MINISTRY OF HIGHER EDUCATION, SCIENCE AND INNOVATION OF THE REPUBLIC OF UZBEKISTAN
FERGANA STATE TECHNICAL UNIVERSITY

O.J.Muradov, A.Djurayev,
B.N.Davidbayev, N.B.Davidbayeva

IMPROVEMENT OF THE DESIGN OF THE SCIENTIFIC BASIS FOR CALCULATION OF WORKING BODIES OF THE SEPARATION AND CLEANING ZONE OF THE FLOW LINE FOR PROCESSING RAW COTTON

(Monograph)

DOI:- https://doi.org/10.37547/gbps-44 **ISBN:- 978-1-957653-53-2**

FERGANA- 2025

Orif Jumaevich Muradov, Anvar Djuraev, Baxtiyordjan Nizamitdinovich Davidbayev, Nargizaxon. Baxtiyordjanovna Davidbayeva. Improving the design and scientific basis for calculating the working bodies of the separation and cleaning zone of the flow line for processing raw cotton.

Reviewers:

Doctor of Technical Sciences, Prof. V.M.Turdaliev

Doctor of Technical Sciences, Prof. G.N.Valiev

The monograph presents the results of research on the development of effective design complex schemes for separation and cleaning of cotton. The results of theoretical studies of separation and cleaning of cotton are presented. The modes of operation of the working parts of cotton cleaners are substantiated. Based on the selection of the best parameters of the sweeping grates, saw drums and determined the ways of effective cleaning of cotton. The results of experiments and comparative production tests are presented.

The monograph is dedicated to researchers, specialists, and doctoral students involved in the creation of designs and research of primary cotton processing machines.

The monograph was approved for publication by the Academic Council of the Fergana State Technical University № may 2025y

CONTENTS

INTRODUCTION

Currently, among natural fibers, cotton is the main raw material used in the textile and light industries. According to statistics from the International Cotton Advisory Committee (ICAC), "the world's leading exporters of cotton fiber are India, the United States, Brazil, Australia and Uzbekistan, and the main importing countries are China, Turkey, Vietnam, Bangladesh and Indonesia." At the same time, these countries pay great attention to the further development of the processing industry using advanced technologies, highly efficient machines and mechanisms that reduce costs and improve the quality of products. Therefore, it is urgent to solve the important task of obtaining high-quality cotton fiber by creating highly efficient, resource-saving machine designs.

Comprehensive theoretical and experimental scientific research aimed at creating new and improving existing techniques and technologies for cleaning medium-fiber cotton varieties in the cotton ginning industry is carried out in leading scientific centers and higher educational institutions of the world.

To intensify the use of modern equipment and technologies, when processing large volumes of contaminated cotton, comprehensive theoretical and experimental scientific research is carried out to improve technology, create a new generation of technological machines, create modern computerized methods for calculating operating parameters, load, and determine operating modes that ensure an increase in the cleaning effect. At the same time, especially important tasks for the industry are the development of highly efficient equipment and technologies that allow optimizing cotton processing in order to maximize the preservation of the natural properties of the fiber.

The implementation of these tasks, in particular, the development of efficient, resource-saving technologies and designs of separators, raw cotton cleaners with a rational arrangement of working parts, taking into account the continuity and compatibility of technologies for separating cotton from air with subsequent cleaning of cotton, allowing for the production of high-quality cotton fiber, is relevant.

CHAPTER 1. ANALYSIS OF RESEARCH ON IMPROVEMENT OF TECHNIQUE AND TECHNOLOGY OF COTTON SEPARATORS AND CLEANERS

1.1. Review of research in the field of cotton separation and cleaning

1.1.1. Review of research on the technique and technology of separating cotton from air

The process of separating cotton from the air flow that carries it has been studied by many scientists. Separation of cotton from the air flow is performed on a separator machine, which is one of the key elements of the technological equipment of cotton plants. The separator separates cotton from dusty air and partially removes small contaminants. The CC-15A separator [3] is widely used in the technological process of cotton ginning plants. Figure 1.1 shows the diagram of the CC-15A separator.

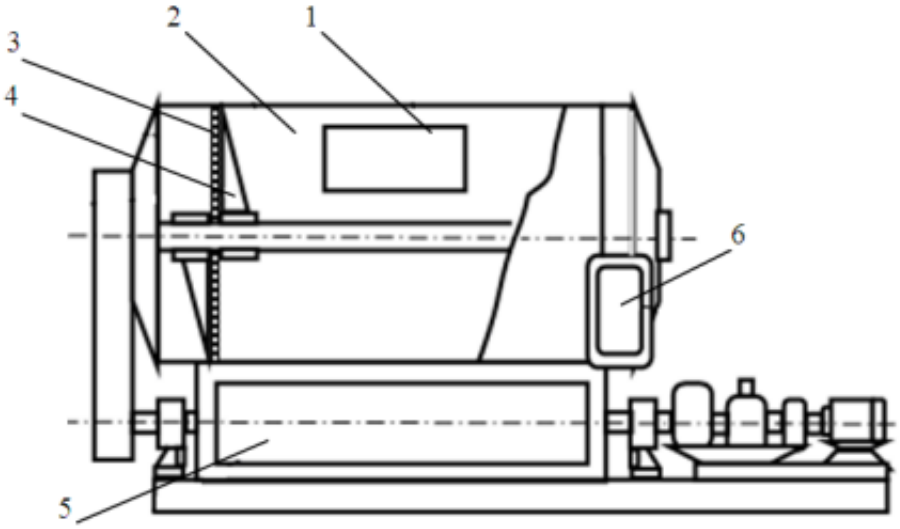

1 - inlet pipe, 2 - separation chambers, 3 - mesh, 4 - scraper, 5 - vacuum valve, 6 - air intake.

Fig.1.1. Separator brand CC-15A

When the separator is operating, cotton enters the separation chamber 2 through the inlet pipe 1 with the air flow. In the chamber, the cotton speed is significantly reduced, and the bulk of the cotton moves under the action of inertia, hitting its wall and entering the vacuum valve under its own weight. A smaller portion is attracted to the surface of the mesh 3 by the air draft. The cotton adhering to the surface of the mesh is removed by the scraper 4 and transferred to the vacuum valve. With the help of the air flow, small contaminants are sucked through the surface of the mesh by means of the pipe 6. The efficient operation of the separator depends on the interaction of the scrapers and the surface of the mesh. If the scraper cleans the surface of the mesh in a timely manner, air will

pass freely. Research [4] studied the formation of a cotton layer on the surface of the mesh and its separation. When rotating, the scraper scrapes only part of the cotton from the surface of the mesh. If we take into account that the separation process is continuous, we can see that the cotton always adheres to most of the surface of the mesh. This leads to an increase in the hydraulic resistance of the separator and a decrease in the pressure in the pipelines.

Since the separator is located next to the fan, there is a pressure drop on the mesh surface of the separator. This leads to a significant suction force that holds the cotton on the mesh surface and draws the fiber into them. The CC-15A separator used has the following disadvantages:

- cotton, entering the working chamber of the separator, hits its rear wall with great force, which leads to damage to the seeds;
- as a result of cotton sticking to the mesh, the moment of resistance on the scraper shaft gradually increases, overloading the drive belt transmission.
- the part of cotton held by the air draft on the mesh surface of the separator within a radius of 200 mm is cleaned by the scraper only on the second or third try. When processing low-grade cotton with a high moisture content, it is difficult to separate the adhered cotton from the mesh surface within a radius of 200 mm. A layer of cotton is formed here, which gradually occupies the entire surface area of the mesh. This leads to the separator stopping; due to the high speed of the air flow sucked in through the holes in the mesh surface of the separator, the cotton sticks to the mesh. As a result, during the separation of the flies, the fiber is torn off from the seeds. The separated fibers are carried away by the air flow into the trash;
- when cotton passes from the separator working chamber through the vacuum valve, it gets between the blades and the shell, which leads to damage to the seeds and fibers;
- As a result of the sticking of particles to the blades of the vacuum valve, it is not completely cleaned in one cycle, the particles accumulate, creating a blockage in the vacuum valve, making it difficult to operate and reducing productivity.

A number of works by domestic and foreign scientists are aimed at overcoming these shortcomings.

In publications by such scientists as V.A. Schwab, F. Zuev, A. Korn, A.M. Dzyadzio, A.S. it was shown that the resistance to movement of a mixture of cotton and air depends on the air flow rate.

In particular, [5], the author proposed to install an additional air-absorbing cushion at the bottom of the mesh surface to reduce the adhesion of cotton to the mesh surface and ensure its faster separation. However, the increase in pressure in

the chamber as a result of the reduction of the useful working surface of the mesh surface was not taken into account.

A number of scientists working on improving the operation of the separator [7-12] wanted to carry out the process of separating cotton from air by abruptly changing the direction of the air flow, using the inertial force created by the movement of cotton, developing so-called pneumatic separators.

Experiments have shown that in pneumatic separators, if the aerodynamic regime is maintained at a constant rate, it is possible to completely separate cotton from the air flow if the cotton is uniformly transferred through the pipes. Otherwise, as a result of a violation of the aerodynamic regime, there is a risk that the cotton will be carried away by the air flow. The inability to uniformly transport cotton through the air ducts in existing cotton processing plants today creates difficulties in the use of pneumatic separators.

The main part of the air separator is the separation zone, in which the separation of the product occurs. It is shown that a large-sized chamber is required to ensure this during the separation from air.

In the work of N.E. Avdiev on the separation of various materials [13], the process of separation of small particles through the surface of the mesh was studied theoretically and experimentally. Particles that are in constant contact with the surface of the mesh are more likely to be separated from the air.

In the work of J. Urban [14], the process of movement of particles of different sizes in the air was studied.

Khasanov M.R. [15] investigated the relationship between air consumption and the speed of material transfer during transportation of material by air flow.

As a result of theoretical and experimental research of the process of pneumatic transportation of raw cotton by P.V. Baidyuk [16], a number of regularities were identified. It was established that the useful surface of the separator mesh and the increase in the total air flow through it leads to a decrease in pressure losses in the separators.

Academician of the Academy of Sciences of the Republic of Uzbekistan H.A. Rakhmatullin [6], taking into account the aerodynamic resistance of air to the transverse movement of cotton, determined the law of its movement in the pipe and put forward the idea that cotton can be separated from the air by inertial forces.

The author proposed a special formula for determining the length of the open part of a bent pipe, which allows the tearing process to be carried out.

Based on the results of research conducted by T.O. Shamsutdinov [17], it was scientifically substantiated that cotton separation occurs at a flow speed of 16 m/s when turning it at an angle of 13°50’

N. Artikov [18] investigated the dependence of the raw cotton movement speed at the entrance to the separation zone of the pneumatic separator on the length of the inclined pipe. According to the author, the separation process is more effective if the length of the inclined pipe is l - 1,9 m and at this length the air flow speed reaches 26,1 m/s. He established a correlation between the coefficients of resistance to the movement of the mixture and its concentration. This made it possible to determine the hydraulic resistance of pneumatic transport with high accuracy.

Based on theoretical research, R. Amirov [19] studied the causes of clogging of the separator mesh surface by gluing pieces of raw cotton to the scraper shaft. He determined the indicators that characterize the cotton layer on the mesh and proposed measures to eliminate clogs. At the same time, R. Amirov [19] found that the geometric parameters of the holes on the mesh surface affect seed damage. Based on the research results, he proposed reducing the diameter of the holes from 6 mm to 5 mm.

R. Amirov also proposed to create a zero-pressure zone where the scraper interacts with the mesh surface. This area would cover the mesh surface behind the scraper and rotate with it.

As a result, the speed of air sucked through the holes in the mesh surface is zero. This should allow cotton stuck to the mesh to be easily separated. However, the device he proposed failed to provide the required level of pressure reduction and the proposed device did not find industrial application.

In the work of Y.D. Yangibaev [20], the movement of cotton on conical mesh surfaces was studied. According to the author, one of the main disadvantages of the air duct is that it consumes a lot of energy during the transportation of cotton. The reason for this is that a certain part of the pressure created by the fan is used to overcome the resistance of the carrier device using the air flow. The device that creates the greatest resistance among the elements of the carrier device using the air flow is the separator. The separator creates resistance when air passes through a mesh located on the side of the working chamber. The author proposed to make it in the form of a cone to increase the useful surface area of the mesh. This increases the useful cross-sectional area of the mesh barrier, reduces the aerodynamic resistance of the separator and increases productivity.

The operation of the vacuum valve has also been studied by many scientists. The efficient operation of the separator is affected not only by the surface of the mesh, but also by the vacuum valve, which is one of its main elements. The results of the studies show that the existing defects of the vacuum valve have not been completely eliminated. The analysis revealed the need for in-depth research to improve the separator and its main working parts.

The vacuum valve is one of the main working elements of the separator, which has the following drawback: when removing cotton from the separation chamber, raw cotton gets between the blades of the vacuum valve and its shell. As a result, the seeds are damaged and various defects are formed.

In the work of R. Muradov [21], the main reasons for cotton getting stuck between the blades of the vacuum valve and the walls of the chamber were studied.

In another study [22], a loss of 20-25% of the total amount of air absorbed by the fan in the vacuum valve is reported. This occurs during the process of lowering a portion of cotton. At this point, air rises from the vacuum valve, in which there is no cotton, into the working chamber filled with cotton. This rising air creates a danger of cotton falling from the upper part of the working chamber sticking to the surface of the mesh. To eliminate these drawbacks, a rotary vacuum valve was created at the "Pakhta sanoati" Research Institute. In this case, the fan pipe is connected to the lower cotton part of the vacuum valve. As a result, air suction through the separator vacuum valve is eliminated.

• Thus, the main directions for improving cotton separation are:

• the need to control the flow of the cotton-air mixture at the entrance to the separator to eliminate the impact of seeds on the wall of the separator and reduce the crushing of seeds:

• the creation of rational conditions for removing a layer of cotton from the surface of the separator mesh;

• the search for a rational shape of the holes on the mesh of the separation chamber, allowing to reduce damage to the fiber and its loss.

1.1.2. Analysis of cotton separator designs

Let us consider the design of the machines used to separate cotton from the cotton-air mixture. Figure 1.2 shows the separator of the XCCH brand, created by Uzbek scientists. In this case, the transported raw cotton, together with air, enters the separation chamber 3 of the separator through a pipe. The size of the separation chamber is much larger than that of the short pipe. Consequently, the air speed decreases from 20-25 m/s to 7-8 m/s.

At this speed, the raw cotton continues to move by inertia and sticks to the mesh 2. The cotton is separated from the mesh surface by a drum with rubber blades and then, under its own weight, enters the vacuum valve 7. The disadvantage of this design is that the cotton entering the separator, moving by inertia, hits the surface of the drum and blade, which leads to crushing of the seeds. The blades on the drum are unevenly pressed against the surface of the drum and clamp individual bats, which leads to ignition of the cotton.

The XCC separator is similar to the XCCH separator. It differs only in its

design dimensions. The rotation frequency of the drum and vacuum valve of the XCC separator has the same parameters as the XCCH separator. At present, all cotton ginning plants use the CC-15A separator (Fig. 1.3) to separate raw cotton from air transported through pipes.

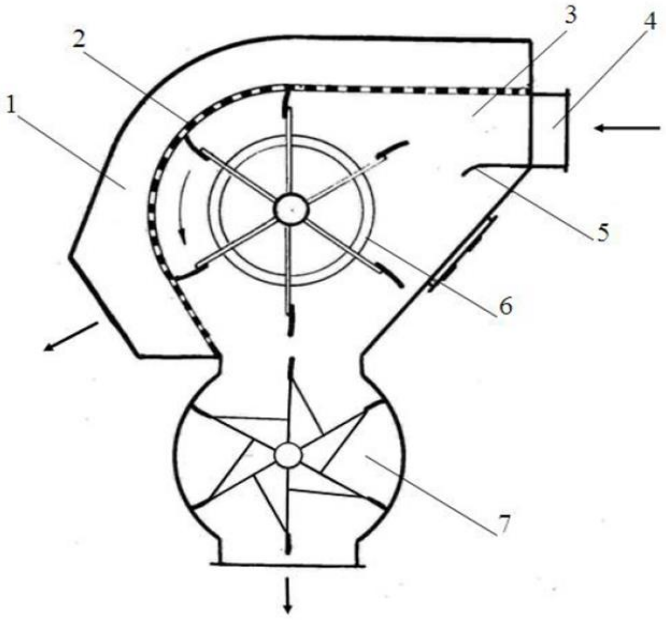

Fig.1.2. Separators of the XCCH brand

1 - air flow; 2 - mesh; 3 - separation chamber; 4 - inlet pipe; 5 - router; 6 - drum; 7 - vacuum valve

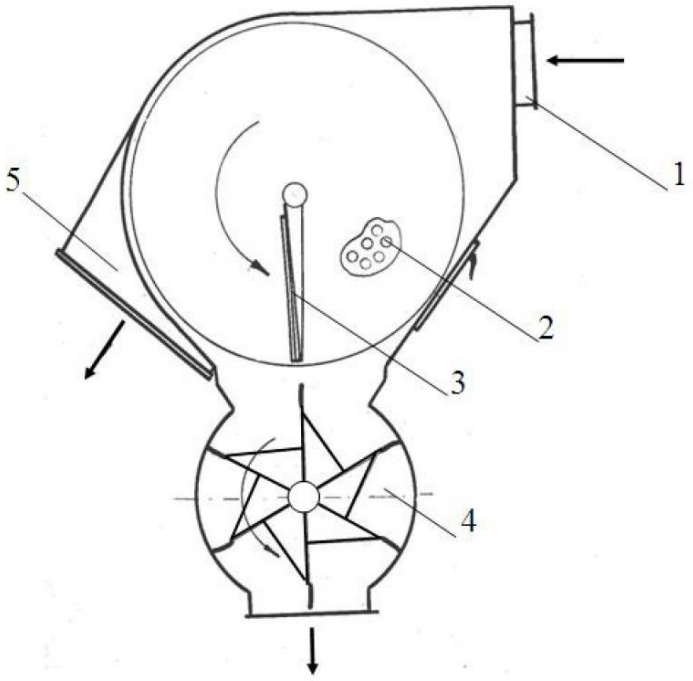

Fig.1.3. Separators CC-15

1-inlet pipe; 2-mesh; 3-scraper; 4-vacuum valve; 5-short suction pipe

The CC-15A and CC-15M separators, originally developed in 1956, have undergone some modifications, but the basic design structure has been retained

[24]. The main difference from the XCCH separator is that the separator does not have a drum with rubber blades.

When the separator is operating, the bulk of the raw cotton entering the chamber moves by inertia, hits the wall of the separating chamber and enters the vacuum valve. A certain part of it is directed by the air flow to the mesh walls and sticks to them. These meshes are installed on the sides of the separator's working chamber.

Cotton is scraped off the surface of the mesh using elastic scrapers (3 Fig. 1.3). The separator capacity is 15 t/hour, the number of revolutions of the scrapers and the vacuum valve shaft is 80 min^{-1}. Some of the small impurities are separated from the cotton and carried away by the air flow through the mesh. The efficiency of the separator cleaning is no more than 5-8%.

The main disadvantages are that during the transfer of raw cotton at low or high humidity during operation, a large amount of cotton sticks to the surface of the side screen. This increases the torque on their shaft and causes the drive belts to slip. As a result, the scraper shaft stops and the separator becomes clogged.

In the short outlet pipe of the separator, the cotton falls between the paddles of the vacuum valve drum and the steel shell. The paddles of the drum strike the cotton against the surface of the shell, causing the seeds to be crushed and the fibers to be damaged.

In addition, the cotton by inertia hits the inner surface of the separator. Due to this, the impact force will be significant. An indirect indicator of the impact force can be the destruction of the wall, which occurs over time, under the action of the cotton flow. The wall of the separator is shown in 1.4.

Fig.1.4. Internal view of the wall of the CC-15A separator after repair.

S. M. Kadyrkhodjaev [23] created a new, more advanced separator CX for

the pneumatic separator shown in Fig. 1.5.

During the operation of the separator CX, cotton enters through the air intake 1. Air is sucked in through a tube through a cylindrical mesh surface 4 using an outlet tube 5. Cotton is separated from the air by inertia and enters the separation chamber 7 through the separation section 3. The mass of cotton, under the action of its own weight, breaks up into 8 parts and is pushed out by the blades.

Some cotton shreds mixed with air will stick to the surface of the mesh 4. The cotton stuck to the surface of the mesh is separated by an elastic drum with blades and transferred to the vacuum valve by a separation chamber.

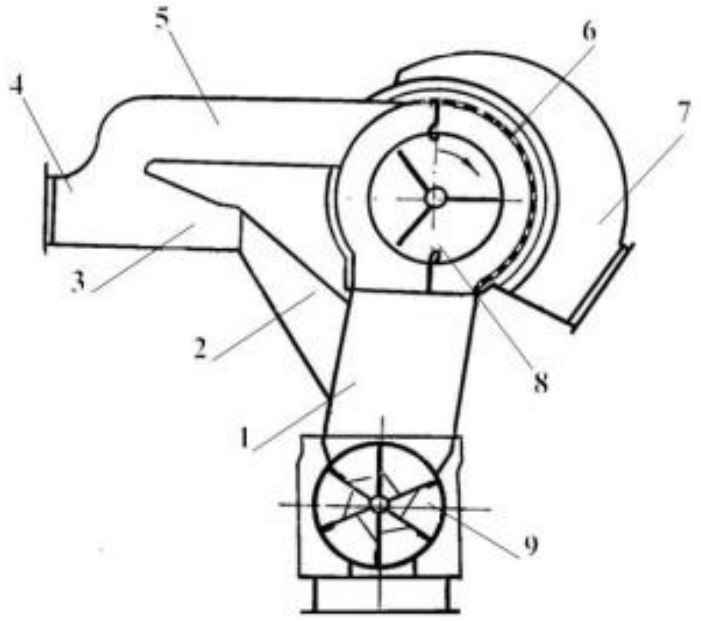

Fig.1.5. Separators

CX 1-working chamber; 2-lower tray; 3-two-way dividing pipe; 4-inlet pipe; 5-upper tray; 6-mesh surface; 7-suction pipe;

In cotton ginning plants, raw materials are unevenly transported through pipes. As a result, cotton moves unevenly through the pipes and enters the working chamber of the separator. Therefore, in pneumatic separators, when separating cotton from air, there are cases when it gets into the fan.

Z.Shodiyev [24] proposed a more advanced design of the CXM pneumatic separator, shown in Figure 1.6.

The proposed separator consists mainly of an input chamber 1, a distribution chamber 2 and an output pipe 3. Cotton is distributed into two streams and enters two air ducts 6 and 7. With the air flow, part of the cotton moves along the air duct 6 and hits the mesh drum 4 and sticks to it. To separate the cotton from the surface of the mesh, a cleaning drum 11 is placed under the drum 4, with the help of which the cotton moves to the vacuum valve 9. Air is released into the atmosphere

through the outlet pipe 3.

Thus, having studied in detail the structure, processing processes and shortcomings of various separator designs, one can be convinced of the need to create an improved separator design.

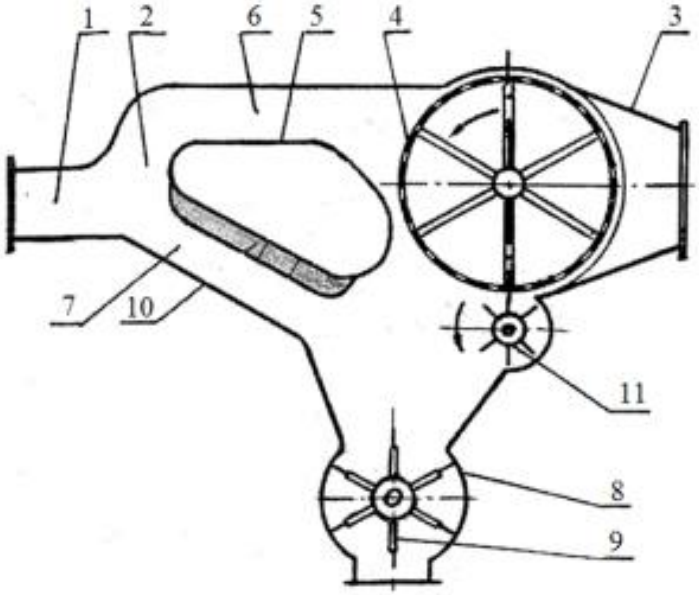

Fig.1.6. Separator

CXM 1-inlet pipe; 2-working chamber; 3-outlet pipe; 4-cell drum; 5-guide edge; 6-air duct; 7-lower tray; 8-shell; 9-vacuum valve; 10-wall; 11-cleaning roller

Hardwick-Etter separators are used in pneumatic conveying installations of cotton ginning plants in the USA (Fig. 1.7) [25].

The flow of raw cotton moving along channel 1 enters wall 2, touching it, is transferred to the vacuum valve and is carried out. Air sucked in by the fan enters pipe 5 through surface 6, which is regularly cleaned by means of rotating separator 4. The company emphasizes the following advantages of the separator.

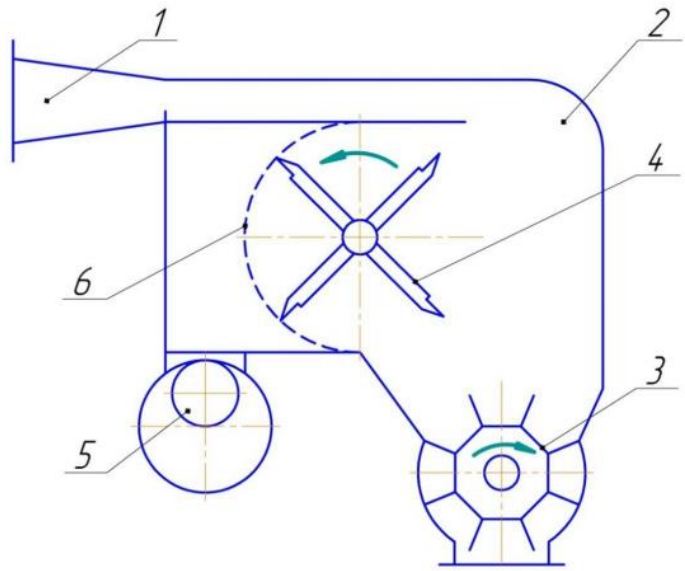

Fig. 1.7. General view of the separator by Hardwick-Etter

1-channel; 2-wall; 3-vacuum valve; 4-rotating separator; 5-pipe; 6-mesh.

The raw cotton does not come into direct contact with the surface of the mesh. This, in turn, prevents it from twisting. The surface of the mesh is regularly cleaned, which ensures a constant supply of air.

Cotton ginning plants in India widely use separators, in particular those similar to the CX brand separator. The main working element of the separator is the brush-scraper, which occupies 1/3 of the working surface of the mesh. Figure 1.8 shows the process flow chart, and Figure 1.9 shows a general view of the BAJAJ brand separator [26]

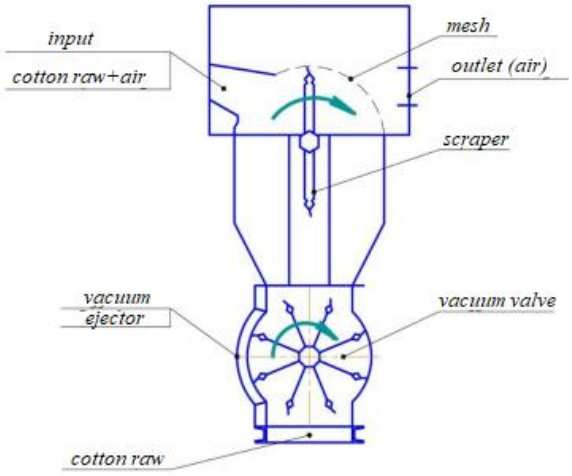

Fig.1.8. Cross-sectional diagram of the separator “BAJAJ”

Fig. 1.9. General view of the separator "BAJAJ"

The Big-J separator has automatic cotton feed control [53].

The separator consists of three pick drums 2, which pre-clean the cotton and direct it to the bunker, where the cotton is loosened and accumulated. Cotton enters the bunker freely in a loosened form (Fig. 1.10.)

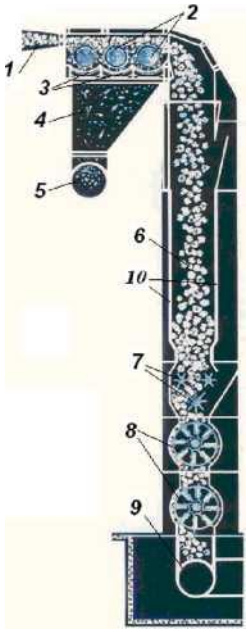

Fig.1.10. General view and process diagram of the Big-J separator

The separator consists of the following parts: 1. Output tunnel. 2. Pin drums. 3. Mesh surface. 4. Impurity accumulation bin. 5. Pipe through which impurities and dirt move. 6. Accumulator bin. 7. Toothed straightening rollers. 8. Vacuum valve. 9. Pneumatic pipe through which cotton moves. 10. Pipe through which air moves.

The separator operates as follows:

Air is removed from the bin through horizontally located transport pipes.

The bin is continuously supplied with a flow of cotton. It is located above the toothed rollers and has a volume that ensures free passage of cotton through the toothed straightening rollers 7.

The toothed straightening rollers move at a variable speed and are provided with a remote control system.

The raw cotton in the bunker is introduced from the bunker using vacuum valves 8 and sent to the drying system. The loosened and controlled cotton flow ensures efficient operation of the drying and cleaning units.

The Chinese company "Swan cotton machinery" produces the MZF-15 cotton separator, the general appearance of which and its process flow diagram are shown in Fig. 1.11

Cotton mixed with air at a speed of 20 rpm enters the separation chamber 6 through the outlet pipe 1.

In the separation chamber, the cotton loses its initial speed due to the expansion of the internal surface. Then it moves to the rotating drum and sticks to it.

The separator consists of the following parts and components: outlet pipe 1, valve 2, drum with mesh surface 3, brush-separator 4, vacuum-valve 5, 1 separation chamber 6, and base 7.

Brush-separator 4 retains cotton segments present on the surface of the drum mesh and cleans the surface. This ensures free access of air to the mesh surface [27].

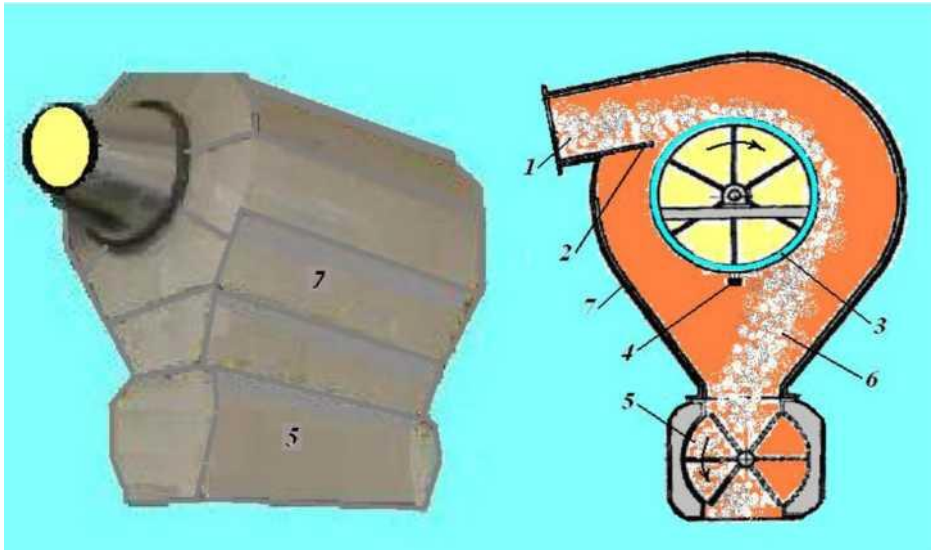

Fig. 1.11. General view of the cotton separator MZF-15

Then the cotton, rotating together with the mesh drum, is separated due to centrifugal force and gravity and enters the vacuum-valve 5 located below, along the inner walls of the unit 7. The vacuum-valve, due to its rotation at a speed of 40 rpm, transfers the cotton loaded into it to the subsequent technological process.

Small impurities pass through the mesh surface, then are removed from the separator together with the air and are transferred to the dust collector unit.

The technology of drying and cleaning raw cotton from foreign impurities at a cotton ginning plant for saw ginning is considered in [28]. The technological process begins with the feed module. The main working element of the feed module is the loosening section, consisting of seven peg drums and a roller platform (Fig. 1.12). The peg drums begin to loosen the raw cotton on one side of the module and evenly transfer it to the pneumatic tube. The movement of cotton is regulated from the main control panel by the operator.

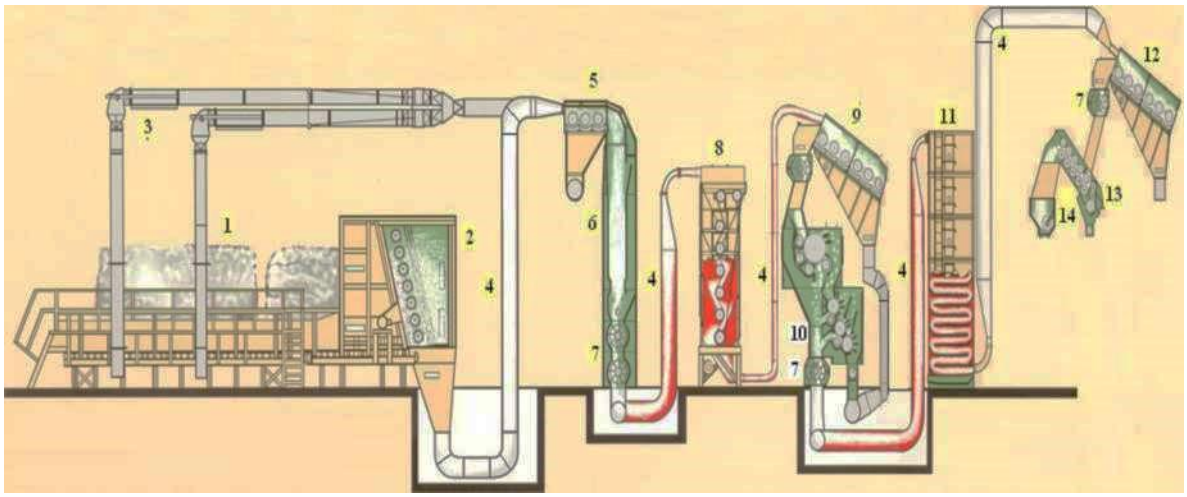

Fig. 1.12. Technological process system for drying and cleaning raw cotton.

In accordance with the amount of cotton, the light flow passing through it changes, which is converted into an electrical signal and changes the speed of the conveyor. Then the raw cotton, located in the pneumatic tube, is transferred to the automatic feeder.

Above the feeder there is a large-volume bin, in the lower part of which there are two vacuum valves 7, as well as a separator with three peg drums. The cotton level in the bin is maintained by the automation system.

Figure 1.12 shows: cotton module 1; opening section 2 consisting of pin drums; catcher for unopened bolls 3; pneumatic tubes 4; separator 5; automatic feeder 6; vacuum valve for cotton discharge 7; vertical flow dryer 8; stone trap 9; saw gin 10; tower dryer 11; inclined drum cleaner 12; fiber cleaner for small and large impurities 13; distribution screw conveyor 14. When cleaning raw cotton from small impurities for the second time, that is, during repeated cleaning, hot air is supplied from the drying system to the cleaner with a pin drum, with the help of which the cleaning process is carried out.

1.1.3. Analysis of research on improving raw cotton cleaning technology

One of the main processes that can preserve the natural properties of raw

cotton is cleaning it from large and small debris. The original raw cotton supplied for its primary processing contains large and small debris. Debris less than 0,8 mm in size is deeply embedded in the fiber and is removed by strong impact and shaking effects on the raw cotton. Large debris is located mainly on the surface of the raw cotton, has weak adhesion to the fiber and is easily separated from it [29]. At the same time, it is the size of the debris that determined the two main directions in the development and improvement of cleaning technology. The work [30] describes in detail the main types of designs of small and large debris cleaners, and provides methods for engineering calculations of their working elements. '

At the current stage of development of the cotton ginning industry, it is important to intensify the cleaning of raw cotton, develop more advanced designs, find new, effective methods for cleaning raw cotton from small and large impurities, as well as select rational modes of movement of the working parts of cotton gins.

At present, ginneries use cleaners CHX-CHM2, CHX-5, 6A-12M1, 1XK, UXK, etc. for cleaning medium-fiber raw cotton, and OXB-10M, CHX-ZM2, etc. for fine-fiber raw cotton [31]. To increase the cleaning effect, a number of scientists, based on theoretical and experimental studies of the cleaning process, have recommended various design changes, substantiated rational technological parameters of the working parts of the cleaners, optimal operating modes of the working parts, etc. Let us analyze the results of work devoted to the technique and technology of cleaning raw cotton.

The works of A.E. Lugachev and U.K. Ziyaev [32] are mainly devoted to studying the influence of the angle of inclination of the lapping brush on the cleaning effect of large debris, as well as the use of a peg leveler in front of the lapping brush. The process of cleaning cotton fiber, recommended by B.S. Kotov et al. [33], was sufficiently intensified by reducing the geometric dimensions of the saw tooth.

G.I. Miroshnichenko, P.N. Tyutin and A.E. Lugachev [34] determined the degree of influence of each factor on the cleaning effect of cotton processing machines operating in production. R.Z.Burnashev [35] and G.I.Miroshnichenko et al. [36], studying the issues of impact interaction of the raw cotton fly with the grate, determined the values of the fly impact impulse on the grate using the strain gauge method, provided the prerequisites for taking into account the dynamic rigidity coefficient of the fly upon impact with the grate, as well as the influence of the fly oscillation frequency on the cleaning effect. R.G. Makhkamov et al. [37] presented the results of studies to determine the force of impact of the fly on various surfaces. G.I.Boldinsky et al. [38] identified the optimal direction of flight

of the cotton fly in the zone of entry into the tooth of the raw cotton cleaner of the flow line.

The work [39] considered the issue of the influence of the number of rotating grates and their rotation speed on the cleaning effect of the coarse debris cleaner. The works [40, 41] present the results of optimization of the technological process of cleaning raw cotton in a flow line from various design and technological factors of machines and mechanisms.

Based on the analysis of the cleaning technology R.Z. Burnashev [37] substantiated the theoretical prerequisites for determining the design and technological parameters of the working elements of cotton cleaning, presented original design developments.

G.P. Nesterov et al. [42] established the influence of the geometric and technological parameters of the grates (the diameter of the grates, the gaps between the grates and saw blades, etc.) on the cleaning effect of the saw sections of the cotton gin. The works [43, 44] are devoted to the study of various issues of the operation of the 1XK flow line for cotton cleaning. The works [45, 46] present the results of studies of the influence of fiber cleaning plans in cleaning modules, as part of flow lines, on the formation of "soft" defects in the fiber. It was found that the disaggregation of raw cotton particles reduces the content of "soft" defects in the fiber.

A.E. Lugachev et al. in [47] investigated the issue of choosing the optimal zone for throwing raw cotton onto a serrated drum. The experimental results showed that there is a significant reserve for increasing the cleaning effect while reducing the amount of fly ash going to waste. A.E. Lugachev [48] presents the results of studies of the effect of feed uniformity on the technological parameters of cotton cleaners. At the same time, the author proposed a number of interesting technical and design solutions that make it possible to increase the cleaning efficiency while preserving the natural properties of cotton fiber.

In [49], the results of studies of the proposed cleaner of fibrous material with differentiated linear speeds are presented, with their increase during the process, where, due to the speed gradient, the material is drawn out and the bond between the debris and the fiber is weakened. This proposal has not found practical application due to the complexity of the design and technological shortcomings.

The rationale for the design parameters of the elements of the module for cleaning raw cotton from large debris is presented in [50, 51, 52]. The authors conducted experimental studies of the impact interaction of raw cotton flakes with the working elements of the cleaner (lapping brush, saw tooth and grate).

In [53, 54] the results of studying the cotton cleaning process in the large debris module are presented; prismatic grates are proposed and their efficiency is

studied on the CHX-3M cleaner. To improve the flow line of the UXK, a comb-type grate was proposed in [49]. However, this design has not found practical application due to its low efficiency.

Cotton cleaning equipment and cotton cleaning complexes abroad are mainly developed by US companies: Murray, Continental Moss Eagle, Continental Consolidation, etc. [55]. The equipment of the Shandong (KHP) machine-building company Lebed has a complex multi-tiered layout in a vertical plane, and the cleaning units are bulky and difficult to maintain [27]. It should be noted that the number of cleaning modules in the flow lines is significantly less than in domestic developments, but the insufficiently high cleaning effect of the equipment is compensated by enhanced cleaning of the fiber after ginning. In practice, the technological line proposed by China is not universal. It is not suitable for processing low-grade cotton.

The Continental Consolidation company uses a shortened technological process for cleaning cotton, where up to three modules for cleaning from large debris in the flow line are used.

In the works of R.Kh. Rasulov [56] a new arrangement of the saw-and-grate system of the large debris cleaner is recommended. It is recommended to install the grates in groups of three grates, while the distance between the saw drum and the first grate is 16 mm, the second grate - 14 mm, the third grate 12 mm. However, this recommendation has not found practical application.

The issues of improving the cleaning process and reducing the loss of material to waste were considered in the work [57, 58]. The author obtained experimental dependencies, and established a relationship between the strength of the fiber and the degree of its fixation with a lapping brush. Models of the process of fixation and interaction of raw cotton fluff with the grate surface are recommended. In order to reduce the amount of cotton going to waste, it was proposed to install a fixing roller in the space between the grates, and to install the last grates of the module with an increasing gap along a parabolic curve. The results have not found practical application.

The results of theoretical and experimental studies of the interaction of cotton with various grate profiles are presented in the work of S. Fazylov [59]. The author gives a detailed analysis of a number of models of the cleaning process, characterizing the grate profile. A grate with variable curvature in the form of an Archimedes spiral is proposed. But the results were not implemented in industry either.

In a number of works by K. Olimov and A. Dzhuraev et al. [60, 61], grates on elastic supports in the form of rubber bushings were studied. Based on theoretical and experimental studies, the authors substantiated the parameters of

the grate and the elastic-dissipative properties of the rubber bushing. The recommendations are used in a number of cotton mills.

Sh. U. Rakhmatkariev in his work [62] mainly presented theoretical studies on the calculation of the working bodies of cotton cleaners, proposed a number of design solutions, which also did not find industrial application due to the complexity of the designs.

The paper [63] presents the results of studies on the impact process of interaction of material particles in the cleaning zone of the large debris module. The paper examines the kinetics of a cotton particle in the grate gap taking into account the force factors arising during the interaction process and obtains a number of mathematical models describing the cleaning process. However, due to the lack of numerical values of some physical and mechanical parameters, such as the damping coefficient, the rigidity of the fiber bundle, etc., during the processes of interaction of fibrous material with the elements of the cleaner, the work was not brought to a numerical solution and did not find practical application.

It is known that during cotton processing at factories, the fibrous mass intensively contacts with the working surfaces. Repeated frictional interaction of cotton with metal working elements leads to significant damage to cotton fibers.

As a result of interaction with transition surfaces, saw teeth and grates, raw cotton can be damaged. Damage occurs both due to the presence of sharp peaks of irregularities and burrs of hard metal surfaces of working elements, and due to the high force of frictional interaction of these surfaces with cotton, especially at high humidity of the latter. In this case, cotton damage reaches 13,7% due to the formation of free fiber, flagella, seed skin with fiber and crushed seeds.

R.G. Makhkamov [64] studied the interaction of raw cotton with the surfaces of structural materials from the position of optimization of surface roughness, aimed at reducing the mechanical damage of cotton fibers. The author showed that the interaction force of raw cotton with metal surfaces increases due to micro-cutting of cotton fibers by micro-protrusions.

From the above analysis of research in the field of cleaning raw cotton and cotton fiber, it can be concluded that most of the research is aimed at developing and modernizing the working elements of cotton cleaners from large debris based on technology using optimization methods. The effect of grates on the operation of large debris cleaners has not been sufficiently studied. There are practically no dynamic studies and the effect of dynamics on the cleaning effect and damage to raw cotton. In addition, it is necessary to clarify the effect of vibration of the working elements on cotton, which allows for a significant increase in the release of foreign impurities.

It should be noted that it is advisable to study increasing the degree of

mobility of the working elements of cleaners, as well as the use of lightweight grates with low rigidity, allowing for controlled vibration and, due to this, variable cotton cleaning modes, which can increase the cleaning effect.

1.2. Features of cotton cleaning technology from small debris in existing cleaners

Cleaners for separating small impurities from raw cotton are installed in drying and cleaning shops at cotton ginning plants. This task is also performed by feeder-cleaners installed on each gin [65; pp. 129-130, 66; pp. 16-17]

Processes for cleaning raw cotton from small impurities are divided into pneumatic, pneumatic-mechanical and mechanical; according to installation in the cleaning process line - into individual and battery.

Small impurities penetrate deeply into the fibers, so their separation is a difficult task. To ensure the necessary effect in these cleaners, the cleaning process is carried out repeatedly.

In a cleaning machine, the main working element affecting cotton is the drum pick. The picks and bars of the drum pull the cotton along the mesh surface of the cleaner.

Foreign companies "Platt-Lummus", "Hardwick-Etter" and "Murray" produce coarse and fine litter cleaners. The cleaning process is especially intensive on cleaners of the company "Continental-Moss-Gordin", which have an increased number of grates and cleaning sections [67; pp. 65, 68; p. 15]. Recently, foreign companies from the USA and China have been producing combined cleaning units, which include sections for coarse and fine cotton cleaning in sequence [69; pp. 381-382].

The cleaning section is designed to separate small impurities from raw cotton; it (Fig. 1.13) has a peg-and-bar drum 1 and a mesh surface 2. The efficiency of this section, assessed by the cleaning effect and seed damage, depends on the design of the drum and the mesh surface, the peripheral speed of the drum and the joint operation of adjacent drums, productivity, gaps and distributions, and air flows in the working volume [29; pp. 134-135].

Cleaning drums and mesh surfaces. By design, cleaning drums are divided into tooth-and-bar, slat, peg and peg-and-slat. Research [70; p. 22] has shown that the greatest cleaning effect is achieved on peg-and-slat cleaning drums.

A number of studies have established that, along with the design of the drum, the design of the mesh surface affects the cleaning effect [29; p. 135].

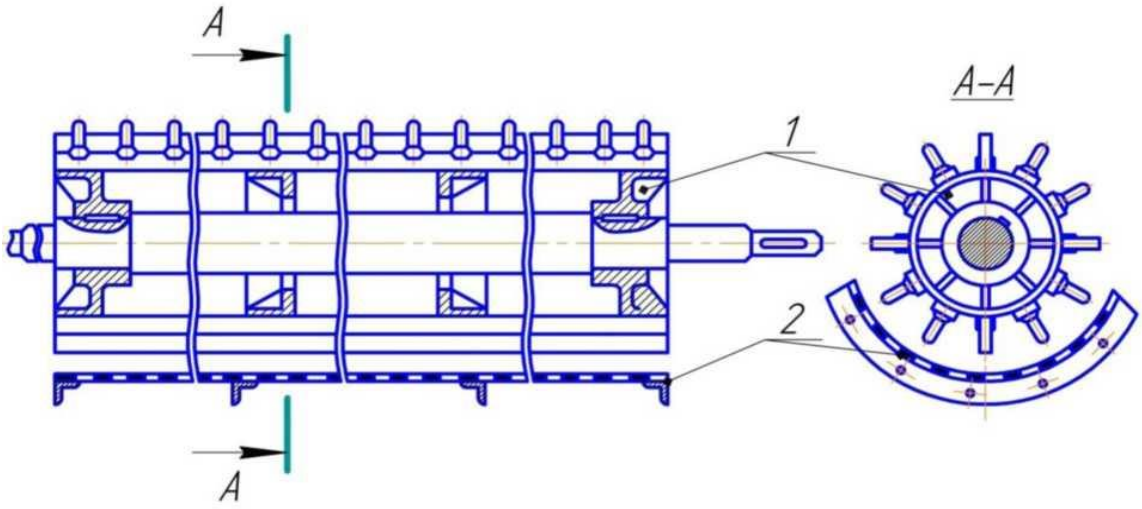

1-pin drum; 2-mesh surface

Fig. 1.13. Cleaning section of drum-and-slat cleaner

Table 1.1 presents the generalized indicators of research of various designs of drums and mesh surfaces, conducted by S.D. Baltabaev, at v_d = 9,42 *m / sec*. [71; c. 65]

Table 1.1

Drums	Cleansing effect %			
	Grate bars	Stamped mesh with holes		Woven wire mesh
		round	oval	
Dentifrices	41,1	42,6	40,8	41,0
Plank	40,4	37,4	36,6	41,0
Pegs	41,4	36,1	38,6	41,5
Peg-slat	35,7	37,8	36,7	39,5

Modern designs of cleaning sections use peg-and-slat drums and stamped mesh surfaces with a hole size of 5×50 mm and the location of the major axis of the holes perpendicular to the movement of cotton in the cleaner. The peg-and-slat drum (Fig. 1.12) is a prefabricated structure consisting of a shaft, disks, a casing made of thin sheet and slats, of which eight are peg-shaped and four are bladed [29; pp. 135-136].

Four rows of slats and eight rows of pegs are installed on the surface of the drum. In this case, the slats in the cleaning zone create a kind of air aerodynamic flow, and the pegs directly interact with the cotton bats and, dragging them along the mesh surface, ensure the separation of impurities from the cotton.

Fig. 1.14 shows the diagram of the combined cotton ginning unit UXK, which includes three sections with four peg-mesh sections and two saw-grate

sections [71 p. 92]. During operation, raw cotton is fed through the loading shaft to the peg drums, which loosen it, pull it along the mesh surface and clean it from small debris, and the first slatted drum of the feeder in the course of the technological process sends it to the saw-type section for cleaning from large debris, then it gets to the first saw-type drum in the direction of movement, is threaded onto the teeth of the saws by a lapping brush and is pulled along the plane of the grate bars to the second saw-type drum, where the process is repeated. Removal from both saw-type drums is performed by one slatted drum, which returns the raw cotton to the feeder to the outlet opening. The separated waste is discharged to the outside through a valve by a screw. The raw cotton, cleaned of large debris, is removed from the cleaning section and sent by the second feeder drum to the picking block for re-cleaning of small debris [66; pp. 18-19].

Fig. 1.15 shows the feed zone (a) and the kinematic diagram of the drive of the first section of the UXK unit. A special feature of the UXK unit is the combined cleaning of raw cotton in several repetitions.

The mesh surfaces of the small debris cleaners are made mainly of two types: stamped with holes and braided wire, as well as rod [66; p. 18].

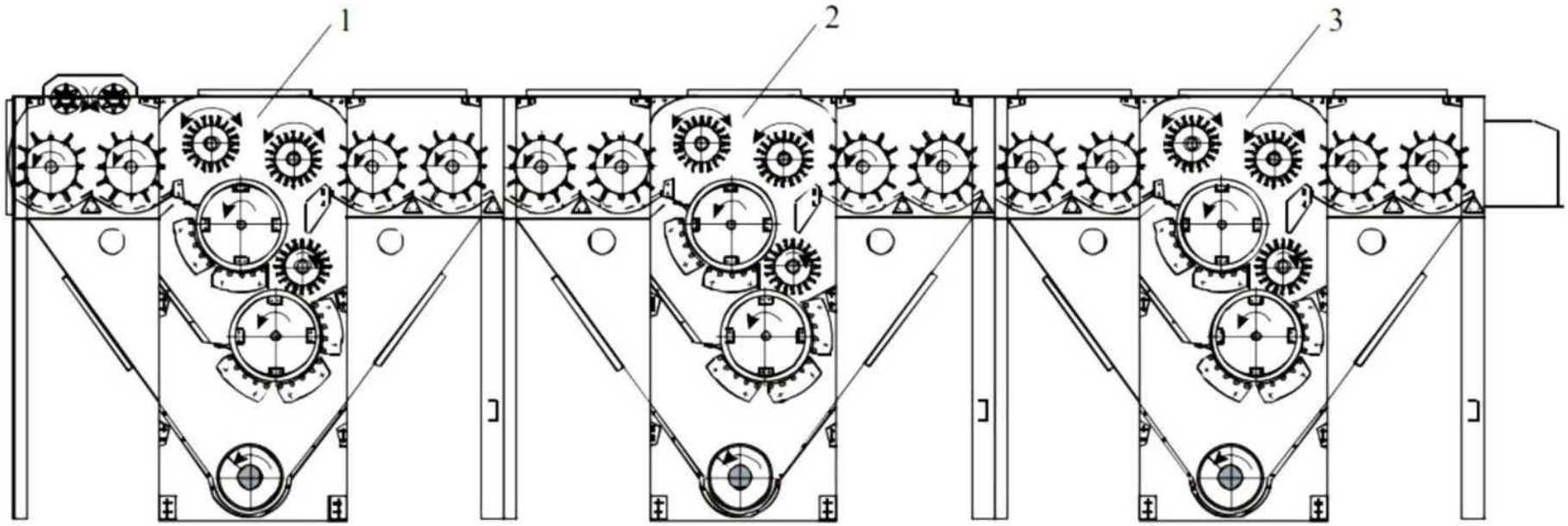

1-Initial cleaning section UXK 01; 2-Intermediate cleaning section UXK 02; 3-Final cleaning section UXK 03.

Fig. 1.14. Scheme of the combined cotton cleaning unit UXK

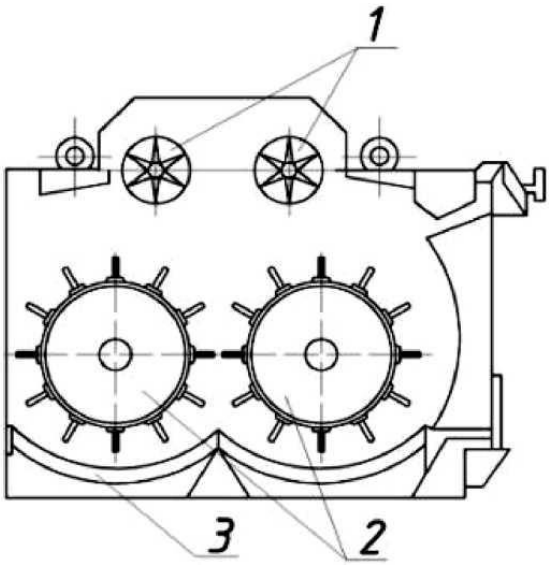

а)

1-feed rollers; 2-pin drums; 3-mesh surface,

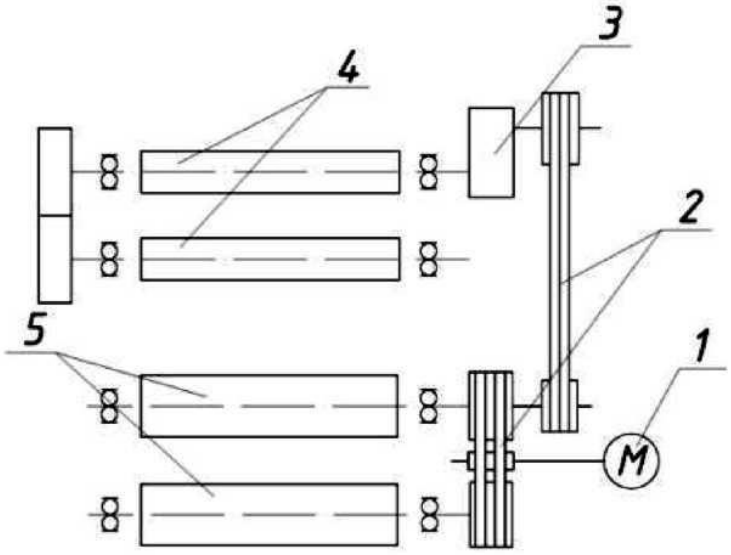

б)

1- electric motor; 2- belt drives; 3-variator; 4-feed rollers; 5-pin drums.

Fig. 1.15. Feed zone (a) and kinematic diagram of the drive of the first section of the UHK unit (b)

For cleaning raw cotton from small debris, the following are mainly used: 1XK, SCH-2 cleaners (Fig. 1.16) and EN-178 peg blocks (Fig. 1.5), which are used in cotton cleaning units of the UXK type or for assembly in 1XK type cleaners with an increased or decreased number of peg drums (a multiple of four). In these cleaners, sections or blocks, peg drums of practically the same design are used, installed in a row one after another in a horizontal plane and working in combination with perforated meshes enveloping them from below, through which debris is separated during cleaning of raw cotton. Above the first two pin drums along the raw cotton flow there is a shaft with feed rollers, the rotation frequency of which is regulated using the IVA variator, thus setting the required productivity. [73; pp. 34-36].

Fig. 1.17 shows the types of mesh surfaces of small debris cleaners [74; p. 64]. The cleaning meshes are installed under the peg-type working bodies of the cleaners and are designed to separate small debris. The cleaning effect of the cleaner, along with the design of the working body and other parameters, largely depends on the design of the mesh surface. The criteria for the technological evaluation of mesh surfaces are: the coefficient of the live section, which is determined by the ratio of the area of the openings of the mesh surface to its entire area, and the coefficient of efficiency of the live section, which shows the influence of the surface design on the cleaning effect [75, 66; pp. 16-24].

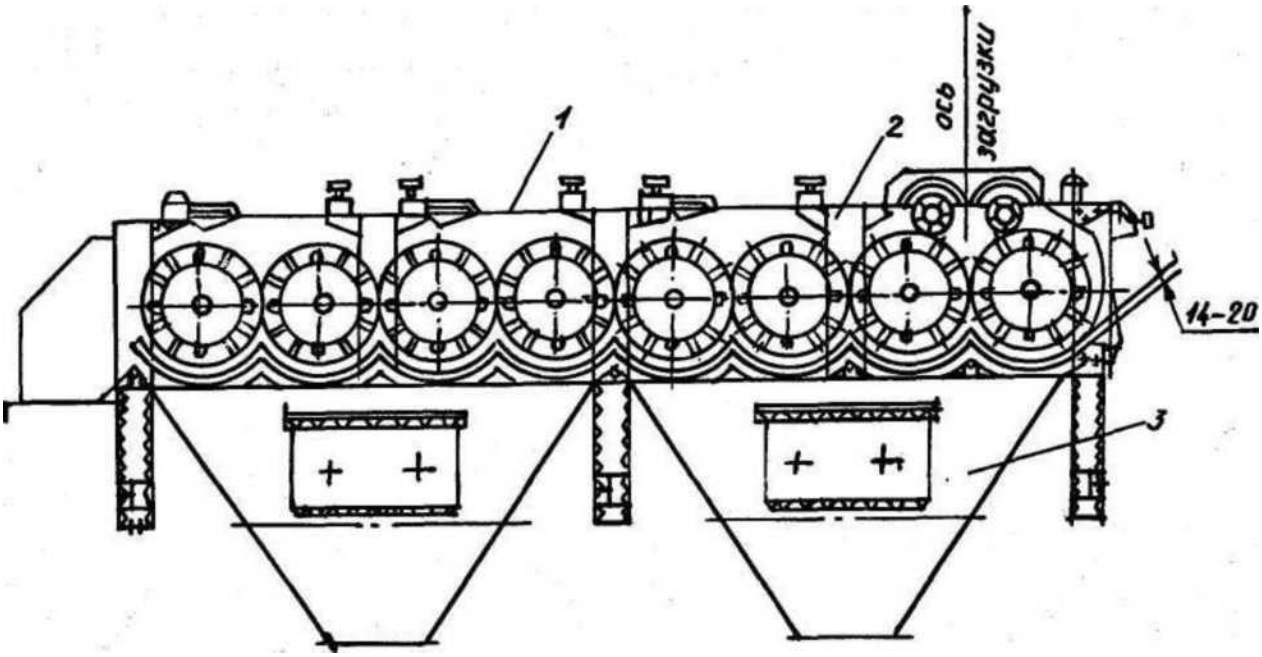

1-pin blocks EN-178; 2-racks; 3-bunkers
Fig. 1.16. Raw cotton cleaner brand 1XK.

Analysis of the designs of small debris cleaners shows that although they have some differences in design, they are generally of the same type and have identical units, such as cleaning mesh surfaces. Researchers have developed and recommended various designs of mesh surfaces and devices used in small debris cleaners in order to improve the cleaning effect [66; pp. 12-22].

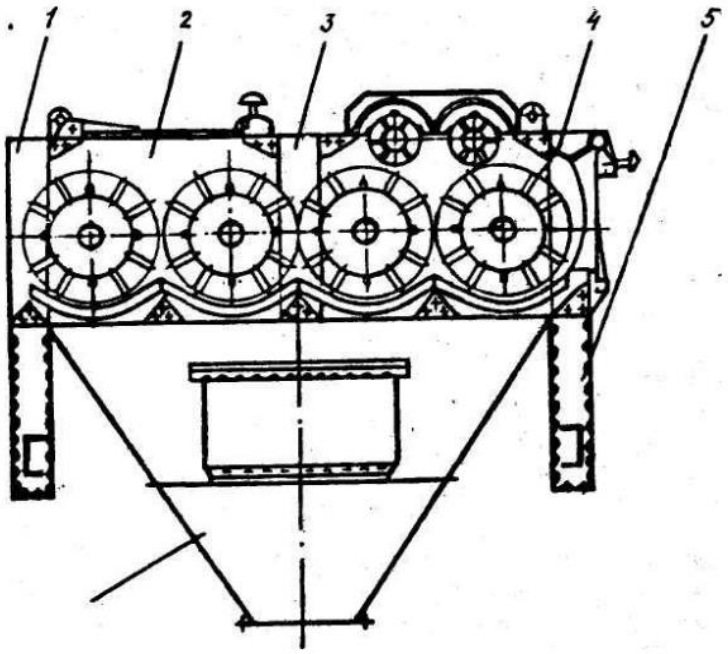

1, 3, 5- racks; 2 - normalized pressing block EN. 178.02; 4 - normalized pin block EN.178.01 (with feed rollers); 6- bunker

Fig. 1.17. Initial section of the 1XK raw cotton cleaner

In the work [76; pp. 52-53] mesh surfaces of the small debris cleaner are proposed, where part of the bridges of each row of holes are made spherical protruding, in a checkerboard pattern (Fig. 1.18). In Fig. 1.18 b, a version of the mesh surface design is shown, where the protruding bridges are made in the form of a broken curve. The advantage of the presented designs of mesh surfaces is that, due to their configuration, they actively affect the mass of raw cotton, however, it should be noted the low efficiency of the separation of foreign impurities compared to other mesh surfaces, since foreign impurities are mainly separated through the lower perforations, as well as the increased damage to the fibers and cotton seeds. The main working element of the feeders, along with the pin drum, is the sifting surface, designed to separate small foreign impurities. In cleaners for raw cotton, the following types of sieving surfaces are used: a woven wire mesh with 10x10 mm cells, a grate made of rods with a diameter of 6 mm, located at a clearance interval of 5 mm, and, finally, a perforated mesh with opening sizes of 20x4.5, 50x5, 50x6, 45x8 mm, etc. (Fig. 1.7) [66; pp. 20-26].

With an increase in the live cross-section of the mesh, the amount of separated trash increases [77; p. 26]. Based on this, and also taking into account that this direction is promising and relevant for the cotton ginning industry, new studies were further developed in this work.

From the analysis of existing designs of trash-separating surfaces, the following effective schemes can be noted. Fiber-processing machine [78; pp. 188-191], where the perforation of the surface is covered by stamped protrusions from

the mesh material.

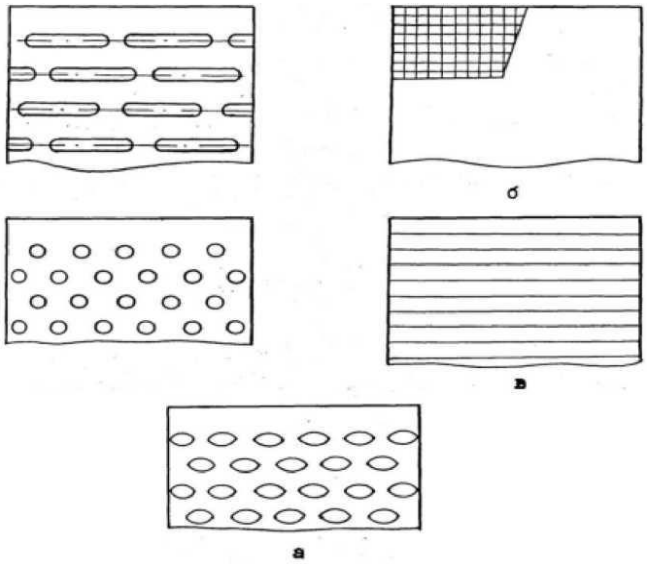

a - stamped from sheet steel with cells of various shapes; b - from woven steel mesh; c - grate.

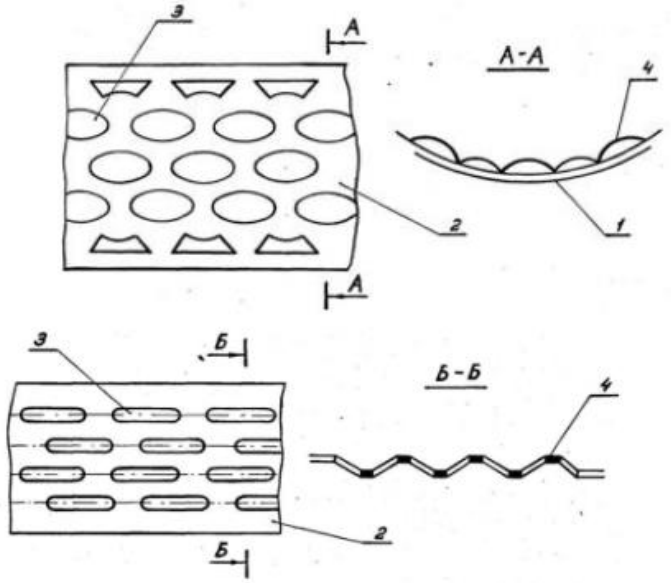

1-arc sidewall; 2-plate; 3-holes; 4-crossbars

Fig. 1.18. Trash-collecting surfaces of small trash cleaners

All mesh openings are located towards the direction of the debris. This design has the following disadvantages: identical uniform perforation, the recesses-openings are located against the rotation of the pin drum, which leads to clogging of the recesses with material. The overlapping elements are made rigid, practically non-oscillating from the mesh material, sharp edges directed towards the movement of the fiber degrade its quality [66; pp. 20-25].

1.3. Features of the technology of cleaning raw cotton from large debris

Existing designs of cotton cleaners for removing large impurities from raw cotton consist of two main parts, a working element in the form of a rotating

serrated drum and a knockout device for knocking out large impurities in the form of grates. The use of fixed grates of round cross-section in the cleaner facilitates the separation of large impurities (see Fig. 1.19). At the same time, the main disadvantage of these grate grates with grate arrangement with gaps is the large loss of cotton flies into waste, which requires the mandatory use of a regeneration section in the flow line for cotton processing [79].

In work [80] it was established that when using triangular grates with an angle of 157° to the radius of the saw-tooth drum and a gap between the grates equal to 40 mm, the cleaning effect of the machine increases significantly.

In the cleaners CHX-3 and CHX-3M, trapezoidal grates with edge sizes of 25, 16, 12 and 10 mm were used. It was found that triangular and trapezoidal grates contribute to significant seed damage. The grates have the same working edge sizes as in triangular grates. The main advantages of grates with a flat working edge (triangular, trapezoidal) are the increase in the force of impact interaction with cotton. This leads to an increase in the cleaning effect of raw cotton. The disadvantage of these grates is an increase in the formation of free fiber, as well as some damage to the fiber and cotton seeds.

Trapezoidal grates were also used in the cleaning section under the serrated drum of the OXP-3 cleaner (Fig. 1.21). When using trapezoidal grates in the CHX-3M cleaners, their working edge was made 12 mm in size. Research has shown that this design was ineffective. Round grates are inferior to grates with a flat working edge in terms of impact force, which allows for intensive separation of impurities and leads to a decrease in the amount of free fibers [81]. It is known that in the OH-2 cleaners, CHX-3M2 "Mehnat", the UXK unit, and in the RH cleaner-regenerator, grates of a round profile are used. Fig. 1.19 shows the cleaning section of the CHX-3M2, "Mehnat" cleaners and the UXK unit. In our opinion, round grates without additional design solutions do not improve the cleaning effect. One of the ways to achieve this is to increase the degree of mobility of round grates.

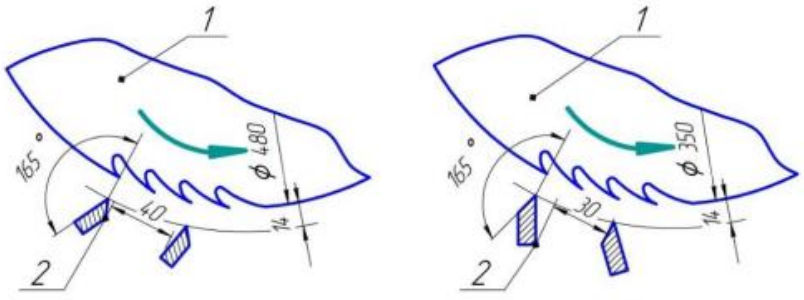

a) *b)*

1-saw-tooth drum, 2-trapezoid grates.

Fig. 1.19. a) Working area of the cleaner CHX-3M2 with trapezoidal grates,
b) Working area of the cleaner OXP-3 with trapezoidal grates

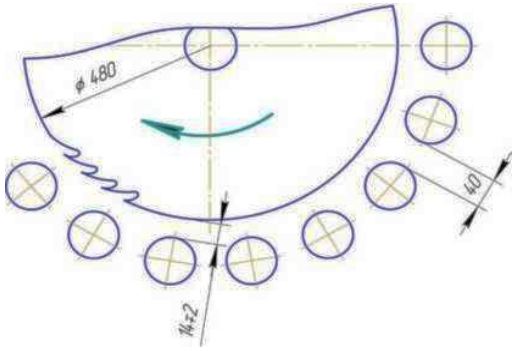

Fig. 1.20. Working area of the UXK cleaner with round grates

Recently, cotton ginning units UXK have been widely used in production [70]. The UXK unit includes successive sections for cleaning raw cotton from small and large debris. Fig. 1.20 shows the basic diagram of the UXK cotton ginning unit, which includes three sections for cleaning cotton from large debris. All three of these sections have two saw-tooth drums 4 and grate bars 5 underneath them. The grate bars have a round cross-section with an outer diameter of 20 mm. It should be noted that with an increase in the cleaning efficiency of each section, it is possible to reduce the number of sections, and thereby the frequency of cotton cleaning [82]. The lower the frequency of cleaning, the less damage to the fiber and seeds.

As noted in the work [83], E.F. Budin et al. proposed elastic grates (Fig. 1.22), which consist of a cylindrical rod with a diameter of 18 mm and a rubber tube mounted on it. During the operation of the cleaner, the grates with a rubber coating cushion the impact of the cotton flies on the grates, which reduces mechanical damage to the seeds and the waste of flies. At the same time, the rubber shell leads to a decrease in the impact impulse. In addition, the rubber coating slows down the pulling of cotton due to increased friction between the cotton and the grates. Therefore, grates with an elastic coating are inactive and have not found application in production. The design of the grate (Fig. 1.23) with grates with ribs on the cylindrical surface has also not found application [84], which leads to damage to the fiber and seeds, the amount of free fiber increases.

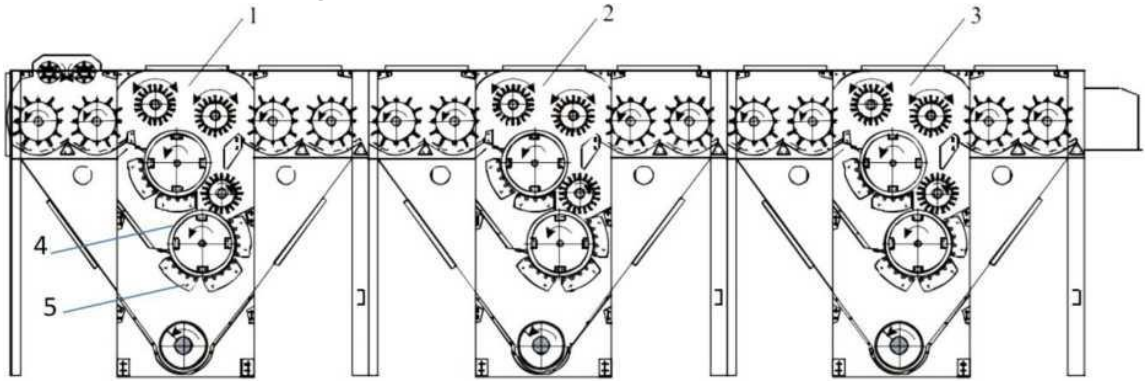

1,2,3-sections for coarse cotton cleaning, 4-saw drum, 5-bar grate with round grates.

Fig.1.21. Scheme of the cotton ginning unit UXK

1-round rod; 2-rubber tube.

Fig.1.22. Round grate with rubber with a nozzle

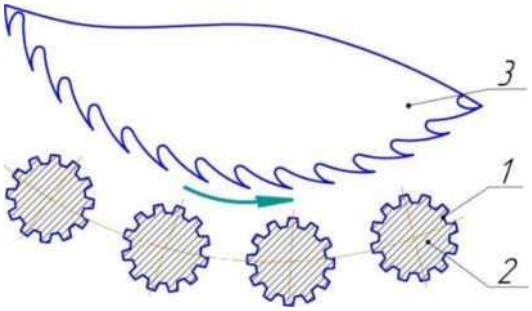

Fig.1.23. Grate of the fibrous material cleaner
with grooved grates 1-grate; 2-riffles (straight); 3-serrated drum

A more efficient design is the grate of the raw cotton cleaner [85], the diagram of which is shown in Fig. 1.24. When the material interacts with the bushings 3, the latter rotate on the rods 2, performing complex movements: oscillatory and rotary - oscillatory due to the free fit of the bushings on the rods with the formation of a gap between them of no more than 0,1-0,15 of the outer diameter of the bushing. With such a complex movement of the bushings 3, additional shaking of the cotton occurs, facilitating better separation of impurities from it.

In the grate [86] the grates are mounted on the side segments by means of elastic supports (see Fig. 1.24). When raw cotton is pulled through, the latter interacts with the grates and imparts an oscillatory motion to them, which facilitates additional shaking of the cotton filaments and the release of impurities.

However, the disadvantage of this design is the limited amplitude and frequency of the grate oscillations, which depend on the characteristics of the rubber bushing.

In [61], a grate for cleaning coarse debris is proposed, where three-sided grates with a circumferential circle diameter of 20 mm, having forced rotation, are installed under a saw-tooth drum. The advantage of a grate with three-sided rotating grates (see Fig. 1.25) is that they allow better separation of debris due to their edges, and somewhat increase the cleaning effect. When the depressions of adjacent three-sided grates coincide, the gap between the grates actually increases, which leads to the loss of raw cotton flakes through them. In addition, in three-

sided grates, a significant number of flakes can fall out into waste, and damage to the fiber and cotton seeds increases.

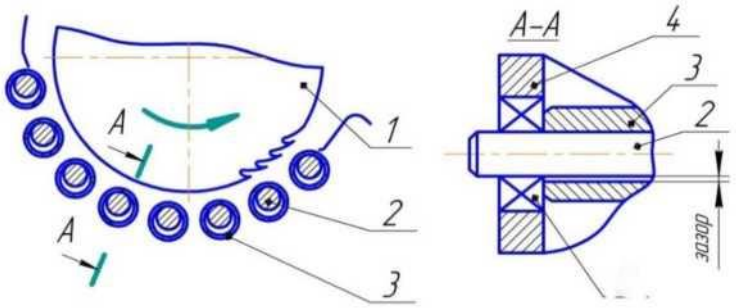

1-saw drum; 2-rod; 3-bushings (grate bars), 4-segment stand, 5-rolling bearings.
Fig. 1.24. Grate with composite grates made of a bushing installed with a gap on the grate rod

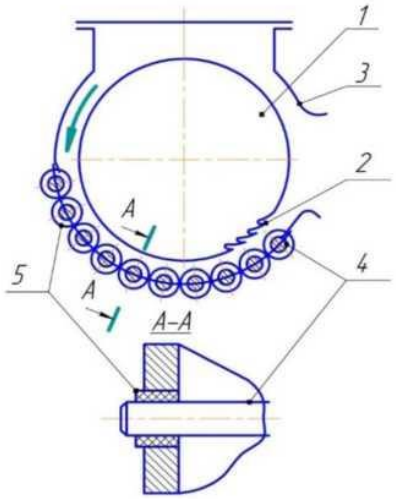

1-working drum, 2-pin, 3-housing, 4-grate, 5-sleeve.
Fig.1.25. Grate bars on elastic supports

In the grate, where between adjacent round grates are installed grates of a multifaceted shape [82], which also have forced rotation (Fig. 1.26). During the operation of the cleaner, the grates with forced rotation shake the cotton to some extent, due to which some additional effect of cleaning the cotton appears. But in this design, there is also a loss of flies into waste and to some extent the mechanical damage of the fiber and seeds increases. Fig. 1.27 shows a cleaner of raw cotton from large foreign impurities. The cleaner works as follows. Raw cotton enters the bin 1, passes through the feed rollers 2, is captured by the serrated drum 4 and fixed by the lapping brush 3. In this case, the raw cotton filaments fixed in this way on the teeth of the serrated drum hit the grate surfaces, due to which some of the impurities are removed and released into the tray 7. The raw cotton filaments captured by the serrated drum hit the first grate harder and bounce back to the surface of the serrated drum. At this moment, additional engagement of the uncaptured fibers by the teeth of the serrated drum occurs. The length of the

connection between the saws and the raw cotton decreases. In this case, the filament hits the nearest second grate. Due to the reduction in the length of the bundles, the fly center moves toward the center and, due to the reduction in the gap between the saw drum and the grate, it is close to the center of the grate, due to which the impact force increases and the cleaning effect is enhanced. The process is repeated in the second and third groups of grates.

When grates of different diameters are installed with constant gaps between us and the saw cylinder, as well as an invariable gap between the grates, the necessary condition for loosening and cleaning the fibrous material is ensured [86]. The cleaning effect is increased by successive impacts of the fibrous material (cotton) on grates of different diameters (due to different cylindrical surfaces, the impact impulse will also be different). In this case, the radius of the grate installation relative to the axis of rotation of the cylinder and the step between them will be different, which correspond to the values of the corresponding grate diameters. Disadvantage is big care flyers to waste.

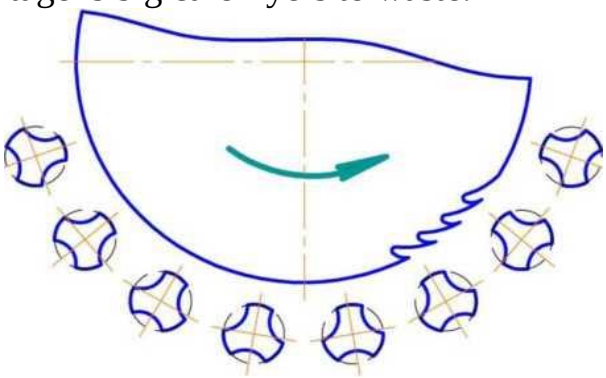

Fig.1.26. Raw cotton cleaner grate with rotating triangular grates

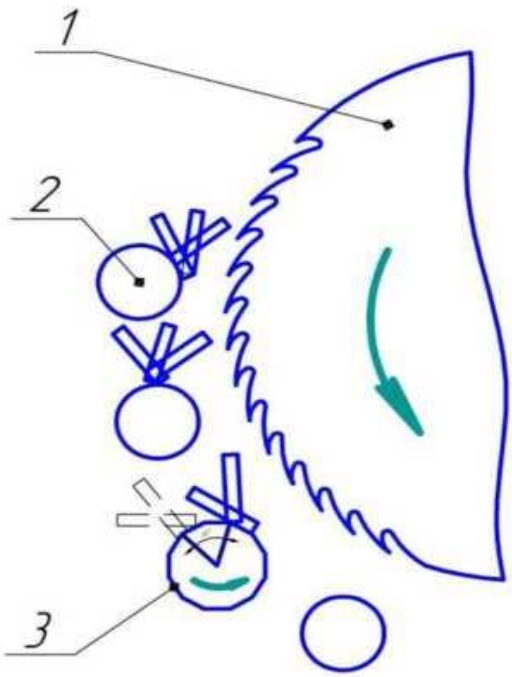

1-saw-tooth drum; 2-round fixed grates;
3-rotating multi-faceted grate.
Fig.1.27. Raw cotton cleaner grate with rotating multifaceted grates

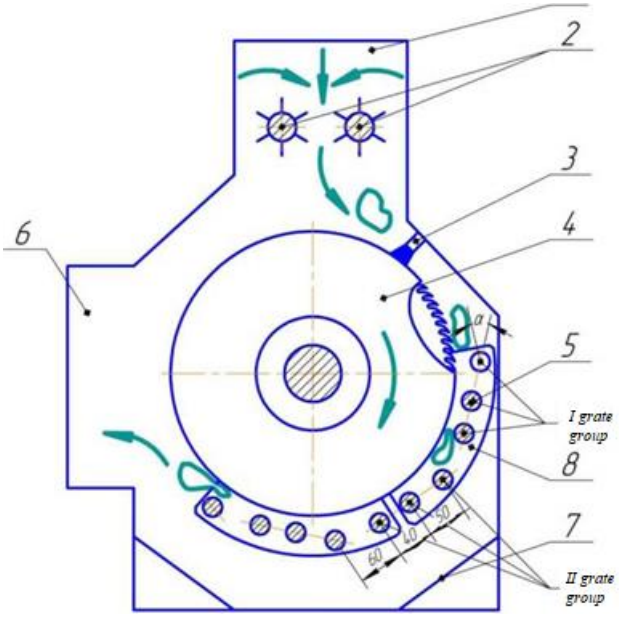

Fig.1.28. Cleaner for removing large impurities from raw cotton

1.4. Conclusions on Chapter 1

1. An analysis of work on cotton separation technology has revealed its main shortcomings, such as increased crushing of seeds, separation of fibers and their disposal as waste, and unstable removal of fibers, which leads to their damage.
2. It has been established that the considered designs of cotton separators and their operating modes do not ensure the preservation of the natural properties of raw cotton.
3. An analysis of the processes of cleaning cotton from small debris made it possible to establish the main directions in which their improvement took place, and the main directions of technology development were identified, which consist in the need to avoid regular movement of the processed material.
4. It has been established that the vibration effect on the processed material is not fully utilized, and its use represents a reserve for increasing the efficiency of cleaning equipment.

In the process of cleaning cotton from large debris, the reserve for increasing efficiency lies in the use of grate vibration to intensify the impact on the processed material.

CHAPTER 2. DEVELOPMENT OF AN EFFICIENT DESIGN OF THE SEPARATION AND CLEANING SECTION OF A FLOW LINE FOR CLEANING RAW COTTON

The flow line for cleaning raw cotton in cotton mills and cluster productions includes a raw cotton separator, 1XK, UXK cleaners. The main disadvantage of the existing designs is: uneven distribution of raw cotton, both in the direction of movement and across the width of the working bodies, low effect of cleaning cotton from large and small foreign impurities, incompatibility of the separator with the cotton cleaners in terms of their productivity, etc. Therefore, in order to eliminate the above disadvantages, increase the cleaning effect, uniformity of the processes of separating cotton from air and cleaning, ensuring their compatibility in productivity, a design scheme of the separation and cleaning section of the flow line for cleaning cotton was developed. In addition, to further increase the effect of separation and cleaning of raw cotton, a number of effective and resource-saving designs of individual working bodies of separators and cotton cleaners were developed, which together provide a high effect of separating air from cotton and cleaning it from large and small foreign impurities.

2.1. Improving the technology in the separation and cleaning section of the cotton cleaning flow line

As noted above [6, 22], the known separation and cleaning section of the cleaning shop includes the CC-15A separator, SHX-screws and two parallel-mounted cleaning units of the UXK. The main disadvantage of the separation and cleaning section of the cleaning shop is the uneven feed of raw cotton by the separator along its working length and the uneven distribution of raw cotton among the cleaning units of the UXK due to the sequential distribution of cotton, as well as the low effect of cleaning cotton from small and large debris due to the imperfection of the working parts of the cleaning unit of the UXK. (Table 2.1) [88. 233-234 pp]

In addition, the design cannot be used in cluster production, where a single flow cleaning line with a capacity of (7÷8) t/h is appropriate.

It should be noted that the cotton cleaning unit UXK consists of successively installed cleaning zones from small and large debris, while the cleaning zone from small debris includes feed rollers and successively installed pin drums and mesh surfaces under them. Cleaning zones from large debris include two saw cylinders and grates under them. In this case, small and large debris fall into one screw conveyor. The main disadvantage of the cleaner is the low cleaning effect of cotton due to the imperfection of the working parts [89].

Table 2.1

Cleansing effect UXK unit

difficult purified by C4880, 149-F, in grades I and II , with an initial moisture content of 8-9% at productivity no more than 7000 kg/h	75-80
in grades III and IV , with an initial moisture content of 9-10% productivity no more than 5000 kg/h	75-80

From the above analysis it can be noted that the existing separator is a chamber divided by a mesh partition into two parts: cotton and air. In the cotton part there is a guide and a scraper, which cleans the raw cotton from the mesh located on the sides, and directs it to the vacuum valve. The vacuum valve is designed to unload the raw cotton from the separator chamber and create a seal that prevents outside air from being sucked into the separator chamber through the discharge opening. The air part of the chamber is limited by a mesh surface on the sides. The raw cotton fed to the separator by the air flow through the branch pipe hits the wall of the working chamber. In this case, the speed of the air flow in the separator drops sharply, and the main part of the raw cotton falls into the vacuum valve, and a certain part reaches the mesh surface and is dumped by the scraper into the vacuum valve. A significant disadvantage of this separator is that during the removal of raw cotton by scrapers, the fiber, pressed by the air flow to the mesh surface, and the seeds are damaged. In addition, the useful area of the mesh surface is limited, which makes it difficult to completely remove part of the cotton [90].

We have proposed a design for a separator for raw cotton, containing a separation chamber with perforated nets in the end walls, the openings of which are made cylindrical at an angle of 45°-60° to the plane of the net. Pipes for the input and output of raw cotton, a vacuum valve, scrapers with elastic blades adjacent to the disks, mounted on a drive shaft [91].

In order to ensure continuity and uniformity of separation of cotton from air in the separator along its length, increase the cleaning effect, ensure the compatibility of the separator and cotton cleaner, allowing use in cluster production with a single flow line for cleaning cotton, we have improved the design, layout and compatibility of separators and cotton cleaner, and the designs of the cleaner elements.

The essence of the design is that the separation and cleaning section of the cleaning shop consists of a separator combined with one cotton cleaner and

includes a separation chamber with inlet and outlet pipes, a perforated end screen with a scraper installed at the end of the chamber, a vacuum valve with an impeller located in the lower part of the chamber, and a guide mounted at the inlet in the chamber, while at the inlet to the separation chamber an upper guide is mounted, oriented from the inlet to the vertical axis of the end screen, made composite, including a curvilinear main rigid plate, to which an outer plate is attached through a gasket having elastic deformation, and a lower guide. In this case, the mesh surfaces are made spherical with a radius of (1,25÷1,35)*R_{cy} (where R_{cy} is the inner radius of the cylindrical part of the chamber), and the clips with elastic blades are also made spherical with a radius equal to the radius of the mesh surface, the cotton cleaner combined with the separator consists of successively installed zones of fine and coarse cleaning, wherein the fine cleaning zone includes feed rollers and successively installed peg drums and mesh surfaces under them. Coarse cleaning zones include two saw cylinders and grates under them and trash collectors made separately for fine and coarse cleaning. The left feed roller is made with a diameter 1,2 times larger than the diameter of the right feed roller, the drum pegs are made multifaceted and in the form of a truncated cone. In the coarse cleaning zones, the gaps between the saw cylinders and the grates are selected to decrease as the cotton is pulled through, with this gap being 17 mm in the initial cleaning zone and 13 mm in the output zone. Chapter 5 shows that the design ensures effective separation of cotton from air, combined operation of the separator and cleaner, and also ensures an increase in the cleaning effect of cotton from small and large debris [91].

The design consists of a separator and a cotton cleaner (Fig. 2.1) The raw cotton separator consists of a separation chamber 2, on the ends of which mesh surfaces 3 are mounted, having a spherical shape with a radius R = (1,25-1,35)*R_{cy} (R_{cy} is the inner radius of the cylindrical part of the chamber). (Fig. 2.1 a and b) Scrapers 5 with elastic blades adjacent to the mesh surfaces 3 are mounted on a drive shaft 4, which are also made spherical with a radius R (see Fig. 2. 1.b). In the center of the chamber there is an inlet pipe 1, on the sides there are outlet pipes 6. A vacuum valve 7 is installed under chamber 2. A shaft 8 is installed at the bottom of the separator and then feed rollers 9.

The cotton cleaner includes a small debris cleaning zone 10 and a large debris cleaning zone 11 installed in a housing 12. In the small debris cleaning zone 10, pin drums 13 are installed and under them a mesh surface 14 and a trash collector 15 for small debris. The large debris cleaning zone 11 includes brush drums 16, saw drums 17, a grate 18 under them, a removable brush drum 19, and at the bottom a screw conveyor 20 for removing large debris.

The feed rollers 9 are made with different external diameters, where d_1 = 1,2

d_2 (see Fig. 2.1.c). The pins 21 of the drum 13 are made in the form of a truncated body (see Fig. 2.1.d). In the large cotton cleaning zone, the gaps between the grate bars 18 and the saw cylinder 17 are made decreasing, wherein Δ_{in} - Δ_{out} =17-13=4 mm (minimum seed size), Δ_{in} is the gap between the saw cylinder 17 and the grate bar 18 in the initial cotton pulling zone, Δ_{out} is the gap in the output part [92].

The separation and cleaning section of the cleaning shop operates as follows. Raw cotton enters the separator through the inlet pipe 1. With the help of the upper and lower guides 4 with a curved working surface, raw cotton and air are directed to the zone of enhanced hovering of raw cotton, i.e. to the central section of the mesh surface 3. In this case, mechanical effects on cotton are significantly reduced. In addition, the lower guide 4 additionally prevents cotton from falling into the gap between the wall of the housing and the mesh surface 3. Guide 4 ensures continuous and uniform distribution of cotton and separation of air from it.

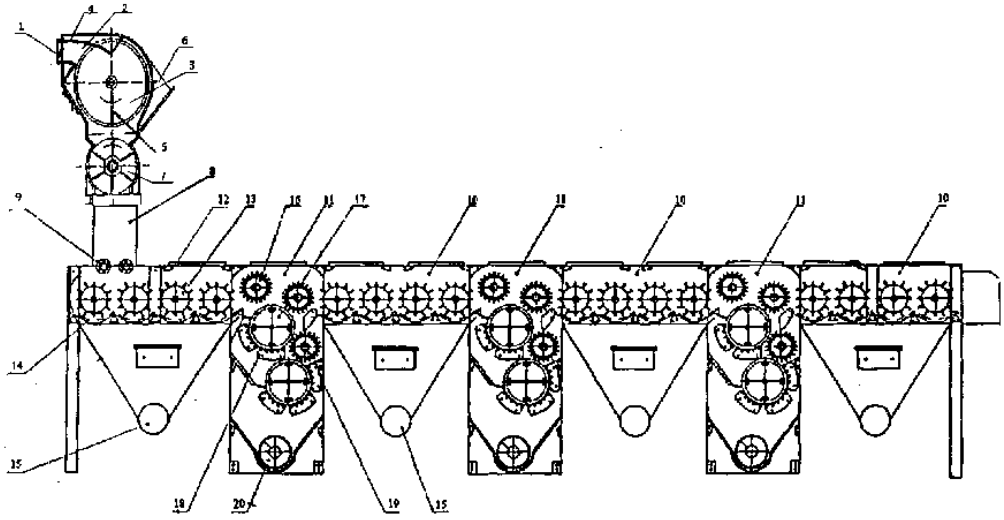

a)

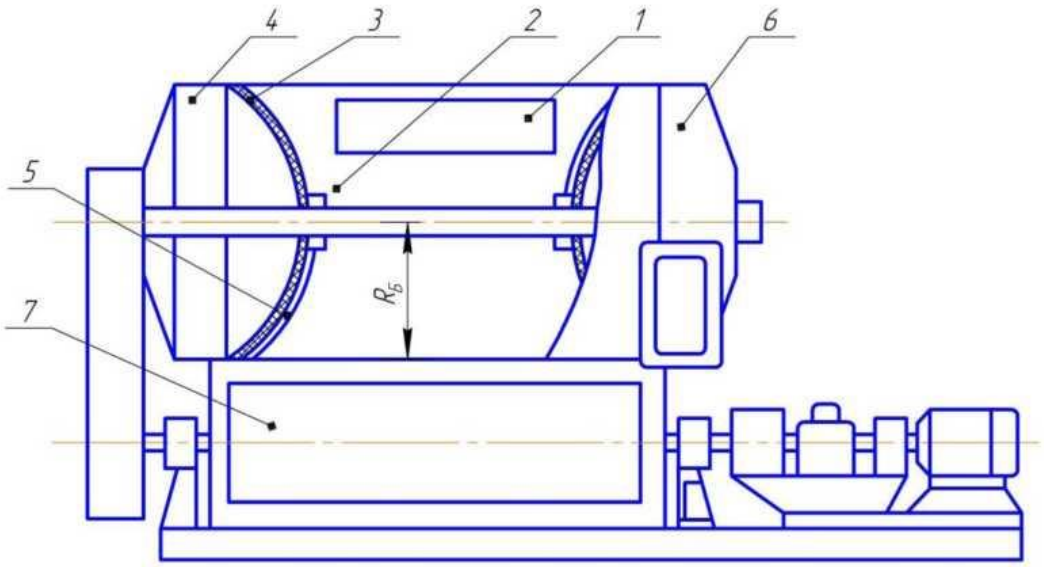

b)

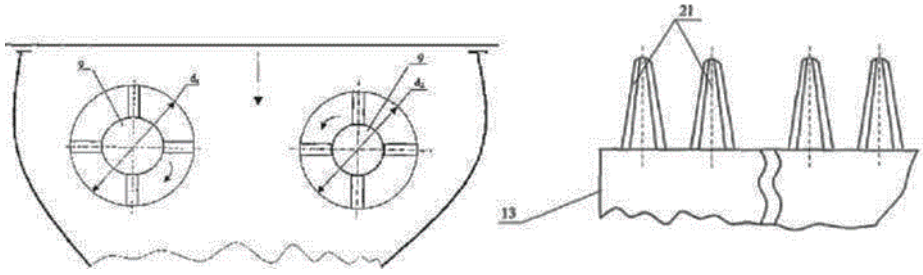

c) d)

a-general diagram; b-separator diagram; c-feed roller diagram; d-drum pin diagram.

Fig.2.1. Separation and cleaning section of the cleaning shop, distribution of cotton and separation of air from it.

In this case, the air is sucked out by the pneumatic system through the mesh surfaces 3 and is carried out of the separator from the outlet pipe 6. The raw cotton hits the mesh, the air flow speed drops sharply, and the bulk of the raw cotton falls into the vacuum valve 7, and some settles on the surfaces of the mesh surfaces 3. It should be noted that due to the implementation of mesh surfaces 3 as spherical with a radius $R=(1,25\text{-}1,35)*R_{cy}$, the working surfaces of meshes 3 are increased. This allows air to be sucked out through meshes 3 without braking. The rotating shaft 4 sets in motion the clips 5, which, moving the cotton bats settled on the spherical mesh surfaces 3, direct them into the vacuum valve 7. In this case, due to the spherical shape of the mesh surfaces 3, the amount of raw cotton settled on them will be evenly distributed and therefore their removal from the holes of the mesh 3 will be easy. In this case, as shown in Chapter 5, the damage to the raw cotton fibers is significantly reduced and the reliability of the separator operation will increase. Then from the vacuum valve 7 through the shaft 8 the cotton goes to the feed rollers 9. To eliminate the faces in the feed zone the left feed roller 9 rotates with a higher linear speed of its blades relative to the linear speed of the blades of the right feed roller 9. In the zone of cleaning cotton from small debris, the conical multifaceted choppers 21 of the drums 13 capture the cotton, dragging it along the mesh surface 14, loosening it. In this case, small debris is removed by the trash collector 15 separately from the cereal debris. In the cotton cleaning zone from large debris, brush drums 16 transport cotton, which falls onto saw cylinders 17. The teeth of saw cylinders 17, capturing cotton volatiles, drag them along the grate bars 18. In the initial cleaning zone, the cotton will be less loosened and therefore the gap between saw cylinder 13 and the grate bar 18 is chosen to be larger δ_{in} = 17 mm, and in the output zone δ_{out} = 14 mm. This is provided effective

selection weeds impurities.

The design ensures efficient separation of cotton from air, combined operation of the separator and cleaner, as well as an increase in the cleaning effect of cotton from small and large debris and the use of the recommended design in cluster production.

At the same time, for the considered section of separation and cleaning of cotton, a number of efficient and resource-saving designs of working parts of separators and cleaners of cotton, mainly from large debris, were developed.

2.2. Separator with curved cotton guides in the inlet part of the chamber

In order to maximally preserve the natural qualities of the manufactured products, eliminate the impact of raw cotton on the back wall and exceptionally extend its service life, the design was improved with the necessary geometric parameters of the separator guides, allowing for a minimal reduction in cotton damage and an increase in the reliability of the separator [92].

The essence of the design is that the separator contains a separation chamber, at the end of which a mesh surface with scrapers is located, in the lower part of the chamber a vacuum valve with an impeller is located, while in the separator chamber at the outlet there are guides made of metal sheets, the working parts of the upper and lower ones are made curvilinear, in the form of a part of a cylinder with a radius $R_H = 1.25\ R_c$ (where R_c is the radius of the mesh surface), and the working surface of the upper guide is located up to the vertical axis of the mesh surface. The working surface of the lower guide is made shortened, and forms a gap with the mesh surface of no more than (10 ÷ 15) mm. The guides are rigidly installed in the separator body (Fig. 2.2).

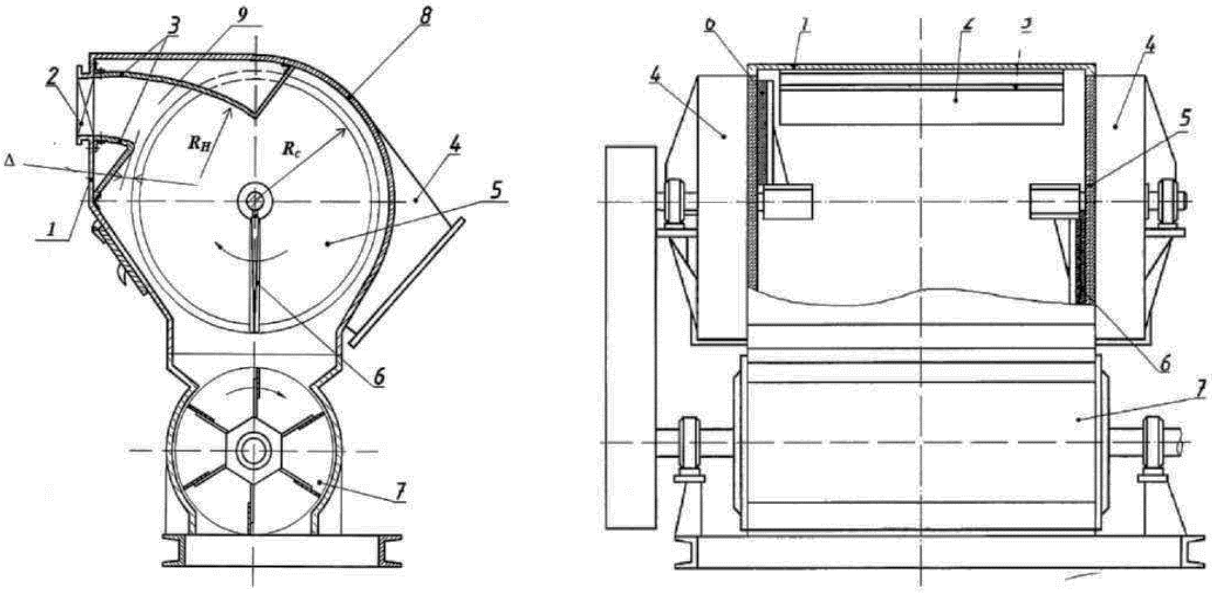

a) b)

a-general diagram of the developed separator; b-cross sections of the separator.

Fig. 2.2. Raw cotton separator.

The raw cotton separator consists of a body 1 (Fig. 2.2), an inlet pipe 2, upper and lower guides 3, an outlet pipe 4, a mesh surface 5, a scraper 6 and a vacuum valve 7.

For suction of air from the air chamber 9, perforated walls 5 are installed in the ends. For cleaning individual cotton bats adhering to the perforated nets 5, there are scrapers 6 installed on the shaft. For removal of raw cotton from the separator, there is a vacuum valve 7 with an impeller installed on the shaft. Rotation of the scraper shaft is carried out by a V-belt transmission from the vacuum valve 7. The working surface of the upper guide 3 is made curved with a radius $R_H = 1{,}25R_c$ (where R_c is the radius of the mesh surface), the length of the working surface 5 of the upper guide 3 reaches the vertical axis of the mesh surface 5. The working surface of the lower guide 3 is also curved, with a radius R_H and makes a gap with the mesh surface 5 within (10÷15) mm.

The separator operates as follows.

Raw cotton enters the separator through the inlet pipe 2. With the help of the upper and lower guides 3 with a curved working surface, raw cotton and air are directed in the zone of increased hovering of raw cotton, i.e. in the central section of the mesh surface 5, and not on the rear wall 8 of the separator housing 1. In this case, mechanical effects on cotton are significantly minimized. In addition, the lower guide 3 additionally prevents cotton from falling into the gap between the wall of the housing 1 and the mesh surface 5. Air is sucked out through the air chamber 9 and discharged through the outlet pipe 4. To clean the separated cotton voles that have stuck to the perforated meshes 5, scrapers 6 dump them into the vacuum valve 7.

The proposed raw cotton separator allows for maximum preservation of the natural qualities of manufactured products and significantly extends their service life.

2.3. Raw cotton separator with composite elastic guide

The design of the separator has been improved, allowing for small vibrations of the guide, reducing damage to cotton and increasing the reliability of the separator (Fig. 2.3).

The essence of the design is that the separator contains a separation chamber, at the end of which a mesh surface with scrapers is located, a vacuum valve with an impeller is located in the lower part of the chamber, while in the separator chamber at the outlet there are guides made of metal sheets, the working parts of the upper and lower are made curvilinear, in the form of a part of a

cylinder with a radius $R_H = 1.25 \cdot R_C$ (where R_C is the radius of the mesh surface), and the working surface of the upper guide is located up to the vertical axis of the mesh surface. The working surface of the lower guide is made shortened and forms a gap with the mesh surface of no more than (10 ÷ 15) mm. The guides are rigidly installed in the separator body. Moreover, the upper guide is made composite from the outer part of the plate made of plastic, which is attached to the main plate by means of a rubber gasket, the thickness of which increases from the outlet part to the axis of the mesh surface. The main plate is rigidly installed in the separator body. The plates and the rubber gasket are connected to each other with a special glue. At the same time, due to the small nonlinear vibrations of the plastic plate, the interaction with the cotton will be soft, and damage to the seeds will be reduced [93].

Raw cotton enters the separator through the inlet pipe 2. With the help of the upper and lower guides 3 with a curved working surface, raw cotton and air are directed in the zone of increased whirling of raw cotton, that is, in the central section of the mesh surface 5, and not to the rear wall 8 of the separator body 1.

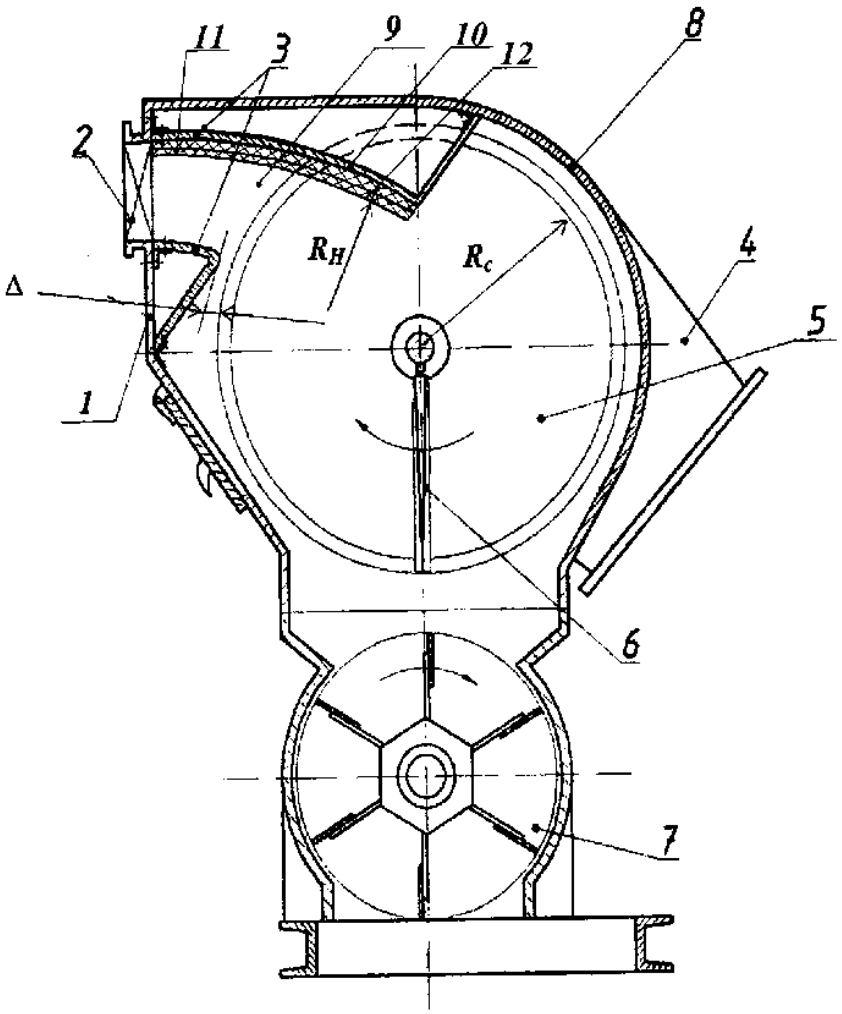

Fig.2.3. Separator with a composite guide with an elastic shock absorber.

In this case, mechanical impacts on cotton are significantly reduced. Air is sucked out through air chamber 9 and discharged through outlet pipe 4. To clean separated cotton bats adhering to perforated nets 5, scrapers 6 dump them into vacuum valve 7. In this case, nonlinear angular oscillations of outer plastic plate 11 occur. Cotton movement is cushioned, and the main part of cotton falls into vacuum valve 7. In this case, cotton damage is significantly reduced. In addition, hard impact interactions of cotton with rear wall 8 of separator housing 1 are virtually eliminated. The reliability of separator operation is increased.

2.4. Cotton separator with improved perforated disc design

In order to reduce damage to cotton fibers during the interaction of scrapers with perforated disks, the separator design was improved to reduce the friction force between cotton fibers and the surfaces of the holes of the perforated disks (nets) (Fig. 2.4). The raw cotton separator consists of a housing 1 with inlet 2 and outlet pipes and a vacuum valve 4 installed in the lower part of the housing 1. A cylindrical chamber 5 is located in the housing 1, along the ends of which perforated nets (disks) 6 are fixed (Fig. 2.4).

To clean individual cotton filaments that have adhered to the perforated meshes 6, there are scrapers 7 mounted on the shaft 8. In this case, the openings 9 of the perforated mesh 6 are made conical with a curved surface, the ratio of the diameters of the main openings 9 is selected $d_2=(1{,}15 \div 1{,}255)\ d_1$ (where d_1 is the diameter of the small base, d_2 is the diameter of the large base of the conical openings) [94].

The separator for raw cotton operates as follows. Cotton is fed by an air flow through the inlet pipe 2 into the separating cylindrical chamber 5 of the separator. In this case, the air is sucked out by the pneumatic system through the perforated mesh 6 and is removed from the separator from the outlet pipe 3. The raw cotton hits the mesh 6, the air flow speed decreases sharply, and the main mass of the raw cotton falls into the vacuum valve 4, and some settles on the surfaces of the perforated mesh 6. It should be noted that, due to the conical design of the holes 9 of the mesh 6, the force holding the cotton fibers on the surface of the mesh 6 is significantly reduced. Therefore, the portion of the cotton mass settling on the surface of the mesh 6 is reduced.

The uniformly rotating shaft 8 sets in motion the scrapers 7, which, moving the cotton flakes settled on the surfaces of the perforated nets, direct them into the vacuum valve 4. In this case, due to the conical openings 9, the main mass of the flake fibers will mainly be located on the side of the large base of the openings 9, and therefore their pulling out of the openings 9 by the scrapers 7 will be with less force. The curvilinearity of the surface of the openings 9 allows for a reduction in

the friction force between the cotton flake fibers and these surfaces due to the coincidence of the generatrices of the openings 9 with the direction of the shear force of the scrapers 7. In this case, the damage to the raw cotton fibers is significantly reduced.

2.5. Separator with a spherical mesh surface of the separating chamber

To ensure maximum preservation of the natural properties of raw cotton, the design of the raw cotton separator has been improved by increasing the useful area of the mesh surface [94].

The essence of the design is that the raw cotton separator contains a separation chamber with mesh surfaces in the end walls, pipes for the input and output of raw cotton, a vacuum valve, clips with elastic blades adjacent to the mesh surface, mounted on a drive shaft, wherein the mesh surfaces are made spherical with a radius of (1.25÷1.35) R_{cy} (where R_{cy} is the inner radius of the cylindrical part of the chamber), and the clips with elastic blades are also made spherical with a radius equal to the radius of the mesh surface.

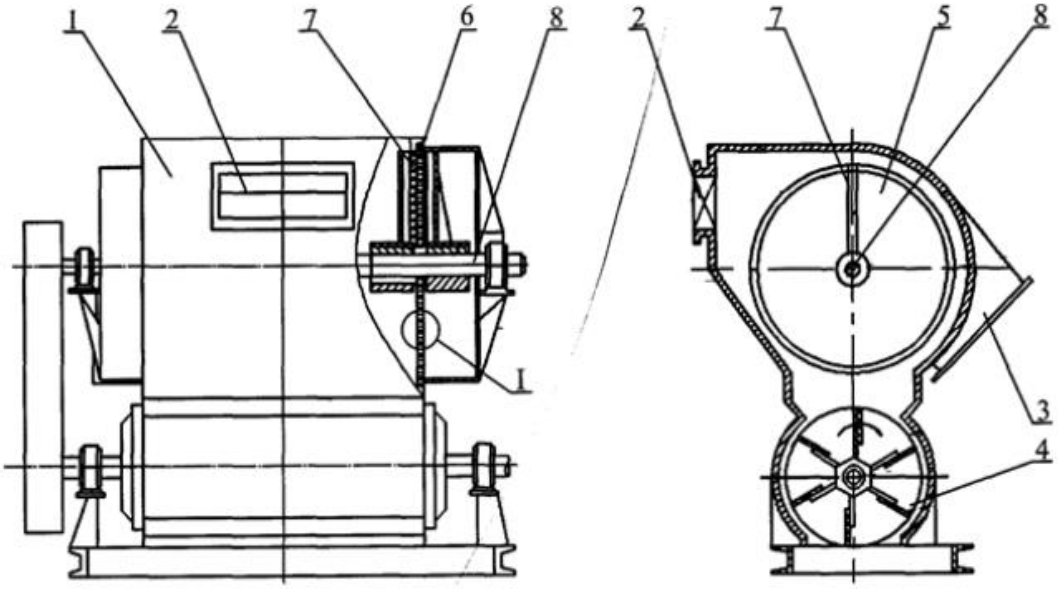

a) b)

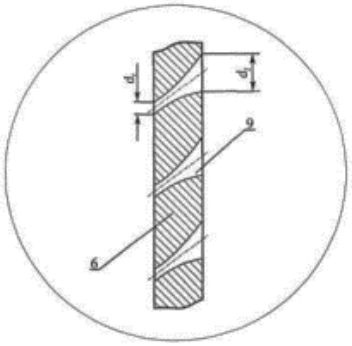

c)

a-general diagram of the separator; b-cross-section of the separator;
c-perforated disc (part).
Fig. 2.4. Raw cotton separator.

The raw cotton separator operates as follows (see Fig. 2.5). Raw cotton is fed by the air flow through the inlet pipe 1 into the separator's separation chamber 2. In this case, the air is sucked out by the pneumatic system through the mesh surfaces 3 and is carried out of the separator from the outlet pipe 6. The cotton hits the meshes 3, the air flow velocity sharply increases, and the main mass of raw cotton falls into the vacuum valve 7, and some settles on the mesh surfaces 3. It should be noted that due to the mesh surfaces 3 being made spherical with a radius R = (1,25-1,35) $R_{cy,}$ the working surfaces of the meshes 3 are increased. This allows air to be sucked out through the meshes 3 without braking.

The uniformly rotating shaft 4 sets in motion the clips 5, which, moving the cotton bats settled on the spherical mesh surfaces 3, direct them into the vacuum valve. In this case, due to the spherical shape of the mesh surfaces 3, the amount of raw cotton settled on them will be uniformly distributed, and therefore their removal from the holes of the mesh 3 will be easy. In this case, the damage to the raw cotton fibers is significantly reduced and the reliability of the separator operation is increased [94].

2.6. Improving the technology of cleaning cotton from small debris

In the technology of cleaning raw cotton from small debris in the cleaning zone, mainly pin drums and mesh surfaces are used.

In order to improve the technology of cleaning cotton from small debris, effective designs of mesh surfaces have been developed [66; pp. 29-31, 95].

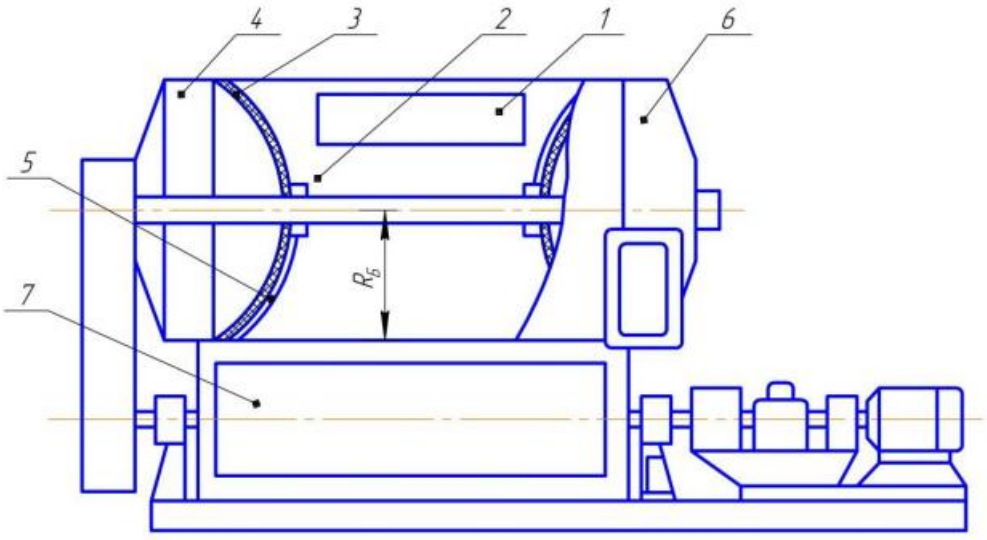

Fig. 2.5. Scheme of a separator with a spherical shape of the mesh surface of the

chamber

In order to increase the effect of shaking the cotton bats over the mesh surface due to their vibrations, a design of a fibrous material cleaner mesh has been proposed [95; pp. 267-270]. In this design, the mesh, rigidly installed in the arcuate sidewalls, is made with rows of holes, part of the crossbars of each row of holes are made protruding, having either a spherical or a broken curve. In this case, the mesh with the recommended crossbars forms a peculiar wavy (there are protrusions and depressions) surface. A disadvantage of the known design is the significant slowdown of the cotton bats on the mesh surface due to the cyclically changing heights of the crossbars between the holes. This significantly increases the damage to the cotton fibers, and also reduces the productivity of the machine.

In a device for drying and cleaning raw cotton [96], containing a vertical chamber with feed units located along the height of the chamber in a checkerboard pattern, perforated (with holes) and solid surfaces, wherein each solid surface of the walls is combined with the wall of the corresponding branch pipe for feeding the heat agent and is made of two different-sized mutually perpendicular sections, the smaller of which is located in the plane adjacent to the perforated surface, wherein the nozzles of the branches are located on the smaller section. In addition, the angle of inclination of the perforated surfaces to the horizon is $50\text{-}55^0$, wherein large sections of the solid surfaces of the walls are connected to subsequent perforated surfaces by vertical shields, with the formation of a zigzag channel for the fiber. The disadvantage of this design is the low effect of cotton cleaning due to the lack of forced mechanical pulling along the zigzag-arranged mesh surface. This design is primarily intended for drying cotton.

In another known design [97], the mesh surface, made of stamped sheet steel with holes, bent along an arc of a circle at four corners (edges), has steel bushings welded to it, into the holes of which pins enter, rigidly connected to the body of the cleaner, and elastic (rubber) bushings are installed between the pins and bushings. As a result, when the fibrous material interacts with the surface of the mesh, oscillations (vibrations) of the mesh occur due to the deformation of the elastic bushings. In this case, the first two elastic bushings, installed in the left corners of the mesh, have a greater thickness relative to the thickness of the two elastic bushings installed in the right corners of the mesh. This ensures the greatest amplitude oscillations of the mesh at the beginning of the interaction of the pulled fiber with the pin drum of the cleaner [98]. The disadvantage of this design is insufficient contact and monotonous movements of the cotton fly being pulled along the surfaces of the bridges between the mesh openings, as well as insufficient pulsed interaction of the cotton fly with the mesh surface and

insufficient braking when pulled along the arc of the inner cylindrical surface of the mesh, which do not allow a significant cotton cleaning effect to be achieved.

A significant increase in the cleaning effect of fibrous material (cotton) from small debris of the debris-collecting mesh of the fibrous material cleaner is achieved by improving the design of the mesh surface by providing a trajectory of movement of cotton bats in the area of its dragging along a broken line along the planes (faces) that make up the mesh surface. In this case, the directions of interaction of cotton bats with the planes of the multifaceted mesh surface will change cyclically. This leads to effective separation of small debris from cotton bats.

The mesh surface of the fibrous material cleaner consists of a trash net with holes (Fig. 2.6). The mesh surface is made in the form of a part of a polyhedral prism with ribs. The holes are made in rows on each face (plane), and between adjacent faces the holes are staggered. The trash net has rigidly connected bushings at the edges in four corners, into which pins enter, rigidly connected to the cleaner body. Elastic (rubber) bushings are installed between the bushing and the pins. A drum with pins is installed above the net in the body.

During operation, raw cotton is captured by the drum pins and pulled along the mesh surface. In this case, the cotton bats will move along the edges of the mesh surface, changing the trajectory of movement, undergoing cyclic interactions with the multifaceted mesh surface. This leads to the effective release of foreign impurities. The foreign impurities released in this case fall out through the holes. At the same time, due to the change in the total mass of cotton located on the mesh surface, some deformations of the elastic bushings occur. Considering that the mass of the raw cotton being pulled changes over time, the deformations of the bushings also change. This leads to vibrations of the mesh with a certain frequency and amplitude.

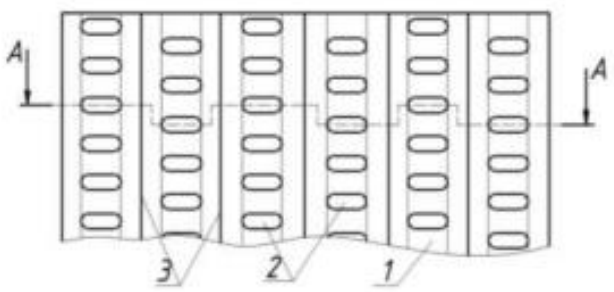

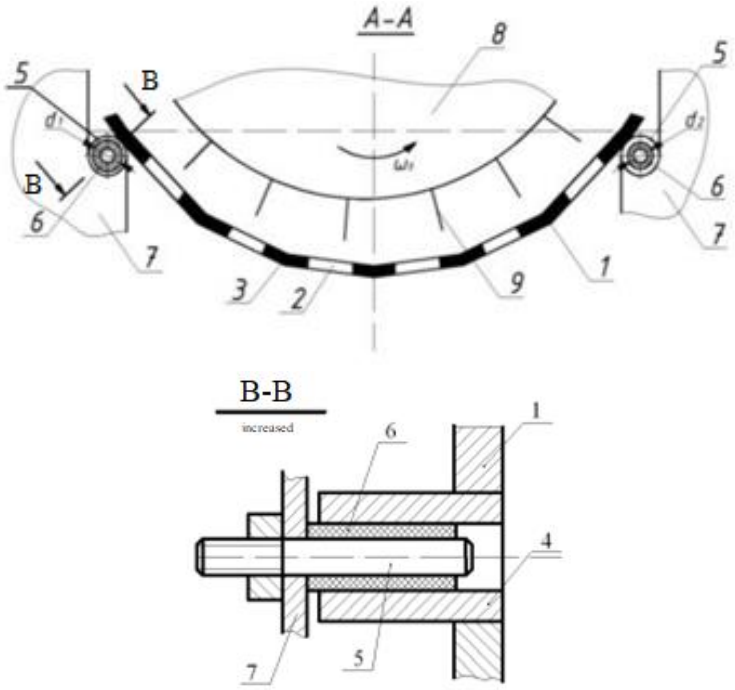

1-mesh surface; 2-holes; 3-prisms with ribs; 4-bushings; 5-finger; 6-rubber bushings; 7-cleaner body; 8-drum; 9-pegs.

Fig. 2.6. Mesh surface of the fibrous material cleaner

In this case, at the beginning of the raw cotton pulling zone, the mesh vibrations will occur with the greatest amplitude due to the larger diameter of the elastic bushings in this zone, and at the end of the raw cotton pulling zone, the mesh vibration amplitude will be the smallest. The frequency and amplitude of the mesh vibrations depend on the rigidity of the elastic bushings, the mass of the mesh, and the change in the mass of the cotton being pulled.

2.7. Improving the efficiency of cotton cleaner grates for removing large debris.

The main disadvantages of the considered grate cleaners for large debris are: low cleaning effect, complex designs, imperfect structural elements, multiple cleaning, insufficient justification of technological and design parameters and rotation modes of the saw-tooth drum.

In order to improve existing designs and increase the cleaning effect, we have developed a number of highly efficient grate designs that allow maximum preservation of the natural qualities of cotton and seeds [99, 100, 101].

In the design recommended by us, the composite grates are installed in the side segments by means of elastic bushings, the thickness of which is selected to decrease as the cotton is pulled through. In this case, the gaps between the grates are also selected to decrease as the cotton is pulled through, and the difference between adjacent gaps between the grates as the cotton is pulled through is

selected to be equal to the difference in the thickness of the elastic bushings between even and odd adjacent grates as the cotton is pulled through. In this case, at the end of the pulling zone, the cotton will be looser, and in order to reduce the loss of cotton fly ash along with the debris, the gaps between the grates will have smaller dimensions.

The design works as follows (Fig. 2.7). Saw cylinder 2 grabbing raw cotton with its teeth, it pulls it along the grates 2. In this case, the grates 2 oscillate due to the impact of the cotton flies on them and the deformations of the elastic bushings 3. The thickness of the elastic bushings 3 is chosen to decrease as the cotton is pulled through and have the following relationships:

$$\Delta_1 = r_1 - R;\ \Delta_2 = r_2 - R;\ \Delta_n = r_n - R;\ \Delta_1 > \Delta_1 > \Delta_n \qquad (2.1)$$

where R is the radii of the grate bars; r_1, r_2 r_n are the outer radii of the elastic bushings 3 of the corresponding grate bars 2; Δ_1, $\Delta_2 \ldots \Delta_n$ are the thickness of the elastic bushings 3 of the corresponding grate bars 2 .

In this case, at the beginning of the pulling zone, the raw cotton will be less loosened and therefore, due to the greater thickness of the elastic bushings 3, the grates 2 in this zone will oscillate with a greater amplitude and lower frequency, which allows not only the separation of foreign impurities, but also some loosening of the cotton. At the end of the cotton pulling zone, due to the smaller thickness of the elastic bushings 3, the grates 2 oscillate with a greater frequency and lower amplitude. This leads to the separation of foreign impurities located deeper in the fibrous mass (fly).

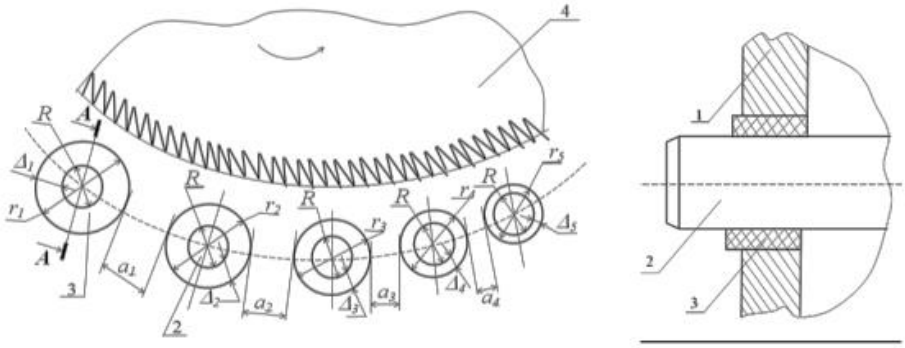

Fig.2.7. Grate of the fibrous material cleaner

The gaps between the bars are also selected to decrease as the cotton is pulled through, which have the following ratios:

$$a_1 - a_2 = \Delta_1 - \Delta_3;\ a_2 - a_3 = \Delta_2 - \Delta_4;\ a_3 - a_4 = \Delta_3 - \Delta_5;\ a_{n-1} - a_n = \Delta_{n-1} - \Delta_{n+1} \qquad (2.2)$$

where a_1, a_2, a_n, - the gaps between the grates 2 along the direction of cotton pulling.

In this case, the difference in the gaps between adjacent grates 2 along the

course of cotton pulling is selected according to (2.2) equal to the difference in the thicknesses of the elastic bushings 3, respectively, between even and odd adjacent grates 2. Along the course of pulling, the cotton will be more divided into strands, and, in order to reduce their falling out through the gaps between the grates 2, these gaps are made decreasing, according to expressions (2.2).

The recommended fibrous material grate allows for a significant increase in the cleaning effect and reduces the loss of cotton flies with the released debris.

The following grate for a fibrous material cleaner has been developed, containing multi-faceted grates with a different number of faces, which, in the course of pulling the fibrous material, are selected in such a way that each subsequent grate has one more face than the previous grate.

The grates are installed in the arc-shaped sidewalls by means of elastic rubber bushings. In the initial cleaning zone, the cotton is exposed to interaction with the grates with a smaller number of edges, ensuring gradual loosening of the cotton with the release of debris. At the end of the cotton pulling zone, due to the larger number of grate edges, the cotton is exposed to multi-frequency interactions with the grate edges in different directions. This also leads to the release of debris located deeper in the cotton.

The proposed design consists of grates 1, which are installed in elastic rubber bushings 3, in arched strips 4 and a rotating saw-tooth drum 2. The grates 1 are made multifaceted. In this case, each subsequent grate 1 has one more face than the previous one. The first grate is made tetrahedral, the second is pentahedral, the third grate, installed along the cotton pulling path, is made hexagonal, and so on. With a three-section grate, each section has five grates 1, then the last grate 1 will have 18 facets (Fig. 2.8).

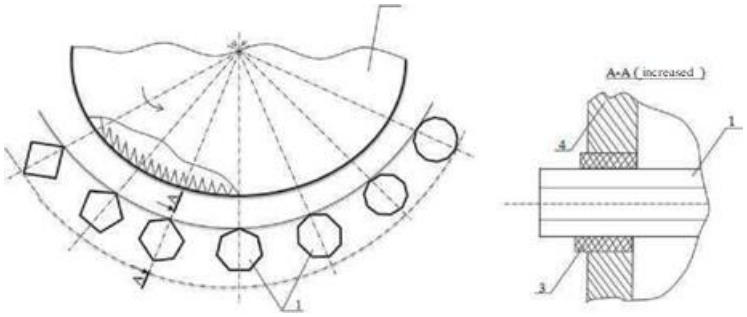

Fig.2.8. Grate of a fibrous material cleaner with multi-faceted grates on elastic supports

During operation, raw cotton (fibrous material) is fed to the saw cylinder 2, the teeth of which grip the raw cotton and drag it along the grates 1. In this case, the cotton hits the multi-faceted grates 1. The force and direction of the impacts along the rotation of the drum 2 will be different due to the different number of grate faces 1. In this case, with an increase in the number of grate faces 1, the force

of the impact of the cotton on the face of the grate 1 decreases, and with a decrease in the number of grate faces 1, on the contrary, the force of the impact increases. Therefore, in the initial zone, raw cotton, hitting the grates 1 with four faces, is subjected to loosening and separation of debris from it with greater force. Further, with an increase in the faces of the grates 1, the force of interaction of the cotton with the faces of the grates 1, although decreases, their frequency and amplitude of interaction increase. This contributes to the effective separation of mainly large debris. In this case, the following ratio is adhered to:

$$K_i = K_{i-1} + 1 \qquad (2.3)$$

where K is the number of faces of the i -th grate 1. K_{i+1} - the number of faces of the $(i-1)$-th grate.

In order to increase the productivity, cleaning effect and reduce the loss of cotton fly ash to the trash chute, the grate design has been improved by providing the required sequence of installing round and multi-faceted grates along the cotton pulling path. During operation, raw cotton (fibrous material) is fed to the saw-tooth drum 3, the teeth of which grip the raw cotton and pull it along the grate. In the area of action of the saw-tooth drum 3, the cotton cyclically strikes the multi-faceted grates 1 and the round grates 2 (Fig. 2.9). In this case, the force and direction of the impacts along the rotation of the saw-tooth drum 3 will be different due to the different number of grate faces 1. In this case, with an increase in the number of grate faces 1, the force of the impact of the cotton on the face of the grate 1 decreases, and with a decrease in the number of grate faces 1, on the contrary, the force of the impact increases. This interaction of cotton with multi-faceted (various quantities) grates 1 facilitates the separation of impurities of varying mass and with varying depth of presence in the cotton from raw cotton.

The alternation of round grates 2 between polyhedral grates 1 during interaction with fibrous material significantly reduces their braking and also makes it possible to change the forces of impulsive interaction and the law of movement of fibrous material in the zone of their dragging [102, 103, 104].

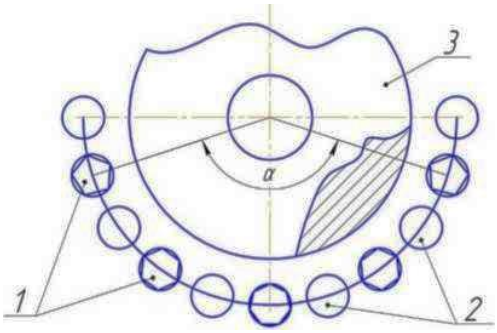

Fig.2.9. Grate of the fibrous material cleaner

In the next design that we recommend, the composite grates are attached to

the side segments using elastic elements [91, 99, 100] Appendix (16a, 16b, 16c).

The design works as follows (Fig. 2.10). Saw cylinder 1, which holds the cotton bats with its teeth, pulls them along mesh 2. In this case, mesh 2, fixed on elastic bushings, vibrates under the action of the pulled cotton tufts. The thickness of elastic bushings 3 decreases as the cotton advances so that ratio (2.2) is satisfied:

$$\Delta_1=r_1-R;\ \Delta_2=r_2-R;\ \Delta_n=r_n-R;\quad \Delta_1>\Delta_2>\ldots>\Delta_n \qquad (2.4)$$

where R is the radii of the grate bars; r_1, r_2, r_n - the outer radii of the elastic bushings 3 of the corresponding grate bars 2; Δ_1, Δ_2,.., Δ_n is the thickness of the elastic bushings 3 of the corresponding grate bars 2.

The use of a composite with a plastic matrix for the manufacture of grates completely eliminates the possibility of cotton ignition from a spark caused by a stone hitting the grates.

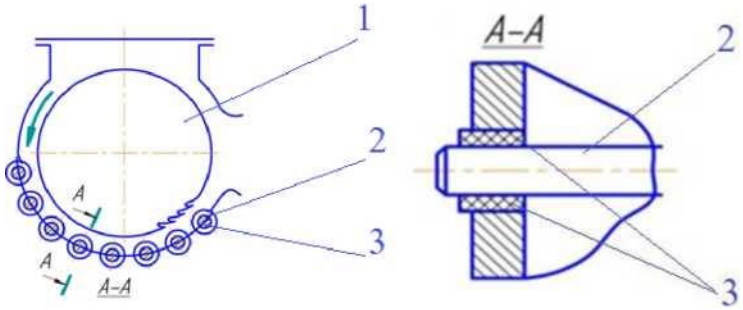

Fig.2.10. Proposed grate for cotton cleaner

The proposed design was studied theoretically in Chapter 4 and tested under production conditions; the results of the testing are presented in Chapter 5.

2.8. Conclusions on Chapter 2

1. Combination and continuity of technologies for separation of raw cotton from air and cleaning are proposed. On this basis, a design scheme of the separation and cleaning section of the flow line for cleaning raw cotton is developed.

2. Effective design schemes of working bodies and elements of cotton separators have been developed:

- separator with curved cotton guides in the inlet part of the chamber;
- diagram of a raw cotton separator with a composite guide with an elastic shock absorber;
- raw cotton separator with improved perforated disc design;
- diagram of a separator with a spherical shape of the design of the mesh surface of the chamber.

3. Based on the analysis of work on improving the technology and technology of cotton cleaning, a modernized technological line for cleaning raw cotton has been developed

4. A cotton cleaning scheme using developed designs of multifaceted mesh surfaces is recommended.

5. Recommended effective design schemes of working bodies and elements of large cotton cleaning sections:

- a cotton cleaner with conical grates on elastic supports, the thickness of which decreases as the cotton is pulled through, while the gaps between the grates are also selected to decrease;
- a raw cotton cleaner with multi-faceted composite grates on elastic rubber supports;
- a cotton cleaner for large debris with combined grates, made in the form of cylindrical and multi-faceted grates, installed in alternation along the cotton pulling path.

CHAPTER 3. THEORETICAL JUSTIFICATION OF THE PARAMETERS OF WORKING BODIES AND TECHNOLOGICAL MODES OF THE ZONE OF SEPARATION OF AIR FROM COTTON IN A COMBINED SEPARATION AND CLEANING UNIT

In the developed design of the separation and cleaning unit, the machines are arranged in series. This ensures continuity and uniformity of the technological processes of separating raw cotton from air, as well as cleaning the cotton. It is important to ensure the efficiency of separating air from cotton, preserving its natural physical and mechanical properties. To minimize damage to fibers and cotton seeds in the zone of separation and cleaning of raw cotton, working elements are used that allow gentle interaction with cotton. To ensure the main parameters of the separation and cleaning unit, complex theoretical and experimental studies were carried out. The results of theoretical studies of the zone of separation of raw cotton are considered below.

3.1. Theoretical study of the processes of formation and removal of a layer of raw cotton from the surface of a separator mesh.

Let's consider the process of movement of the cotton layer in the separator. Such a layer is formed on the surface of the mesh under the action of a continuous flow of cotton, as a result of separation of the raw material by a scraper. The thickness of the layer on the surface changes, when rotating, the scraper scrapes it off the surface, and under its own weight it gets into the vacuum valve zone.

We select a polar coordinate system (h, 0), which is located at the central point of the surface. The layer thickness is determined as follows $h = h(\bar{\theta})$, where h is the thickness of the cotton on the surface of the mesh, the angle of inclination $\bar{\theta}$ is calculated based on the position of the scraper and depends on time t (Fig. 3.1).

Since the scraper has a constant speed, the process is stationary and the thickness of the feedstock depends on the difference $\theta = \bar{\theta} - \omega t$ (where ω is the angular velocity of the scraper rotation). Using the stationarity condition, we consider the process actions in the interval $0 < t < T\ (T = 2\pi/\omega)$, and the interval of change of the angle θ we will take as $0 < \theta < 2\ \pi$. In this case, the air flow through the surface dS will:

$$dQ = \rho(\theta)U(\theta)dS, \tag{3.1}$$

where $\rho\ (\theta)$ and $U\ (\theta)\ dS$ are the density and velocity of air on the surface.

We assume that the air density is constant $\rho(\theta) = \rho_0$.

Let us consider the coordinate system as shown in Figure 3.1, in this case $dQ = \rho_0 U(\theta)dS$, and the air flow rate $dQ = \rho_0 U(\theta) r dr d\theta$.

To determine the air flow in a sector with a central angle of θ along the surface, we write the previous expression as follows:

$$Q = Q(\theta) = \rho_0 \int_{R0}^{R} r dr \int_0^{\theta} U(\theta) d\theta = \rho_0 \frac{R^2 - R_0^2}{2} \int_0^{\theta} U(\theta) d\theta \tag{3.2}$$

where: R_0 and R are the inner and outer radii of the mesh surface.

This equation is obtained from the steady state of the air flow

$$Q_0 = \rho_0 \frac{R^2 - R_0^2}{2} \int_0^{2\pi} U(\theta) d\theta \,, \tag{3.3}$$

where Q_0 - general air flow to the surface.

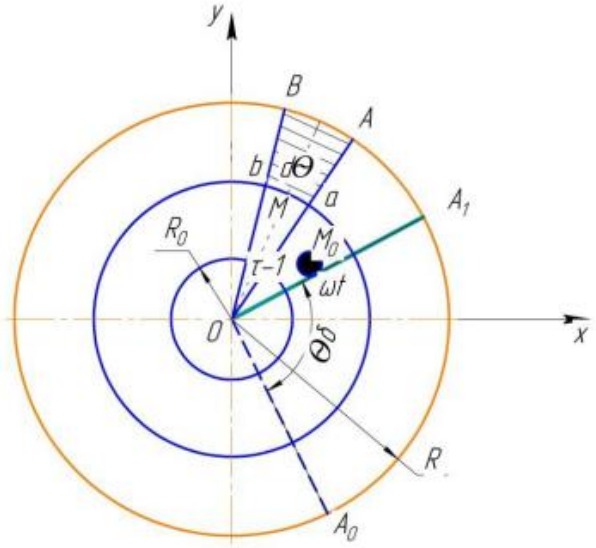

Fig.3.1. Scheme of movement of the scraper along the separator grid

The air suction rate varies based on equation (3.3). The equation is a first-order integral equation with multiple solutions. To obtain a unique solution, it is necessary to know the law of air suction along the surface of the mesh. To do this, consider the process of air passing through the layer based on filtration theory. According to this theory, the speed at which air passes through the layer (filtration) is proportional to the pressure gradient in it.

$$U = k_0 \frac{dp}{dh} \tag{3.4}$$

where $k_0 = k / \rho_0 g$ (m^4 / Ns), k is the filtration coefficient (varies depending on the thickness of the cotton layer), m/s, ρ_0 is the air density. Considering $h = h(\theta)$, then according to formula (3.2), the air flow rate will take the form:

$$Q = Q(\theta) = \rho_0 \int_{R0}^{R} r dr \int_0^{\theta} U(\theta) d\theta = \rho_0 k_0 \frac{R^2 - R_0^2}{2} \int_0^{\theta} \frac{dp}{dh} d\theta \tag{3.5}$$

Thus, the air flow in the layer is determined by the pressure gradient, which is a function. Let us give a special case.

$$p = A_1 (h - h_0)/h_1 + p_0 \quad (h_1 = h(0)) \tag{3.6}$$

Here is A_1 - a constant, - depending on the values of $\theta_0 = 0$, the thickness of the layer h_0 and the pressure in it p_0. Using condition (3.3), we determine the constant A_1.

$$A_1 = \frac{Q_0 h_1}{\pi (R^2 - R_0^2) k_0 \rho_0} \tag{3.7}$$

Thus, we obtain the following formulas for air flow, its speed and pressure:

$$U = \frac{Q_0}{\pi(R^2 - R_0^2)\rho_0} \quad (3.8)$$

$$Q = \frac{Q_0\theta}{2\pi} \quad (3.9)$$

$$p = \frac{Q_0[h(\theta) - h_0]}{\pi(R^2 - R_0^2)k_0\rho_0} + p_0 \quad (3.10)$$

Since the pressure is in a linear dependence (3.4) on the layer thickness on the surface of the grid, the air flow does not change according to formulas (3.9), its flow is limited by a linear law relative to the angle in. We assume that the maximum $h_1 + h_0$ and the minimum will be equal to $\theta = 0$ and $\theta = 2\pi$, respectively, in this case the ratio will be the following $h = h_1(2\pi)/2\pi + h_0$, then the air pressure in the raw material is calculated as follows.

$$p = \frac{Q_0 h_1(2\pi)}{2\pi^2(R^2 - R_0^2)k_0\rho_0} + p_0 \quad (3.10)$$

Let us consider theoretically the laws of distribution of the speed and density of cotton raw material on the surface of the net. Let the movement of the raw material flow occur only in the angular direction, and its speed v_n depends on the angle θ. In the layer under the action of the scraper, we determine the pressure p_n, which depends on the change in the angle θ. The element of the OAB highlighted in Fig. 3.1 moves along the surface of the grate, the Coulomb friction force acts on it $f(p - p_0)Sd\theta$, the surface area can be expressed through $S = \pi(R^2 - R_0^2)$ $ds = R_c d\theta$, then the Euler equation for the stationary motion of an element along an arc MM_0 can be expressed as follows:

$$\rho v_n S_0 \frac{dv_n}{ds} = -\frac{d(S_0 p_n)}{ds} - fS(p - p_0), \quad (3.11)$$

where $S_0 = h(\theta)(R - R_0)$ is the surface area of the layer, the center of which is located at point M.

Equation (3.11) includes three unknowns: velocity v_n, pressure p_n and thickness of the initial material $h(\theta)$, so to solve it we will use two additional equations. The first equation is the law of conservation of mass, due to the stationarity of the process (Q_n is the consumption of raw materials)

$$\rho_n v_n h_n = \rho_{n0} v_{n0} h_{n0} = Q_n/(R - R_0) \quad (3.12)$$

In addition, the equation of state of the raw material has the form

$$\rho = \rho_{n0}\{1 + A(p_n - p_{n0})\} \quad (3.14)$$

where p_{po}, v_{n0}, h_{n0} are, respectively, the density, speed and thickness of the raw material layer in the area of action of the scraper, in the initial area $\theta = 0$. Since the raw material and the scraper move together, $v_{n0} = v_0 = R_c\omega$.

A is the experimental constant, p_{n0} is the pressure exerted by the scraper on the surface of the raw material. With the same pressure of the raw material and air, we will take the pressure equal to p_0. If the consumption of raw materials is designated by Q_n, then the following equation is valid

$$\rho_{n0} = Q_n/h_{n0} v_0 (R - R_0) \quad (3.15)$$

Using equation (3.10), we determine the velocity by pressure for the case $A < 1$:

$$v = v_{n0}[1 - A(p - p_{n0})] \quad (3.16)$$

From equation (3.9) we find that pressure is expressed in terms of density

$$p_n = p_{n0} + \frac{1}{A}\left(\frac{\rho_n}{\rho_{n0}} - 1\right) \quad (3.17)$$

For $\theta=2\pi$ the densities of the raw material and air are close to each other. Therefore, the pressure on the scraper surface can be determined by taking the equations $p_n = p_0, \rho_n \approx \rho_0$ в (3.17).

$$p_{n0} = p_0 + \frac{1}{A}\left(1 - \frac{\rho_9}{\rho_{n0}}\right) \quad (3.18)$$

Let the following linear relationship be known between the properties of raw cotton and pressure.

$$p_n = B(h - h_0) + p_0 \quad (3.19)$$

where $h = h(\theta)$ is the thickness of the material as a function of the polar angle, which must be determined, $B = (p_{n0} - p_0)/(h_n - h_0)$, $C = (p_0 h_n - p_{n0} h_0)/(h_n - h_0)$, and with equations (3.16) and (3.19) $s = R_c\,\theta$, taking into account that in the equations $(R_c = R/2)\left(\frac{dv_n}{d\theta}\right)$ и $\frac{d(hp_n)}{d\theta}$, we will write the equation of the variable θ relative to $h\,(\theta)$:

$$\frac{2\bar{h}m + \bar{C} - m}{\bar{h}m + \bar{C}} \frac{d\bar{h}}{d\theta} = -\lambda \quad (3.20)$$

Where $\bar{h} = h/h_n$, $m = \frac{1-\bar{p}_0}{1-\bar{h}_0}$, $\bar{C} = \bar{p}_0 - \bar{h}_0 m$ $\lambda = \pi f(R + R_0)/2h_n$, $\bar{h}_0 = h_0/h_n$ $\bar{p}_0 = p_0/\rho_{n0}v_n^2$

Equation (3.19) is an equation for the angle θ to determine the thickness $h(\theta)$ of the original material, in which case the solution satisfying the condition $h(\theta)=1$ looks like this:

$$\theta = \frac{1}{\lambda}\left[\frac{C+m}{m} ln \frac{\bar{h}m + C}{m + C} - 2(\bar{h} - 1)\right] \quad (3.21)$$

Expression (3.21) determines the thickness of the layer h as a function of the continuity of the angle θ. In Fig. 3.2, the graphs of the dependence of the thickness of the raw cotton layer on the surface of the mesh on the angle are given for two values of the parameter A.

Let us take the following numerical values: h_0 = 0,03 m, $R = 0{,}05m$, p_0=10 kg/m ^{3}, p_n = 80kg/ m^3, ω = 15s $^{-1}$, f = 0,2, $\bar{p}_0$ = 10.

From the analysis of the graphs it can be noted that the thickness of the layer of the initial material changes according to a linear law relative to the angle θ, the same as the pressure (3.13). If $\theta = 0$, given the thickness of the original material h_0, its thickness can be calculated at any angle using the graphs in Figure 3.2. Let us introduce the concept of the bulk compression modulus $K = 1/A$.

For example, if A = 0,001 Pa $^{-1}$, ($K = 1/A$ = 10^3 Pa) h = h $_0$ = 0,03 m, then the thickness of the original material on the surface of the scraper is h_n = 0,0833 m. The consumption of raw material distributed over the surface of the grid is Q_n = 1250 kg/s. In other words, the volume of raw material decreases, while the thickness of the layer in front of the scraper and the consumption of raw material decrease, i.e. h_n = 0,066 m and Q=900 kg/ s. Q_n=900 kg/s.

Figure 3.3 shows the angular changes in pressure in the feedstock for two values of parameter *A*. The highest pressure value is created when the screen surface contacts the scraper, and an increase in parameter *A* (i.e. a decrease in the bulk compression modulus K) leads to a significant decrease in pressure.

A= 0,001Pa^{-1} h_0 = 0,03m, h_n = 0,0883m, A = 0,005Pa $^{-1}$ h_0 = 0,03m, h_n = 0,066m,

$Q_n = 1125\ kg/s$ $Q_n = 900\ kg/s$

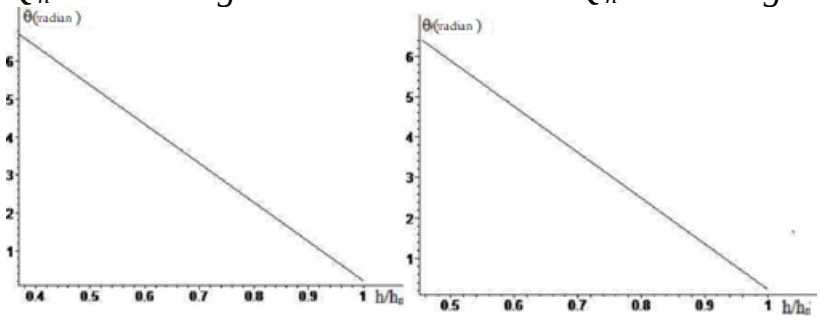

Fig.3.2. Graphs of the dependence of the raw material layer thickness h / h_n at different values of the pole angle θ.

A = 0,001Pa $^{-1}$ A = 0,005Pa $^{-1}$

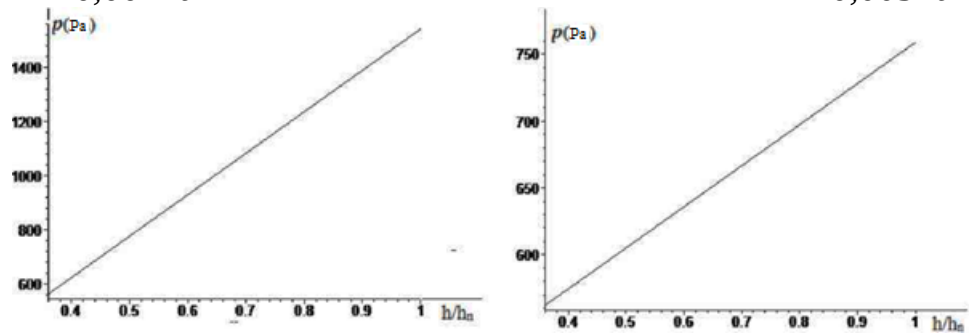

Fig.3.3. Graphs of pressure dependence on h / h_n for different values of parameter A

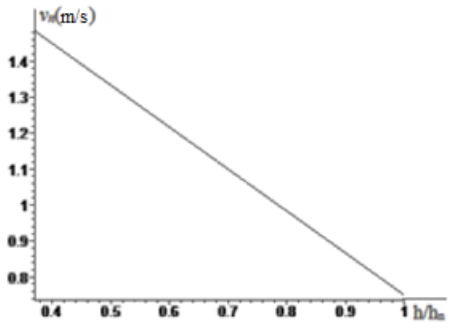

Fig.3.4. Graph of air flow velocity dependence v_n from h/h_n

Figure 3.4 shows the changes in the speed of the scraper with respect to the angular θ when the linear velocity $v_{n0} = v_0 = R\omega$ = 0.75 m/s. The graph of the change in density with respect to the angle with such a ratio p_0 = 10kg/ m^3 and p_p = 100 kg/ m^3 is shown in Fig. 3.5. Since the surface pressure is linearly related to the angle, the velocity and density of the initial material on the surface also turned out to be linearly related.

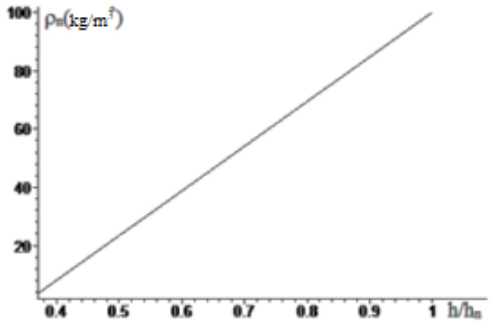

Fig.3.5. Graph of raw material density dependence p_n from h / h_n

Thus, in the chosen scheme, i.e. when the pressure changes proportionally to the layer thickness, the speed of movement of the raw material increases on the surface of the grid relative to the polar angle and decreases with density.

3.2. Analysis of the change in tension of cotton fibers when removing a layer from the surface of the net and its effect on seed damage and the formation of free fibers

The raw cotton is in constant contact with the surface of the net during movement. Under the influence of external pressure due to friction against the net surface, especially against the surface of the net holes, some fibers are stretched, which can lead to their detachment from the seed. To analyze this phenomenon, we set the value of the friction force in the fiber per unit area, based on Coulomb's law of friction, assume that the tension is equal to the product of the friction force and the area of the contact surface of the scraper with the net surface. In this case, the tensile strength is calculated using the formula:

$$T = fS_k p(\theta) \qquad (3.22)$$

Here S_k contact area, which can be calculated using the following formula. $S_k = (R - R_0) H_k$, where H_k - the width of the scraper contact. Thus, taking into account the change in pressure on the surface, the formula for calculating the maximum tension is presented in the following form:

$$T = fp(2\pi)(R - R_0)H_k \qquad (3.23)$$

For numerical calculation we assume that f = 0.2, h_0 = 0.03m, R = 0.05 m, H_k =0.01 m. The results of calculations for different values of parameter A and the ratio $p_0/\rho_n v_0^2$ are given in Table 3.1.

Results of calculation of the tension parameter A and the ratio $p_0/p_n v_0^2$ for different values:

Table 3.1

A = 0,001 Pa $^{-1}$ (K = 10 ^{3} Pa)									
$p_0/\rho_n v_0^2$	0,5	1	1,5	2	2,5	3	3,5	4	5
$T(N)$	5,04	5,18	5,32	5,46	5,6	5,74	5,88	6,02	6,31
A = 0,005Pa $^{-1}$ $(K = 5 \cdot 10^2\ Pa)$									
$p_0/\rho_n v_0^2$	0,5	1	1,5	2	2,5	3	3,5	4	5
$T(N)$	0,75	0,84	0,93	1,03	1,12	1,22	1,31	1,4	1,6

From the analysis of the calculation results given in Table 3.1, it is evident that the extension increases with increasing external pressure and the raw material compression modulus (or decreasing the parameter A). Such a change can be more abrupt as the modulus K increases. For example, when $K=10^3\ Pa$, the stress at $\frac{p_0}{\rho_n v_0^2} = 1$ is equal to $T = 5{,}18\ N$, and at $p_0/\rho_n v_0^2 = 5$ the stress is $T = 6{,}31\ N$. At K = 5·10 ^{2} Pa, these values are equal to $T = 0{,}84\ N$ and $T = 1{,}6\ N$. respectively, that is, the voltage increases by 1,22 and 1,9 times, respectively, when the pressure increases by 5 times, and the voltage increases by 6 times, when the modulus increases by five times, respectively, an increase of 3,94 times is observed.

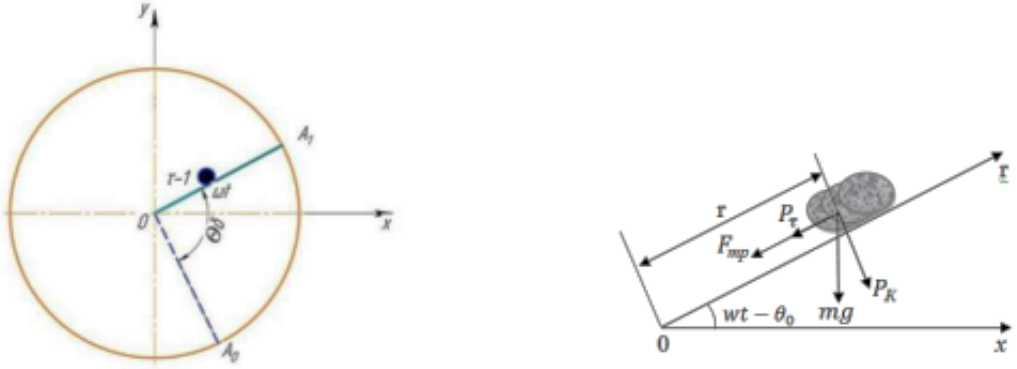

A b

Fig.3.6. Scheme of particle movement on the surface of the scraper

Let us formulate the equation of motion of a particle on the surface of the scraper at any time t >0. If the particle is at a distance r at an arbitrary time on the surface of the scraper, we determine the forces acting on the particle, taking into account the friction between the surface and the particle. For clarity, let us assume that the particle's motion along the axis of the vector is positive *o* $\vec{r}$. In this direction we will determine the forces acting on the area:

1. Projection of the particle's gravity force onto the direction of the tangent to the scraper.

$$P_\tau = mg\ sin(wt - \theta_0), \qquad (3.24)$$

where ω is the angular velocity of the scraper

2. If ṙ> 0, then according to Zhukovsky's method the Coriolis force of inertia is

directed
normal to the plane of the drawing and inversely proportional to the particle velocity, its value can be expressed as:

$$P_K = 2\dot{r}\omega m \tag{3.25}$$

3. This force presses the particle against the scraper and creates an additional friction force. The total friction force on the scraper will be:

$$F_{fr} = -f_0 m\left[g\cos(\omega t - \theta_0) + 2\dot{r}\omega\right] \tag{3.26}$$

where: f_0 - coefficient of friction between particles and scraper.

4. On the surface of the mesh, the particle is subject to pressure - Po from the suction air flow. If we assume that the surface in contact with the surface is S, then this pressure creates a friction force.

$$P_0 = -fP_0S \tag{3.27}$$

f - coefficient of friction between the mesh surface and the particle.

5. In addition to the pressure, using Euler's formula we determine the tension force T of the fiber on the surface of the holes.

$$T = T_0 e^{-f_1\alpha} \tag{3.28}$$

where f_1 is the coefficient of friction between the fiber and the hole surface. α is the angle of coverage. T_0 is the external tensile force. Stress also creates a friction force.

$$P_t = -f_2T_1 = -f_2T_0e^{-f_1\alpha} \tag{3.29}$$

Under the action of the indicated forces, equation (3.16) of the particle's motion along the scraper is written as follows:

$$m\ddot{r} - m\omega^2 r = -fmg[sin(\omega t - \theta_0) + f_0\, cos(\omega t - \theta_0)] - 2f_0\dot{r}\omega m - fP_0S - f_2T_0e^{-f_1\alpha} \tag{3.30}$$

According to the accepted condition, when t =0, $\ddot{r}>0$ ($r = r_0$, r =0, t =0), the condition must be satisfied. Using equation (3.30), we obtain the following inequality:

$$m\omega^2 r_0 - mg(f_0\cos\theta_0 - Sin\theta_0) - f_2P_0S - f_2T_0e^{-f_2\alpha} > 0 \tag{3.31}$$

From this inequality follows the following condition for the angular velocity. If the condition $\omega^2 > \omega_x^2$ is satisfied, the particle moves under the action of gravity in the direction from the center of the grid. Assuming that condition (3.19) is satisfied, we present the equation in the following form:

$$\ddot{r} - \omega^2 r + 2f_0\dot{r}\omega = -g[Sin(\omega t - \theta_0) + f_0\, cos(\omega t - \theta_0)] - \bar{P}_0 - \bar{P}_1 \tag{3.32}$$

Where $\bar{P}_0 = f\frac{P_0S}{m}$; $\bar{P}_1 = \frac{T_0e^{-f_0\alpha}}{m}$;

The general solution of equation (3.32) is as follows

$$r = C_1e^{k_1t} + C_2e^{k_2t} + \frac{g(1-f^2)}{2\omega^2(1+f^2)}sin(\omega t - \theta_0) + \frac{f_0g\,cos(wt-\theta_0)}{\omega^2(1+f^2)} + \frac{P_0}{\omega^2} \tag{3.33}$$

where $K_{1,2} = \omega(\pm\sqrt{1+f_0^2} - f_0)$, C_1 and C_2 are constant coefficients determined from the initial conditions.

For r = 0, $\dot{r}$= 0, t = 0 we construct using the following conditions:

$$C_1 = \frac{g}{\omega^2(1+f_0^2)(K_2-K_1)}\left[\frac{(1-f_0)}{2}(K_2\sin\theta_0 - \cos\theta_0)\right] + f_0[(K_2\cos\theta_0 + \sin\theta_0)]\cdot C_2 =$$

$$\frac{g}{\omega^2(1+f_0^2)(K_1-K_2)}\left[\frac{(1-f_0)}{2}(K_1\,sin\,\theta_0 - Cos\theta_0)\right] + f_0[(K_1\,cos\,\theta_0 + sin\,\theta_0)] \quad (3.34)$$

From equation (3.34) one can determine the radius r and the stress using formula (3.29).

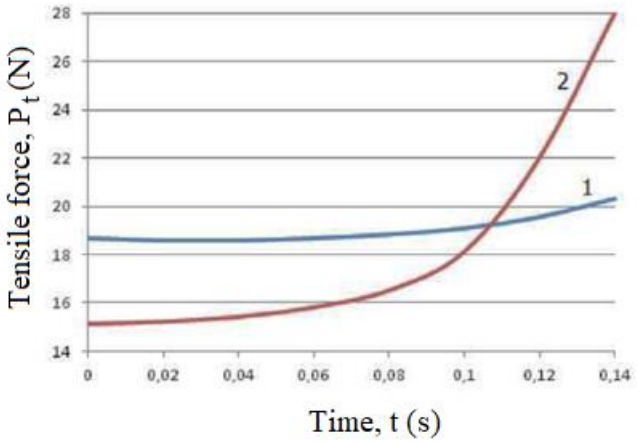

Fig.3.7. Dependence of the tensile force acting on the fiber on time (1) ω =15 s $^{-1}$ (2) ω =20 s $^{-1}$

Based on the graph in Fig. 3.7, we can recommend an angular speed of scrapers ω = 15 s $^{-1}$, at which the tensile force is more stable, which helps to reduce fiber damage.

3.3. Justification of the parameters of perforated meshes with conical holes

As noted above, the creation of conical holes in the perforated meshes with a curved surface allows the scrapers to smoothly remove cotton fluff when they interact with the perforated meshes. Part of the meshes 1 with holes 2 are shown in Fig. 3.8.

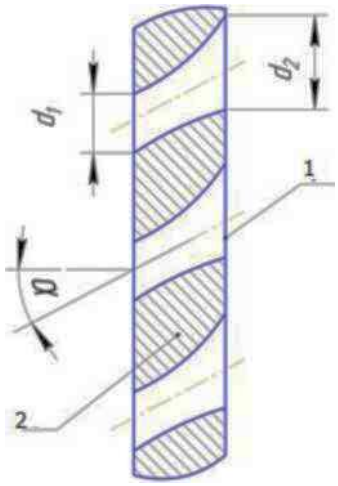

Fig.3.8. Grid hole pattern.

For efficient removal of cotton attached to perforated nets, the holes 1 have a conical shape with a curved surface. The ratio of the diameters of the base of the holes 2 is d_2 = (1,15 ÷ 1,255) di (where d_1 is the diameter of the small base, d_2 is the diameter of the large base of the conical holes).

In order to reduce the amount of free fibers, it is important to study the process of removing cotton fluff from the separator screens with a scraper. Fig. 3.21 shows the calculation scheme for determining the force and torque on the separator shaft.

In this case, the following forces act on the cotton located on the net. F_{f1} is the friction force of the fibers on the surface of the net of holes. G is the weight of the fibers and seeds in the hole, F_s is the suction force of the air flow on the fibers in the cross-section of the holes and the friction force of the seeds on the surface of the nets.

The friction force of the fibers on the surface of the hole is determined from expression (3.55):

$$\vec{F}_{fr1} = f_1 \cdot N_1 \qquad (3.35)$$

where f_1 - coefficient of friction between the fibers and the surface of the mesh.
The pressure on the surface of the mesh is determined from the expression.

$$N_1 = m_f g + F_f \qquad F_f = kV^2 \qquad (3.36)$$

where is m_f - mass of fibers located in the mesh opening; g - acceleration of gravity; V - air velocity in the opening; k - coefficient of aerodynamic force in the transverse direction.

Substituting (3.36) into (3.35) we obtain

$$F_{fr1} = f_1\left(m_f g + kV^2\right)$$

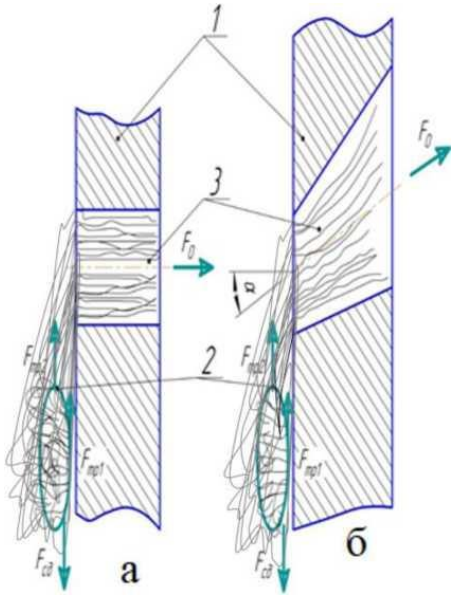

Fig.3.9. Calculation scheme for determining the force of removal of the fly from perforated mesh a - existing mesh; b - recommended mesh; 1-net; 2-seed; 3-fibers.

Friction force of fibers when bending around a hole

$$F_{fr1} = nF_0 e^{f_2\beta}$$

where n is the number of fibers in the hole;
F_0 - tension of fibers in the hole;
f_2 - coefficient of friction of fibers on the curved surface of the hole; β is the angle of coverage of the curved part of the hole.
Then the total friction force of the fly on the grid

$$F_{fr1} = f_1\left(m_f g + kV^2\right) + nF_0 e^{f_2\beta} \tag{3.37}$$

Then the shear force, that is, the force of removing the cotton tufts from the surface of the mesh, must be greater than the friction force between them and the surface of the mesh.

$$F_{sh} \geq F_{fr}$$

$$F_{sh} \geq f_1\left(m_f g + kV^2\right) + nF_0 e^{f_2\beta} \tag{3.38}$$

For the existing option β = 90 ^{o} for the recommended β = 90 ^{o} - α where, α is the angle of inclination of the hole axis.
In addition, it is necessary to take into account that in a conical inclined hole there is a smaller number of fibers. As a result, we finally get.

$$F_{sh} = f_1\left(am_f g + kV^2\right) + nF_0 e^{f_2(90-\beta)} \tag{3.30}$$

where a is a coefficient that takes into account the reduction in the number of fibers in the conical hole.

Let us assume that the shear force of the cotton particles falling into each mesh hole will be the same. However, the moment relative to the scraper axis from this force will be different, depending on the radius of the hole relative to the mesh axis and the scraper. In this case, the total separation moment is determined from the expression for the recommended mesh option:

$$M_c = (K_1R_1 + K_2R_2 + \cdots + K_nR_n)\left[f_1(am_в g + kV^2) + nF_0 e^{f_2\beta}\right] \tag{3.40}$$

where, K_1 , K_2,...K_P is the number of holes on the same grid radius $R_{1;}$ R_2 ,... R_n .
The numerical solution of (3.68), (3.72) and (3.73) is performed with the following initial values of the parameters:

$$m_f = (0,7 \div 0,9)\,g;\ F_{fr1} = (0,24 \div 0,34)\cdot 10^{-3}\ N;\ F_f = (60 \div 150)\cdot 10^{-3}\ N;$$

$$V_f = (10 \div 20)\,m/s;\ K = (1,0 \div 2,5);\ \alpha = (30^o \div 45^o);\ n = (150 \div 200);$$

$$F_0 \leq (10 \div 15)\,N;\ f_1 = (0,3 \div 0,4);\ f_2 = (0,45 \div 0,55);\ f_3 = (0,35 \div 0,5);$$

Based on the solution, graphical dependencies of the change in shear force on the suction force of fibers in the mesh openings of comparable versions of the mesh separator were constructed. The moisture content of raw cotton was taken into account by the values of the friction coefficients. The obtained dependencies are presented in Figure 3.10. Analysis of the graphs shows that with an increase in the suction force of fibers, the shear force of fibers along the mesh by scrapers increases linearly. It should be noted that an increase in F_o = 3,0·10 $^{-2}$ N , the tension of fibers from friction against the rim of the opening, leads to an increase

in F_{cd} = 6,2·10^{-2} N in the recommended version and up to (12-15)·10^{-2} in the existing version of the openings of the meshes of the compared separators.

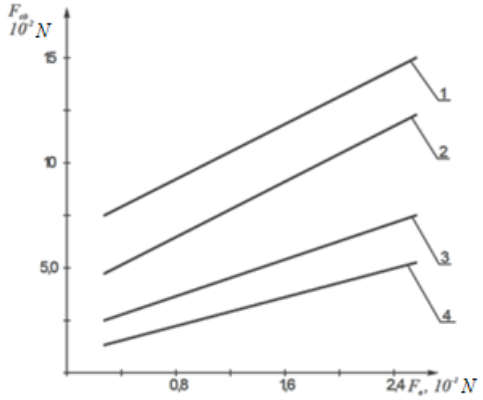

Fig. 3.10. Graphic dependences of the shear force of a cotton bundle on the change in the suction force of cotton fibers by air.
1.2 - for the existing option; 3.4 - recommended option, 1.3 - with cotton moisture content of 10,5%; 2.4 - with cotton moisture content of 9.0%.

The influence of the angle of inclination of the axis and the mesh holes on the force of removing cotton particles from the mesh surface is important. Analysis of the graphs in Fig. 3.23 shows that increasing the angle of inclination of the hole from 50 ^{0} to 46 ^{0} leads to a decrease in the force from 14,7·10^{-2} N to 4,82·10^{-2} N with a bulk compression modulus of K = 2,5 N/m, and at K = 2,5 N/m the force value decreases to 2,1·10 $^{-2}$ N at $\alpha = 46^{0}$. It follows that for guaranteed removal of raw cotton it is desirable to increase the angle of inclination of the axis of the grate openings in the direction of the scraper movement. The recommended values of the angle of inclination of the axis of the grate opening are $\alpha = 40^{0} \div 48^{0.}$

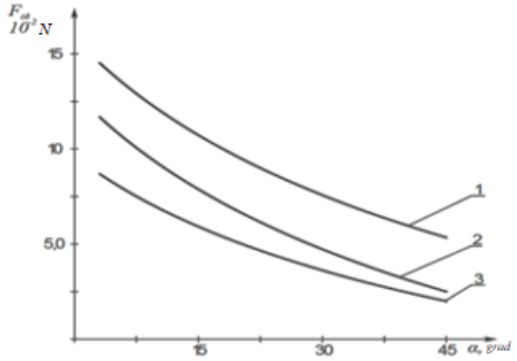

Fig. 3.11. Graphic dependences of the change in the shear force of a fiber bundle on the surface of the mesh on the change in the angle of inclination of the axis of the holes.
1-at K = 2,5 N/m; 2-at K = 2,0 N/m; 3-at K = 1,5 N/m

The force of pulling and moving the fibers and cotton seeds stuck in the holes depends largely on the coefficient of friction of the fibers on the surface of the mesh holes. It should be noted that an increase in the number of fibers in the holes increases the friction force. In the recommended conical hole, the number of fibers in it is significantly less than in the cylindrical hole. This decrease in expressions (3.72) and (3.73) is taken into account by the coefficient "a". Fig. 3.12 shows the change in the shear force of the cotton bundle on the surface of the separator mesh

from a change in the coefficient of friction of the fibers on the surface of the mesh holes.

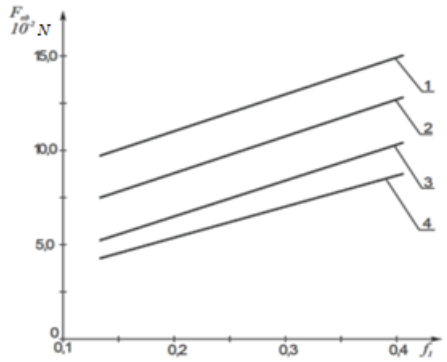

Fig. 3.12. Dependences of the change in the shear force of the bundle on the surface of the separator mesh on the change in the coefficient of friction of the fibers on the surface
grids.
1.2 - for the existing version; 3.4 - for the recommended version,
1.3 - at V_f -20 m/s, 1,3 - at V_f -15 m/s

3.4. Theoretical study of the removal of raw cotton from the surface of the separator mesh in the presence of an isolating chamber.

Using the suction pressure Δp on the surface of the mesh, let's assume that the cotton flow is Q_0 (Fig. 3.5). We will represent the isolating chamber as a sector abcd moving with an angular velocity ω, moving to clean the raw cotton stuck to the surface of the grid. The back part of the sector is closed, and the raw cotton in this sector is in a free state. It falls freely due to its own weight and the rotation of the separator shaft. The size of the isolating chamber is characterized by the angle α.

a

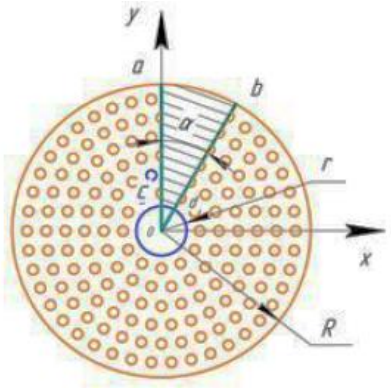

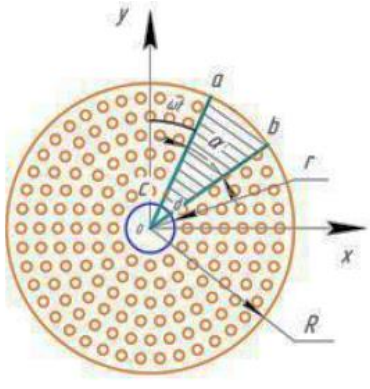

b

c d

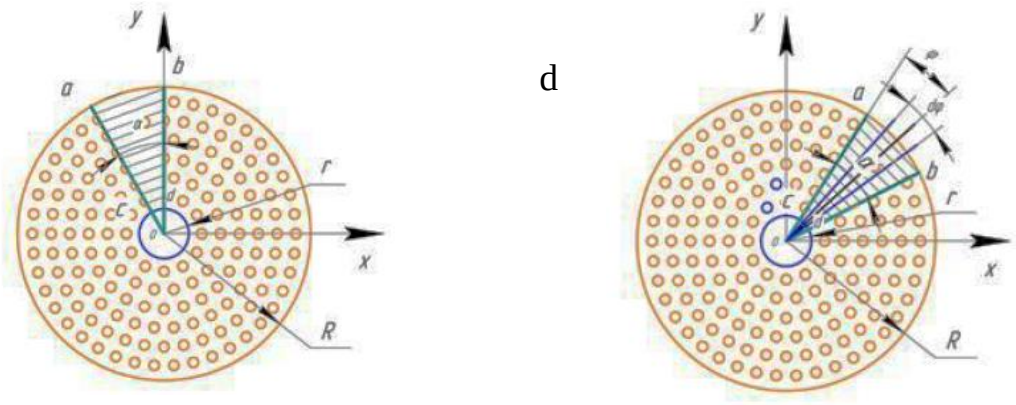

Fig. 3.13. Schematic diagram of the arrangement of a sector moving at an angular velocity along the surface of the mesh to clean it from cotton lobes stuck to it. raw material.

Under initial conditions $t = 0$ (a), $t > 0$ (b), $t = (2\pi - \alpha)/\omega$ (c) and (d) is the location of the scraper at any time.

Let the total weight of raw cotton that is not located within the sector region (within the moving sector) on the surface of the network be equal to m_0.

During rotation, the surface sector of the mesh is cleaned and filled with portions of fresh cotton.

If the edge bd of the sector is located in the direction of the Oy axis, the time it takes for the sector to pass through the grid is $t = T = (2\pi - \alpha)/\omega$ (c), then the moving sector abcd occupies the position shown in Figure 3.5.

In this case, the total mass of cotton seeds (including the mass of cotton) on the net is determined by the following expression:

$$m_0 = \frac{Q_0}{\omega} \tag{3.41}$$

If the current processes are stationary, then it is assumed that $m = m_0$, and the angle changes as follows: $\varphi = \theta - \omega t.$

In this case, the location of the edges ac and bd depends on the change in angle φ:

$$\varphi = 0 \; and \; \varphi = \alpha$$

Let us denote the total density of raw cotton c by p. It is subject to excess pressure. Depending on the change in pressure at any point on the surface of the net, its volume is determined as follows.

$$\rho = \rho_0(1 + B\Delta p) \tag{3.42}$$

where: ρ_0 - density of raw cotton on the surface of the mesh, $\Delta p = p - p_0$ - value of pressure change, where $p = p(\varphi)$ and p_0 are the current and initial pressure.

We assume that in the absence of cotton on the surface of the sector $\Delta p = 0$.

Since the pressure and thickness of the seed cotton layer vary depending on the mesh surface and sector area, its weight also changes.

Let us assume that the mass of raw cotton on the surface of the sector and the net are equal to m_1 and m_2, respectively. Let us determine the mass of the layer on the above surfaces in $d\varphi$ (Fig. 3.8, g):

$$dm_1 = \pi(R^2 - r^2)\rho_0 h(\varphi)d\varphi \; 0 < \varphi < \alpha \quad (3.43)$$

$$dm_2 = \pi(R^2 - r^2)\rho_0(1 + B\Delta p)h(\varphi)d\varphi \quad \alpha < \varphi < 2\pi - \alpha \quad (3.44)$$

where: $h(\varphi)$ is the sector being determined and the thickness of the raw cotton on the surface of the mesh.

By integrating equations (3.36) and (3.37), we write the law of change in the mass of a layer of raw cotton as follows:

$$m_{сл} = m_1 + m_2$$

$$m_1 = \pi(R^2 - r^2)\rho_0 \int_0^{\varphi} h(\varphi)d\varphi \quad \text{при } 0 < \varphi < \alpha,$$

$$m_2 = \pi(R^2 - r^2)\rho_0 \int_{\alpha}^{\varphi}(1 + B\Delta p)h(\varphi)d\phi] \quad \text{при } \alpha < \varphi < 2\pi - \alpha \quad (3.45)$$

According to equation (3.23), if the total mass of cotton is m_0, we obtain the following equations using this condition:

$$m_{сл} = m_1(\alpha) + m_2(2\pi - \alpha) = \frac{Q_0}{\omega}. \quad (3.46)$$

Taking into account equations (3.27), we obtain the following expressions:

$$\pi(R^2 - r^2)\rho_0\{\int_0^{\alpha} h(\varphi)d\phi + \int_{\alpha}^{2\pi-\alpha}(1 + B\Delta p)h(\varphi)d\varphi] = \frac{Q_0}{\omega}$$

Let us express this equation in the following form:

$$\int_0^{2\pi-\alpha} h(\varphi)d\varphi + B\int_{\alpha}^{2\pi-\alpha} \Delta p h(\varphi)d\varphi = \frac{Q_0}{\pi\omega(R^2-r^2)\rho_0} \quad (3.47)$$

The integral equation (3.41) is used to determine the thickness of the raw cotton layer on the contact surface.

Let us consider the modeling process at different performance levels of the grid surface.

Since the above equation is difficult to solve by mathematical methods, we will consider several cases in which the thickness of the raw cotton layer is taken based on experiments to solve the equation.

In computer calculations we take the pressure change as follows:

$$\Delta p = \Delta p_0 = p_1 - p_0 = const$$

1. If we assume that the thickness of raw cotton on the surface of the mesh is h_0, then:

$$h_0 = \frac{Q_0}{\pi\omega(R^2-r^2)[2\pi-\alpha+2B\Delta p_0(\pi-\alpha)]} \quad (3.48)$$

Fig. 3.9 shows the change in the relative central angle a (grad) from the thickness of raw cotton on the surface of the mesh at different productivity Q_0 $(kg/hour)$ and pressures Δp_0 (Pa).

Let's take the following data into account in the calculations: R = 0,5m, r = 0,045m, B = 0,0001m^2/N, ω = 15s^{-1}.

According to the analysis of the graphs (Fig. 3.14), with the increase of the central angle value, the sector width increases linearly. There are several options for the selected angle values.

2. The thickness of the raw cotton layer decreases according to a linear law as follows:

$$h = h_0(1 - k\varphi) \tag{3.49}$$

where k - proportionality coefficient, $k < 1/(2\pi - \alpha)$,

h_0 - thickness of the raw cotton layer at the beginning of the sector.

Substituting the values of h into (3.28), we calculate the integrals and determine the relationship between h_0 and k:

$$h_0 = \frac{1}{\pi\rho_0\omega(R^2-r^2)} \frac{2kQ_0}{1-[1-k(2\pi-\alpha)]^2+B\Delta p_0\{(1-k\alpha)^2-[1-k(2\pi-\alpha)]^2\}} \tag{3.50}$$

Fig. 3.15 shows the graphs of the dependence of the value of the parameter k from the angle α of the parameter ho at Q_0 = 12000 kg/h. According to calculations, the thickness of the raw cotton layer has virtually no effect on the change in pressure at height h_0, therefore, the calculations were carried out for the value Δp_0 = 1100 Pa. As shown in the graph, a sharp increase in the thickness of the cotton layer is observed as the deflection angle k increases, and this value approaches the value $k_t = 1/(2\pi - \alpha)$.

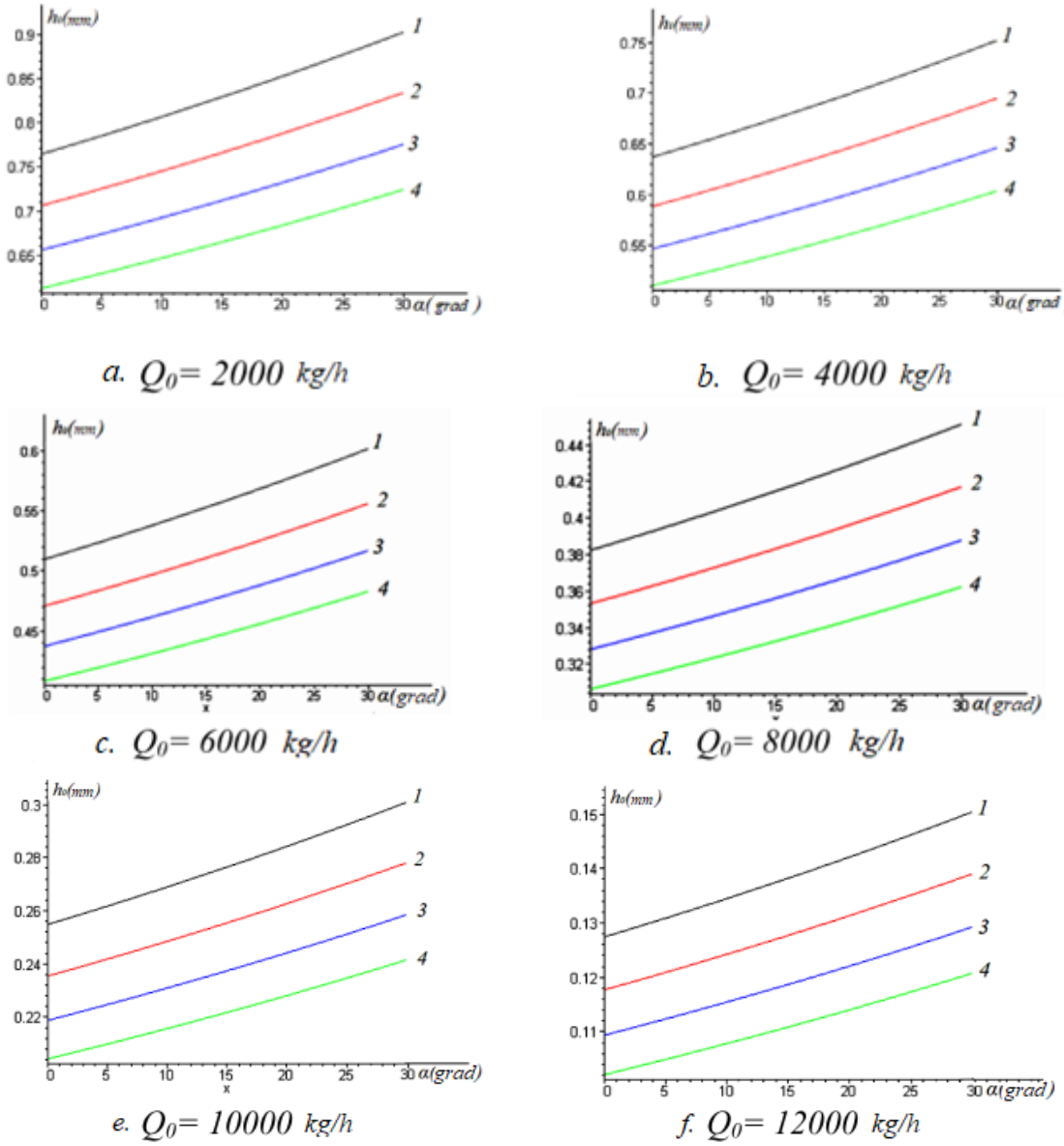

Fig. 3.14. Graphs of cotton thickness dependence on the size of the isolating

chamber (a), productivity @ $_0$ (kg/hour) and pressure change
Δp_0 (Pa): 1 - Δp_0 = 1050, 2 -p_0 = 1100, 3 - Δp_0 = 1150, 4 - Δp_0 = 1200

The efficiency of the separator mesh surface at $Q_0 = 12000$ kg/h depends on the angle φ of the raw cotton layer, and different values of the parameter k are shown in Fig. 3.11. According to calculations, it was found that the values of the height h and the angle φ of the cotton layer do not depend on the change in pressure. However, it was found that these values depend on the parameter k.

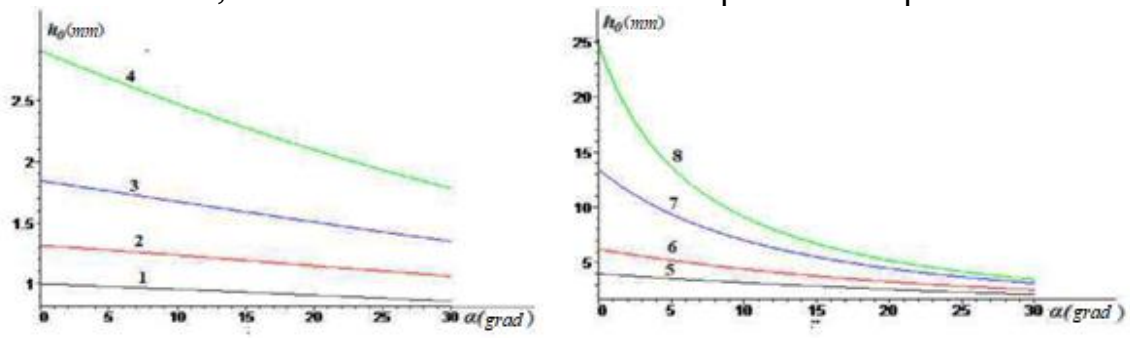

Fig. 3.15. Dependence of the thickness of the layer ho on the size of the insulating chamber a for different parameters k: 1 - k = 0,11; 2 - k = 0,12; 3 - k = 0,13; 4 - k = 0,14; 5 - k = 0,145; 6 - k = 0,15; 7 - k = 0,155; 8 - k = 0,158.

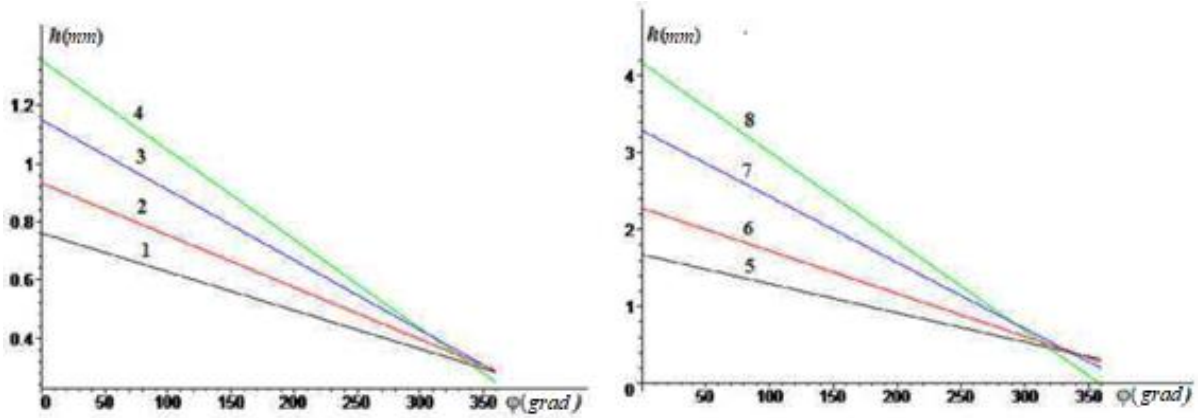

Fig. 3.16. Dependence of the layer thickness h on the angle φ for different values parameter k
1 - k = 0,10; 2 - k = 0,11; 3 - k = 0,12; 4 - k = 0,13; 5 - k = 0,14; 6 - k = 0,15; 7 - k = 0,155; 8 - k = 0,16.

It is evident from Fig. 3.15 that the initial thickness of the cotton h_0 decreases asymptotically with increasing angle α, which characterizes the size of the insulating chamber. The change in h_0 at α = 15 ° practically does not occur, therefore this value can be considered recommended.

3.5. Effect of air flow on separator performance

In order to study the movement of the air flow in the separator and determine its aerodynamic components, we will consider the change in the cross-sectional

area of the flow (Fig. 3.17) during horizontal movement in the pipe.

Let us assume that the air flow density is constant and that it is one-dimensional in each zone ABCE and BDEK. In this case, using the Euler equation, we write the air flow equation in both zones as follows:

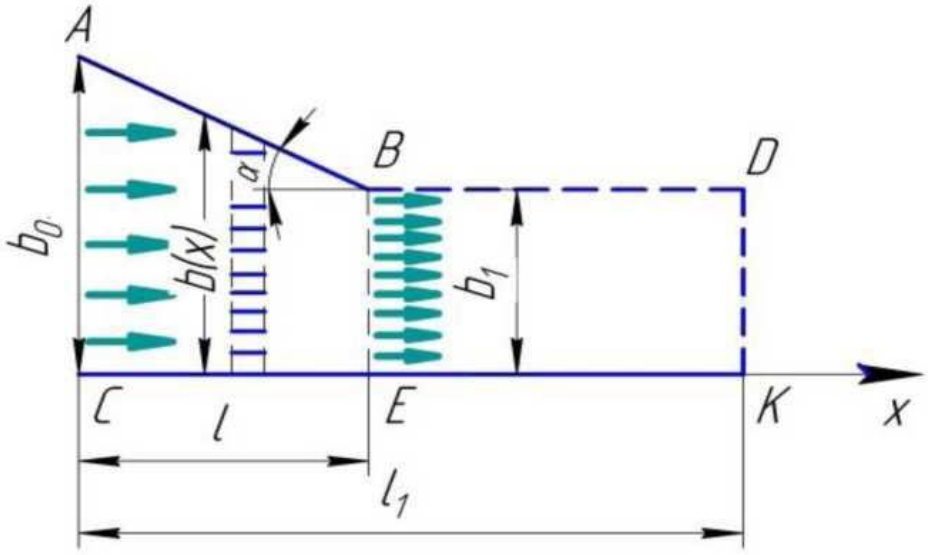

Fig. 3.17. Air movement diagram in a pipe.

In zone ABDX: (zone 1)

$$\rho_1 v_1 S_1 \frac{dv_1}{ax} = -\frac{d(S_1 p_1)}{ax}, \qquad 0 < x < l \tag{3.51}$$

In the BDEK zone: (zone-2)

$$\rho_2 v_2 \frac{dv_2}{ax} = -\frac{dp_2}{ax}, \qquad l < x < l_1 \tag{3.52}$$

where ρ_1, ρ_2 - density in zones; speed in zones - v_1, v_2, p_1, p_2 - pressure in zones; $S_1 = b(x)\ L$ - law of change of pipe height in zone 1 along coordinate x, L - length of separator.

When integrating equations (3.51) and (3.52), we accept the following conditions: The air density does not change, the air flow movement is stationary. In this case, the amount of mass per unit of time does not change, that is,

$$\rho_1 v_1 S_1 = \rho_0 v_0 S_0 = Q_0 \tag{3.53}$$

where, Q_0 is the mass flow rate

Based on these assumptions, we will determine the air flow and pressure in each zone. For clarity, we will express the linear law of change of the x coordinate. That is,

$$S_1 = (b_0 - kx)L\ , \tag{3.54}$$

where k is a constant, b_0 is the height of the surface in the section at $x = 0$, $k = tg\alpha$, α is the angle formed by the segment AB with the axis OX: Let us determine the speed, when ρ=const in equation (3.52).

$$v = v_1 = \frac{Q_0}{\rho_0 S_1} = \frac{Q_0}{\rho_0 L(b_0 - kx)} \tag{3.55}$$

The pressure is determined by integrating $p = p_0$ at $x = 0$ equation (3.45):

$$p_1 = \frac{b_0}{b_0 - kx} p_0 \left[1 - \frac{Q_0^2}{L^2 b_0^2 p_0 \rho_0} \left(\frac{kx}{b_0 - kx} \right) \right] \quad (3.56)$$

Equations (3.54), (3.55) represent the distribution laws in a pipe where the cross-sectional area of velocity and pressure is variable. In particular, if the cross-sectional area is constant, we obtain the values

$$k=0, p = p_0, \qquad v = v_0 = \frac{Q_0}{\rho_0 L b_0} \quad (3.57)$$

where the pressure and velocity $v = v_2$ in the section $l < x < l_1$.

The cross-section of the pipeline is constant and can be expressed as follows:

$$v_2 = v_1(l) = \frac{Q_0}{\rho_0 L (b_0 - kl)} \quad (3.58)$$

Where : $k = \frac{b_0 - b_1}{l}$ and the connection between $v_2 = v_1 \frac{b_0}{b_1}$

The obtained velocity is valid in the interval $l < x < l_1$ of the pipeline. Equation (3.56) shows the air flow velocity in the second zone, the value of which is times $n = \frac{b_0}{b_1}$ greater than the flow velocity in the separator. According to the formula we determine the pressure (3.42) on the section $x = l$.

$$p_2 = p_1(l) = \frac{b_0}{b_0 - kl} p_0 \left[1 - \frac{Q_0^2}{L^2 b_0^2 p_0 \rho_0} \left(\frac{kl}{b_0 - kl} \right) \right] \quad (3.59)$$

The calculation scheme assumes that the pressure during the transfer process at an arbitrary section is positive. This requirement must be met so that the process is resolved in a stationary form. If this condition is not met, the flow movement cannot be considered stationary. This condition occurs because the pressure has a positive value, so expression (3.44) will take the following form:

$$1 - q^2 \frac{kl}{b_0 - kl} > 0 \quad (3.60)$$

From this inequality we obtain the condition for the boundary angle

$$tg\alpha = k < \frac{b_0}{l} \cdot \frac{1}{q^2 + 1} \quad (3.61)$$

Where $q = \frac{Q^2}{L^2 b_0^2 p_0 \rho_0}$ b_0 height l, - length.

Taking into account the pressure, density and air flow rate in the transition section, $\alpha = arctg \frac{b_0}{l(1+q^2)}$, it is possible to select the boundary angle b_0 satisfying inequality (3.46). Figure 3.18 shows the graphs of the relationship between the angle a and the air flow rate Q for different values of the ratio b_0 / l ($L = 1.5м$, $b_0 = 0.5м$) and

$\rho_0 = 1.2кг/м^3$ pressure at values

$p_0 = 850\ Pa$ $p_0 = 1000\ Pa$

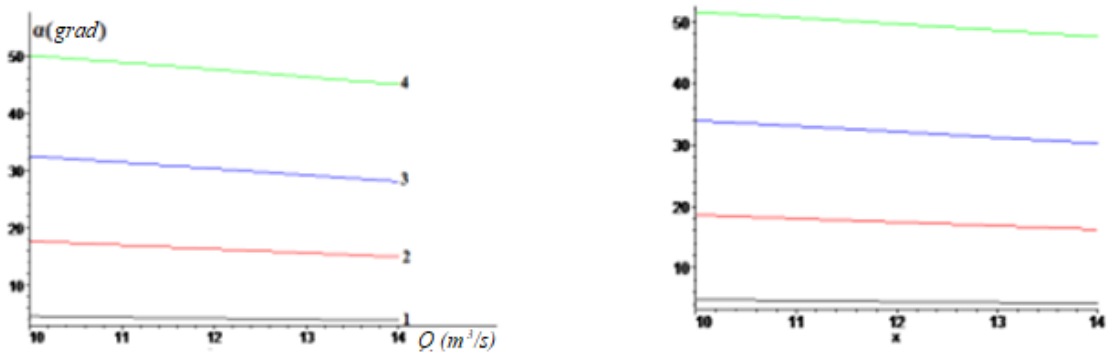

Fig. 3.18 Graphs of changes in air flow Q (m^3/s) depending on the pressure p_0 (Pa), the ratio b_0/l and the boundary angle a (deg) 1. b_0/l, 2. $b_0/l = 0{,}4$, 3. $b_0/l = 0{,}8$, 4. $b_0/l = 1{,}5$.

$\alpha = 15^0$ $\alpha = 35^0$

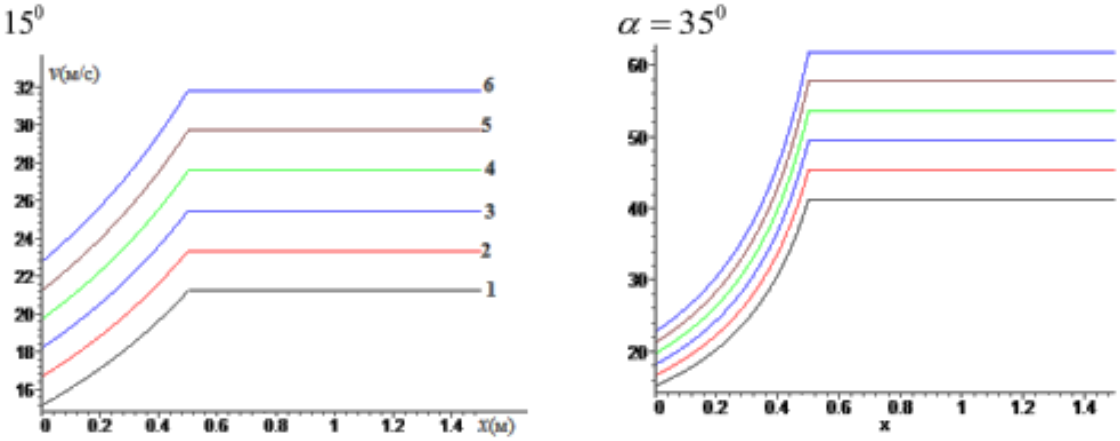

Fig. 3.19. Graphs of the dependence of air flow rate on angle.

Q (m^3 / s). 1. - Q = 10, 2.- Q = 11, 3. - Q=12, 4. - Q=13, 5. - Q=14, 6. - Q = 15,

$p_0 = 1200 Pa$ $p_0 = 1000\ Pa$

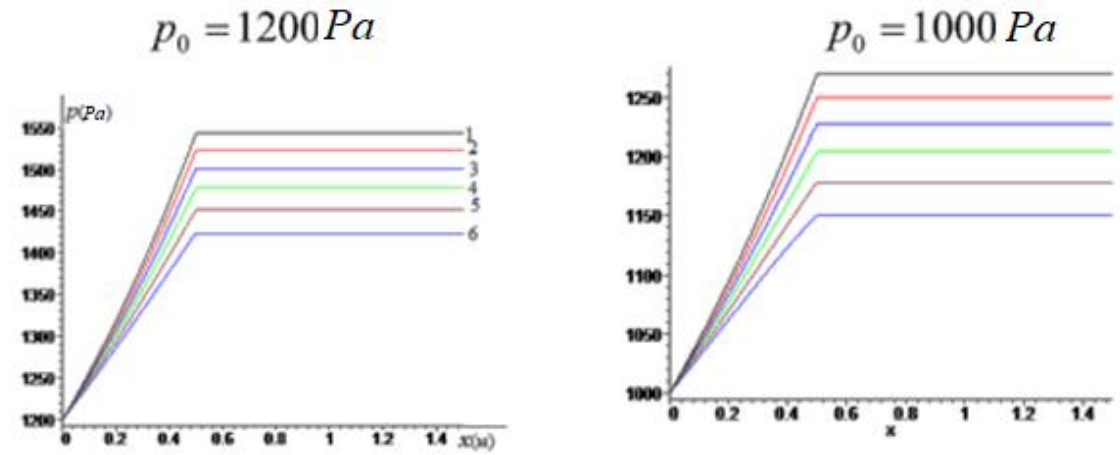

Fig. 3.20. Graphs of the dependence of air flow pressure on the x *coordinate* at an angle α = 15^0, and two values of the initial pressure and different values of air flow rate Q (m^3 / sec):

1 - Q = 10, 2.-Q = 11, 3. - Q = 12, 4.- Q = 13, 5. - Q = 14, 6.-Q = 15.

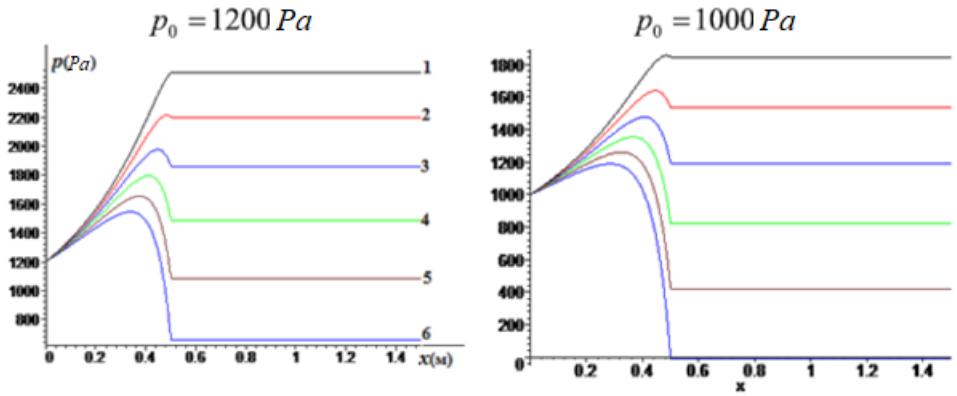

Fig. 3.21 Graphs of the dependence of air flow pressure on the x coordinate at an angle α = 35^0, and two values of the initial pressure and different values of air flow Q (m ^{3} / sec):
1- Q = 10, 2 - Q = 11.3 -Q = *12*, 4 -Q = 13., 5 - Q = 14, 6 - Q = 15.

Based on the graphs shown in Fig. 3.13-3.16, it is possible to determine the limiting value of the deflection angle a to ensure a continuous air flow in the pipe. For example, at b_0 = *0,5 m*, l = *0,5 m*, Q = 10 m ^{3} / s, α < 35° should correspond to the limiting angle for transmitting the air flow at a steady-state pressure of p_0 = 1000 Pa, that is, the value of the angle α should be less than 35 ^{0} to ensure steady-state movement. At the same pressure,
if the flow rate is Q = 10 m^3 / s, then α < 40°. That is, the taper of the branch pipe should be less than 40 ^{0}.

3.6. Study of the movement of cotton flakes in the guide chamber of the separator.

The separator chamber has a non-uniform cross-section. Let us assume that a particle moving with the air flow in the chamber does not exert a large influence on it. On a moving particle of mass m under the influence of the air flow, the active driving force of air F acts (Fig. 3.22).

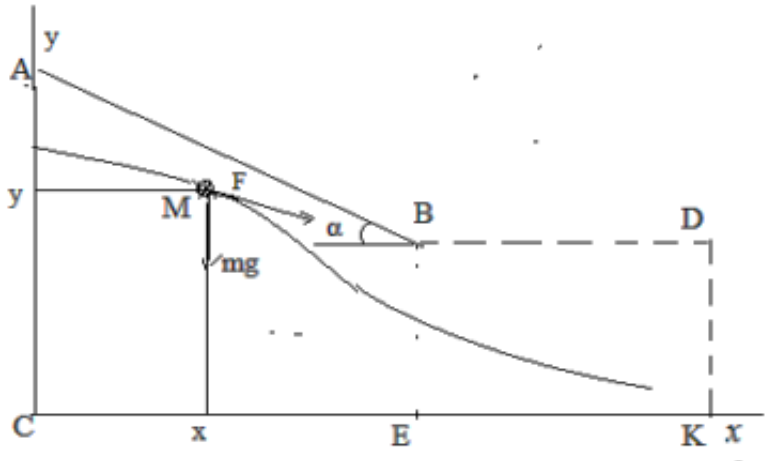

Fig. 3.22. Scheme of cotton fly movement in the separator chamber

Let us assume that the modulus of this force is proportional to the square of

the difference between the particle velocities and the air velocity $v_0 > 10$ m/s. In addition, taking the condition $tg\alpha = k < 1$, there will be no transverse motion in section AB. In this case, the equation of particle motion can be considered in a two-dimensional plane along the *xy axes*. In this case, we will express the fly as point *C* of the initial section of the pipe, direct the *OX axis* in the direction of the air flow, and the *OY axis* perpendicular to it, and the motion of the fly can be represented by the following equations:

$$m\ddot{x} = c\sqrt{(v_0 - \dot{x})^2 + \dot{y}^2}(v_0 - \dot{x}) \tag{3.62}$$

$$m\ddot{y} = c\sqrt{(v_0 - \dot{x})^2 + \dot{y}^2} + mg \tag{3.63}$$

where *c* is the proportionality coefficient of the air flow force,

v_0 - air flow rate, and its expression is expressed by the formulas:

$$v_0 = \frac{Q_0}{L\rho_0(b_0 - kx)}, \quad 0 < x < l \tag{3.64}$$

$$v_0 = v_1(l), l < x < l_1 \tag{3.65}$$

where l_1 is the length of the pipe. We see the following special case, in practice $\dot{y} < L(v_0 - \dot{x})$ the condition is satisfied. Therefore, we write equations (3.62) and (3.63) in the following form:

$$\ddot{x} = n(v_0 - \dot{x})^2 \tag{3.66}$$

$$\ddot{y} = n(v_0 - \dot{x})^2 + g \tag{3.67}$$

where $n = c/m$.

Equations (3.57) and (3.58) are nonlinear and require numerical integration. If the air flow velocity is not high enough, $v_0 < 5$ m/s, the air resistance force can be obtained in linear form.

$$m\ddot{x} = C_0(v_0 - \dot{x}) \tag{3.68}$$

$$m\ddot{y} = C_0\dot{y} + mg \tag{3.69}$$

The solution of equations (3.45) can be carried out on the basis of initial conditions.

$$x = 0,\ y = y_0,\ \dot{x} = v_n,\ \dot{y} = 0$$

where y_0 is the initial ordinate of the fly, $v_n < v_0(0)$ is the initial velocity of the fly in the pipe (separator chamber), to determine it, the separator performance can be used. $v_n = Q_n / Lb_0\rho_1$, Q_n - specific productivity per unit time, (kg/s), ρ_1 - raw material density. Taking into account formula (3.45) in the expression v_0 is the air flow velocity. Equation (3.51) takes the following form:

$$\ddot{x} + 2n_0\dot{x} = \frac{2n_0Q_0}{\rho_0 L(b_0 - kx)}, \qquad 2n_0 = \frac{C_0}{m} \tag{3.70}$$

Equation (3.70) is nonlinear and can be solved numerically. To transform it into a linear equation, we set the condition $\varepsilon = (b_0 - b_1)/b_0 < 1$ for the following case $\varepsilon^2 \approx 0$.

$$\frac{1}{b_0 - kx} = \frac{1}{b_0[1 - \frac{b_0 - b_1}{b_0 l}x]} \approx \frac{1}{b_0}$$ y (3.73)

$$\ddot{x} + 2n_0\dot{x} - 2n_0\varepsilon x / l = 2n_0 v_0$$

Where $\varepsilon = 1 - \frac{b_1}{b_0}$; $v_0 = \frac{Q_0}{\rho L b_0}$

Equation (3.71) is linear, and its general solution is as follows:

$$x = C_1 e^{k_1 t} + C_2 e^{k_2 t} - \frac{l}{\varepsilon} \qquad (3.72)$$

Under the following boundary conditions $x(0)=0$; $\dot{x}(0) = v_n$ we get the coefficients

$$C_1 = \frac{lk_2 - v_n\varepsilon}{k_2 - k_1};\ C_2 = \frac{v_n\varepsilon - lk_1}{k_2 - k_1}$$

Where $k_1 = -n(1 + \sqrt{1+\beta})$, $k_2 = -n(1 - \sqrt{1+\beta}$, $\beta = 2n\varepsilon / nl$, $n = C_0 / m$.

The motion of a particle along the axis ***oy*** (3.69) is determined by integrating the equation $y(0) = y_0$, $\dot{y}(0) = 0$ under the following boundary conditions. Its general solution is as follows:

$$y = A_1 e^{-2nt} + \frac{g}{2n} A_2$$

The coefficients A_1 and A_2 will be equal to:

$$A_1 = \frac{g}{4n^2};\qquad A_2 = y_0 - \frac{g}{4n^2}$$

And the equation of motion of a particle along the ordinate will take the following form:

$$y = -\frac{g}{4n^2}(1 - e^{-2nt}) + \frac{g}{2n}t + y_0 \qquad (3.73)$$

(3.48) solutions $0 < x < l$ as obtained for the interval. The equation in the range $l < x < l_1$ at $v_0 = v_1(l) = \frac{Q_0}{\rho_0 L(b_0 - kl)}$ should be written as follows

$$m\ddot{x} = (v_1 - \dot{x})C_0 \qquad (3.74)$$

Solving equation (3.74) for values $x(t_0) = l$, $\dot{x}(t_0) = v_{1n}$, we obtain the following roots of the equation:

$$v_{1n} = C_1 k_1 e^{k_1 t} + C_2 k_2 e^{k_2 t} \qquad (3.75)$$

At t_0 we obtain a particular solution $C_1 e^{k_1 t_0} + Ce^{k_2 t_0} - \frac{b_0}{\varepsilon} = l$.

$$x = x_2 = v_0 - (v_0 - v_{1n})[1 - \exp(-2nt)]/2n \qquad (3.76)$$

When studying the movement of the fly in the separator chamber at the angle of the guide wall of the branch pipe *a*, collisions with it are minimal. At such an angle of deviation of the guide, the fly does not experience impact in this zone. The following parameters were taken as a calculation: L = 1,1m, l = 0,5m, b_0 = 0,5m n = 0,35, p_0 = *1,2 kg* / m^3, p_1 = 50 kg / m^3, Q_n = 12000 kg/h.

Fig. 3.23 shows the trajectory of the flyer at two angle values in the first zone, where the line determines the trajectory of the flyer. From the analysis of the graphs it is evident that the trajectory of the flyer is a straight line in the direction of movement, and the speed of the flyer decreases along the angle α of the guide wall.

Figure 3.24 shows graphs of the change in particle velocity in the separator chamber over time for two values *of α*. It is shown that with an increase in the angle of the guide to the horizon, the velocity of the fly increases, and the location of the hole can partially reduce the velocity of the fly.

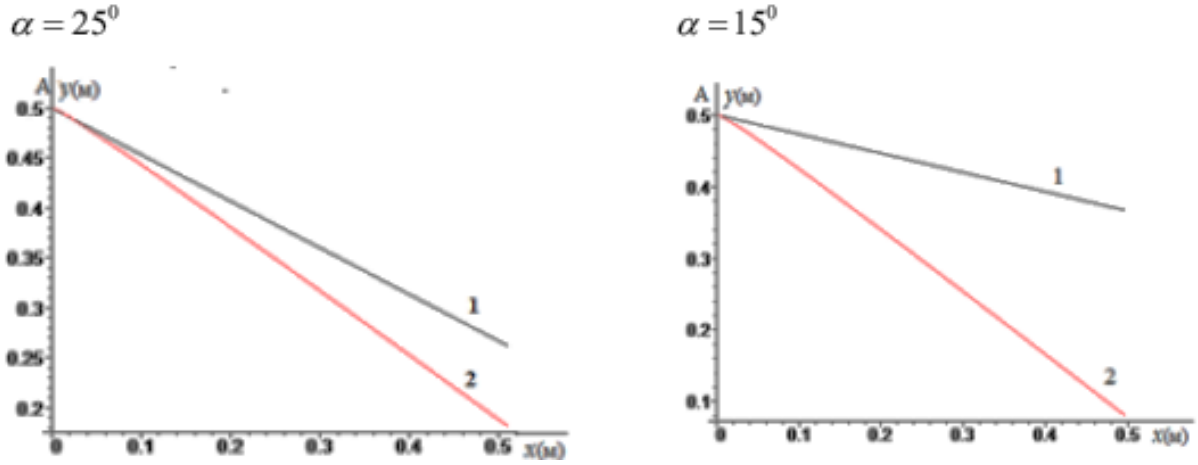

Fig. 3.23. Trajectory of the raw cotton fly in the first zone for two angle values (1 - position of the air duct wall, 2 - trajectory of the fly)

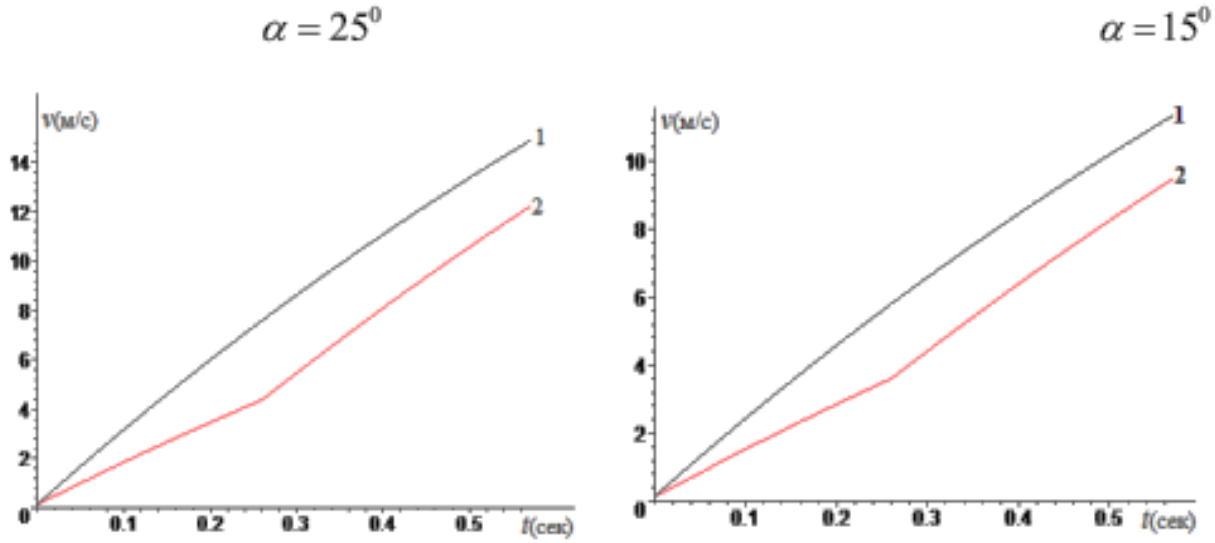

Fig. 3.24. Change in particle velocity over time in the separator chamber without a guide (line 1) and with a guide (line 2).

3.7. Justification of cotton separator parameters.

An analysis of the graphs (Fig. 3.25) shows that with an increase in the coefficient of friction of the fibers on the surface of the mesh holes, the force required to remove the cotton decreases. At an air speed of 20 m/s for the existing version of the separator, it reaches $14{,}65 \cdot 10^{-2}$ N, and for the recommended version, F_{cd} decreases to $8{,}9 \cdot 10^{-2}$ N.

At an air speed of 15 m/s for the recommended version of the separator mesh it is $7{,}6 \cdot 10^{-2}$ N. When the separator is operating it is necessary to ensure the lowest possible torque on the scraper shaft. Calculations were carried out using expression (3.76) for the recommended version of the mesh. Fig. 3.26 shows a graphical dependence of the change in torque on the scraper shaft on the total mass of cotton stuck to the mesh.

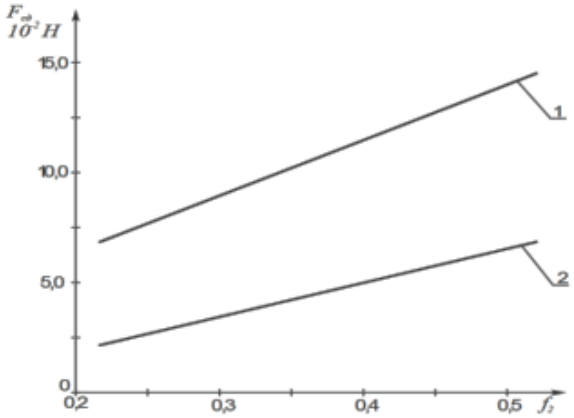

Fig. 3.25. Graphic dependences of the change in the shear force of cotton on the mesh surface of the separator on the change in the coefficient of friction of the fiber on the mesh
1-for the existing option; 2-for the recommended option

Analysis of the obtained graphs shows that with an increase in the total weight of cotton on the surface of the mesh from 1,22 kg to 6,0 kg, the torque on the scraper shaft increases from 0,51 *Nm* up to 4,29 *Nm* in the recommended version of the grid at v = 20 m/s. In the existing version of the grid, the torque on the scraper shaft reaches 5,24 *Nm*. It should be noted that the low torque value on the scraper shaft for the recommended version of the grid is explained by the fact that the friction force of the fibers on the surface of the grid hole will be less due to the small number of fibers, as well as the reduction in the projection of the friction force due to the angle α.

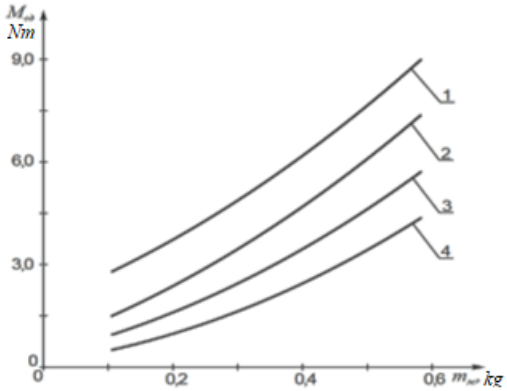

1.3 - for the existing option; 2.4 - for the recommended option,
1.3 - at v = 20 m/s; 2.4 - at vu = 15 m/s

Fig. 3.26. Dependences of the change in torque on the scraper shaft on the total mass of cotton on the screen.

Fig. 3.27 shows the graphical dependence of the change in moment on the change in the angle of inclination of the axis of the conical holes of the grid.

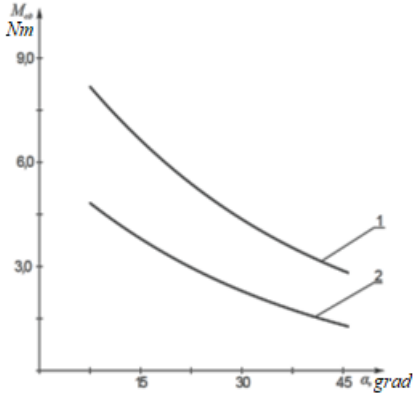

1-at m_{sl} = 7,0 kg; 1-at m_{sl} = 5,0 kg;

Fig.3.27. Variation of the torque on the scraper shaft from a change in the axis tilt mesh holes.

To justify the angle of inclination of the axis of the conical holes of the separating mesh, corresponding experiments were carried out for five variants of meshes with cylindrical and conical holes at an angle α (Fig. 3.20) of inclination of the axes of the holes: 0^0, 15^0, 30^0, 45^0, 60^0. The experiments were carried out at three moisture contents of cotton W = 12.5%, 10.5%, 9.5%, respectively.

Based on the results of the experiments, dependencies were obtained (Fig. 3.28) for the change in the amount of free fiber from the change in the angle of inclination of the cylindrical and conical holes of the separator mesh. Analysis of the graphs shows that at an inclination angle of the axes of the mesh holes of 45^0 for both cylindrical and conical holes, the amount of free fiber is the smallest. But with conical holes at $\alpha = 45^0$ and a humidity of 12.5%, there will be less free fiber, (0.3 - 0.4) 10^{-2} % compared to the serial version of the mesh. At a cotton humidity of 9.5%, this difference reaches (0.35 - 0.45) 10^{-2} %.

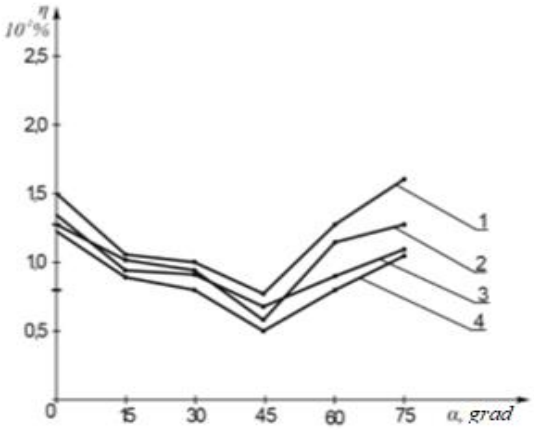

1 and 2 - at - W = 12,5%; 3 and 4 - at - W = 9,5%; 1 and 3 - with cylindrical holes; 2 and 4 - with conical holes.

Fig.3.28. Amount of free fiber depending on the change in angle inclination of the holes of the dividing grid.

Therefore, in the recommended variant α = 45° the free fiber is significantly reduced. It should be noted that in the recommended variant of the mesh with conical holes with an axis inclination of 45 ° the seed damage is reduced by (20÷30)% compared to the serial variant.

3.8. Analysis of the movement of a cotton particle along the curved surface of a separator guide

The calculation scheme of a particle with a curved surface, guiding is shown in Fig. 3.29.

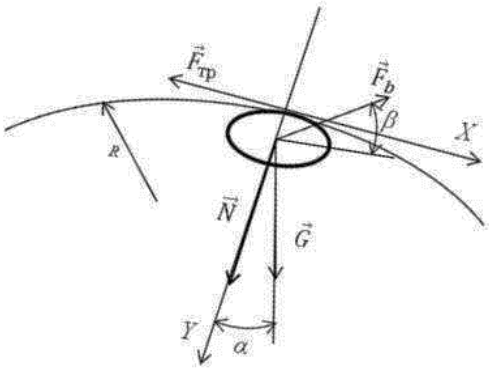

Fig.3.29. Calculation scheme of a guide with a curved surface

The forces acting on a cotton particle are: G - the force of weight, N - the reaction force, F_b - air force (blowing flow), F_{fr} - friction force between the cotton particle and the surface of the guide. Let us write the basic equation of dynamics in projections on the Lagrange coordinate axes:

$$m\ddot{x} = F_b cos\beta - F_{тр} + Gsin\alpha$$
$$m\ddot{y} = Gcos\alpha - F_b sin\beta - N \qquad (3.77)$$

When a cotton particle interacts with the surface of the guide, its movement along the *y- axis* will be limited, because the cotton particle in this zone will be in

contact with the surface, i.e. y=0.

Then the second equation of the system takes the following form.

$$N = G\cos\alpha - F_b\sin\beta \quad (3.78)$$

Moreover, given that $G = mg$; $F_b = kv^2$,

and, substituting (3.77) into (3.78), we have

$$m\ddot{x} = mg\sin\alpha + kv_b\cos\beta - f(mg\cos\alpha - kv_b^2\beta) \quad (3.79)$$

where m is the mass of the cotton particle; g is the acceleration of gravity; kv_b is the air velocity; α is the angle between the vector of the weight force and the *y*-axis; β is the angle between the vector of the aerodynamic force and the *x*-axis; f is the coefficient of friction of the cotton on the surface of the guide.

From (3.79) after integration we obtain an expression for determining the law of motion of a cotton particle along the x-axis:

$$x = \frac{1}{kv_b^2(f\sin\beta-\cos\beta)}\ln\left\{\frac{[gf-kv_b^2(f\sin\beta-\cos\beta)]}{[g(\sin\alpha+f\cos\alpha)-kv_b^2(f\sin\beta-\cos\beta)]}\right\} \quad (3.80)$$

In this case, the speed of movement of the cotton particle is determined taking into account $x = R\sin\beta$

$$V = \sqrt{\frac{[g(\sin\alpha+f\cos\alpha)-[gf-kv_b^2(f\sin\beta-\cos\beta)]e-R\sin\beta(f\sin\beta-\cos\beta)}{f\sin\beta-\cos\beta}} \quad (3.81)$$

Figure 3.30 shows the graphical dependences of the velocity of the ejection of a cotton particle when leaving contact with a curved surface on the velocity of the supplied air. Analysis of the graphs shows that with an increase in air velocity, the velocity of the ejection of cotton particles increases according to a nonlinear pattern.

It should be noted that a change in the moisture content of the original cotton leads to a change not only in the mass of the cotton particles, but also to an increase in the friction coefficient. The higher the friction coefficient, the lower the cotton ejection velocity (see Fig. 3.30, a, b, c, curves 1,2,3). The location of the cotton particles in the initial interaction zone with the guide surface is important. In this case, the greater the angle a, the greater (see Fig. 3.30, c) V_x. An increase in the radius of the separator guide surface also leads to an increase in the cotton particle ejection velocity. This is explained by the fact that with an increase in R, the surface approaches the plane, which leads to a decrease in the braking of the cotton particles (see Fig. 3.31, curves 1,2,3).

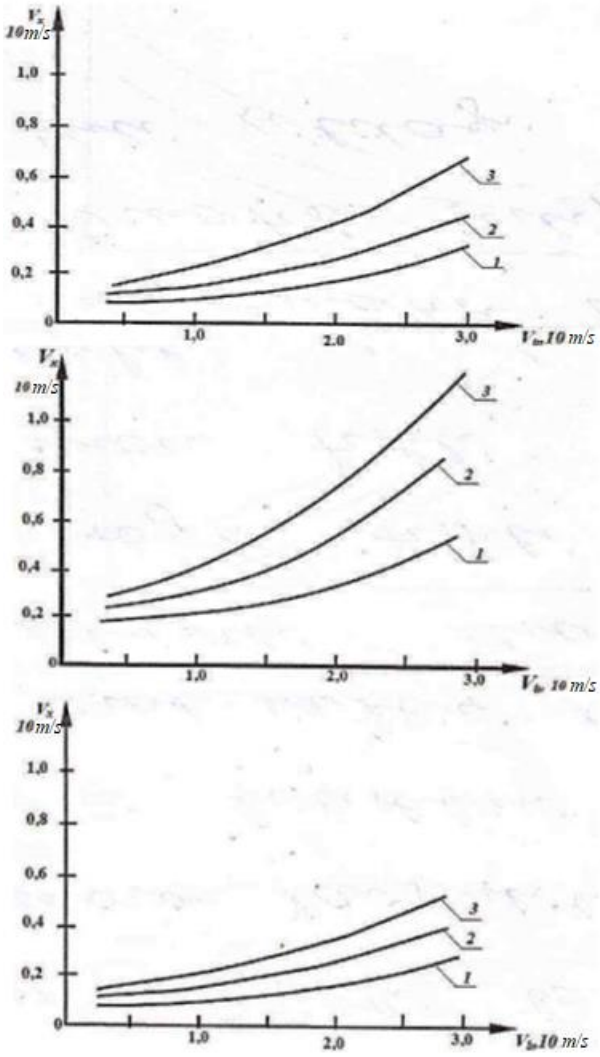

a- at $\alpha = 20^0$

b- at $\alpha = 35^0$

c- at $\alpha = 45^0$

Fig. 3.30. Graphical dependence of the change in the velocity of the ejected cotton particle upon exiting contact with the surface is directed from the change in the velocity of the supplied air. 1 – at f =0,35; 2 – at f =0,30; 3 – at f =0,25.

An increase in the coefficient of friction leads to a decrease in the speed of the height of the cotton particles (see Fig. 3.32).

Results of comparative production tests of a cotton separator-cleaner.

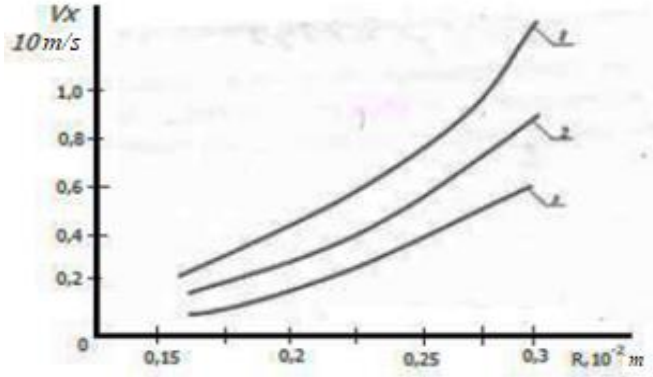

Fig.3.31. Graphic dependences of the change in the velocity of the ejection of a cotton particle when leaving contact with the surface of the direction from the

change in the radius of curvature of the guide

Based on the substantiated parameters of the separator, a prototype of the design was designed and manufactured. Comparative production tests of the separator were conducted.

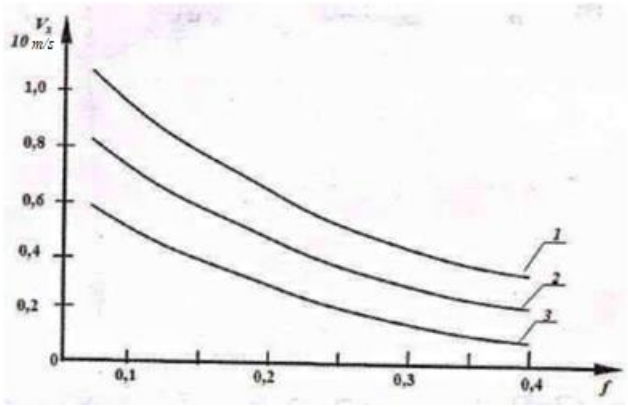

Fig.3.32. Regularities of change in the velocity of the ejection of a cotton particle with curved surface of the guide from the coefficient of friction.

3.9. Finite element modeling of the movement of cotton-air mixture in a cotton separator

Section 2.2 examines the operation of the SS-15 cotton separator, designed to separate raw cotton from the air flow transporting it.

One of the shortcomings of the separators currently in use is the increased crushing of the seeds, which occurs as a result of the impact of the cotton voles, moving by inertia, on the wall of the separating chamber. In this section, design measures are proposed to eliminate this shortcoming. They boil down to installing a guide 3 (Fig. 2.2), which deflects the air flow entering the separating chamber and, thus, reduces the force of the impact of the raw cotton voles on the wall. In [105], the position of the visor, which ensures an acceptable level of seed crushing, is experimentally determined.

For a more detailed study of the aerodynamic processes occurring in the CC-15A cotton separator, finite element modeling was carried out in the ANSYS environment. CFX. Since the separator design has a plane of symmetry, half of the design was used as a geometric model. Fig. 3.33 shows a model of a cavity in which a mixture of air and raw cotton moves with a finite element mesh applied to it. The mesh is tetrahedral, the maximum element size is 3 cm. For better flow resolution in the boundary layer, orthogonal layers of a regular mesh of 10 layers with a total thickness of 40 mm were created near the walls. In total, the model has about 600 thousand elements and 140 thousand nodes.

To simulate the perforated wall, 3 (Fig. 3.33.) between the separating and air chambers holding back the cotton particles, the model included two domains, the interface between which allowed the pressure difference to be set according to a given law. In this model, the difference was calculated depending on the average air velocity through the interface surfaces according to the Darcy-Weisbach formula for local resistance in the flow [106]

$$\Delta P = \xi \frac{v^2}{2} \rho \quad (3.82)$$

where ΔP is the pressure loss due to hydraulic resistance

ξ — local resistance coefficient (loss coefficient);

ρ - air density;

v - flow velocity.

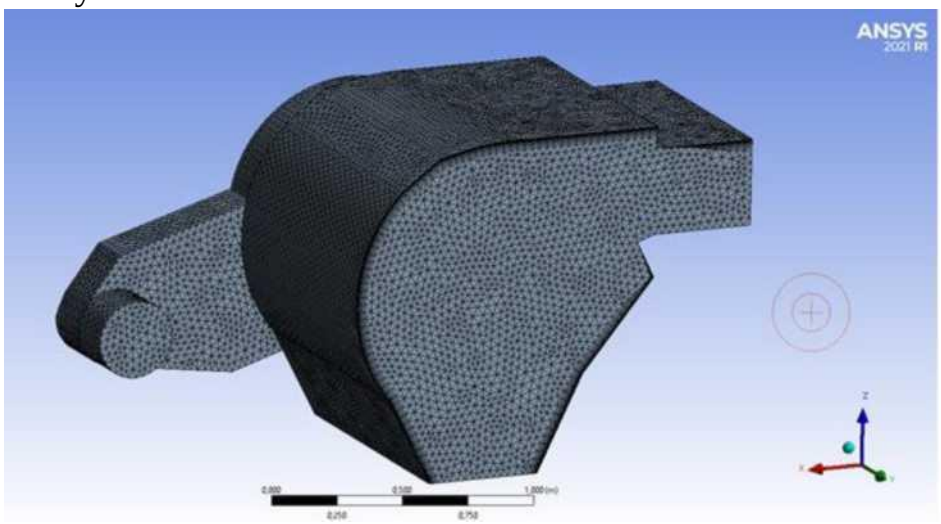

Fig. 3.33. Geometric model with finite element mesh

In the simulation, the cotton fly particles were represented as balls with a mass equal to the mass of the fly particle and a diameter that ensured a hovering speed equal to the hovering speed of the fly.

The mass of the fly was taken to be 0,25 g [29]. In [107] the average value of the volume of cotton fly is given, which is 5,2 cm ^{3}. This allows us to calculate the radius of the sphere simulating the fly in this calculation, which is 1.6 cm.

The number of particles in the flow is calculated as follows. The separator capacity of the machine is 3 - 7 t/h. At maximum capacity, 1,9 kg/s of raw cotton will pass through the inlet pipe, which corresponds to 9500 volatiles per second.

Based on the calculation results, a comparison was made between two variants of the cotton separator design: a serial one (Fig. 3.33) and a modernized one, in the inlet pipe of which a guide was installed, which should ensure the deviation of the cotton-air mixture towards the vacuum valve (Fig. 3.34). Fig. 3.34 shows the trajectories of cotton volatiles in the volume of the separator's separation chamber and in the central section (Fig. 3.35)

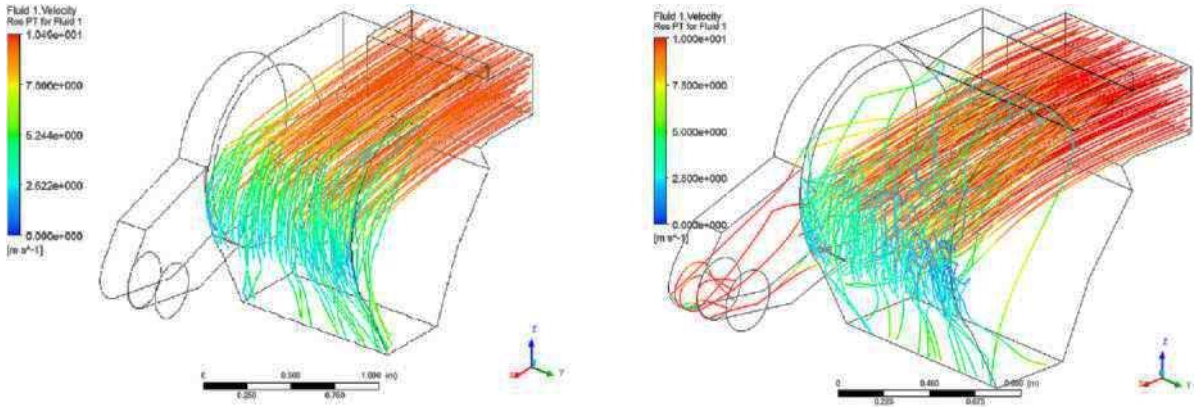

Fig. 3.34. Trajectories of cotton particles (3D picture) in section (a - existing separator scheme, proposed separator scheme)

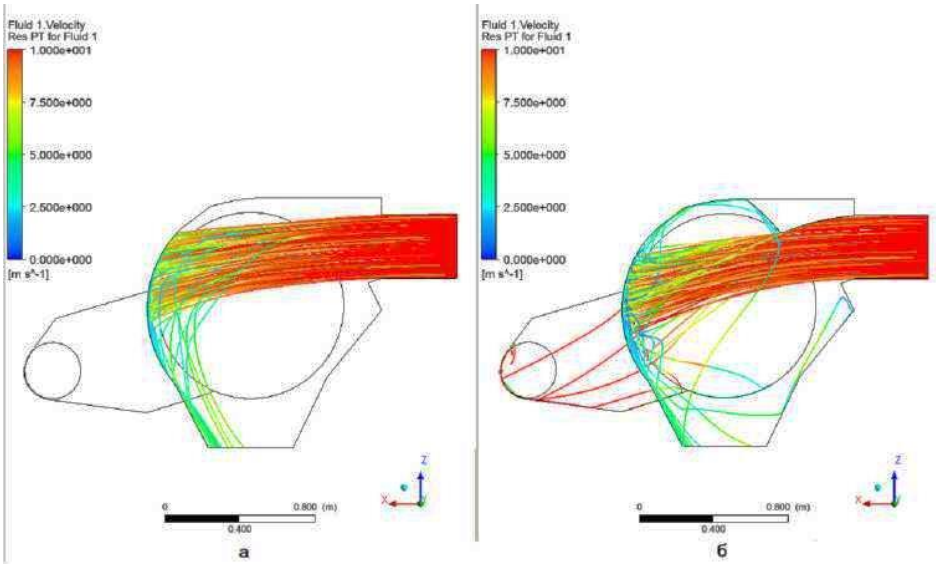

Fig. 3.35. Trajectories of cotton particles in the central section (a - existing separator scheme, b - proposed separator scheme)

From the figures it is clear that the installation of the guide results in the deflection of the flow of fly ash downwards towards the vacuum valve.

The air flow lines for the two variants are shown in Fig. 3.36.

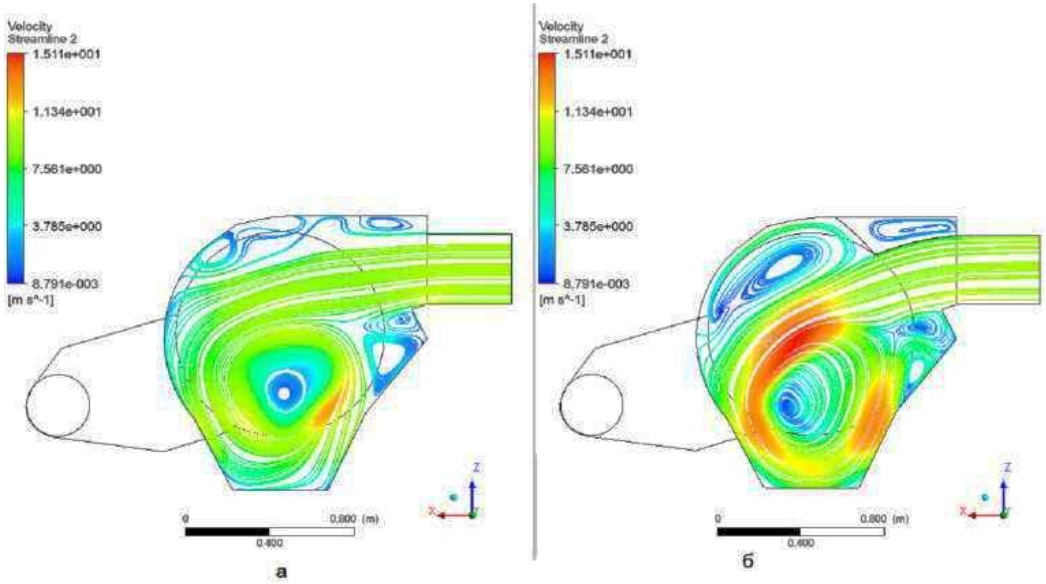

Fig. 3.36. Air flow lines (a - existing separator scheme, b - proposed separator scheme)

The flow line pattern shows that when a guide is installed in the upper part of the separation chamber, a vortex is formed, the maintenance of which consumes a certain amount of flow energy, which can contribute to a decrease in the flow velocity in the central part of the chamber. This is confirmed by the turbulent viscosity distribution pattern shown in Fig. 3.37.

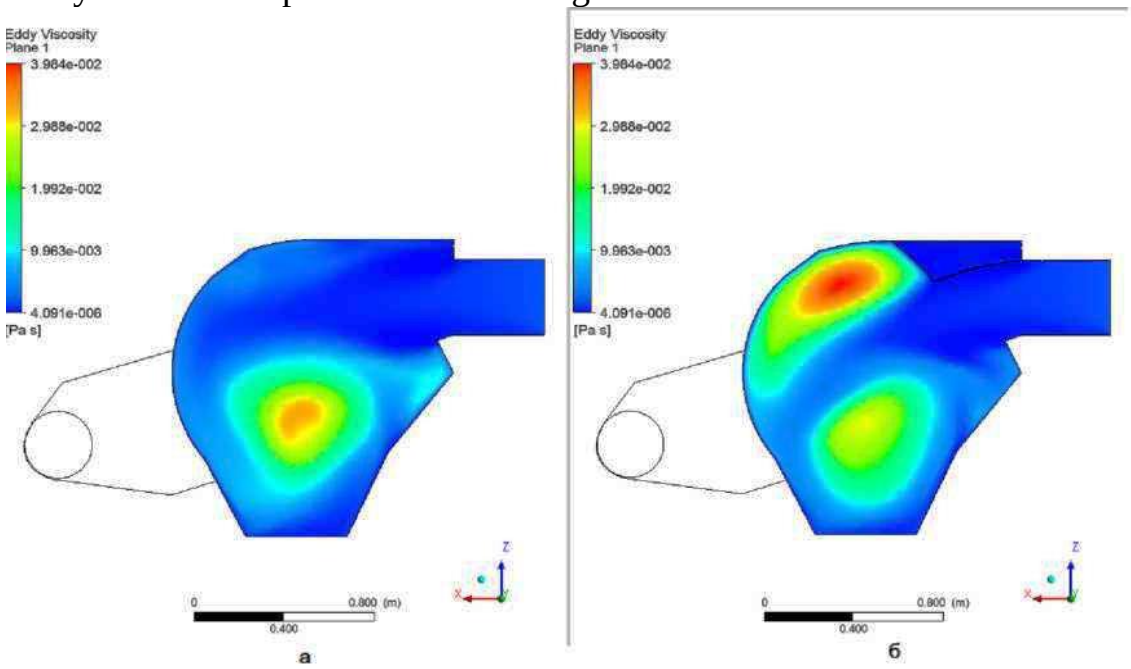

Fig. 3.37. Turbulent viscosity (a - existing separator scheme, b - proposed separator scheme)

Fig. 3.38 shows the field of air flow velocities in the separating chamber. Comparison of the figures shows that compression of the flow by the guide leads to an increase in the air velocity in the separating chamber. However, as can be seen from Fig. 5, the velocities are directed tangentially to the wall, so an increase in velocity as a whole should not lead to an increase in the velocity of impact of the flies with the wall of the separating chamber and crushing of the seeds.

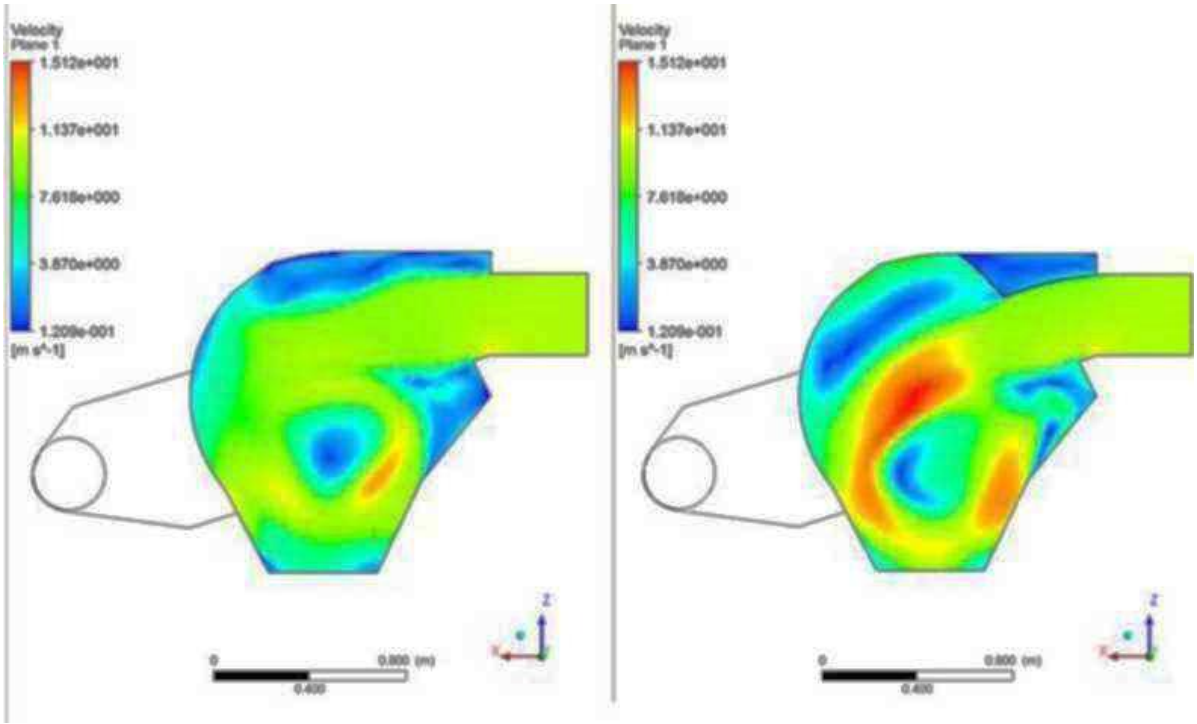

Fig. 3.38. Air velocity field in the separation chamber (a - existing separator design, b - proposed separator design)

ANSYS C FX has a software module that allows for computational experiments to determine the mutual influence of various factors included in the mathematical model. In this way, it is possible to construct the dependences of the averaged pressure force of cotton buds on the wall of the separation chamber calculated within the framework of the developed model. This parameter does not allow for obtaining the impact force of each bud and assessing the probability of seed destruction, but it does allow for comparison of various technological modes and design options.

Fig. 3.39 shows the dependence of the average force of pressure of the flywheels on the wall of the separation chamber on the velocity of the flywheels at the inlet for the compared design options.

As can be seen from the graphs provided, the proposed version of the separator with a flow guide in the separation chamber provides a reduction in the impact force of the flywheels on the wall of the separation chamber by up to 18%, which, as experiments show, allows the flywheels to be deflected from a direct impact with the wall of the separation chamber and the flow velocity to be reduced due to the formation of a turbulent vortex behind the visor, which intensively absorbs energy.

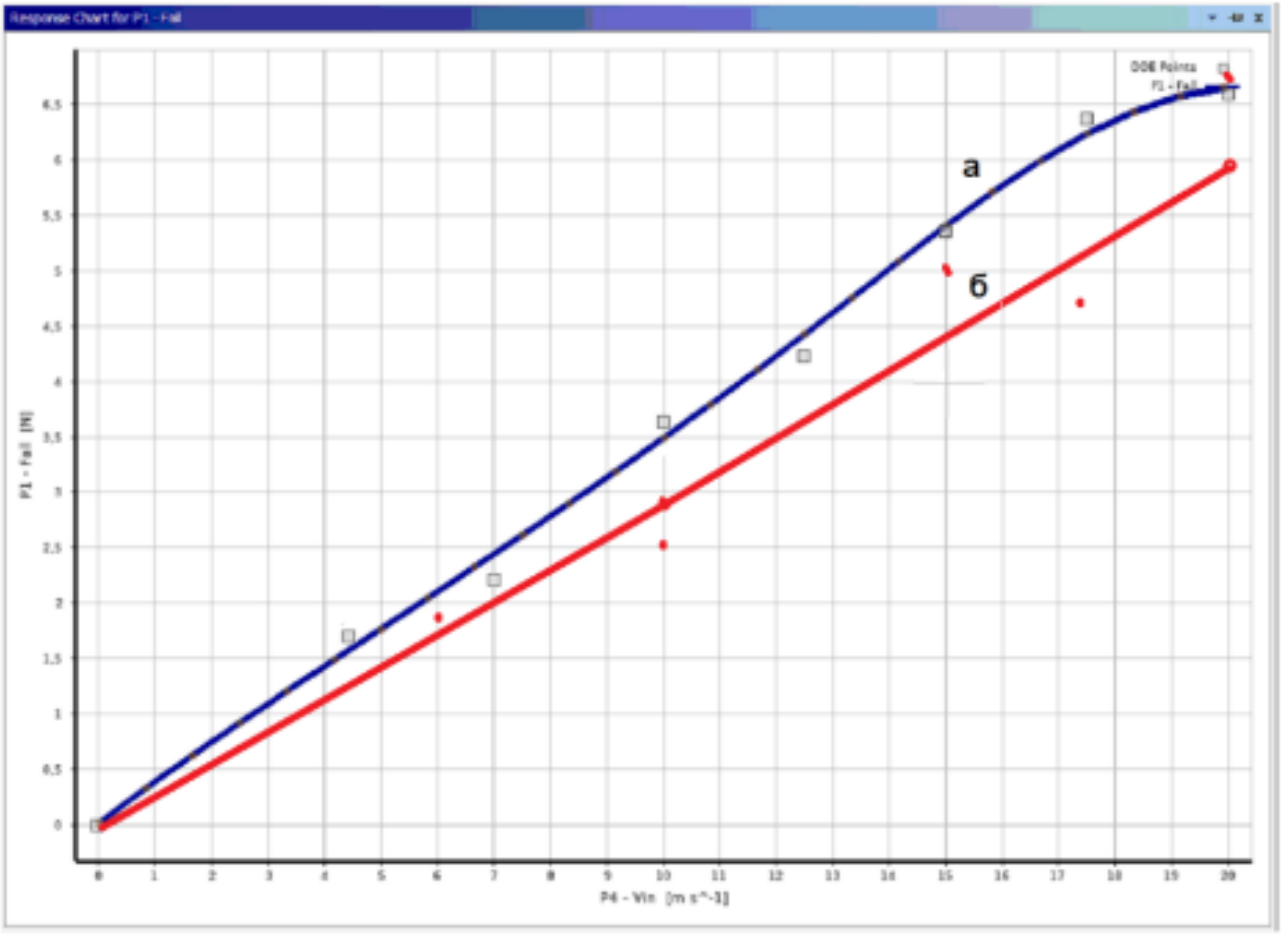

Fig. 3.39. Total force of particle impact on the walls depending on the velocity of the cotton-air mixture at the inlet
(a - existing separator scheme, b - proposed separator scheme).

3.10. Conclusions on Chapter 3

1. The law of distribution of the velocity and density of raw cotton on the surface of the perforated mesh of the separator is determined. Graphic dependences of the change in the thickness of the layer and the density of cotton on the surface of the mesh on the change in the pole angle and pressure are constructed. Their values are substantiated.
2. It was found that the change in pressure is proportional to the thickness of the cotton layer, the speed of which increases on the surface of the mesh relative to the polar angle and decreases from the density value.
3. The patterns of movement of a part of cotton on the surface of the net are determined. A formula for calculating the radius of the location of cotton particles on the surface of the net is obtained.
4. The influence of the law of motion of the separator scraper on the fixation of cotton bats on the net and on the efficiency of removing raw cotton from the surface of the nets is determined. The required angular dependence of the

speed of the scrapers is determined for different parameters of the net.

5. The dependence of the height of the raw cotton layer and the value of the pole angle on the air pressure in the separating chamber was established. As a result of theoretical and practical research, a separator with an isolating chamber was proposed.

6. Approximate calculation formulas for determining the speed and pressure of a stationary air flow in a channel with a variable cross-section are obtained. The condition for the stationarity of the flow speed is determined, at which the magnitude of the channel expansion angle is practically independent of the air flow rate.

7. The regularities of cotton fly movement in the separator are determined taking into account the flow guide. The dependences of the trajectories and speeds of cotton fly movement on the change in the separator guide angle are obtained.

8. A formula has been obtained for calculating the force required to shift a layer of cotton on a separator mesh, taking into account the shape of the holes in the meshes.

9. Graphic dependencies of the change in the shear force of cotton bats are constructed taking into account the change in the angle of inclination of the holes, their coordinates, the coefficient of friction and air speed. The parameters of the grid and conical holes are substantiated, at which the minimum value of their shear forces is ensured.

10. A formula for determining the displacement and speed of a cotton particle on the curved surface of a composite separator guide has been obtained.

11. Based on finite element analysis, the distribution of air flows, the trajectories of the fly particles and the force of interaction of the fly particle flow with the wall of the separator separation chamber were determined. The efficiency of the flow guide installed at the entrance to the separation chamber was confirmed.

CHAPTER 4. THEORETICAL JUSTIFICATION OF TECHNOLOGICAL PARAMETERS OF COTTON CLEANERS

4.1. Small debris cleaners

4.1.1. Influence of the flyer movement mode on the interaction of cotton with the mesh

In the technology of cleaning raw cotton in a fine debris cleaner using a multifaceted mesh, it is important to determine the reaction force, which depends on the angle of interaction and the angular velocity of the drum. Fig. 4.1 shows the calculation scheme of the cleaning zone. It is known that at the moment of the cotton fly flying out from the end of the drum peg, it is mainly affected by the centrifugal force. At the same time, in the free flight zone, the fly is additionally affected by the forces of air resistance and the force of gravity. Considering that the gap between the ends of the pegs and the mesh surface is small, and, in the first approximation, only the centrifugal force was taken into account as the main one, as well as the variability of the rotation of the peg drum, we have:

$$F_{cen} = m_l R_K \left(\omega_{av} + \omega \sin \alpha t\right)^2 \tag{4.1}$$

where, m_l - mass of the fly, R_K - radius and amplitude of the variable part of the angular velocity of the peg drum.

It should be noted that, as noted in the work of G. I. Miroshnichenko [29; pp. 137-140], the speed of interaction of the fly with the mesh surface is determined from the expression:

$$V_l = \sqrt{\frac{m_l g}{c_1}} \tag{4.2}$$

where g is the acceleration of gravity, c_1 is the drag coefficient, $c_1 \approx 0.65$.

But the expression does not take into account the centrifugal force acting on the fly. At the same time, taking into account the centrifugal force according to [108], we obtain:

$$\omega_d = \frac{\left(1 + k_b\right)\cos\alpha}{t_i} \tag{4.3}$$

where, k_b *is* the coefficient of recovery of the fly on impact, *(0,3 – 0,35);* α is the angle of inclination of the fly's flight speed, t_i is the time of impulse interaction *(0,015÷0,030) s.*

The reaction forces, according to Fig. 4.1, are determined from the expressions for the elastic interaction of the flyer with the grid:

$$\overline{F_1} = \overline{F_1'} + \overline{F_2}\,;\ \overline{F_2} = \overline{F_2'} + \overline{F_2''}\,;\ \overline{F_3} = \overline{F_3'} + \overline{F_3''}\,;\ \overline{F_4} = \overline{F_4'} + \overline{F_4''} \tag{4.4}$$

or $F_1' = F_1 \cos\alpha_1;\ F_2' = F_2 \cos\alpha_2;\ F_3' = F_3 \cos\alpha_3;\ F_4' = F_4 \cos\alpha_4;$

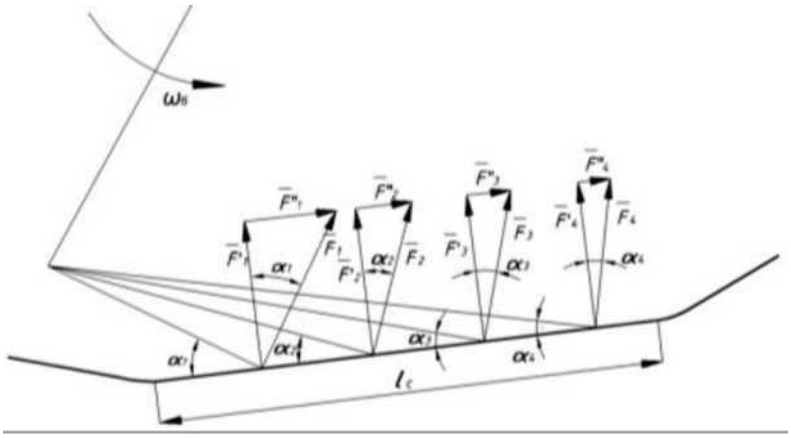

Fig. 4.1. Calculation scheme of the cotton cleaning zone from small debris

It is known that the linear velocity of cotton flies when interacting with the net should not exceed *11,5 m/s,* at which the damage to seeds and cotton fibers increases significantly [109; pp. 7-8]. Therefore, it is advisable to accept, taking into account (4.2) and (4.4)

$$\alpha_i \geq \arccos\left[\frac{\left(\omega_{av} + \omega_0 \sin\alpha t\right) t_i}{1 + k_b}\right] \tag{4.5}$$

To ensure condition (4.5) with the initial values of the cleaning zone parameters, the angle α_i is obtained within the limits:

$$\alpha_i = \left(\frac{2\pi}{9} \div \frac{\pi}{4}\right) \tag{4.6}$$

4.1.2. Analysis of the interaction of cotton filaments with the multifaceted mesh surface of the cleaner

During the process of cleaning cotton from small debris, the fly hits the mesh surface and the impurities are released from it. In this case, the cotton fly flies off the surface of the splitter under the action of centrifugal force. Given the relatively small gap between the splitters and the mesh surface, in the first approximation, the speed at the moment of impact of the fly with the mesh surface will be determined by:

$$V_l \leq \omega_d \cdot R_k \tag{4.7}$$

where ω_b is the angular velocity of the peg drum, R_k is the radius of the tops of the drum pegs.

At the same time, as R.Z. Burnashev notes, the loss of speed in the zone of

the fly reaches 10% [110; pp. 7-8]. According to the calculation scheme, taking into account the angle of inclination of the cotton fly speed P, the vertical component of which determines the actual impact impulse, and the horizontal component determines the speed of the fly movement along the mesh surface of the cleaner:

$$\overline{V}_l = \overline{V}'_l + \overline{V}''_l;\ \overline{V}_{l0} = \overline{V}'_{l0} + \overline{V}''_{l0}; \tag{4.8}$$

Where $V'_l = V_l \cos\beta;\ V''_l = V_l \sin\beta;\ V'_{l0} = V_{l0} \cos\beta;\ V''_{l0} = V_{l0} \sin\beta;$

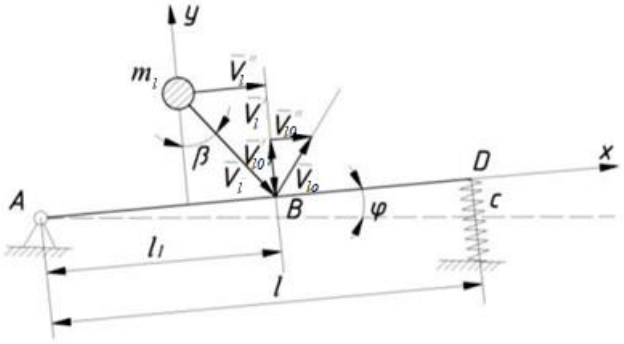

Fig.4.2. Calculation scheme for determining the interaction of the fly with the mesh surface

In this case, the interaction of the cotton fly with the mesh surface is considered elastic, therefore the angle of reflection will also be *β*. The determination of the post-impact velocities of the cotton fly and the mesh surface was carried out using the Lagrange method [111; pp. 38-40], according to the calculation scheme in Fig. 4.2. In this case, the generalized coordinates were taken *to be y* for the fly and *φ* for the mesh surface.

The kinetic energy of the system will be equal to:

$$T = \frac{1}{2} m_{cl} \dot{y}^2 + \frac{1}{2} \frac{m_c l^2}{3} \dot{\varphi}_c^2 \tag{4.7}$$

The derivatives of kinetic energy will be:

$$\frac{\partial T}{\partial \dot{y}} = m_{cl}\dot{y};\quad \frac{\partial}{\partial t}\left(\frac{\partial T}{\partial \dot{y}}\right) = m_{cl}\ddot{y};\quad \frac{\partial T}{\partial \dot{\varphi}} = \frac{ml^2}{3}\dot{\varphi};\quad \frac{\partial}{\partial t}\left(\frac{\partial T}{\partial \dot{\varphi}}\right) = \frac{ml^2}{3}\ddot{\varphi}; \tag{4.8}$$

It should be noted that the velocity of the cotton fly at the beginning of the impact on the mesh surface is equal to $\overline{V_l}$, and its projection on the y-axis is negative, according to (4.6) $\overline{V_l}'$. At the beginning of the impact, the mesh surface on the elastic base is at rest, i.e. the initial angular velocity of the mesh is zero. At the end of the impact, the velocity of the cotton fly along the y-axis will be $\overline{V_{l0}}'$,

and the velocity of the mesh after the impact will be $\dot{\varphi}'_c$.

Based on these considerations, the increments of the partial derivatives (4.8) of the kinetic energy of the system with respect to the generalized velocities are equal to:

$$\Delta\left(\frac{\partial T}{\partial \dot{y}}\right) = m_{cl}(\dot{y} + \dot{y}); \quad \Delta\left(\frac{\partial T}{\partial \dot{\varphi}_c}\right) = \frac{m_c l^2}{3}\dot{\varphi}'_c; \tag{4.9}$$

According to the calculation scheme, the generalized impulses are determined as follows:

$$P_{ly} = \frac{\delta A}{\delta \dot{y}}\Big|_{\delta\varphi_c=0} = \frac{S\delta y}{\delta y} = S,$$
$$P_{cy} = \frac{\delta A}{\delta \dot{\varphi}_c}\Big|_{\delta y=0} = \frac{Sl_1\delta\varphi_c}{\delta\varphi_c} = Sl_1 \tag{4.10}$$

It is known [111; pp. 19-20] that the Lagrange equations for impact are linear equations relative to the velocities of the cotton fly and the net after impact. For the system under consideration, they are written in the following form:

$$m_l(\dot{y}' + \dot{y}) = S$$
$$\frac{m_c l^2}{3}\dot{\varphi}_c = S \cdot l_1 \tag{4.11}$$

In a cotton cleaner for small debris, the impact of the cotton flakes occurs when it interacts with the surface of the mesh. Its speed determines subsequent vibrations of the mesh. The relationship between the speeds is achieved through the coefficient of recovery during impact. This coefficient takes into account the relative speeds of the interacting elements, in projections on the y-axis. In this case, we have:

$$k = -\frac{\left(\dot{y}' + \dot{\varphi}'_c l_1\right)}{-\dot{y}} \tag{4.12}$$

From equation (4.35) we obtain the dependences of the velocities before and after the impact.

$$k\dot{y} = \left(\dot{y}' + \dot{\varphi}'_c l_1\right) \tag{4.13}$$

Then the system of linear equations will be:

$$\left(\dot{y}' + \dot{\varphi}'_c l_1\right) = k\dot{y}$$
$$\dot{y}' - \frac{m_c l^2 - \dot{\varphi}'_c}{3m_n l_1} = -\dot{y} \tag{4.14}$$

Having solved (4.14), we obtain the velocity of the cotton fly after impact with the mesh surface

$$\dot{y}' = \left(\frac{km_c l^2 - 3m_n l_1^2}{m_n l^2 + 3m_n l_1^2}\right)\dot{y}$$

and the angular velocity of the net after impact

$$\dot{\varphi}'_c = \left(\frac{3m_1 l_1 (k+1)}{m_c l^2 + 3m_1 l_1^2} \right) \dot{y}$$

Taking into account (4.6), we have the velocity of the flyer along the *y axis*

$$V_l' = \left(\frac{\left(\cos\beta + \frac{\dot{\varphi}'_c l_1}{V_l} \right) m_l l^2 - 3m_l l_1^2}{m_c l^2 + 3m_l l_1^2} \right) V_l \cos\beta ; \qquad (4.15)$$

On the *x- axis* we have: $V_l'' = V_l \sin\beta$;

The important thing here is the amount of rebound of the cotton bats after hitting the mesh surface:

$$h_l = \left[\frac{\left(\cos\beta + \frac{\dot{\varphi}_c l_1}{V_x} \right) m_l l^2 - 3m_l l_1^2}{m_c l^2 + 3m_l l_1^2} \right] t_n; \qquad (4.16)$$

Based on the numerical solution of expressions (4.15) and (4.16), graphical dependencies of the change in the speed and the magnitude of the rebound of the cotton fly after impact with the mesh surface are constructed depending on the parameters of the system. Fig. 4.3 shows graphical dependencies of the change in the speed of movement of the cotton fly on a multifaceted mesh surface on the change in the angle of inclination of the flight of the fly in the cleaning zone.

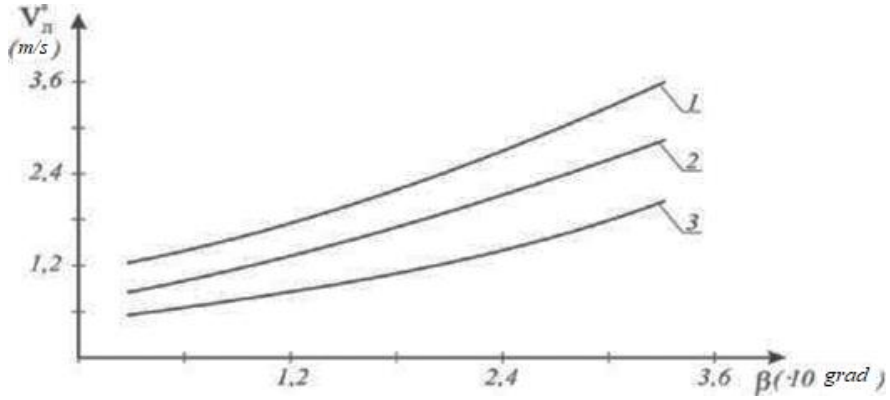

Fig.4.3. Graphic dependencies of the change in the speed of movement of a cotton fly on a multifaceted mesh surface on the change in the angle of inclination of the trajectory of the fly in the cleaning zone.

1. m_l = 0,25 g; 2. m_l = 0,5 g; 3. m_l = 0,85 g.

Analysis of the obtained graphical dependencies shows that an increase in the angle of flight of the cotton fly from *4,5* ^{0} to *31,5* ^{0} leads to an increase in the speed of movement of the cotton fly along the polyhedral mesh surface according to a nonlinear law. Thus, with an increase in the angle *f* with a mass of m_l *= 0,25 g,* the speed V_l'' increases from *1,2 m / s* to *3,49 m / s,* and with a mass of the cotton being pulled equal to *0,85 g,* the speed increases only to *1,83 m / s*. Therefore, to increase the rapid movement of cotton voles in the cleaning zone, it is necessary to loosen the cotton sufficiently so that the mass of the raw cotton lump being pulled does not exceed *(0,5÷0,7) g.* In this case, the speed of pulling

the cotton will be within the range of *(3,0÷3,5) m/s*.

Figure 4.4 shows the graphical dependences of the change in the speed of movement of cotton bats along a multifaceted mesh surface on the change in the length of the edges and the length of the flight of the bats in the cleaning zone. It is evident from the calculation scheme (see Figure 4.2) that the speed of movement of the cotton bat along the mesh surface depends on the length l of the mesh edges and on the length l_1 flight of a fly in the cleaning zone.

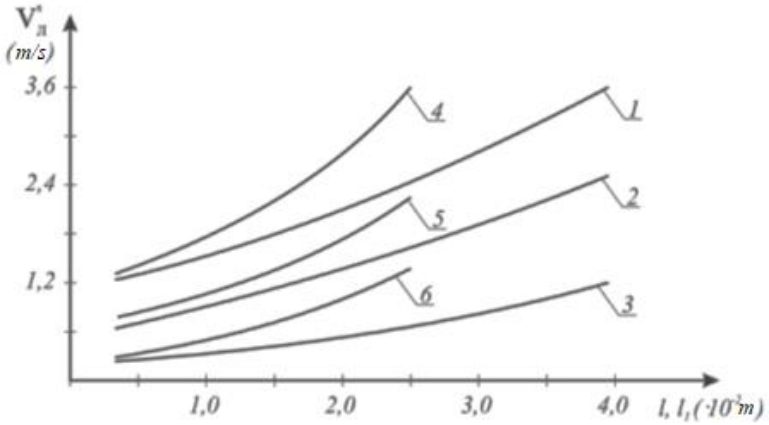

Fig.4.4. Graphic dependences of the change in the speed of movement of cotton bats on a multifaceted mesh surface on the change in the length of the edges and the length of the flight of bats in the cleaning zone.
1,2,3 - $V_l'' = f(l)$; 4,5,6 - $V_l'' = f(l_1)$ *1,4 - at* $t_l = 0,25$ *g; 2,5 - at* $t_l = 0,5$ *g; 3,6 - at* $t_l = 0,85$ *g;*

Analysis of the graphs shows that with increasing l and l_1 the speed of advancement of the bats increases according to a nonlinear pattern. In this case, an increase in the length of the mesh edges to $4,0 \cdot 10^{-2}$ *m* leads to an increase *in* V_l'' to *3,5 m/s* at $m_l = 0,25$ *g,* and at a cotton lump mass of more than *0,85 g*, the speed of cotton movement along the mesh surface reaches only *0,95-1,2 m/s*. Therefore, to ensure the speed of cotton filament movement along the mesh surface of up to 3,0-3,5 m/s, the recommended length of the mesh edges is $l = (3,2 – 4,5) \cdot 10^{-2}$ m. From curves 4, 5, 6 in Fig. 4.4 it is evident that the speed of filament pulling along the multi-faceted mesh surface reaches *3,0÷3,5 m/s* at a filament mass *of 0,25-0,30 g* and at $l_1 = (2,0 – 2,5) \cdot 10^{-2}$ *m*.

It is important to study the rebound value h_{of} the flyer after interaction with the surface of the polyhedral mesh.

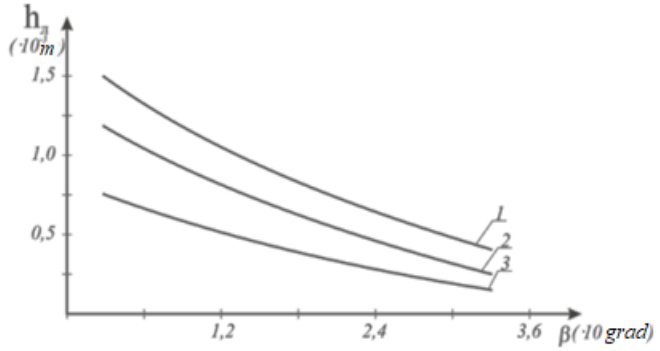

where, *1 - t_n = 0,4 s;* 2 - t_n = 0,2 s; 3 - t_n = 0,08 s;

Fig.4.5. Graphic dependences of the change in the rebound value of a cotton fly on the change in the angle of its trajectory in the cleaning zone

Figure 4.5 shows the obtained graphical dependencies of the change in the rebound value of a cotton fly on the change in the angle of inclination of its flight trajectory in the cleaning zone.

Analysis of the technology of cleaning cotton from small debris shows that the value of the angle of flight of the fly mainly depends on its mass, as well as on the angular velocity of the peg drum of the cleaner. An increase in the angle of flight of cotton flies from $4{,}4^0$ to 32^0 leads to a decrease in the value of the fly rebound on cotton from $1{,}5\cdot10^{-3}$ *m* to $0{,}46\cdot10^{-3}$ *m* at a pulse time of $t = 0.4$ *s*, and at $t = 0{,}08$ *s* the value of the fly rebound decreases from $0{,}75\cdot10^{-3}$ *m* to $0{,}21\cdot10^{-3}$ *m*. This is explained by the fact that at smaller values of the angle β the impact of the fly will be significant, and thus the rebound value will be greater. In this case, the separation of debris will be more effective. But the speed of pulling the cotton fly will be significantly reduced. In addition, the damage to the fibers and seeds of cotton may increase. Therefore, the recommended values are $\beta \leq 25^0$ -35^0. Fig. 4.6 shows the graphical dependencies of the change in the rebound value of the cotton fly on the change in the interaction zone on the mesh.

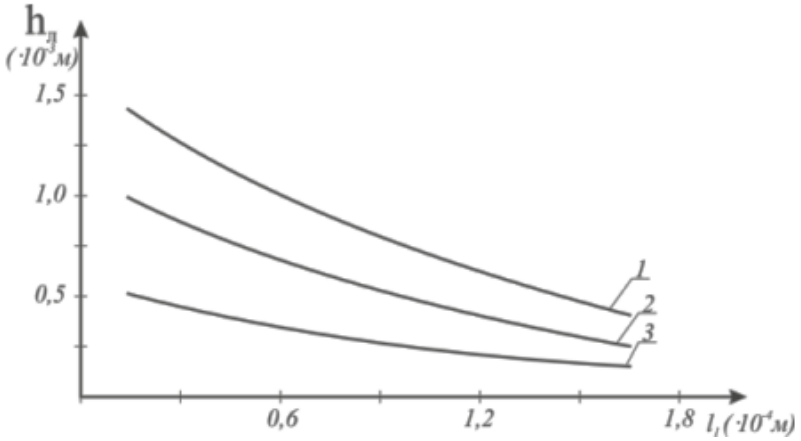

Fig.4.6. Graphic dependences of the change in the rebound value of the cotton fly on the change in the length of the interaction zone with the mesh.
1 - m_l = 0,25 g; 2 - m_l = 0,5 g; 3 - m_l = 0,85 g

An analysis of the graphs in Fig. 4.6 shows that an increase in the flight speed of the fly when leaving the surface of the peg also leads to an increase in the flight length, while the rebound value of the fly after impact with the mesh

polyhedral surface is significantly reduced. It should be noted that with an increase in the flight length l_1 the impact interaction of the cotton fly with the polyhedral mesh surface decreases. With an increase in l_1 from $0{,}2 \cdot 10^{-4}$ m to $1{,}76 \cdot 10^{-4}$ m the rebound value of a cotton fly from a polyhedral mesh surface along the y-axis decreases from $1{,}46 \cdot 10^{-3}$ m to $0{,}47 \cdot 10^{-3}$ m at $t_l = 0{,}25$ g, and at $h_l = 0{,}85$ g the rebound value decreases from $0{,}52 \cdot 10^{-3}$ m to $0{,}19 \cdot 10^{-3}$ m according to a nonlinear pattern. In this case, the greater h_l, the greater the probability of debris release and the possibility of cotton fly movement due to the reduction of its contact with the mesh. Therefore, the recommended values of the flight length (projection along the x- axis of the polyhedral mesh surface) are $l_1 = (2{,}0 \div 2{,}5) \cdot 10^{-2}$ m

4.1.3. Determination of the reaction during the interaction of cotton filaments with the multifaceted mesh surface of a fine debris cleaner

When cotton is pulled by a pin drum over a mesh surface, the force of interaction between the cotton and the mesh surface is random [112; pp. 152-154]. In this case, the vertical component of the disturbing force is determined from the expression:

$$F(t) = F_b(t) \cdot \sin\beta \qquad (4.17)$$

where $F_b(t)$ is the resultant disturbing force, β *is* the angle of inclination of the disturbing force with the horizontal axis (Fig. 4.7).

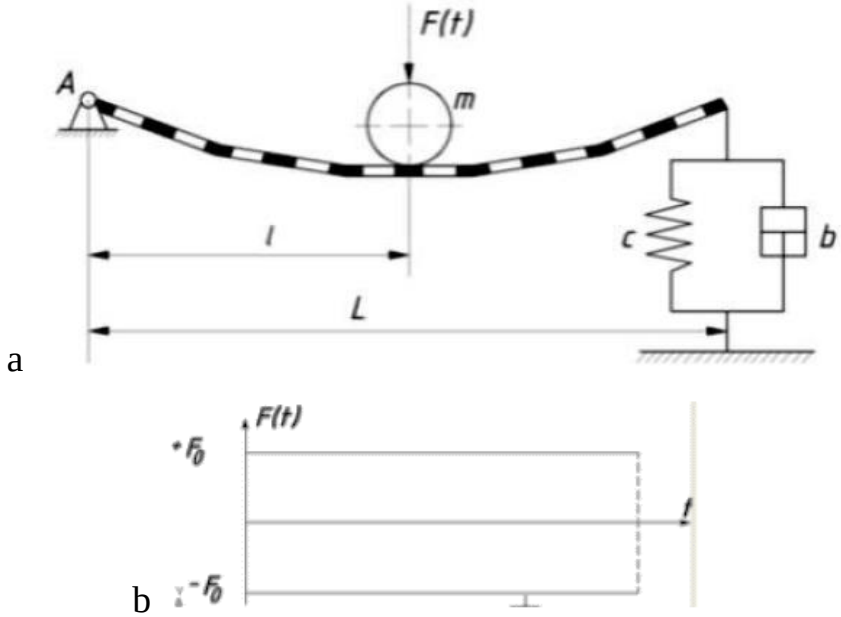

Fig. 4.7. a - Diagram of interaction of cotton with mass *"t"* on the mesh surface of a cotton cleaner; b - graph of the disturbing force from cotton

Due to the fact that the mesh surface is attached to elastic supports, when interacting with cotton, its angular vibrations occur.

Using the d'Alembert principle [111], one can obtain differential equations for the motion of the cotton being pulled and the mesh surface of the fine debris cleaner:

$$m\ddot{y} + N - F(t) = 0$$

$$I_{c.n.}\ddot{\varphi} + bL^2\dot{\varphi} + cL^2\varphi = -NL \qquad (4.18)$$

where N - reaction force;
L - distance between the supports of the mesh surface;
y is the vertical displacement of cotton of mass m;
φ - angular displacement.

In this case, excluding the reaction force from the system of equations (4.18) and taking into account small displacements of the mass m vertically:

$$y = l\varphi \qquad (4.19)$$

we can write:

$$(I_0 + ml^2)\ddot{\varphi} + bL^2\dot{\varphi} + cL^2\varphi = fF(t) \qquad (4.20)$$

where, I_0 is the moment of inertia of the mesh surface relative to the left support. Reducing (4.43) to standard form, we obtain:

$$\ddot{\varphi} + 2n\dot{\varphi} + p_0^2\varphi = \frac{lF(t)}{I_0 + ml^2} \qquad (4.21)$$

Where $2n = \frac{\alpha L^2}{I_0 + ml^2};\ p_0^2 = \frac{cL^2}{I_0 + ml^2}$

Fig. 4.8 shows the mass of cotton m and the mesh surface at an arbitrary moment in time.

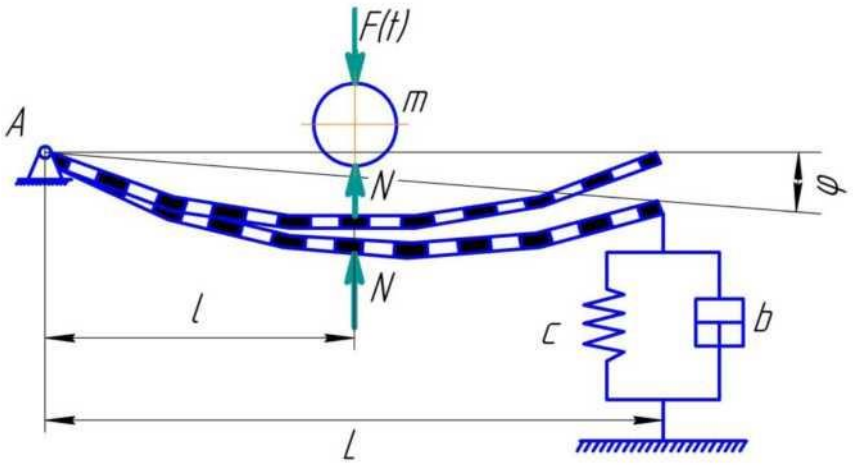

Fig. 4.8. Scheme of the working position of the mesh surface

c, b - coefficients of rigidity and viscous friction of the elastic support.

The solution of the differential equation (4.21) according to the methodology [113; p. 120] can be represented as:

$$\varphi = \frac{1}{(I_0 + ml^2)p_1}\int_0^t l^{-n(t-\tau)} \sin p_1(t-\tau)F(t)dt \qquad (4.22)$$

Where $p_1 = \sqrt{p_0^2 - n^2}$

Taking into account the relationship between y and f from the first differential equation of system (4.41), we determine the dynamic reaction:

$$N = F_b(t)\sin\beta - ml\frac{d^2\varphi}{dt^2} \qquad (4.23)$$

Taking the time derivatives (4.22) and substituting them into (4.19) we have:

$$N = F_b(t)\sin\beta - \frac{F_b(t)ml^2}{I_0 + ml^2} + \frac{ml^2\sqrt{p_0^4 + 4n^2p_1^2}}{(I_0 + ml^2)p_1}\cdot\int_0^t l^{-n(t-\tau)}\sin\left[p_1(t-\tau) - \gamma\right]F_b(t)d\tau \qquad (4.24)$$

Where, $\gamma = arctg\frac{2np_1}{p_0^2}$

The dynamic reaction reaches its maximum value when the raw cotton fly is torn off from the mesh surface of the fine debris cleaner. In this case, the disturbing force $F_b(t)$ sin β takes the values ± F_0, and the integrand remains positive all the time. The moment of discontinuity of the function F(τ) is determined from the condition [114; pp. 20-26]:

$$\sin(p_1\varepsilon_k + \gamma) = 0,\ p_1\varepsilon_k + \gamma = k\pi$$

at the same time $\varepsilon_k = \frac{k\pi - \gamma}{p_1}.$

Then, by integrating (4.47), we can determine the maximum value of the dynamic reaction during the interaction of cotton with the mesh surface of the cleaner:

$$N = \frac{I_0F_0}{I_0 + ml^2} - A\left[l^{-n\varepsilon}\sin(p_1\varepsilon + \gamma + \gamma_1)\Big|_0^{\varepsilon_1} - l^{-n\varepsilon}\sin(p_1\varepsilon + \gamma + \gamma_1)\Big|_{\varepsilon_1}^{\varepsilon_2} + \ldots\right] \qquad (4.25)$$

Where $A = \frac{ml^2F_0\sqrt{p_0^2 + 4n^2p_1^2}}{p_0p_1(I_0 + ml^2)};\qquad \gamma_1 = arctg\frac{p_1}{n}$

In order to obtain the values of the dynamic response N_{max}, the upper limit is taken to be equal to infinity. In this case, we obtain:

$$N_{\max} = \frac{I_0F_0}{I_0 + ml^2} - A\left[\sin(\gamma + \gamma_1) + 2\sin\gamma_1\sum_{k=1}^{k=\infty} l^{\frac{-n(k\pi-\gamma)}{p_1}}\right] \qquad (4.26)$$

into account $\sum_{k=1}^{k=\infty} l^{\frac{n(k\pi-\gamma)}{p_1}} = \frac{l^{\frac{-n(k\pi-\gamma)}{p_1}}}{1 - l^{-\frac{n\pi}{p_1}}}$

Finally, we obtain an expression for calculating the maximum dynamic response in the form:

$$N_{\max} = \frac{I_0 F_0}{I_0 + ml^2} - A\left[\sin\gamma\cos\gamma_1 + \cos\gamma\sin\gamma_1 + 2\sin\gamma_1 \frac{l^{-\frac{n(\pi-\gamma)}{p_1}}}{1 - l^{-\frac{n\pi}{p_1}}}\right] \quad (4.27)$$

Where $\gamma_1 = \arcsin\frac{p_1}{\sqrt{p_0^2 + n^2}}$

For small values of the coefficient of viscous friction of the elastic support of the mesh surface of the cleaner, we can write:

$$\sin\gamma \approx \frac{2n}{p_0}; \qquad \cos\gamma \approx 1; \qquad \sin\gamma_1 \approx 1; \qquad \cos\gamma_1 \approx \frac{n}{p_0}$$

Then, expanding $l^{-\frac{n\pi}{p_1}}$ and $l^{-\frac{n\lambda}{p_0}}$ in a series and keeping only the linear terms of the expansion, from (4.27) we obtain:

$$N_{\max} \approx \frac{2F_0 p_0 ml^2}{\pi n(I_0 + ml^2)} \quad (4.28)$$

The dynamic reaction when cotton interacts with the surface of the fine debris cleaner mesh will be:

$$N = \frac{ml^2 F_0 p_0^2}{(I_0 + ml^2)^2 2np_0}\sin(\frac{\pi}{2} + p_0 t) + F_0 \sin p_0 t \quad (4.29)$$

During the operation of the cotton cleaner from small debris, about 40-60 flies are concentrated in one row of pins. In this case, F_0 changes within the range of $(12{,}8 \div 20)\cdot 10^{-2}$ N. The maximum value of the dynamic response with pulsed disturbance from cotton reaches 30% and more, compared to the harmonic change $F(t) = F_0 \sin \omega t$.

4.1.4. Analysis of small vibrations of a polyhedral mesh under the influence of technological load from cleaned raw cotton

The recommended technology for cleaning cotton from small debris includes pulling the cotton bats and raw cotton along a multifaceted mesh surface with pegs. A special feature of this technology is the small vibrations of the multifaceted mesh due to the mesh being installed in elastic (rubber) supports. The calculation scheme for calculating small vibrations of the multifaceted mesh is shown in Fig. 4.9. According to the calculation scheme, the mesh of the cleaner was taken as a beam, fixed at one end to the body with a hinge, and the other end was installed by means of an elastic support. In this case, the generalized coordinate of the oscillatory system we take the angle of deflection of the mesh φ_c.

Then the kinetic energy of the polyhedral mesh of the cotton cleaner from small debris will be [115; pp. 56-58]:

$$T = \frac{J_c \dot{\varphi}_c^2}{2} = \frac{1}{2}\left(\frac{m_1 l^2}{3}\right)\dot{\varphi}_c^2 \qquad (4.30)$$

where, J_c - moment of inertia of the mesh, m_1 - mass of the polyhedral mesh, l - length of the mesh, $\dot{\varphi}_s$ - angular velocity of the grid

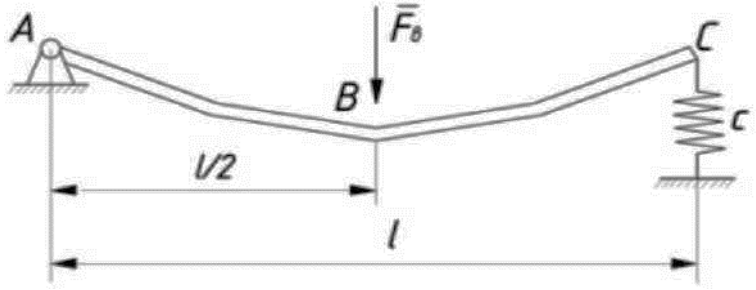

Fig. 4.9. Calculation scheme of the polyhedral mesh of the cleaner

The potential energy of the system will be:

$$П = \frac{1}{2} c l^2 \varphi_c^2 \qquad (4.31)$$

where c is the coefficient of rigidity of the elastic support, φ_c - angular movement of the grid.

In this case, having designated $p_C = \sqrt{\frac{c}{2m_1}}$, we obtain the law of small angular oscillations of a polyhedral grid in the form:

$$\varphi = A_\varphi \sin(p_c t + \beta) \qquad (4.32)$$

where *t is* the time, *β is* the initial angular phase of the polyhedral grid installation, *and φ is* the amplitude of small oscillations of the polyhedral grid.

From expression (4.55) after differentiation we obtain

$$\dot{\varphi} = A_\varphi p \cos(p_c t + \beta) \qquad (4.33)$$

Taking into account the initial conditions at t = 0, φ = 0, $\dot{\varphi} = \dot{\varphi}_s$

$$0 = A_\varphi \sin\beta; \quad \dot{\varphi}_c = \omega_c \cos\beta \qquad (4.34)$$

In this case, we obtain the law of small oscillations of a polyhedral grid:

$$\varphi_c = \frac{A}{p}\sin(p\ t + \beta) \qquad (4.35)$$

Where $A = \frac{1}{J_c\sqrt{2(1-\cos pt)}}$; $\beta = arctg\frac{\sin pt}{1-\cos pt}$;

In the calculations we take the following parameter values $F_в = 123{,}8\ H$

$$J_в = (1{,}042 \div 1{,}5)\ кгмс^2;\ c = 1{,}4 \cdot 10^4 Нм/рад.$$

Based on the numerical solution of the problem, graphical dependencies of

the parameters of the polyhedral mesh on elastic supports are obtained. In this case, it is important to determine the angular displacements of the polyhedral mesh. Since at large values of the span $\Delta\varphi_c$ the gap between the pegs and the mesh can increase, this leads to the fact that the pegs stop moving the cotton, there is a decrease in the cleaning effect and a decrease in the productivity of the cleaning section of the unit.

Fig. 4.10 shows the graphical dependences of the change in the amplitude of oscillations $\Delta\varphi_c$ a polyhedral mesh on the circular stiffness of the elastic support.

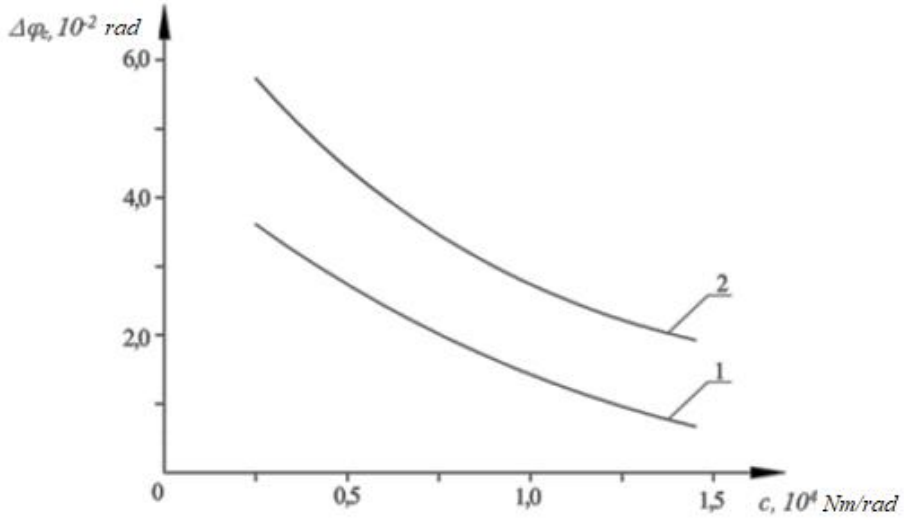

Fig. 4.10. Graphic dependences of the change in the amplitude of oscillations of a polyhedral mesh on the increase in the torsional rigidity of an elastic support
1- with m_1 =14,5 kg; 2 - with m_2 =10 kg

The analysis of the constructed graphs shows that the increase in the circular stiffness of the elastic support of the polyhedral mesh within the range of *(0,25 – 1,45)·10 ^{4} Nm/rad* leads to a decrease in the magnitude of the mesh oscillation amplitude $\Delta\varphi_c$ according to a nonlinear pattern from *3,68·10 $^{-2}$ rad* to *3,68·10 $^{-2}$ rad* with a mesh weight *of 14,5 kg.* With a weight of *10,0 kg,* with an increase in the circular stiffness of the support, it leads to a decrease in the oscillation amplitude $\Delta\varphi_c$ from *5,81·10 $^{-2}$ rad* to *1,93·10 $^{-2}$ rad.* In order to ensure the required permissible values of the technological gap between the pegs and the mesh of no more than *(18,0-20,0)·10 $^{-3}$ m,* the values of the amplitude $\Delta\varphi_c$ should be selected within the range of *(3,8-5,6)·10 $^{-2}$ rad.* The recommended values of the coefficient of circular stiffness of the elastic support of the polyhedral mesh are *(0,42-1,05)·10^4 Nm/rad.*

It is known that the greater the moment of inertia of a polyhedral mesh, the more difficult it is to ensure oscillations of the polyhedral mesh with the required amplitude and frequency. Therefore, it is important to reduce the mass of the mesh. Figure 4.11 shows the graphical dependences of the change in the oscillation range $\Delta\varphi_c$ a polyhedral mesh on the increase in the moment of inertia.

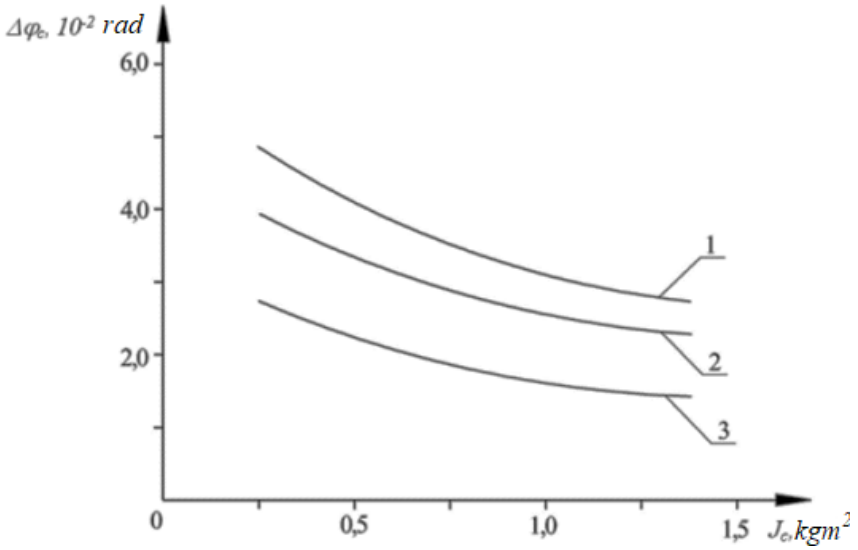

Fig. 4.11. Graphical dependencies of the change in the amplitude of oscillations of a polyhedral mesh on the increase in the moment of inertia
1 - at $c = 0{,}55 \cdot 10^{4}$ *Nm/rad; 2* - at $c = 1{,}05 \cdot 10^{4}$ *Nm/rad;* 3 – at $c = 1{,}45 \cdot 10^{4}$ *Nm/rad*

The analysis of the graphs shows that an increase in the moment of inertia of the polyhedral mesh from *0,25 kg m* ^{2} to *1,35 kg m* ^{2,} the amplitude of mesh oscillations $\Delta\varphi_c$ decreases from $4{,}72 \cdot 10^{-2}$ *rad* to $2{,}94 \cdot 10^{-2}$ *rad* with a circular stiffness coefficient of the elastic support of $0{,}55 \cdot 10^{4}$ *Nm/rad.* With an increase in the value of *c* to $1{,}45 \cdot 10^{4}$ *Nm/rad,* the amplitude of angular oscillations $\Delta\varphi_c$ the polyhedral mesh decreases from $2{,}47 \cdot 10m^{-2}$ *rad* to $1{,}78 \cdot 10^{-2}$ *rad.* To ensure the required values $\Delta\varphi_c = (3{,}8 \div 5{,}6)\ 10^{-2}$ *The* recommended values of the moment of inertia of a polyhedral mesh are *(0,21÷0,65) kgm*^{2}. In this case, the mass of the polyhedral mesh should be selected to be no more than *(7,5÷9,5) kg*.

4.1.5. Justification of the rigidity of the elastic support of the mesh surface taking into account the impact of raw cotton during its cleaning

The proposed design of the mesh surface of the fibrous material cleaner is illustrated by the drawing, where Fig. 4.12. a shows the general diagram of the mesh surface in the working position, and Fig. 4.12. b shows the section A-A [116; pp. 31-33].

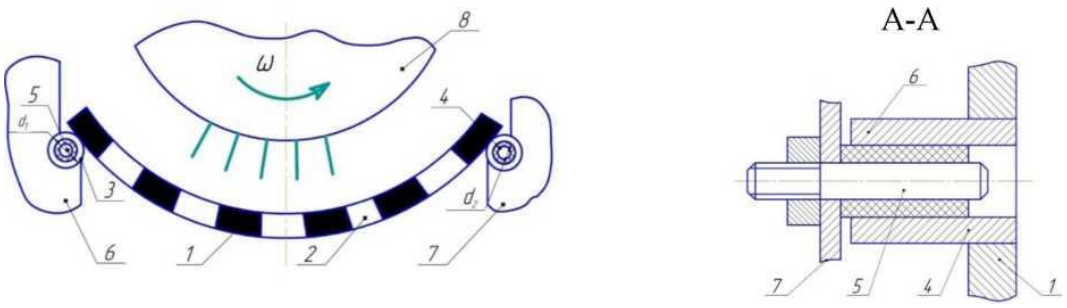

a b

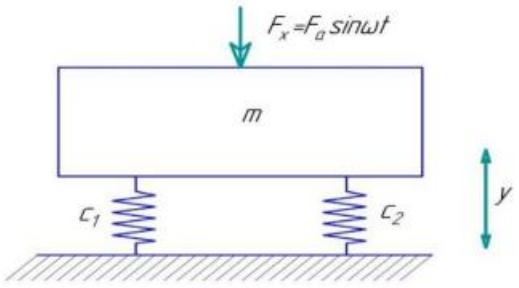

c

Fig.4.12. Schematic (a and b) and calculated (c) diagrams of the mesh surface on elastic supports of a cotton cleaner for small debris

During operation, raw cotton is captured by the pins of the drum 8 and pulled along the mesh surface 1. In this case, the cotton in the contact zone is subjected to cyclic action by the edges of the holes 4. As a result, the cotton receives high-frequency vibrations and is shaken. The dirt released in this case falls out through the holes 4. In this case, due to the large mass of cotton located on the surface of the mesh 1, some deformations of the elastic bushings 6 occur. Considering that the mass of the raw cotton being pulled changes over time, the deformations of the bushings 6 also change. This leads to vibrations of the mesh 1 with a certain frequency and amplitude. In this case, at the beginning of the raw cotton pulling zone, the vibrations of the mesh 1 will occur with the greatest amplitude due to the larger diameter ($d_1 > d_2$, thickness) of the elastic bushings 6 in this zone, and at the end of the raw cotton pulling zone, the vibration amplitude of the mesh 1 will be the smallest. The frequency and amplitude of the oscillation of the mesh 1 depends on the rigidity of the elastic bushings 6, the mass of the mesh 1 and the change in the mass of the cotton being pulled through. The oscillations of the mesh 1 significantly intensify the release of impurities, which leads to an increase in the cleaning effect by 12 - 17%.

The calculation scheme for the oscillations of the mesh surface on elastic supports of a cotton cleaner for small debris is shown in Fig. 4.16c. According to this scheme, using the d'Alembert principle [117; pp. 114-118], we will compose a differential equation for the oscillations of the system:

$$m\ddot{y} + b\dot{y} + (c_1 + c_2)y = F_0 \sin\omega t \qquad (4.36)$$

where m is the mass of the mesh surface, b is the coefficient of dissipation of elastic supports, c_1, c_2 are the stiffness coefficients of elastic supports, F_0 - the amplitude of oscillations of changes in technological resistance from the raw cotton being pulled through, ω - the frequency of changes in technological resistance.

In this case, the amplitude of forced vibrations of the mesh surface on the

elastic supports of the cotton cleaner:

$$y_0 = \frac{y_{cm}}{\sqrt{(1-\frac{\omega^2}{p_0^2})^2 + (\frac{2n\omega}{p_0^2})}} \qquad (4.37)$$

Where $y_{ст} = \frac{F_0}{c_1 + c_2}$

It is important to determine the recommended values of the vibration amplitude of the mesh surface. Since a significant increase in the vibration amplitude of the mesh surface leads to a decrease in the gap between the ends of the drum pins and the mesh surface. This can lead to increased damage to the fibers and cotton seeds, and in some cases, to the slaughter of cotton [118; pp. 256-260].

Figure 4.13 shows the graphical dependencies of the change in the amplitude of forced oscillations of the mesh surface on elastic supports in the steady-state mode on the change in the amplitude of the external technological load from raw cotton at different values of the mesh surface mass. They show that an increase in the amplitude of the disturbing force from *0,2·10 ^{2} N* to *0,71·10 ^{2} N* leads to an increase in the amplitude of oscillations of the mesh surface of the cleaner in the steady-state mode from *0,4·10^{-3} m* to *2,93·10 $^{-3}$ m* at *m = 13 kg*, and at a mesh surface mass *of 15 kg*, y_0 accordingly increases according to a linear pattern from *0,18·10 $^{-3}$ m* to *0,94·10 $^{-3}$ m*.

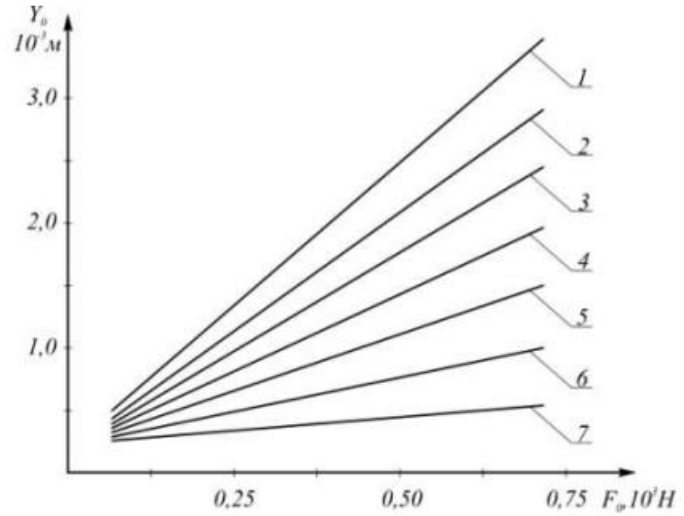

Fig.4.13. Dependences of the change in the amplitude of oscillations of the mesh surface on elastic supports on the change in the amplitude of the technological load. 1-for *m=12 kg;* 2-for *m=12,5 kg;* 3-for *m=13 kg;* 4-for *m=13,5 kg;* 5-at *m=14,4 kg;* 6-at *m=14,8,2 kg;* 7-at *m=15,1 kg*

To ensure the required gap between the ends of the pegs and the mesh surface of *0,014-0,016 m,* the recommended parameter values are: *m = 13,5,0-14,4 kg; y_0 = (1,1-2,4)·10 $^{-2}$ m; F_0 = (0,45-0,60)·10 ^{2} N.*

4.2. Theoretical research on the substantiation of the parameters of the large debris cleaner

4.2.1. Effect of the rotation frequency of the saw drum on the deviation value of the captured cotton fly

In cotton cleaners for large debris, it is usually assumed in studies that the saw drum rotates with a constant angular velocity [29]. But in reality, the angular velocity of the saw drum is variable [83, 119], especially with a lightweight version of the saw drum [120]. Variability in the rotation of the saw drum occurs due to errors in the installation of the pulleys and debris getting into the grooves of the pulleys. Let us consider the effect of the variable speed of the saw cylinder on the movement of the flyers in the cleaning zone. The angular velocity of the saw drum can be determined according to [121]:

$$\omega_n = \omega_0 + \omega \cdot \sin k_K t \qquad (4.38)$$

where ω_0 is the average angular velocity of the saw drum in the steady state of cotton cleaning; ω_1 is the amplitude of the angular velocity oscillations, t - time.

Figure 4.14 shows the interaction diagram of a serrated drum tooth with a single fly in a raw cotton cleaner. According to the calculation diagram, the fly participates in the transfer movement together with the serrated drum and relative to the center of oscillation (at the point where the drum teeth capture the strand of raw cotton fly).

The angle formed between OM and OB is designated by φ , and the angle between the radius of the drum and the flyer strand MN by β .

According to the works [122, 123, 124, 125], when analyzing the relative oscillation of the flyer, it is necessary to take into account the translational and Coriolis forces of inertia of the flyer.

The transfer force of inertia is directed along the straight line OB and is determined by

where:

$$P_i = m_l l \omega^2 \qquad (4.39)$$

Where $l = \frac{R + l_1 + \cos\beta}{\csc\varphi}$.

t_l - mass of the fly, l - distance from the center of rotation of the serrated drum to the center of mass of the fly seed, l_1 - the length of a strand of cotton wool.

The Coriolis force of inertia is directed along the straight line *NM*, and the moment of this force relative to the rolling point N is zero. Therefore, we discard this force [126].

The fly is affected by the force of inertia, the force of weight, and the force of resistance.

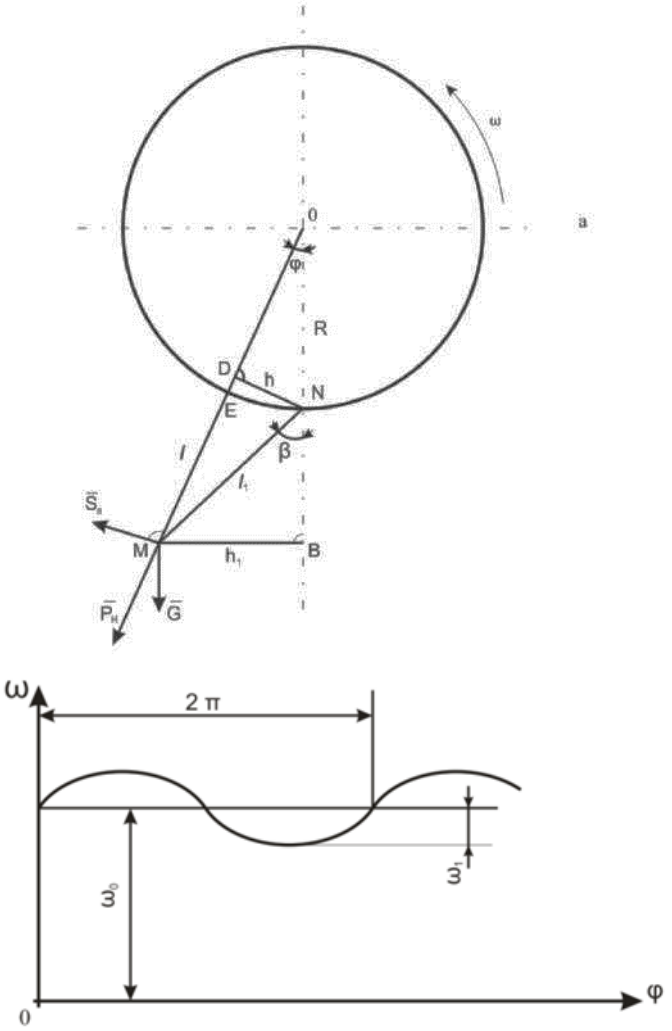

Fig. 4.14 Calculation scheme (a) and graph of the angular velocity of the saw drum (b).

In this case, the air resistance force is determined [140] from:

$$S_b = F_m \cdot \theta_l \cdot \frac{\rho v^2}{2} l_1 \tag{4.40}$$

where F_m is the midsection; ρ is the air density; v is the transport speed of the flyer; θ_l is the drag coefficient.

From ΔDON and Δ OBM we have:

$$\sin\varphi = \frac{DN}{ON} = \frac{h}{R} = \frac{h_1}{l};$$

$$OB = ON + NB = R + l_1 \cos\beta; \tag{4.41}$$

$$l = MD + DO = \sqrt{l_1^2 - h^2} + R\cos\varphi,$$

$$tg\varphi = \frac{h_1}{R + l_1\cos\beta} \tag{4.42}$$

The equation of moments of forces relative to point N, taking into account (4.41), (4.42) and (4.40), has the form:

$$m_l l_1^2 \ddot{\beta} + m_1(\omega_0 + \omega_1 \sin K_K t)^2 \cdot \left[\sqrt{l_1^2 + R^2\sin^2\varphi} + R\cos\varphi\right] \times$$

$$\times R\sin\varphi + m_l g h_1 + \sqrt{l_2 + R_2\cos^2\varphi} \cdot F_l\theta_l \cdot \frac{\rho v^2}{2} l_1 = 0 \tag{4.43}$$

During the operation of the fly cleaner, in the period between impacts on adjacent grates, it makes small oscillations and, due to the smallness of the angle *β,* it can be written:

$$\beta = \frac{h_1}{l_1} \tag{4.44}$$

In addition, to simplify the problem, we do not take into account the last term in (4.43) due to its smallness. Then, taking into account (4.44), (4.43) will be rewritten as:

$$\frac{d^2 h_1}{dt^2} + \frac{R h_1}{l_1}(\omega_o + \omega_1 \sin K_\kappa t)^2 + \frac{g}{l_1} - h_1 = 0 \tag{4.45}$$

According to the methodology given in the work [127], we reduce the differential equation (4.19) to the standard form of the Mathieu equation:

$$\frac{d^2 h}{dt^2} + (a + 2q\cos 2\tau) = 0 \tag{4.46}$$

Where,

$$a = \frac{\varphi R {\omega_o}^2}{l_1 {K_k}^2} + \frac{g}{l_1 \cdot {K_k}^2}; \qquad \tau = \frac{K_k t}{2}$$

$$2q = \frac{\varphi 2\omega_o \omega_1 R}{l_1 K_\kappa^2} \tag{4.47}$$

where K_k - grate rigidity; R - radius of the saw-tooth drum; ω_1 - frequency of change of technological resistance; ω_0 - average angular velocity of the saw-tooth drum; l_1 - length of the strand of cotton fly;

The solution of equation (4.47) is oscillatory in nature and depends crucially on the values of the parameters *a* and q. In this case, if the amplitude of the oscillations remains limited, the system will be stable; otherwise, resonance occurs

and the system is unstable. For practical purposes, the boundaries between the regions of stable and unstable solutions are of greatest importance. This issue has been sufficiently studied in [127] and is presented in the form of the Ince-Strutt diagram. According to this diagram, specific parameters of the serrated drum and the frequency of change of its angular velocity can be recommended, at which the process of cleaning raw cotton from large debris will proceed favorably due to intensive shaking of the captured fluff.

Numerical calculations were carried out at the following parameter values: ω_0 = 31,4 rad/ s; ω_1 = 2,5 rad/ s; R = 0,16m; l_1 = 0,02m; $\beta_n = 8^0$; K_K = 45; $m_l = 0{,}2 \cdot 10^{-3}$ kg.

Moreover, according to the Ince-Strutt diagram [128, 129], the intersection points of the coordinates of the values of the coefficients, a = 0,21 and q = 0,34, are in the unshaded zone, that is, the oscillatory motion of the fly is in the stable zone.

Changing the values of the system parameters may lead to unstable motion modes. Therefore, the following values of the parameters are recommended: ω_0 = 31 - 35 rad/s; ω_1 = 2,0 – 2,6 rad/ s; R = 0,15 – 0,17 m; l_1 – 0,02 – 0,022 m; K_K -35 - 45, according to the calculations for which a = 0,24 – 0,83; q = 0,3 i – 0,46.

If the saw-tooth drum of the cleaner rotates with a constant angular velocity, then expression (4.19) can be rewritten as follows:

$$\frac{d^2 h_1}{dt^2} + \left(\frac{\omega^2 R}{l_1} + \frac{g}{l_1} \right) h_1 = 0 \qquad (4.48)$$

In this case, the natural frequency of the flyer oscillations will be equal to

$$f_{св} = \sqrt{\frac{R\omega^2 + g}{l_1}}$$

The solution of the differential equation (4.22) can be represented in the form [76]:

$$h_1 = c_1 \sin f_{св} t + c_2 \cos f_{св} t \qquad (4.49)$$

or

$$h_1 = d \sin\left(f_{cb} t - \alpha\right).$$

The integration constants are determined from the initial conditions:

$t = 0$; $v = v_0$; $h_1 = h_{1.0}$; $C_1 = \frac{v_0}{f_{сб}}$; $C_2 = h_{1.0}$

$$d = \sqrt{{h_{1.0}}^2 + \frac{{v_0}^2}{f_{св}}}; \qquad \alpha = arctg \frac{h_{1.0}}{v_o}$$

Then the solution will be:

$$h_1 = h_{1.0} \cos f_{cв} t + \frac{v_o}{f_{cв}} \sin f_{cb} t \qquad (4.50)$$

or, taking into account (4.48)

$$h_1 = h_{1.0} \cos f_{cв} t + \sqrt{\frac{v_o^{\,2} l_1}{R\omega^2 + g}} \sin f_{cв} t \qquad (4.51)$$

Analysis (4.50) shows that at the initial moment, when t = 0, the value of $h_1 = h_{1.0}$ and, according to the data of E.F. Budin [83], the angle of deviation of the strand of fibers of the fly from the radius of the saw-tooth drum is 60^0 - 62^0. Taking into account the length of the strand of the fly of 0.022 m, $h_{1.0}$ will be equal to 0.019 m.

Let us use the method proposed by H. Tursunov [125]. At a rotation frequency of the saw drum of 300 rad/ s, ω = 31.4 rad/ s, and the location of adjacent grates forms an angle of 0.17 rad with the axis of rotation of the drum. Then the fly between adjacent grates is in accordance with the proportion of 0,009 s. In this case, $\sin f_{cв} t \approx 1.0$, $h_1 \approx 0.019$ m.

4.2.2. Oscillations of a grate on an elastic foundation with nonlinear rigidity

In order to reduce damage to cotton fibers and raw cotton seeds, it is advisable to reduce the frequency of interaction of working parts with cotton during the primary processing of cotton.

It is important to increase the efficiency of interaction of cotton with working bodies by improving their design. We recommend a new design of the grate of the cotton cleaner from large debris [130,131,132] with composite grates on elastic supports.

In this case, the recommended grate design significantly reduces the friction resistance of raw cotton against the side surfaces. In addition, the elastic bushings 4 are installed eccentrically in the sidewalls 3 of the grate. In this case, the elasticity of the supports will actually be nonlinear. According to the well-known technique [99], the elastic element can have nonlinear rigidity (see Fig. 4.15 b). Fig. 4.15 a shows a diagram of the installation of composite grates 1 on elastic supports 2 in sidewalls 3. In this case, the elastic bushings 2 are made eccentric and have a variable thickness during their installation. From the experimental data obtained, it can be noted that the grates on elastic supports perform mainly vertical oscillations [133]. In this case, the load distribution will be more uniform, both in the middle and in the extreme zones of the grates, which is confirmed by the results of the experiments given in [102, 103].

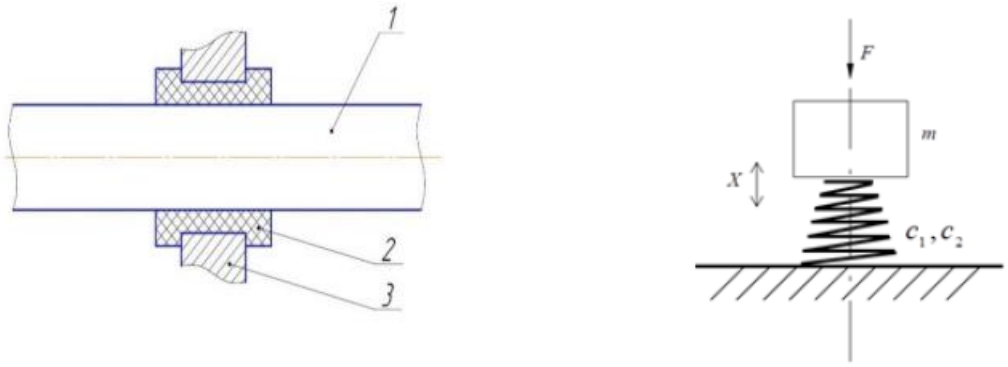

a-composite grates of sectional design (large diameter) b-calculated scheme of oscillations of a composite grate

1-composite grates, 2- rubber bushing with variable thickness, 3- body (side, segment) of the grate

Fig.4.15. Scheme of composite grate on elastic supports and calculation scheme

When choosing the calculation scheme, taking into account the above, in the first approximation we considered only the vertical oscillations of the grate, which directly affect the cleaning effect of cotton, and assumed a conventional single-mass oscillatory system. It should be noted that during operation the position of the eccentricity can change (there are slight circular movements). Therefore, the value of the eccentricity e_k composite grates 1 does not exceed $(2,0\text{-}3,0)\cdot 10^{-3}$ *m*, according to the work of A. Dzhuraev [89]. According to the calculation scheme (Fig. 4.15 b), we will compose an equation describing the oscillation of the grate. During the cotton cleaning process, the grate is acted upon by the inertial force, the restoring force of the elastic support and the random disturbing force from the raw cotton. It should be noted that in the existing design, the mathematical expectation of the load on the metal grate is 12,5 N, and the random component is within the range of (0,8-1,1) N [134].

$$F_b = (F_b) \pm \delta(F_b) \tag{4.51}$$

where (F_b); δ (F_b) is the mathematical expectation or average value of resistance from the cleaned cotton and the random component of resistance.

Considering that the rubber support is eccentric and its rigidity is nonlinear, the restoring force takes the form:

$$P = c_1 x + \frac{c_2}{\mu} x^3 \tag{4.52}$$

where c_2, c_1 are the values of the stiffness coefficients of the rubber support and the composite grate;

x_1 - movement of the grate in the vertical direction.

It should be noted that the technological load from the cotton fly is insufficient to ensure the oscillations of the metal rod grate. When using composite

grates, their mass is reduced by 4-5 times. In this case, the grates perform forced oscillations. It is known that taking into account the dissipation of the rubber grate supports leads to a decrease in their oscillation amplitude due to energy absorption. Without taking into account dissipation, it is possible to estimate the maximum values of the grate oscillation amplitude.

Without taking into account the absorption of energy in the rubber bushings, the oscillations of the grate are described by the following differential equation:

$$m\ddot{x} + c_1 x + \frac{c_2}{\mu} x^3 = F \qquad (4.53)$$

where m *is* the reduced mass of the composite grate; μ is the constant nonlinearity coefficient; F *is* the disturbing force from the raw cotton being cleaned.

It can be noted that the solution to problem (4.53) can be used to justify the necessary parameters of the system, which ensure an increase in the cleaning effect of raw cotton cleaners from large debris.

In the process of cleaning raw cotton from large debris, the cleaning effect due to the oscillations of the composite grate on rubber supports is specific. After the impact of cotton flies on the composite grate, the latter performs free oscillations for a short period of time. During repeated interaction of cotton flies with the grate, the influence of the frequency and amplitude of natural oscillations of the composite grate is important. Therefore, we further considered the nature of free oscillations of the composite grate on eccentric rubber supports.

4.2.3. Study of the influence of the parameters of a composite grate on elastic supports with nonlinear rigidity on the oscillation frequency

When raw cotton is pulsed onto lightweight composite grates, the elastic supports are instantly deformed. It is important to determine the oscillation frequency of composite grates, which affects the cleaning effect.

In this case, let us assume [135] that when determining the values of the deformations of the composite grate supports, the kinetic energy of the raw cotton being dragged along with the grate during the impact with the cleaner grate is converted into the potential energy of the deformable rubber support:

$$T = \frac{mV_y^2}{2} \qquad \Pi = \int_0^{x_{max}} \left(c_1 x + \frac{c_2}{\mu} x^3 \right) dx \qquad (4.54)$$

where T is the kinetic energy of raw cotton and the composite grate; m *is* the total mass of the composite grate and raw cotton; V_y *is* the rate of interaction of raw cotton with the grate during the cleaning process from coarse particles.

litter; c_1 — linear component of the stiffness coefficient of the elastic support of

the composite grate; c_2 *is* the nonlinear component of the stiffness coefficient; *П is* the potential energy of the deformable elastic support of the composite grate;

Taking into account the accepted interaction condition, the speed can be determined:

$$V_y = \sqrt{\frac{2}{m}\int_0^a c_1 x dx + \int_0^a \frac{c_2}{\mu} x^3 dx} \tag{4.55}$$

where, *a is* the maximum value of deformation of the rubber support of the composite grate.

According to the results of studies [136, 137], with nonlinear rigidity of the elastic element of a single-mass oscillatory system of a composite grate under conditions from $x=0$ until $x=a$ the period of oscillation will be

$$t = 4\sqrt{\frac{n}{\alpha}} \cdot \frac{1}{\alpha^{n-1}} \int_0^1 \frac{d\xi}{\sqrt{1-\xi^{2n}}} \tag{4.56}$$

where a and n are constants, $n = 1,2...,; \xi = x/a$,with the restoring force equal to αx^{2n-1}.

The period of oscillation of a composite grate on an elastic support with nonlinear rigidity is determined from the expression:

$$t = 4\sqrt{m}\left[\sqrt{\frac{1}{c_1}}\int_0^1 \frac{d\xi}{\sqrt{1-\xi^2}} + \sqrt{\frac{2\mu}{c_2 a^2}}\int_0^1 \frac{d\xi}{\sqrt{1-\xi^4}}\right] \tag{4.57}$$

where μ is a coefficient taking into account the nonlinearity of the elastic characteristics of the rubber support of the composite grate.

Using tables of special functions, according to works [86, 90, 138], we have (4.58)

$$t = 4\sqrt{m}\left[6{,}28\sqrt{\frac{1}{c_1}} + \frac{1{,}8541}{\alpha\sqrt{c_2^2/\mu}}\right] \tag{4.58}$$

In this case, the frequency of free oscillations of the grate, taking into account $\rho = 2\pi/t$:

$$\rho_k = \frac{0{,}25a\sqrt{c_1 c_2/\mu}}{\sqrt{m}(2\pi\alpha\sqrt{c_2/\mu} + 1{,}85\sqrt{c_1}} \tag{4.59}$$

According to (4.59), the natural frequency of oscillations decreases nonlinearly with the increase in the reduced mass of the composite grate with cotton.

It should be noted that, with an increase in the amplitude of oscillations and

the stiffness coefficients c_1 and c_2, the frequency of natural oscillations changes according to a nonlinear relationship.

In numerical calculations, the following initial parameters were adopted:

$$m = 0{,}8 - 1{,}4\ кг;\ c_1 = 1{,}5 \cdot 10^4\ Н/м;\ c_2 = 0{,}8 \cdot 10^4\ Н/м;$$

$$\mu = 0{,}5 - 1{,}0\ м^2;\ a = (1{,}0 - 1{,}2) \cdot 10^{-3}\ м.$$

Fig. 4.16 shows the graphical dependences of the relative value of the natural frequency of oscillations of the composite grate on its reduced mass. Analysis of the graphs shows that the relative value of the natural frequency decreases according to a nonlinear pattern with an increase in the reduced mass of the grate. The magnitude of the amplitude (deformation of the elastic support) does not actually affect this pattern, that is, an increase in the amplitude leads to a parallel upward displacement of the curve of the pattern with a difference of ρ_k / ρ_n = 0,25 – 0,05 (with an increase in a from 0,8·10 ^{3} *m* to 1,2·10 ^{3} *m)*.

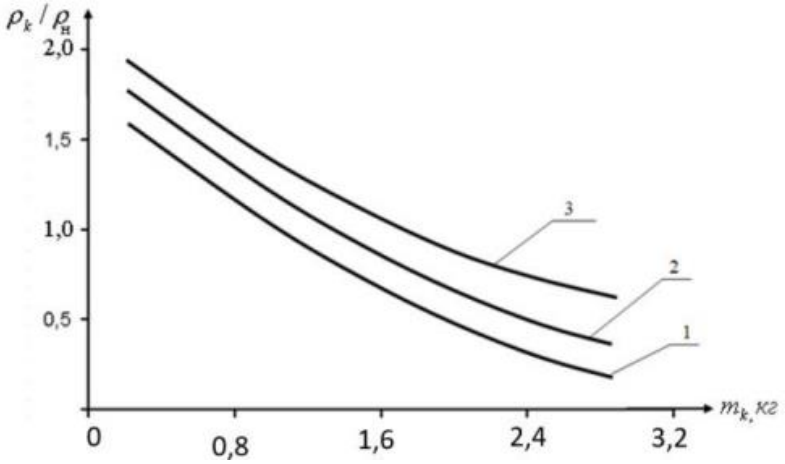

1-for $a=0{,}8\cdot10^{-3}\ m$; 2-for $a=1{,}0\cdot10^{-3}\ m$; 3-for $a=1{,}2\cdot10^{-3}\ m$

Fig.4.16. Graphic dependences of the change in the relative value of the natural frequency of oscillations of a composite grate on the increase in its reduced mass

Fig. 4.17 shows graphs of the change in the relative value of the oscillation period of the grate on an elastic support with a nonlinear characteristic from the change in the amplitude of natural oscillations. Thus, with an amplitude value of 0,5 · 10^{-3} *m* oscillation period t_k / t_n = 1,9, at m_k = 1,8 *kg*, and with a = 1,75·10 $^{-3}$ m and m_k = 1,2 *kg*, the oscillation period t_k / t_n = 1,49. This means that the amplitude of the grate oscillations has little effect on the period and frequency of oscillations. In this case, the mass of the composite grate includes the average mass of cotton (flyers) located on the surface of the grate on average.

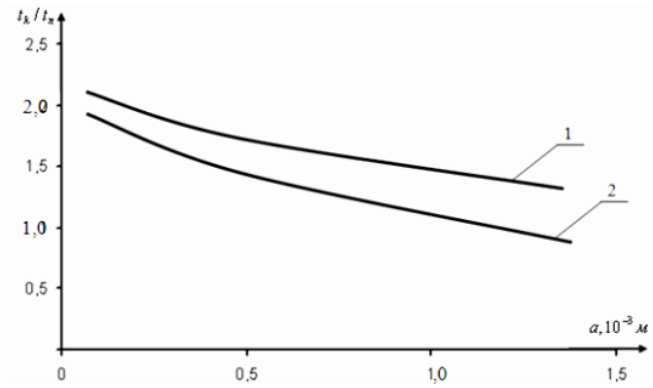

1 – m_k=1,8 кг; 2 – m_k=1,2 кг

Fig.4.17. Graphic dependences of the change in the relative value of the oscillation period of the composite grate on the change in the maximum amplitude.

It should be noted that the amplitude of natural oscillations itself depends on the magnitude of deformations of the elastic support, i.e. on its rigidity characteristic. Fig. 4.7 shows the graphical dependencies of the change in the relative value of the natural frequency of oscillations (the ratio of the current value of the natural frequency to the calculated one) on the change in the stiffness coefficients of the elastic support. It is evident from the graphs that an increase in the rigidity of the elastic support leads to an increase in the natural frequency of the system according to a nonlinear pattern. The nonlinearity of the elastic support depends on the location of the eccentric rubber bushing through which the composite grates are installed in the body of the cotton cleaner from large debris.

When calculating the stiffness coefficient c_1 and c_2 are given for rubber bushings per grate. With a stiffness coefficient *of* c_2 = 1.3 -10 ^{4} *N/m* increase in stiffness coefficient c_1 to 0.6-10 ^{4} *N/m* up to 2.1 10 ^{4} *N/m*, the relative frequency value increases almost twice from p_k / p_n = *1.12* to 2.21. With a decrease in the value c_2 to 0.8 10 ^{4} *N/m* the intensity of the increase in the natural frequency of the grate oscillations decreases (see Fig. 4.18 curve 2).

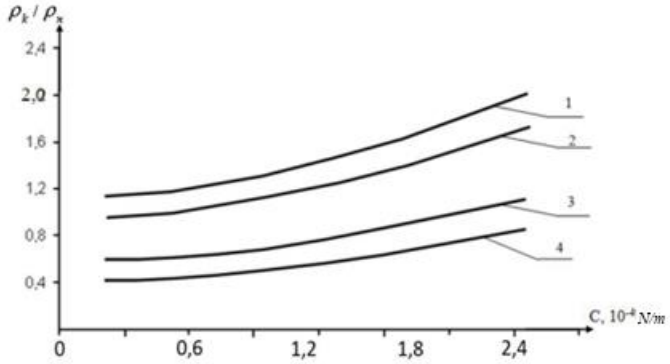

Fig.4.18. Graphic dependences of the change in the relative values of the natural frequency of oscillations of the composite grate on the change in the stiffness coefficients of the elastic support with a nonlinear characteristic

1 - at c_2 = 0,810 ^{4} N/m; 2 - at c $_2$ = 1,010 ^{4} N/m; 3 - at c $_2$ = 1.410 ^{4} N/m; 4 - at c $_2$ = 1.210 ^{4} N/m;

At a constant value of c_2 with an increase of c_1 from 0,6·10^4 *N/m* up to 2,1·10^4 *N/m* leads to an increase in p_k / p_n from 0,55 to 1,15, also by a factor of two. This means that to increase the values of the natural frequency of oscillations of the composite grate, it is advisable to increase the rigidity of the elastic support (reduce the thickness of the rubber bushing).

Taking into account the limits of changes in the disturbing force on the grate from the side of the raw cotton being pulled through, the natural frequency should change within insignificant limits. Therefore, it is advisable for the oscillatory system under consideration c_1 = (1,2-1,4)·10 ^{4} N/m, c_2 = (0,80- 1,0)·10 ^{4} *N/m*, at m $_k$ = 1,1-1,3 *kg*.

4.3. Determination of natural frequencies and modes of free vibrations of the grate.

The grate is a system with distributed parameters. Therefore, the results obtained in the previous sections for the single-mass model are a rather rough approximation. For a more accurate determination of the entire spectrum of natural oscillation frequencies of the grate, modeling was carried out in the ANSYS system Mechanical APDL using the Modal analysis type.

Previously constructed in the ANSYS environment. The grate consists of five identical sections. Therefore, one section shown in Fig. 1 is used for the analysis. It is a frame consisting of sidewalls 1 and longitudinal steel bars of circular cross-section 2. Intermediate supports 3 are attached to the bars. The frame serves as a support for five grates 4, which are rods of circular cross-section made of composite material.

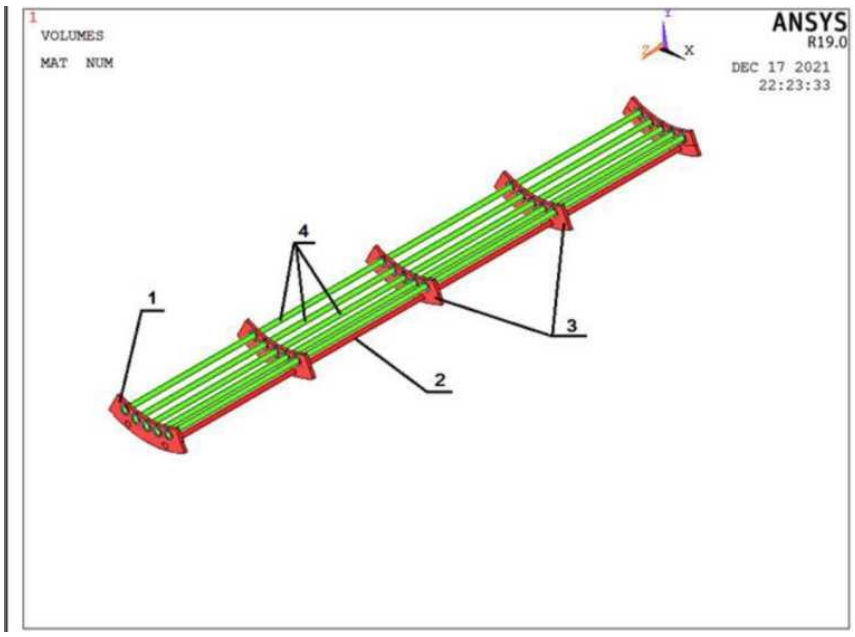

Fig. 4.19. Geometric model of the grate

The grates are attached to the frame through elastic rubber bushings 5, shown in the enlarged fragment of the geometric model (Fig. 20).

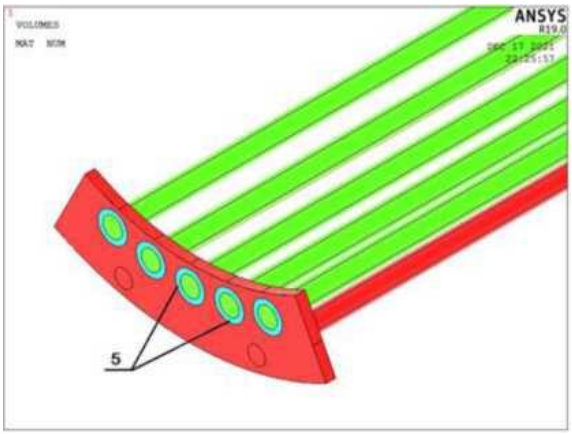

Fig. 4.20. Fastening the grate bars to the frame

The frame was secured along the sides, which were prohibited from moving along the three coordinates. The grate bars were secured along the end surfaces, and movement along the Z axis was prohibited on them. This fastening scheme corresponds to the real fastening of the grate.

An elastic isotropic material model was used for all structural elements. For the frame material, the elastic modulus $E=2\cdot10^{11}$ Pa, Poisson's ratio 0,3, density 7800 kg/m ^{3}. For the grate material, the elastic modulus $E=1,4\cdot10^{9}$ Pa, Poisson's ratio 0,4, density 900 kg/m ^{3}, and for the rubber bushings, the elastic modulus $E=10^{6}$ Pa, Poisson's ratio 0,4, density 1000 kg/m^3.

SOLID 185 element was used as a finite element for all volumes. The model was divided into tetrahedral finite elements with a side of 1 cm. A fragment of the model with a finite element mesh applied to it is shown in Fig. 4.21.

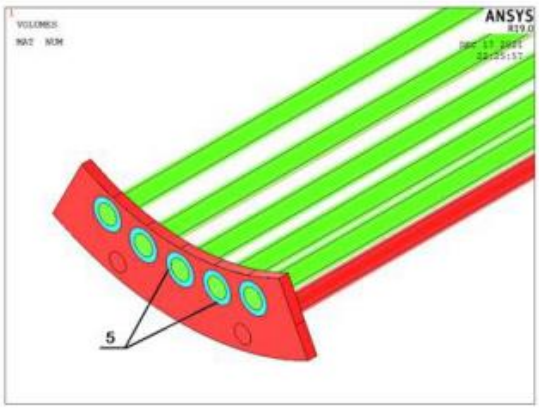

Fig.4.21. Fragment of finite element mesh

In the Modal module settings, a search for 12 natural frequencies of the system in the range from 0 to 50 Hz is assigned. The calculation results are shown in Fig. 4.22.

SET,LIST Command

File

***** INDEX OF DATA SETS ON RESULTS FILE *****

SET	TIME/FREQ	LOAD STEP	SUBSTEP	CUMULATIVE
1	2.579	1	1	1
2	2.582	1	2	2
3	2.582	1	3	3
4	2.582	1	4	4
5	2.585	1	5	5
6	2.586	1	6	6
7	2.588	1	7	7
8	2.594	1	8	8
9	2.596	1	9	9
10	2.598	1	10	10
11	2.602	1	11	11
12	2.692	1	12	12

Fig.4.22. Results of calculation of 12 natural frequencies of the grate

The first column gives the harmonic number, and the second column gives the corresponding frequency. As follows from the calculation results, all frequencies are located in a fairly narrow range of 2,579 to 2,692 Hz. Fig. 4.23 shows the vibration modes for the corresponding frequencies. The image in Fig. 4.24 helps to understand why the frequencies are located so close to each other. The grate consists of five identical grates divided into 4 identical spans. Each of the frequencies determined as a result of the calculation is the first vibration mode for the corresponding span in the horizontal or vertical plane. Theoretically, these frequencies should coincide; the existing small discrepancy is due to the features of fastening the middle and outer spans, as well as the difference in the flexibility of the sidewalls and intermediate supports in the case of applying a load in the middle or outer openings.

As will be shown below, during operation the grate performs forced vibrations caused by random impacts from the cotton being processed.

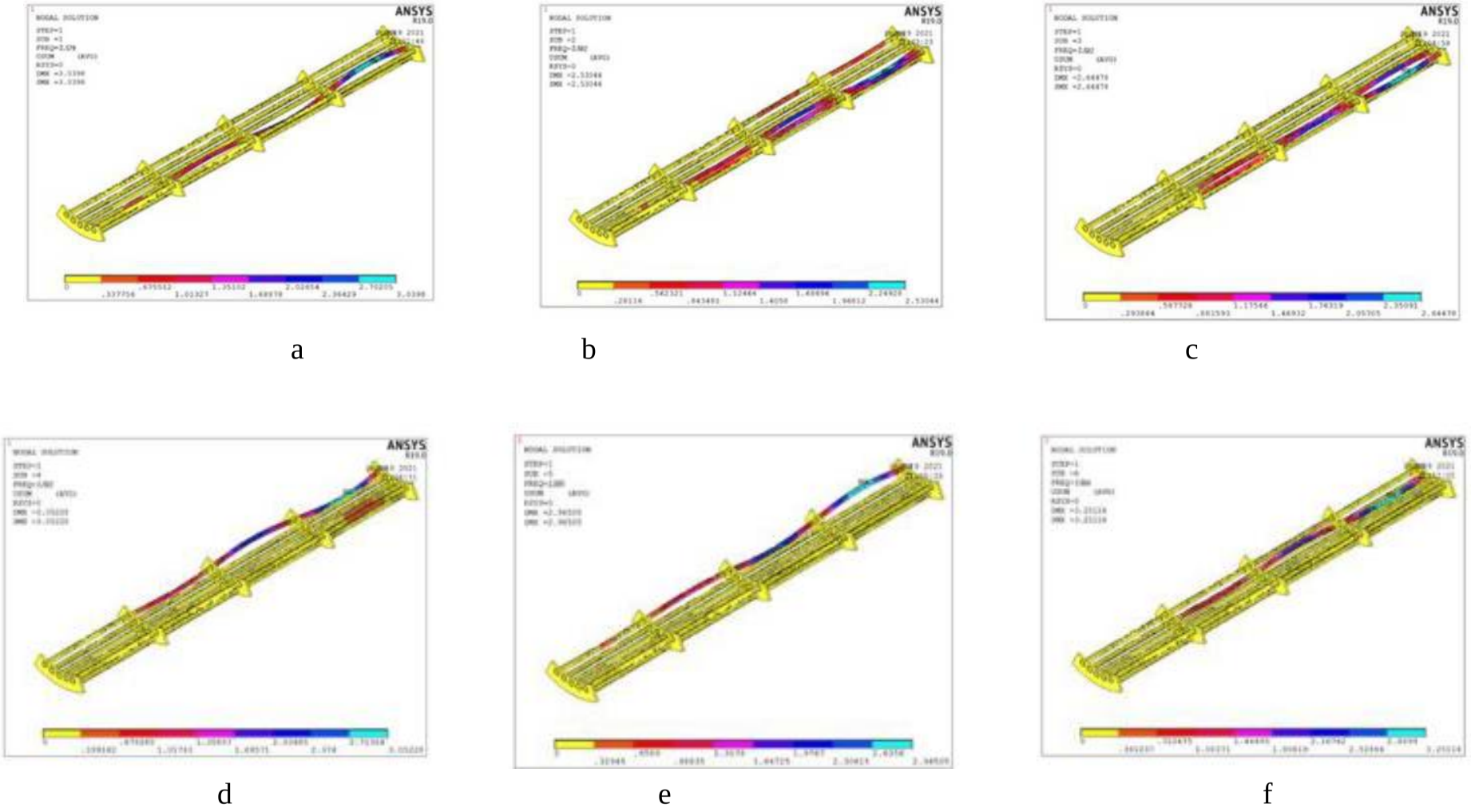

Fig.4.23. Forms of oscillations of the grate corresponding to natural frequencies

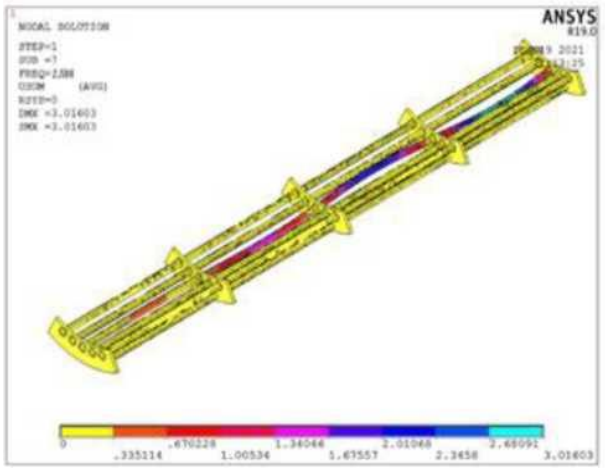

g

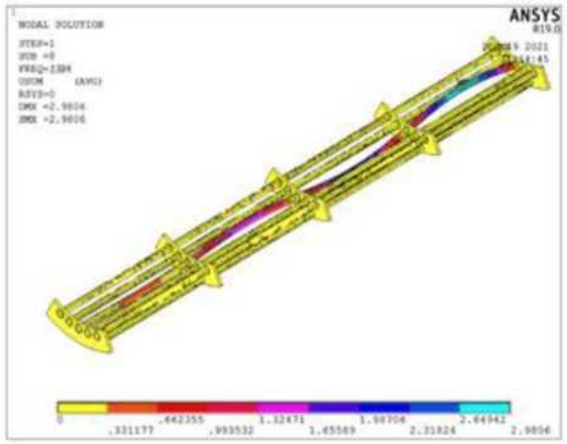

h

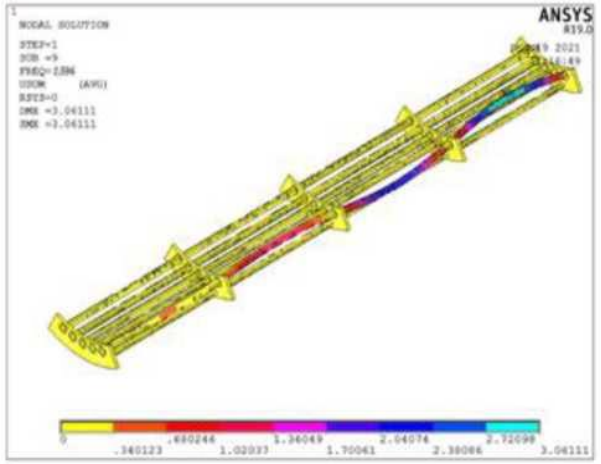

i

j

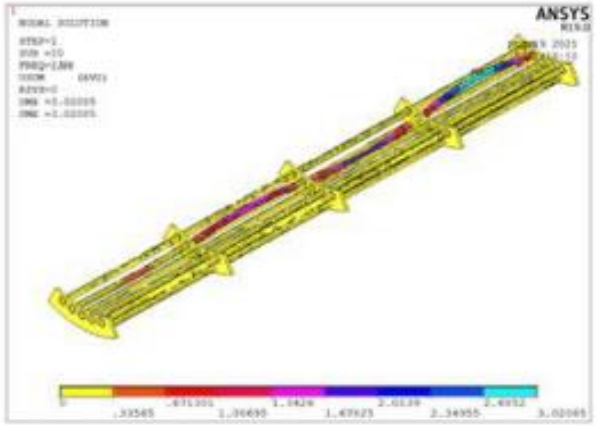

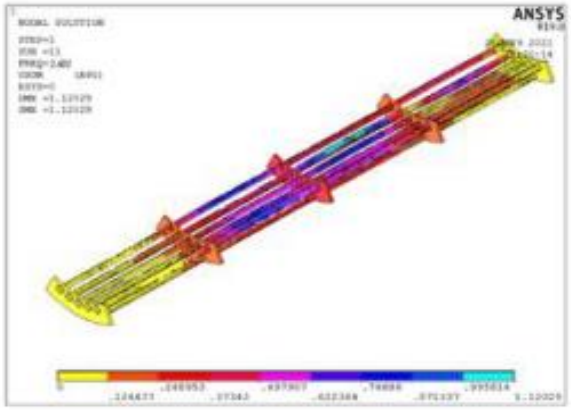

k

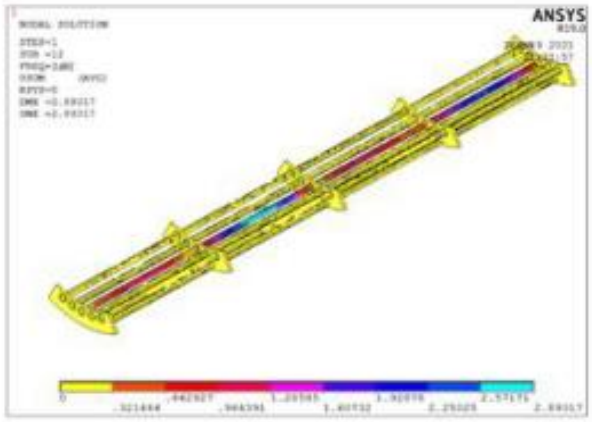

l

Fig.4.24. (continued) Forms of oscillations of the grate corresponding to natural frequencies

4.4. Analysis of grate oscillations on elastic supports with nonlinear stiffness and with random resistance from raw cotton

In a cotton cleaner, the captured fly spools are pulled through the grate bars by a saw-tooth drum to remove large debris. In this case, each grate bar is cyclically exposed to interaction with the fly spools of raw cotton. That is, the loads from the fly spools are the disturbing force of forced vibrations of lightweight composite grate bars on elastic supports with nonlinear rigidity. In fact, this force is a random function [138]. The studies conducted in [139] showed that the resistance of the interaction of raw cotton on grate bars with an elastic support depends mainly on the productivity (angular velocity of the saw-tooth drum) of the cotton cleaner. Usually, the characteristics of the random resistance function are determined experimentally, and the mathematical expectation, correlation function and spectral density are determined based on correlation analysis. The obtained data are taken into account in the form of approximate mathematical models.

It should be noted that composite grates actually perform complex oscillations. Therefore, expression (4.53) will only approximately describe the data of a composite grate. That is, they do not take into account random resistance. The grates will actually perform vertical oscillations. Taking into account the random function of the disturbing force from raw cotton, the nonlinearity of the restoring force of the elastic support, its dissipative characteristics, taking into account the work [140], we can write the equation of the oscillatory motion of the grate in the form:

$$m\frac{d^2x}{dt^2}+в\frac{dx}{dt}+c_1x+\frac{c_2}{\mu}x^3=M(F_в)\pm\delta(F_в) \qquad (4.60)$$

where b is the coefficient of internal resistance of the elastic support of the grate.

Solving (4.60) by analytical methods presents a certain difficulty. The solution can be carried out by approximate methods. To conduct a machine experiment, the solution of the problem is carried out by a numerical method on a PC using standard programs. In this case, the following calculated values of the parameters were taken into account:

m =0,8-1,0 $N{\cdot}s^2$ / m; c_1 = (0,8-1,0) 10^4 N /m; c_2 = (1,2-1,4)·10^4 N /m; b = 50 - 60 Ns / m; μ = 1,0 m^2;

$M(F_b) \pm\delta(F_b)$ = 19,67 + 0,98sin(t + 55°12') + 7,83sin(2t +112°14') +1,8 sin(3t +103°23') + 3,37sin(4t + 4°39') + 6,96sin(5t + 93 ^{0} 24') + 2.7 sin $6t$.

The last formula was obtained as a result of processing experimental oscillograms using the harmonic analysis method.

To determine the best dynamic parameters of composite grates on elastic supports with nonlinear rigidity, taking into account the randomness of

technological disturbance from clapping, the following variations of parameters were carried out.

a) We vary the mass of the lightweight composite grate within the range of m = 0,8-1,5 Ns^2/m. Reducing the mass of the grate allows us to reduce metal consumption and also ensure the required parameters of grate vibrations.

b) Rigidity coefficients of elastic supports. As noted above, the dependence of deformation on the load of an elastic support (rubber bushing) is nonlinear, i.e. with increasing load, the intensity of the increase in deformation decreases. In this case, the rigidity coefficients (changed by changing the thickness of the rubber bushings) varied within the range of $c_1 = (0,8\text{-}1,0)\cdot 10^4$ N/m and $c_2 = (1,2\text{-}1,4)\cdot 10^4$ N/m. In this case, the nonlinearity coefficient of the rigidity characteristic is assumed to be constant.

c) The coefficient of dissipation of the elastic support of the composite grate. For each type (brand) of rubber, the coefficient of internal friction has different values. The coefficient of dissipation of the elastic support characterizes the rate of attenuation of natural oscillations of a composite grate.

Considering that the natural frequency of the grate oscillations changes depending on the amplitude of the oscillations, it is advisable to quickly damp the natural oscillations. For the rubber grades used, NO-68, taking into account their operating conditions (low-frequency mode) [141], the variation of the dissipation coefficient was accepted within the range of *b=50-60 N s/m*.

d) Disturbing force - technological load on the composite grate from raw cotton. This force mainly depends on the machine productivity. With the productivity of the cotton cleaner UXK P_p = 6,0 t/h, the technological load on the grate will be $M\ (F_{b)}$ = 19,7-0,9 *N*.

The accounting of the technological load from cotton on lightweight composite grates is due to the fact that its value during the cleaning process has a random character, which actually forms the oscillation of the composite grate. The character and magnitude of the technological resistance force were determined experimentally by the strain gauge method (Fig. 4.25).

of disturbance from the clap on the grate and its possible variations in both frequency and amplitude were determined.

To study forced oscillations of composite grates on elastic supports with nonlinear characteristics, an algorithm for implementation on a PC was developed. It included taking into account the force of a random technological load from cotton using a random number generator [142] with a frequency of 2 Hz and an amplitude of 18 N, which correspond to the experimental result obtained in Chapter 5. As a result of implementing the mathematical model of the oscillatory system of the grate of a cotton cleaner from large debris on a PC with variations in

parameters, graphical dependencies were obtained.

Fig. 4.8 shows a fragment of displacement, velocity and acceleration composite grate on an elastic support with nonlinear restoring force at m = 1,0 kg, c_x = 0,8 ·10 ^{4} N/m, c$_2$ = 1,2 ·10 ^{4} N/m, M **(**F_b) = 10,5 N, δF_b = (0,7 ÷ 1,0) N. It should be noted that the grate oscillation frequency is 1,5-2,5 Hz. The high-requency component of the grate oscillations is 14,7-17,8 Hz.

The low-frequency component of forced oscillations corresponds to the rotation frequency of the saw-tooth drum of the UXK unit, and the high-frequency component corresponds to the technological load, taking into account the number of grates in the section. From Fig. 4.8 it is evident that during forced oscillations the grate deviates on average by the value X_{av} = (1,4-1,6)·10 $^{-3}$ m, and the amplitude of oscillations at the calculated values of the parameters is ΔX = (1,8 - 2,1)·10^{-3} m. For metal grates on elastic supports, according to work [143], the amplitude of oscillations is ΔX = (1,5 — 1,8)·10 $^{-3}$ m. Comparison of the results shows that in the proposed design of the composite grate, the amplitude of oscillations increases by 10-15% due to the lightweight design of the grate. The values of $\dot{X}$ and $\ddot{X}$ change in a similar way. The amplitude of velocity oscillations reaches from 0,6 m/s to 1,25 m/s, and the amplitude of acceleration oscillations at the calculated parameters of the system varies within the range of 6,5-10 m/s^2. The frequency of velocity and acceleration oscillations corresponds to the high-frequency component of the technological load from cotton.

$\dot{X}$ and $\ddot{X}$ change in a similar manner. The range of speed fluctuations reaches from 0,6 m/s to 1,25 m/s, and the amplitude of acceleration fluctuations at the calculated parameters of the system changes within the range of 6,5·10 m/s ^{2} . The frequency of speed and acceleration fluctuations corresponds to the high-frequency component of the technological load from cotton.

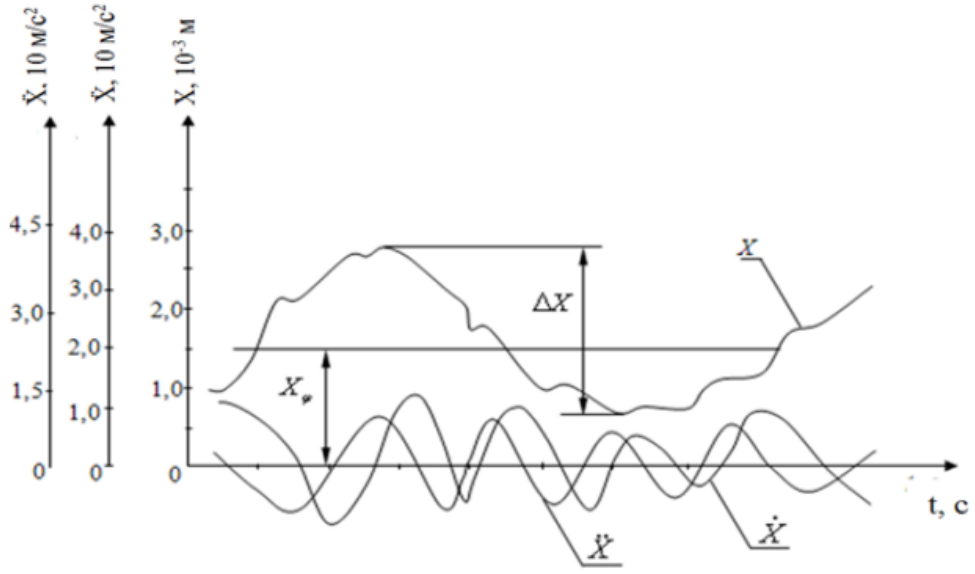

Fig. 4.25. Changes in displacement, speed, acceleration of a composite grate on an

elastic support under random disturbance at $m = 1,0\ Ns^2/m$; $c = 0,8\ 10^4\ N/m$;
$c_2 = 1,2 \cdot 10^4\ N/m$; $M(F_b) = 10,5$ N $\delta F_b = (0,7 \div 1,0)$ N

Fig. 4.9 shows the graphical dependencies of the change in the range of movements, speed and acceleration from the increase in the mass of the grate bar. It is known that with an increase in the mass of the oscillating system, a greater force is required to disturb it, that is, with an increase in mass, the amplitude of oscillations of the composite grate decreases. With an increase in the mass of the grate from 0,7 *kg* to 1,5 *kg* the oscillation range of the composite grate decreases from $1,85 \cdot 10^{-3}$ *m* to $0,65 \cdot 10^{-3}$ *m* according to a nonlinear pattern. Regarding the oscillatory system under consideration, it should be noted that with an increase in the grate mass, the decrease in speed and acceleration is also nonlinear. The peculiarity is that the intensity of the decrease in the oscillation range ΔX, $\Delta\dot{X}$ and $\Delta\ddot{X}$ decreases with increasing mass. This is explained by the nonlinear rigidity characteristic of the elastic support. At the same time, with increasing load on the grate, the intensity of deformation of the elastic support decreases, which leads to a decrease in the amplitude of the grate oscillations (see Fig. 4.26). Comparison of the results of studies with studies of a metal grate on an elastic support [60] show that the amplitude of the oscillations of the speed and acceleration $\dot{X}$ and $\ddot{X}$ in the recommended version by 10-13% more than in cylindrical composite grates. This means that the impulse force acting on raw cotton from the composite grates is 12-15% more than in the existing cleaner grates. The recommended values for the mass of composite grates are 1,1-1,3 *kg*.

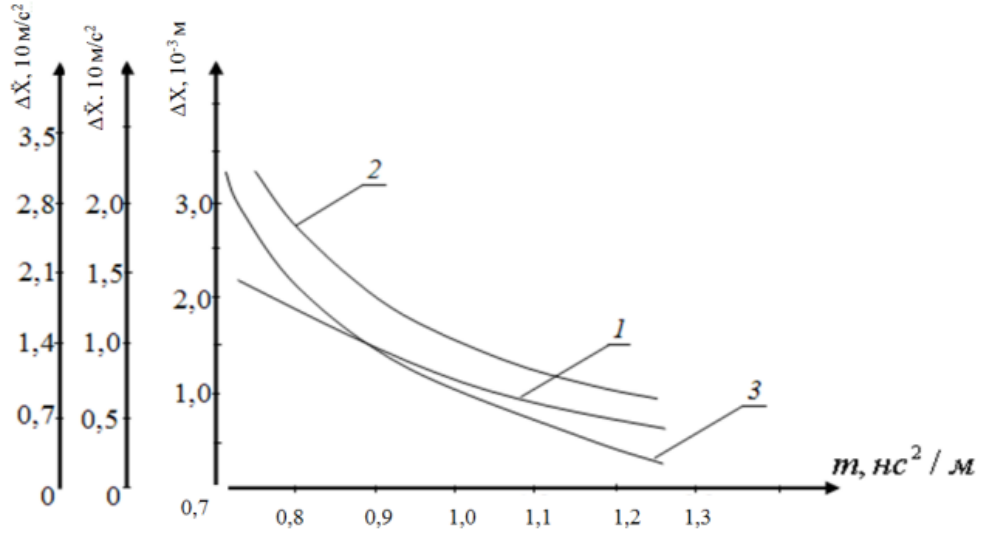

1 -$\Delta X = f(m)$; 2 -$\Delta\dot{X} = f(m)$; 3 -$\Delta\ddot{X} = f(m)$;
at $c_1 = 2,5 \cdot 10^4$ N/m; $c_2 = 1,2 \cdot 10^4$ N/m; deviations $\delta\Delta X$, $\delta\Delta\dot{X}$, $\delta\Delta\ddot{X}$ = 10-12%

Fig. 4.26. Graphical dependencies of the change in the amplitude of oscillations of displacement, speed and acceleration of the composite grate on the change grate masses

In the process of cleaning raw cotton from large debris, it is important to limit the amplitude of the grate oscillations, since these oscillations directly affect the size of the gap between the grate and the saw cylinder. The values of the amplitude of oscillations of the composite grate in our case are regulated by the nonlinear rigidity characteristics of the elastic support. Fig. 4.27 shows the obtained graphical dependencies of the change in the amplitude of movement, speed and acceleration of oscillations of the composite grate on the variation of the nonlinear component of the rigidity coefficient of the elastic supports. With an increase in the load on the grate, the deformation of the rubber bushings due to the variability of the thickness increases with decreasing intensity. This ensures oscillations of the composite grate with the required amplitude and frequency at high machine productivity. With a variation in the rigidity coefficient of the elastic support c_2 values c_1 remained unchanged, $c_1 = 1{,}0 \cdot 10^4\ N/m$. From Fig. 4.10 it is evident that an increase in c_2 leads to a decrease in ΔX, $\Delta\dot{X}$ and $\Delta\ddot{X}$ according to a nonlinear pattern. Thus, with a stiffness coefficient of $c_2 = 0{,}4 \times 10^4\ N/m$, the amplitude of the oscillations of the composite grate movement is $2{,}15 \times 10^{-3}\ m$, and with $c_2 = 1{,}35 \times 10^4\ N$ /m, the value of the amplitude ΔX is $0{,}82 \times 10^4\ m$. In this case, the amplitude of oscillations of the composite grate decreases by 2,4 times. An increase in the stiffness coefficient c_2 of the elastic support also leads to a decrease in the amplitude of oscillations, speed and acceleration of the composite grate. In this case, the amplitude of oscillations of speed $\Delta\dot{X}$ decreases by three times, and the amplitude of accelerations $\Delta\ddot{X}$ decreases by two times. It should be noted that the influence of the random component of the load from the clap affects the values of the amplitude of oscillations ΔX, $\Delta\dot{X}$ and $\Delta\ddot{X}$ within 8,0-10%. The graphs show their average values.

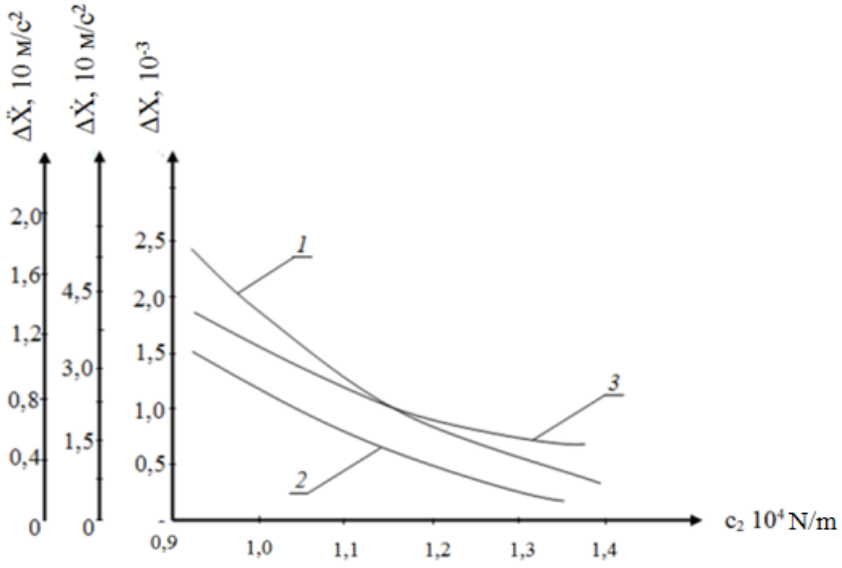

1- $\Delta X = f(c_2)$; 2 - $\Delta\dot{X} = f(c_2)$; 3 - $\Delta\ddot{X} = f(s_2)$;
deviations 8,0-10%; $m = 1{,}4\ kg$; $c_1 = 1{,}2 \cdot 10^4\ N/m$

Fig.4.27. Dependencies of change ΔX, $\Delta \dot{X}$, $\Delta \ddot{X}$ from the coefficient of rigidity with $_2$ elastic support of the composite grate.

In this case, the deviations δx, $\delta \dot{x}$, $\delta \ddot{x}$, = 8,0 -10% c_1 = 1,0·10 ^{4} *N/m* c_2 = 1,2·10 ^{4} *N/m* . Research has shown that an increase in the stiffness coefficient c_1 elastic support leads to a proportional decrease in the amplitude of oscillations of the composite grate bars. To ensure oscillations of the composite grate bars with an amplitude of (0,6-1,2) 10 $^{-3}$ *m* nonlinear component of the elastic support stiffness coefficient should have values of (0,8-1,0)·10 ^{4} N/m, and the stiffness coefficient c_1 = (1,2 – 1,4)·10^4 *N / m* . The change in the thickness of the rubber bushing is up to (2,0 – 2,5)·10 ^{3} *m* (for rubber grade NO-68).

Experimental studies (Chapter 5) have shown that composite grates on elastic supports experience loads from the raw cotton being pulled through in the middle of the grate by 2,0 times, and in the extreme positions by 1,5 times less in relation to grates on rigid supports. In relation to the existing metal grates on rigid supports in production, in the proposed version the load is reduced by 2,3-2,5 times in the middle, and in the extreme positions by 1,6-2,0 times. The attenuation of natural oscillations and part of the forced oscillations of composite grates is ensured by the dissipation coefficient of the elastic support made of rubber grade NO-68. Considering that there are no resonant modes during operation, since the frequencies of natural and forced vibrations have large discrepancies. But, to ensure only forced vibrations of composite grates with relatively fast absorption of free vibrations of composite grates, the recommended values of the dissipation coefficient are 50-60 *Ns/m*, which correspond to the characteristics of rubber grade NO-68 [129, 141].

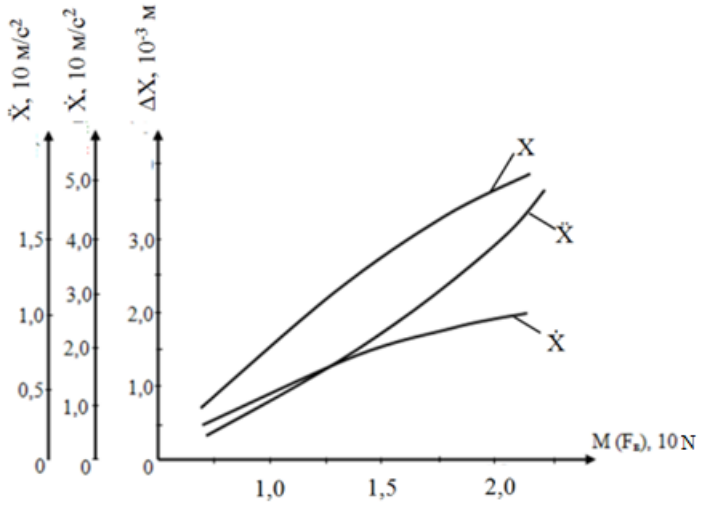

Fig. 4.28. Changes in displacement, speed and acceleration of composite grates depending on the technological resistance of cotton.

Figure 4.28 shows the graphical dependencies of the change in displacement, speed and acceleration of composite grates on elastic supports with nonlinear rigidity with varying load from raw cotton. With an increase in resistance from cotton from 8.5 N to 20 N (average value), the movement of the grate increases from 0,65 10^{-3} *m* to 2,6 10^{-3} *m*. In this case, the oscillation speed increases according to a nonlinear pattern to 2,45 m/s, and the acceleration increases to 17 m/s^2. In this case, the deviations δx , $\delta \dot{x}$and $\delta \ddot{x}$, depending on the random component of the load are within 8,0-10%. To prevent the loss of flyers between the grates, due to the large amplitudes of the grate oscillations and the reduction of the technological gap between the saw drum and the grates, the amplitude of the composite grates, according to the results of experiments, should not exceed (1,0 – 1,4)·10^{-3} *m* **.**

Therefore, to ensure the required vibration amplitudes of the composite grate bars, it is advisable to select resistance from raw cotton within the range of 15-20 N, which corresponds to 5.0-7.0 t/h in the UHK machine.

4.5. Conclusions on Chapter 4

1. A formula for calculating the speed of impact interaction of a cotton fly with a multifaceted mesh surface has been obtained. A formula for determining the rebound value of a cotton fly after interaction with the mesh has been derived.

2. Graphic dependences of the change in the speed of movement of cotton bats on a multifaceted mesh surface on the change in the angle of inclination of the flight of bats in the cleaning zone are constructed. It is revealed that in order to increase the speed of movement of cotton bats in the cleaning zone, it is necessary to ensure sufficient loosening of the cotton, such that the mass of tufts of raw cotton does not exceed 0,5-0,7 g, while the speed of pulling cotton is within 3,0-3,5 m/s.

3. Graphic dependences of the change in the speed of movement of cotton bats on a multifaceted mesh surface on the change in the length of the edges and the length of the flight of bats in the cleaning zone were obtained. It was established that in order to ensure the speed of movement of cotton bats on the mesh surface up to 3.0-3.5 m/s, the recommended mesh edge length is (3,2-4,5)·10^{-2} m.

4. The dependences of the change in the rebound value of the cotton fly on the change in the angle of inclination of its trajectory in the cleaning zone are determined. It is revealed that at smaller values of the angle β, the impact of the fly will be significant, thereby the rebound value will be greater. In this case, the separation of debris will be more effective. However, this reduces the speed of pulling the fly. In addition, damage to fibers and cotton seeds can increase.

Therefore, the recommended values are $\beta \leq 25°\text{-}35°$;

5. Graphic dependences of the change in the rebound value of the cotton fly on the change in the length of the interaction zone with the mesh are constructed. It is revealed that an increase in the flight speed of the fly when leaving the surface of the splitter also leads to an increase in the trajectory length, while the rebound value of the fly after hitting the mesh polyhedral surface decreases significantly. It should be noted that with an increase in the trajectory length, the force of the impact interaction of the cotton fly with the polyhedral mesh surface decreases.

6. The analytical method was used to solve the problem of determining the reaction during the interaction of cotton filaments with the multifaceted mesh surface of a small debris cleaner. The maximum value of the dynamic reaction during random disturbance from the layer of processed cotton is 30% greater than during harmonic disturbance.

7. Small oscillations of a polyhedral mesh under the effect of technological load from the cleaned cotton are studied. Graphic dependences of the change in the amplitude of oscillations of the polyhedral mesh on the increase in the torsional rigidity of the elastic support and on the moment of inertia of the mesh are constructed. To ensure the required values $\Delta\varphi_c = (3{,}8 - 5{,}6)\cdot 10^{-2}\ rad$ The recommended values for the moment of inertia of a polyhedral mesh are 0,21–0,65 kg m^2 . In this case, the mass of the polyhedral mesh should be selected to be no more than 7,5–9,5 kg.

8. A method for determining the rigidity of an elastic support of a polyhedral mesh is proposed. Dependences of changes in the amplitude of oscillations of the mesh surface on elastic supports on changes in the amplitude of the process load are obtained.

9. A differential equation for the oscillatory motion of a lightweight composite grate on an elastic support with nonlinear rigidity is obtained.

10. Formulas for determining the period and frequency of natural oscillations of a grate on an elastic support with a nonlinear restoring force are obtained. It is revealed that with an increase in the reduced mass of the grate, the frequency of its natural oscillations decreases according to a nonlinear pattern.

11. The dependences of the change in the grate oscillation period on the increase in the oscillation amplitude are obtained. It is established that an increase in the rigidity of the elastic support leads to an increase in the relative frequency of the grate's natural oscillations according to a nonlinear pattern.

12. The first twelve natural frequencies of composite grates were calculated using finite element modeling methods. It was shown that their values are located in a narrow range, which allows using resonance modes to increase cleaning

efficiency.

13. A mathematical model of oscillations of composite grates on elastic supports with nonlinear rigidity under random resistance from raw cotton has been developed. Based on the numerical solution of the problem, the nature and shape of oscillations of the composite grate of a cotton cleaner for large debris have been obtained.

14. The dependences of the change in the oscillations of the displacement, speed and acceleration of the composite grate are constructed depending on the rigidity coefficient of the elastic support of the grate. It is revealed that with an increase in the load on the composite grate, the values of displacement, speed and acceleration increase according to nonlinear patterns, and the influence of the random component of the load is within 8,0-10%. To ensure the required amplitudes of oscillations of the composite grate $(1,0\text{-}1,4)\cdot 10^{-3}$ m, the average value of the disturbing force should not exceed 15-20 N.

15. Formulas for determining the distance and angle of deviation of the cotton fly with variable rotation of the saw-tooth drum are obtained. Dependencies of the change in the angle of deviation of the fly from the saw-tooth drum with an increase in its diameter are constructed.

CHAPTER 5. RESULTS OF EXPERIMENTAL STUDIES OF THE MAIN WORKING ELEMENTS OF THE SEPARATION AND PURIFICATION UNIT

5.1. Test results of the upgraded separator.

Chapter 2 describes the measures to improve the CC15-A cotton separator, and Chapter 3 provides a theoretical justification for the parameters of the new separator elements and their operating modes.

The separator was modernized in the following directions.

5.1.1. Ensuring control of the movement of the cotton-air mixture at the entrance to the separator

To prevent increased crushing of seeds in the separator, it is proposed to install a guide at the entrance to the separating chamber, which will ensure control over the flow of the cotton-air mixture. The design parameters of this guide are substantiated. The parameters of its interaction with the cotton-air mass are established by finite element modeling.

The experimental sample of the guide was manufactured in two versions. In the first version, shown in Figure 5.1, it is rigidly fixed to a frame that is installed on the inlet pipe of the separator. Such a guide was installed on the separator in the Chelak Pakhta Tozalash Joint-Stock Company in Samarkand (Republic of Uzbekistan).

Fig. 5.1. Cotton-air mixture flow guide (option 1)

The second version of the guide was installed directly in the separating

chamber and allowed the position to be adjusted in such a way as to deflect the flow of the cotton-air mixture entering the separator to a greater or lesser extent. The appearance of such a guide is shown in Fig. 5.2. This version of the guide was tested at the Sherabad cotton mill (Termiz, Republic of Uzbekistan)

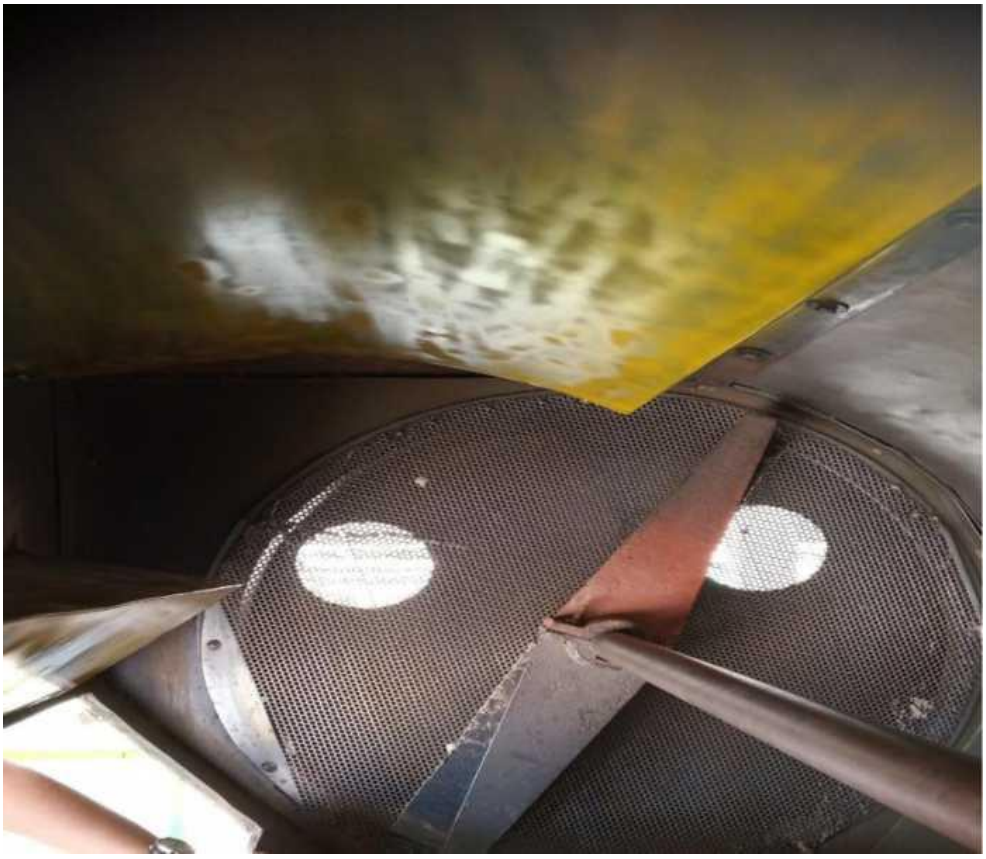

Fig. 5.2. Cotton-air mixture flow guide (option 2)

To assess the impact of the proposed recommendations, a full factorial experiment was conducted, in which the output parameter was mechanical damage to seeds, and the factors were the air velocity in the separator inlet pipe, the angle of the guide, and the equipment performance. The air velocity in the separator inlet pipe was set by changing the fan impeller speed, which was changed by replacing the pulley on the fan drive shaft. The air velocity was monitored using an electronic anemometer based on a PCE - PFM -2 Pitot tube, which has an operating range of flow velocity measurement of up to 80 m/s and pressure of up to 50 *mbar*._The angle of visor deviation a from the horizontal was set using a conveyor fixed to the separating chamber body. The required separator performance level was ensured by setting the appropriate feed rate of raw cotton by the conveyor.

The experimental conditions are given in Table 5.1.

Table 5.1

No.	Name of the factor, symbol	Coded designation	Actual values of the factor			Variation Interval
			-1	0	+1	
1	Air velocity in the inlet pipe v, m/s	x_{11}	$x_{11min} = 20$	$x_{11c} = 27,5$	$x_{11max} = 35$	$\Delta_{11} = 7,5$
2	Guide inclination angle α, deg.	x_{21}	$x_{21min} = 15$	$x_{21c} = 22,5$	$x_{21max} = 30$	$\Delta_{21} = 7,5$
3	productivity P, t/hour	x_{31}	$x_{31min} = 10$	$x_{31c} = 12,5$	$x_{31max} = 15$	$\Delta_{31} = 7,5$

The experiments were carried out in triplicate based on the design matrix (Table 5.2). In this case, the number of experiments $N = 2^3 = 8$, the number of repetitions $m = 3$, and the total number of experiments $N \cdot m = 8 \cdot 3 = 24$.
The obtained values of the output parameter, their mean values and variance are presented in Table 5.2.

Table 5.2

Experimental Design Matrix

No.	Factor range			Seed damage (in percent)						
				Deviation						
	X_1	X_2	X_3	y_{i1}	y_{i2}	y_{i3}	y_u	$S^2\{y\}$	y_{Ru}	$(y_u - y_{Ru})^2$
1	-	-	-	1,24	1,26	1,25	1,25	0,000100	1,22	0,000733
2	+	-	-	1,4	1,5	1,4	1,43	0,003333	1,44	6,26E-05
3	-	+	-	0,95	1,01	1,03	1,00	0,001733	1,02	0,000733
4	+	+	-	1,3	1,22	1,23	1,25	0,001900	1,24	6,26E-05
5	-	-	+	1,31	1,4	1,32	1,34	0,002433	1,35	0,000126
6	+	-	+	1,43	1,4	1,55	1,46	0,006300	1,46	6,26E-05
7	-	+	+	1,17	1,16	1,17	1,17	0,000033	1,15	0,000126

8	+	+	+	1,27	1,28	1,28	1,28	0,000033	1,26	6,26-05

We check whether the homogeneity of variances *S is ensured*, which characterizes the distribution of results over the number *m* of parallel experiments [144].

$$S_u^2 = \frac{\sum_{p=1}^{m}(y_{up} - y_u)^2}{m-1} \qquad (5.1)$$

where *u* is the serial number of the option *p* is the serial number of parallel experiments (*p* = 1 , 2 , 3.. m), *m* - number of parallel experiments, $y_u = \frac{1}{m}\sum_{p=1}^{m} y_{up}$ - the average value of the results of a parallel experiment. *m* = 3 for the case of *S* and ^{2} we enter the values into the table and calculate this statistic.

$$G = \frac{S^2_{maz}}{\sum_{u=1}^{N} S_u^2} = \frac{0{,}00630}{0{,}01586} = 0{,}3972 \quad G = \frac{S^2_{u(\max)}}{\sum_{u=1}^{N} S_u^2} \qquad (5.2)$$

where $S^2_{u\,(max)}$ is the maximum value of the dispersion given in Table 5.2.

We examine the distribution of variance in two parallel experiments using Cochran's test, $G_{\alpha,\ k1,\ k2}$ - values are given in the table, α - significant level ($0 < \alpha < 1$), $k_1 = N$, $k_2 = m - 1$ - The degree of freedom in our case *is* α = 0,05, *m* = 2, *N* = 8 , $G_{\alpha\ ,\ k\ 1,\ k\ 2} = G_{0{,}05,8,1} = 0.52$. If the following inequality is satisfied

$$G < G_{\alpha\ ,\ k\ 1,\ k\ 2}\ , \qquad (5.3)$$

then the dispersions can be considered homogeneous.

Let's calculate the reproducibility variance

$$S_y^2 = \frac{1}{N}\sum_{u=1}^{N} S_u^2 = \frac{0{,}01586}{8} = 0{,}001982$$

3. We make a regression equation for *k* = 3

$$y = b_0 + \sum_{i=1}^{k} b_i x_i + \sum_{i<1}^{k} b_{ij} X_i X_j + \sum_{i<j<l}^{k} b_{ijl} X_i X_j X_l$$

The regression coefficients are calculated using the following formulas (N = 8).

$$b_0 = \frac{1}{N}\sum_{u=1}^{N} \bar{y}_u\ ,\ b_i = \frac{1}{N}\sum_{u=1}^{N} X_{iu}\bar{y}_u\ ,\ b_{ij} = \frac{1}{N}\sum_{u=1}^{N} X_{iu}X_{ju}\bar{y}_u\ ,\ b_{ijk} = \frac{1}{N}\sum_{u=1}^{N} X_{iu}X_{ju}X_{ku}\bar{y}_u$$

$$b_0 = 1{,}272; b_1 = 0{,}0829; b_2 = -0{,}0995;\ b_3 = 0{,}03958;\ b_{12} = 0{,}00791;$$

$$b_{13} = -0{,}0262;\ b_{23} = 0{,}00958;\ b_{123} = -0{,}00958$$

Thus, the regression equation looks like this:

$$Y=1,272+0,0829X_1–0,0995X_2+0,0395X_3+0,00791X_1X_2–0,0262\ X_1X_3+0,00958\ X_2X_3–0,00958\ X_1X_2\ X_3 \quad (5.4)$$

4. We use the Student's criterion to determine the significance level of the regression coefficients. To do this, we calculate the dispersion of the regression coefficients [144]

$$S^2\{b_i\} = \frac{1}{N \cdot m} S^2\{Y\} = \frac{1}{8 \cdot 3} 0,001982 = 0,00008258$$

$$S\{b_i\} = 0,00908$$

Calculated value of the Student's criterion

$$t_R\{b_i\} = \frac{|b_i|}{S\{b_i\}}$$

$$t_R\{b_1\} = \frac{0,082917}{0,00908} = 9,13,\ t_R\{b_2\} = \frac{0,09958}{0,00908} = 11,05,\ t_R\{b_3\} = \frac{0,03958}{0,00908} = 4,35$$

$$t_R\{b_{12}\} = \frac{0,007916}{0,00908} = 0,87;\ t_R\{b_{13}\} = \frac{0,02625}{0,00908} = 2,89;\ t_R\{b_{23}\} = \frac{0,009583}{0,00908} = 1,05$$

$$t_R\{b_{123}\} = \frac{0,009583}{0,00908} = 1,05$$

Confidence for regression coefficients.

Tabular value of the Student's criterion $t_{0.05,16} = 2.31$, i.e. coefficients b_{12}, b_{23} and b_{123} are insignificant. The final regression equation will look like this.

$$y = 1,2720 + 0,0829X_1 - 0,0995X_2 + 0,0395X_3 - 0,0262X_1X_3 \quad (5.5)$$

To check the adequacy of the obtained model, we determine the variance due to inadequacy using the formula.

$$S^2_{\text{ад}}\{Y\} = \frac{m \sum_{u=1}^{N} (y_{u\text{ср}} - y_{Ru})^2}{N - N_k} = \frac{3 \cdot 0,00197}{8-5} = 0,00197$$

where y_{Ru} - the value of the output parameter calculated according to (5.5),

y_{and} - the actual value of the output parameter,

N - number of options,

N_k - the number of significant regression coefficients.

The calculated value of Fisher's criterion will be

$$F_R = \frac{S_y^2}{S_{\text{ад}}^2\{Y\}} = \frac{0{,}001982}{0{,}00197} = 1{,}006$$

Tabular value of Fisher's criterion

$$F_T[p_D = 0{,}95;\ f_1 = 8(3-1) = 16;\ f_2 = 8-5 = 3] = 8{,}69$$

Since $F_R < F_T$, the hypothesis about the adequacy of the regression model (5.5) is not rejected.

The model in natural values of factors has the form

$$Y = 0{,}3251 + 0{,}0284v - 0{,}0132\alpha + 0{,}0542П - 0{,}00139vП$$

The resulting model allows predicting seed damage depending on technological factors.

5.1.2. Facilitating the removal of fiber from the perforated wall of the separator.

During the operation of the separator, some of the cotton is pressed by the air draft against the perforated walls located between the separating and air chambers. This cotton forms a layer on the wall surface. To remove the formed layer, movable scrapers mounted on a rotating shaft are used. The process of removing the cotton layer is accompanied by the destruction of seeds and the formation of free fibers, which are carried away by the air into the waste.

To eliminate this phenomenon, two measures are proposed. One of them is the production of specially shaped holes in the perforated walls, theoretically justified in 2.5.

Another measure is the installation of a scraper with an additional insulating chamber in the modernized SS-15A separator (Fig. 5.3).

During the process of separating cotton by scraper 3, insulating chamber 1, located on the rear side of perforated surface 2, covers the air flow. In this case, the pressure difference between the inner and outer surfaces of the wall is zero, i.e. the insulating chamber blocks the air suction process. The friction force between the cotton and the perforated surface is sharply reduced. This reduces the mechanical impact on the seeds and prevents fiber breakage. As a result, the number of free fibers is reduced. Scraper 8 freely cleans the perforated surface from cotton. Cotton falls into the vacuum valve under the action of its own weight. Figure 5.4 shows a general view of the installation on the CC15-A separator. Figures 5.5 and 5.6 show the rear view and the location of the scraper elements [145].

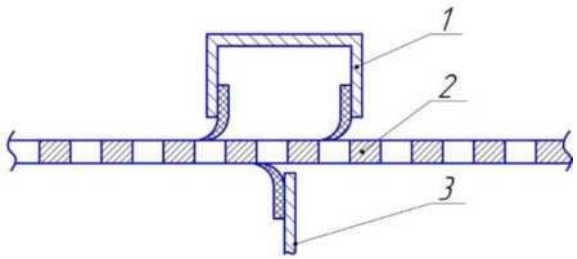

Fig. 5.3. Location of the isolation chamber in relation to the main scraper

Fig. 5.4. View from the scraper side

Fig. 5.5. View from the separating chamber

Experiments to test the effectiveness of the proposed changes in the separator design were conducted at the enterprise JSC "Korasuv Pakhta Tozalash" in the Tashkent region (Republic of Uzbekistan). As a control option, a serial separator SS-15A was used, which was compared with a modernized one equipped with an isolating chamber.

Figure 5.6 shows the improved CC-15A separator installed in the process

flow (Figure 5.6).

Fig.5.6. General view of the SS-15A UHK separator.

The main criterion for efficiency was the amount of free fibers entering the waste. The following method was used to determine it. A burlap filter was installed in the outlet pipe of the separator. The waste coming from the separator was collected on it for 10 minutes of operation. After that, they were weighed with an accuracy of 0.01 g. Then, fibers were manually removed from the sample and weighed again. The degree of mechanical damage to the seeds was determined using the standard method UzDSt 598: 2008 and UzDSt 597: 2008, "Method for determining the mass fraction of defective seeds" [146; 3- c].

The experiment used raw cotton of the Sultan selection variety of industrial grades I, II, III, IV and V. The air flow rate in both separators was the same, and the productivity was 10 t/h. Tables 5.3 and 5.4 show the levels of contamination and moisture content of the cotton during the experiment, as well as the results of the experiment [147; 1-5 c].

Analysis of Table 5.3 shows that the use of a separating chamber allows to reduce the content of combined fibre in litter by 33 - 39%, and the beneficial effect is more pronounced in low grades. This is due to the fact that they contain a greater number of immature and damaged fibres, which are more easily separated by mechanical action. Therefore, reducing the load when using an isolating chamber helps to preserve a greater number of fibres.

Table 5.3

Effect of an isolation chamber on the content of free fibers in litter

Variety cotton	Amount of free fibers in litter, %			
	Level of contamination and moisture content of cotton,%	Serial separator CC-15A	Upgraded separator CC-15A	Reduction in the amount of free fibers in litter,%
I	Z=2,05 W=8,6	0,26	0,17	33
II	Z=2,05 W=8,6	0,37	0,24	35
III	Z=3,98 W=10,92	0,51	0,32	37
IV	Z=6,8 W=13,5	0,63	0,39	38
V	Z=11,4 W=16,5	0,78	0,48	39

The results of the experimental determination of the number of damaged seeds are given in Table 5.4.

Table 5.4

Effect of an Isolation Chamber on Seed Crushing

Variety cotton	Seed damage, %			
	Level of contamination and moisture content of	Serial separator CC-15A	Modernized bathroom separator CC-15A	Reduction in the number of damaged - seeds,%
I	Z=2,05 W=8,6	1,08	1,32	22%
II	Z=2,05 W=8,6	1,21	1,41	16.5%
III	Z=3,98 W=10,92	1,38	1,55	12%
IV	Z=6,8 W=13,5	1,87	2,05	9,6%

V	3=11,4 W=16,5	2,15	2,38	7,3%

Table 5.4

Effect of an Isolation Chamber on Seed Crushing

Variety cotton	Seed damage, %			
	Level of contamination and moisture content of	Serial separator CC-15A	Modernized bathroom separator CC-15A	Reduction in the number of damaged - seeds,%
I	Z=2,05 W=8,6	1,08	1,32	22%
II	Z=2,05 W=8,6	1,21	1,41	16,5%
III	Z=3,98 W=10,92	1,38	1,55	12%
IV	Z=6,8 W=13.5	1,87	2,05	9,6%
V	Z=11,4 W=16.5	2,15	2,38	7,3%

Let us present the results obtained from the experiments graphically. Figure 5.7 shows a graph of the change in the amount of free fiber in the separator waste. When we analyze this graph, we see that the amount of free fiber in the CC-15A separator is on average 33-39% greater than the amount of free fiber in the improved separator. As a result, the torn fiber passes through the mesh surface and is collected in the dust collector with the air flow [148]. Amount of free fiber in raw material, %

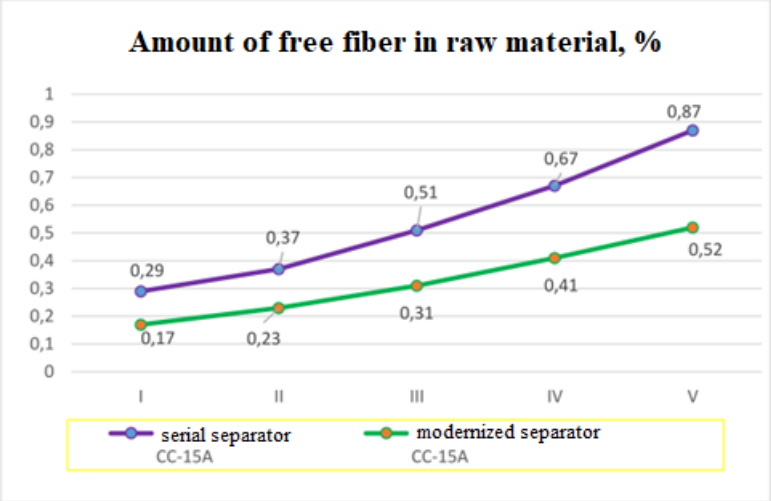

Fig. 5.7. Graph of changes in the amount of free fiber in raw cotton depending on the type of cotton

As can be seen from the graph, the amount of free fiber in the waste increases with decreasing industrial grade of cotton. Figure 5.8 shows the effect of the improved CC-15A separator on the degree of mechanical damage to seeds. This graph shows that the degree of mechanical damage to seeds increases with a change in industrial cotton grades: the degree of mechanical damage to seeds in industrial grade I cotton ranges from 1.08% to 1.32%; industrial grade II cotton from 1.21% to 1.41%; grade III cotton from 1.38% to 1.55%; industrial grade IV cotton from 1.87% to 2.05%; industrial grade V cotton ranged from 2.15% to 2.38%.

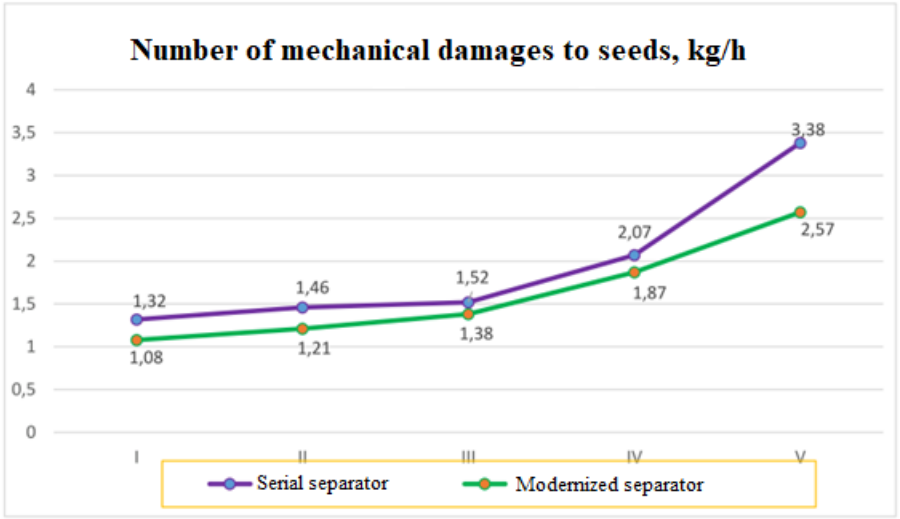

Figure 5.8. Change in the degree of mechanical damage to seeds depending on the industrial variety of cotton

The use of an insulating chamber reduces the amount of free fiber by reducing the pressure force on the surface of the perforated wall, as well as by uniformly distributing the cotton layer on it.

The technical solutions and recommendations obtained as a result of completing the dissertation have been implemented in:

- Karasuv and Piskent cotton factories in Tashkent region.
- Kagansky and Peshkunsky cotton factories of the Bukhara region.
- Chelak cotton factory in Samarkand region.
- Sherabad cotton factory, Surkhandarya region.

This is confirmed by the relevant implementation acts (Appendix 1-6).

5.2. Improving the technology of cleaning raw cotton from small foreign impurities

Nearby scientists from JSC “Paxtasanoat ilmiy markazi” and TITLP have studied to a sufficient extent the factors influencing the amount of fine debris released during the process of cleaning raw cotton. In particular, the influence of the rotation frequency, the size of the pick drum, the design parameters of the mesh, the gap between the drum and the mesh, and others have been studied [149]. They have proposed recommended values for these parameters. However, these parameters do not exhaust the possibility of increasing the efficiency of fine debris cleaners.

As shown by the theoretical analysis in Chapter 4, there is a significant reserve for increasing the cleaning effect in improving the parameters of the cleaning zone of the purifiers from small debris. Experiments were conducted in production conditions to confirm this position.

5.2.1. Methodology for conducting technological experiments

Technological experiments were carried out on 1XK cotton purifiers in the production conditions of the “Korasuv pakhta tozalash” cotton mills (Republic of Uzbekistan).

The aim of the study was to compare the existing cotton cleaning technology using a cylindrical mesh surface with the proposed cleaning technology using a multifaceted mesh surface based on the results of theoretical studies (Fig. 5.9, Fig. 5.10- *a* and *b*).

The experiments were carried out in the following variants:

— existing technology for cleaning cotton from small debris;

— technology for cleaning cotton from small debris using a multi-faceted mesh surface;

— comparison of the cleaning process of the proposed and existing technology when changing the gap between the pins and the grid.

— The experiments were carried out on the selection variety "Namangan-

77" II and III industrial grades

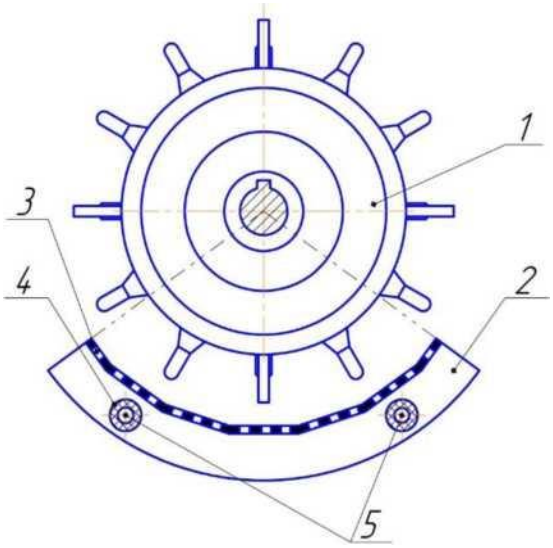

Fig. 5.9. General view of the cleaning zone using a multifaceted mesh surface. 1-pin drum; 2-mesh sidewall; 3-mesh surface; 4-rubber bushings; 5-supports

Samples for analysis were taken after the cotton cleaner. For each variant, the moisture content, contamination, and cleaning effect were determined. These indicators were determined according to the standards OzDst 6432006, O'zDst 6442006, O'zDst 5922008 [150, 151]. Cotton moisture was measured on a VKhS-M1 device using VLKT laboratory scales. The cleaning effect was determined on a LKM laboratory unit.

Fig. 5.10. a - Photographs of the cotton cleaning area using drums with multifaceted screens

Fig. 5.10. b - Photographs of the cotton cleaning area using a multi-faceted mesh surface

5.2.2. Effect of mesh surface design options on the cleaning effect of cotton on small debris

When conducting experiments, the following options were used and compared in terms of cleansing effect:

- existing version of the mesh surface;
- mesh surfaces with 4, 5, 6 and 7 faces
- design options with a change in the gap between the tops of the pegs and the mesh surface.

Figure 5.11 shows the graphical dependencies of the change in the cleaning effect on the machine productivity with different numbers of faces (4, 5, 6, 7 faces) and face widths (*l_w:* 106 mm; 85 mm; 70,8 mm; 60,7 mm). Analysis of the constructed graphs shows that with an increase in the number of faces or a decrease in the face width, the cleaning effect decreases. With a mesh face width of 53,1 mm and a productivity of 5,0 t/h, the cleaning effect reaches 44,2%, and with П=9,0 t/h, it reaches 37,2%.

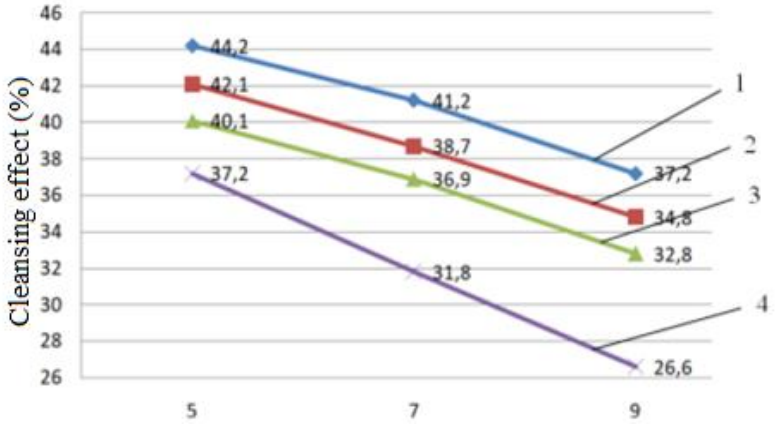

Fig. 5.11. Change in cleaning effect from machine productivity with different number of mesh faces:

1 - mesh surface with 4 edges (1w=106 mm); 2 - mesh surface with 5 edges (1w=85 mm); 3 - mesh surface with 6 edges (1w=70.8 mm); 4 - mesh surface with 7 edges (1w=60.7 mm).

Accordingly, when $l_{w\ is\ reduced}$ to 60.7 mm (7 edges), the cleaning effect of cotton decreases to 37.2% at P = 5.0 t/h, and at a productivity of 9.0 t/h, the cleaning effect decreases to 26.6%. However, an increase in the width of the edges of the mesh surface leads to significant slowing down of the cotton, increasing the interaction with the mesh and pins. This leads to some increase in damage to the fibers and seeds of the cleaned cotton [152]. Therefore, the recommended values are $p_g = 6;\ l_w = 70.8\ mm$.

Fig. 5.12 shows the experimental dependences of the change in cleaning effect on the change in productivity, using the existing and recommended mesh design options.

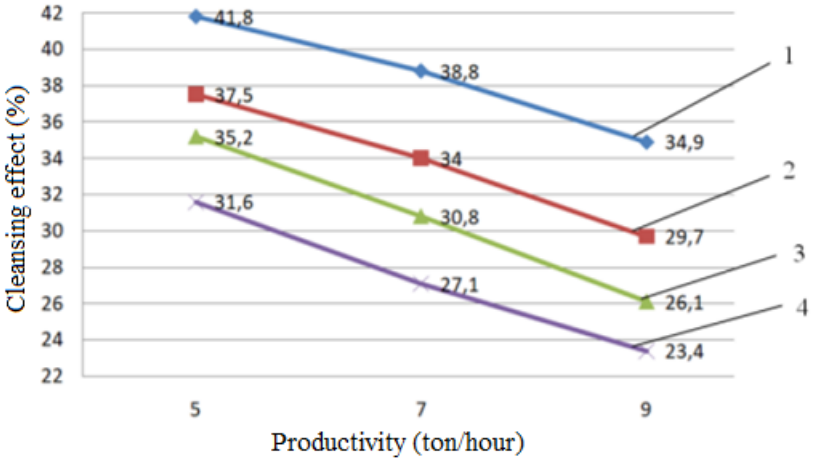

Fig. 5.12. Change in the cleaning effect of cotton with increasing machine performance.1- mesh surface (II grade); 2- existing mesh surface (II grade);3- mesh surface (III grade); 4- existing mesh surface (III grade).

At a capacity of 5,0 t/h, the cleaning effect for small debris for the existing mesh version, when cleaning grade I cotton, will be 37,5%, and for a multi-faceted (6 faces, l_g = *70,8 mm)* mesh, the cleaning effect reaches 41,8%. At a capacity of 9.0 t/h, the cleaning effect for
the existing version will be 29.,7%, and for the recommended design of the multi-faceted mesh it reaches 34,9%. When cleaning grade III cotton, the cleaning effect at P=5,0 t/h for the existing version of the mesh will be 31,6%, and for the recommended version it will be 35,2%. It should be noted that the cleaning effect at different productivity and grades of cleaned cotton in the recommended multi-faceted mesh compared to the existing version will be higher by an average of 2,7-5,7%. In the recommended multi-faceted mesh, the incoming cotton fly hits with different force. In addition, the fly is dragged along a flat mesh surface, which enhances the interaction. This leads to intensive removal of debris and an increase in the cleaning effect.

It is important to study the effect of the gap 5 between the tops of the pegs and the multifaceted mesh. The obtained graphical dependencies are presented in Fig. 5.13. Analysis of the graphs shows that an increase in the gap between the ends of the pegs and the multifaceted mesh surface leads, as in the serial version of the mesh, to a decrease in the cleaning effect.

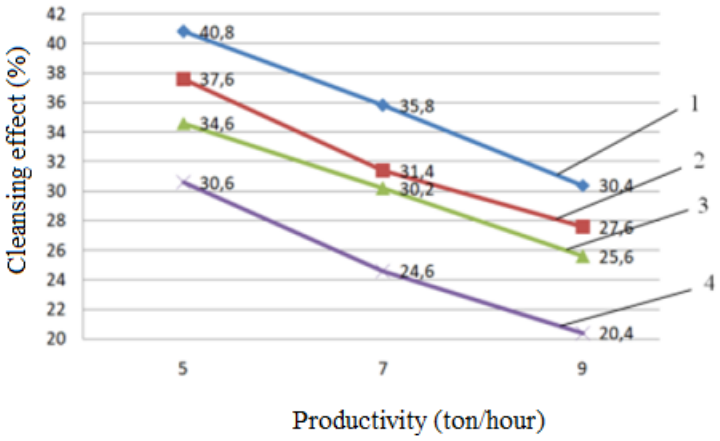

Fig. 5.13. Graphic dependencies of the change in the cleaning effect from the increase in productivity and from the gap between the ends of the pegs and the mesh surface.1 - mesh surface at δ=13,0 mm;2 - existing mesh surface at δ =13,0 mm;3 - mesh surface at δ =15,0 mm;4 - existing mesh surface at δ =15,0 mm.

In the recommended version of the multi-faceted mesh with P=5,0 t/h and δ =13,0 mm, the cleaning effect is 40,8%, and with P=9,0 t/h it decreases to 30,4%. With the existing version of the mesh, the cleaning effect will be 37,6% and 27,6%, respectively. That is, the difference between the compared options reaches 2,8-4,4%. With an increase in the distance between the ends of the pegs and the

mesh to 15,0 mm, with the recommended version of the multi-faceted mesh, the cleaning effect will be 4-5,8% greater than when using the serial mesh. The recommended gap values will be 14,0-15,0 mm, when using a multi-faceted mesh l_w = 70,8 mm (6 faces).

5.2.3. Cleaning cotton using a mesh on elastic supports

Chapter 4 proposes a design for a fine juice cleaner mesh, which is mounted on elastic supports. A theoretical analysis of the interaction of such a mesh with the cotton transported through it is carried out, and rational values for the mesh parameters are proposed.

Experiments were conducted to confirm the effectiveness of the elastic mesh fastening and its effect on the cleaning effect in the conditions of the cotton mill "Korasuv pakhta tozalash" (Republic of Uzbekistan). Cotton of the selection variety Namangan-77 of II and III grades was used for processing. The results obtained are presented in Table 5.5.

Table 5.5

Results of experimental tests of a multifaceted mesh surface on elastic supports (II grade)

No.	Indicators	Number of mesh faces	Productivity, t/h		
			3	5	7
1	Moisture content, %		8.6		
2	Amount of debris in the source material, %		4.6 (2.0 - small, 2.6 - large)		
3	Amount of debris after the cleaner, %	4	1,19	1,32	1,41
		5	1,20	1,37	1,42
		6	1,15	1,21	1,37
		7	1,29	1,38	1,45
		Serial grid	1,30	1,40	1,47
	Cleansing effect, %	4	0,405	0,34	0,295
		5	0,4	0,315	0,29
		6	0,425	0,395	0,315
		7	0,355	0,31	0,,275
		Serial grid	0,35	0,3	0,265

Table 5.6

Results of experimental tests of a multifaceted mesh surface on elastic supports (III grade)

No.	Indicators	Number of mesh faces	Productivity, t/h		
			3	5	7
1	Moisture content, %		8,6		
2	Amount of debris in the source material, %		4,6 (2,0 - small, 2,6 - large)		
3	Amount of debris after the cleaner, %	4	1,25	1,43	1,56
		5	1,2	1,48	1,52
		6	1,21	1,51	1,65
		7	1,29	1,49	1,75
		Serial grid	1,29	1,4	1,47
	Cleansing effect, %	4	0,375	0,345	0,290
		5	0,387	0,390	0,299
		6	0,405	0,415	0,330
		7	0,325	0,37	0,225
		Serial grid	0,31	0,33	0,222

5.2.4. Experimental studies of a multifaceted mesh surface on elastic supports of a small debris cleaner

The cleaning effect is the main indicator characterizing the feasibility of using new technological solutions in the separation and cleaning section of a cotton mill. According to the results of the preliminary experiment, it was established that the influence of factors on the cleaning effect is nonlinear, therefore, the matrix of the central composite rotatable experiment CRCE is used to conduct the experiment. In the studies, the following factors were adopted:

x_1 — number of faces of a polyhedral mesh surface; m

x_2 — gap between the peg drum and the mesh surface, *mm*.

x_3 — coefficient of rigidity of elastic supports, *N/m;*

The values of the factor levels are given in Table 5.5.

Table 5.7

Levels of variation of experimental factors

No.	Name and designation of factors	Designation coding meaning	Factor values					Interval variation
			-1,682	-1	0	+1	+1,682	
1	Number of faces of a polyhedral mesh surface;*n*	x_1	3	4	6	8	9	2
2	Gap between the peg drum and the mesh surface, *mm*.	x_2	12,6	14	16	18	19,4	2
3	Rigidity coefficient of elastic supports, $\times 10^3$ *N/m;*	x_3	0,5	1,5	3	4,5	5,5	1,5

For this purpose, we make a planning matrix. The experiments were carried out in 3 - fold repetition at each point of the planning matrix. In this case, the number of experiments is determined by the following expressions:

$$N=2^k+2k+n_0=2^3+2\cdot3+6=20 \qquad (5.1)$$

In this case, the arithmetic mean values of the cleansing effect obtained as a result of the experiments are filled into Table 3.4 [144; pp. 121-126]. Then the mean value of the results is determined from the expression:

$$\overline{Y}=\frac{\overline{Y}_{i1}+\overline{Y}_{i2}+\overline{Y}_{i3}}{3} \qquad (5.2)$$

Table 5.8

Central compositional experiment design matrix

u	x_1	x_2	x_3	$(x_1)^2$	$(x_2)^2$	$(x_3)^2$	$x_1 x_2$	$x_1 x_3$	$x_2 x_3$	*Yu*
1	+	+	+	+	+	+	+	+	+	86,6
2	+	+	-	+	+	+	+	-	-	86,8
3	+	-	+	+	+	+	-	+	-	87,1
4	+	-	-	+	+	+	-	-	+	85,3
5	-	+	+	+	+	+	-	-	+	85

6	-	+	-	+	+	+	-	+	-	84,8
7	-	-	+	+	+	+	+	-	-	84,6
8	-	-	-	+	+	+	+	+	+	84
9	1,682	0	0	2,83	0	0	0	0	0	86,8
10	-1,682	0	0	2,83	0	0	0	0	0	85,2
11	0	1,682	0	0	2,83	0	0	0	0	87
12	0	-1,682	0	0	2,83	0	0	0	0	86,8
13	0	0	1,682	0	0	2,83	0	0	0	87,1
14	0	0	-1,682	0	0	2,83	0	0	0	86,2
15	0	0	0	0	0	0	0	0	0	88,9
16	0	0	0	0	0	0	0	0	0	88,7
17	0	0	0	0	0	0	0	0	0	89,1
18	0	0	0	0	0	0	0	0	0	88,9
19	0	0	0	0	0	0	0	0	0	88,8
20	0	0	0	0	0	0	0	0	0	89

To determine the regression coefficients based on the formulas from [144; p. 187], we calculate the sums of the corresponding columns in Table 3.3

$$\sum x_{1u}Y_u = 10{,}1 \qquad \sum x_{2u}x_{3u}Y_u = -2{,}4$$

$$\sum x_{2u}Y_u = 2{,}53 \qquad \sum x_{1u}^2Y_u = 1170{,}63$$

$$\sum x_{3u}Y_u = 3{,}914 \qquad \sum x_{2u}^2Y_u = 1176{,}05$$

$$\sum x_{1u}x_{2u}Y_u = -0{,}2 \qquad \sum x_{3u}^2Y_u = 1174{,}63$$

$$\sum x_{1u}x_{3u}Y_u = 0{,}8$$

After which the corresponding coefficients of the model can be determined.

$$b_0 = g_1\sum_{u=1}^{N}\overline{Y}_u - g_2\sum_{i=1}^{M}\sum_{u=1}^{N}x_{iu}^2\overline{Y}_u = 0{,}1663\cdot 1736{,}7 - 0{,}0568\cdot(1170{,}63+1176{,}05+1174{,}63) = 88{,}8$$

$$b_1 = g_3\sum_{u=1}^{N}x_{1u}\overline{Y}_u = 0{,}0732\cdot 10{,}1 = 0{,}739$$

$$b_2 = g_3\sum_{u=1}^{N}x_{2u}\overline{Y}_u = 0{,}0732\cdot 2{,}53 = 0{,}185$$

$$b_3 = g_3\sum_{u=1}^{N}x_{3u}\overline{Y}_u = 0{,}0732\cdot 3{,}91 = 0{,}286$$

$$b_{12} = g_4\sum_{u=1}^{N}x_{1u}x_{2u}\overline{Y}_u = 0{,}125\cdot(-0{,}2) = -0{,}025$$

$$b_{13} = g_4\sum_{u=1}^{N}x_{1u}x_{3u}\overline{Y}_u = 0{,}125\cdot 0{,}8 = 0{,}1 \quad b_{23} = g_4\sum_{u=1}^{N}x_{2u}x_{3u}\overline{Y}_u = 0{,}125\cdot(-2{,}4) = -0{,}3$$

$$b_0 = g_1\sum_{u=1}^{N}\overline{Y}_u - g_2\sum_{i=1}^{M}\sum_{u=1}^{N}x_{iu}^2\overline{Y}_u = 0{,}1663\cdot 1736{,}7 - 0{,}0568\cdot(1170{,}63+1176{,}05+1174{,}63) = 88{,}8$$

$$b_1 = g_3\sum_{u=1}^{N}x_{1u}\overline{Y}_u = 0{,}0732\cdot 10{,}1 = 0{,}739$$

$$b_2 = g_3\sum_{u=1}^{N}x_{2u}\overline{Y}_u = 0{,}0732\cdot 2{,}53 = 0{,}185$$

$$b_3 = g_3\sum_{u=1}^{N}x_{3u}\overline{Y}_u = 0{,}0732\cdot 3{,}91 = 0{,}286$$

$$b_{12} = g_4\sum_{u=1}^{N}x_{1u}x_{2u}\overline{Y}_u = 0{,}125\cdot(-0{,}2) = -0{,}025$$

$$b_{13} = g_4\sum_{u=1}^{N}x_{1u}x_{3u}\overline{Y}_u = 0{,}125\cdot 0{,}8 = 0{,}1 \quad b_{23} = g_4\sum_{u=1}^{N}x_{2u}x_{3u}\overline{Y}_u = 0{,}125\cdot(-2{,}4) = -0{,}3$$

$$b_{11} = g_5\sum_{u=1}^{N}x_{1u}^2\overline{Y}_u + g_6\sum_{i=1}^{M}\sum_{u=1}^{N}x_{1u}^2\overline{Y}_u - g_2\sum_{u=1}^{N}\overline{Y}_u = 0{,}0625\cdot 1170{,}83 + 0{,}0069\cdot(1170{,}83+1176{,}05+$$
$$+1174{,}64) - 0{,}0568\cdot 1736{,}7 = 1{,}46$$

$$b_{22} = g_5\sum_{u=1}^{N}x_{2u}^2\overline{Y}_u + g_6\sum_{i=1}^{M}\sum_{u=1}^{N}x_{2u}^2\overline{Y}_u - g_2\sum_{u=1}^{N}\overline{Y}_u = 0{,}0625\cdot 1176{,}05 + 0{,}0069\cdot(1170{,}83+1176{,}05+$$
$$+1174{,}64) - 0{,}0568\cdot 1736{,}7 = -0{,}84$$

$$b_{33} = g_5\sum_{u=1}^{N}x_{3u}^2\overline{Y}_u + g_6\sum_{i=1}^{M}\sum_{u=1}^{N}x_{3u}^2\overline{Y}_u - g_2\sum_{u=1}^{N}\overline{Y}_u = 0{,}0625\cdot 1174{,}64 + 0{,}0069\cdot(1170{,}83+1176{,}05+$$
$$+1174{,}64) - 0{,}0568\cdot 1736{,}7 = -0{,}93$$

Taking into account the obtained values of the coefficients, the model accepts:

$$Y = 88{,}8 + 0{,}739x_1 + 0{,}185x_2 + 0{,}286x_3 - 0{,}025x_1x_2 + 0{,}1x_1x_3 - 0{,}3x_2x_3 + 1{,}46x_1^2 - 0{,}84x_2^2 - 0{,}93x_3^2 \quad (5.4)$$

We determine the dispersion of the regression coefficients:

$$|S\{b_0\}| = \sqrt{S^2\{b_0\}}; \qquad S^2\{b_0\} = g_1 \cdot S^2\{Y\} = 0{,}1663 \cdot 0{,}54 = 0{,}089; \qquad S\{b_0\} = 0{,}298;$$

$$|S\{b_i\}| = \sqrt{S^2\{b_i\}}; \qquad S^2\{b_i\} = g_3 \cdot S^2\{Y\} = 0{,}0732 \cdot 0{,}54 = 0{,}039; \qquad S\{b_i\} = 0{,}197;$$

$$|S\{b_{ij}\}| = \sqrt{S^2\{b_{ij}\}}; \qquad S^2\{b_{ij}\} = g_4 \cdot S^2\{Y\} = 0{,}125 \cdot 0{,}54 = 0{,}0675; \qquad S\{b_{ij}\} = 0{,}259;$$

$$|S\{b_{ii}\}| = \sqrt{S^2\{b_{ii}\}}; \qquad S^2\{b_{ii}\} = g_7 \cdot S^2\{Y\} = 0{,}0695 \cdot 0{,}54 = 0{,}0038; \qquad S\{b_{ii}\} = 0{,}062;$$

The significance of the regression coefficients is checked using the Student's criterion . The calculated value of the Student's criterion:

$$t_R\{b_0\} = \frac{|b_0|}{S\{b_0\}} = \frac{88{,}8}{0{,}298} = 297{,}98; \qquad t_R\{b_1\} = \frac{|b_1|}{S\{b_i\}} = \frac{0{,}739}{0{,}197} = 3{,}75;$$

$$t_R\{b_2\} = \frac{|b_2|}{S\{b_i\}} = \frac{0{,}185}{0{,}197} = 0{,}939; \qquad t_R\{b_3\} = \frac{|b_3|}{S\{b_i\}} = \frac{0{,}286}{0{,}197} = 1{,}451;$$

$$t_R\{b_{12}\} = \frac{|b_{12}|}{S\{b_{ij}\}} = \frac{0{,}025}{0{,}259} = 0{,}096; \qquad t_R\{b_{13}\} = \frac{|b_{13}|}{S\{b_{ij}\}} = \frac{0{,}1}{0{,}259} = 0{,}38;$$

$$t_R\{b_{23}\} = \frac{|b_{23}|}{S\{b_{ij}\}} = \frac{0{,}3}{0{,}259} = 1{,}158; \qquad t_R\{b_{11}\} = \frac{|b_{11}|}{S\{b_{ii}\}} = \frac{1{,}46}{0{,}062} = 23{,}54;$$

$$t_R\{b_{22}\} = \frac{|b_{22}|}{S\{b_{ii}\}} = \frac{0{,}84}{0{,}062} = 13{,}54; \qquad t_R\{b_{33}\} = \frac{|b_{33}|}{S\{b_{ii}\}} = \frac{0{,}93}{0{,}062} = 15;$$

The calculated values of the Student's criterion for the coefficients are compared with the tabular value.

$$t_R > t_T; \qquad t_T\left[P_D = 0{,}95; \quad f\left\{S_u^2 = 6 - 1 = 5\right\}\right] = 2{,}57; \qquad (5.6)$$

If the given condition is met, then the calculated values of the regression equation coefficients are considered significant, otherwise, these regression coefficients are considered insignificant and are output.

Thus, as a result of the calculation, b_0, b_1, b_{12}, b_{11}, b_{22} and b_{33} coefficients are considered significant and the calculations continue with these coefficients. In this case, the regression equation has the form:

$$Y = 88{,}8 + 0{,}739x_1 + 1{,}46x_1^2 - 0{,}84x_2^2 - 0{,}93x_3^2 \qquad (5.7)$$

To check the adequacy of the obtained results, we use the Fisher criterion. To do this, we compare the calculated and experimental values of the output factors [144]:

Table 5.9

Results of calculations of the output factor using regression Equation

No.	$\overline{Y}_U$	Y_R	$\overline{Y}_U - Y_R$	$(\overline{Y}_U - Y_R)^2$
1	86,6	86,56	0,04	0,0016
2	86,8	86,38	0,42	0,1764
3	87,1	86,84	0,26	0,0676
4	85,3	85,46	-0,16	0,0256
5	85	84,93	0,07	0,0049
6	84,8	85,16	-0,36	0,1296
7	84,6	85,11	-0,51	0,2601
8	84	84,14	-0,14	0,0196
9	86,8	85,91	0,89	0,7921
10	85,2	85,43	0,23	0,0529
11	87	86,73	0,27	0,0729
12	86,8	86,11	0,69	0,4761
13	87,1	86,65	0,45	0,2025
14	86,2	85,69	0,51	0,2601
15	88,9	88,8	0,1	0,01
16	88,7	88,8	-0,1	0,01
17	89,1	88,8	0,3	0,09
18	88,9	88,8	0,1	0,01
19	88,8	88,8	0	0
20	89	88,8	0,2	0,04
Sum				2,702

We calculate the variance of the output parameter:

$$S^2\{Y\} = \frac{\sum_{u=1}^{n_0} (\overline{Y}_u - Y_{Ru})^2}{n_0 - 1} = \frac{2,7}{5} = 0,54 \tag{5.8}$$

$$F_R = \frac{S^2_{ad}\{Y\}}{S^2\{Y\}} = \frac{S^2_{nad}\{Y\}}{S^2\{\overline{Y}\}}; \tag{5.9}$$

$$S^2_{ad}(Y) = \frac{\sum_{u=1}^{N} (\overline{Y}_u - Y_{Ru})^2 - \sum_{u=1}^{n_0} (\overline{Y}_u - Y_{Ru})^2}{N - n_0 - (n_0 - 1)} = \frac{2,7 - 0,15}{20 - 6 - (6 - 1)} = 0,283; \tag{5.10}$$

$$F_R = \frac{S^2_{ad}\{Y\}}{S^2\{Y\}} = \frac{0,283}{0,54} = 0,52; \tag{5.11}$$

We find the Fisher criterion in the table [144; p. 183]:

$$F_T\left[P_D = 0,95;\ f\{S_{nad}\{Y\}\} = 20 - 6 - (6 - 1) = 9;\ f\{S_u^2\} = 6 - 1 = 5\right] = 3,48 \tag{5.12}$$

Therefore, $F_R < F_T$, therefore the model is adequate.

The coefficients in the regression equation express the output factors and are important. Equation (5.7) is inconvenient for practical calculations, so the transition from coded values *(x 1 , x 2 , x 3)* to the actual values of the factors *(n,* 8 *s)* is carried out according to the following expressions

$$x_1 = \frac{n - n_0}{\Delta n}; \quad x_2 = \frac{\delta - \delta_0}{\Delta \delta}; \quad x_3 = \frac{c - c_0}{\Delta c}; \qquad (5.13)$$

where $p_{0,}\ \delta_{o,}\ C_O$ - actual values of the main equations, *Δn , Δ8 , Δc* - intermediate values. Substituting into formula (5.13) the values of n_0 , δ_o, c_o And *Δn, Δ8, Δc* we get:

$$x_1 = \frac{n - 6}{2}; \quad x_2 = \frac{\delta - 16}{2}; \quad x_3 = \frac{c - 3 \cdot 10^3}{10}; \qquad (3.14)$$

From expression (5.14) we obtain the factor equation in the following form: ***M*** = -

$$M_z = -98{,}94 + 10{,}76n - 0{,}158n\delta - 0{,}0705nc + 12{,}37\delta + 1{,}515c - 0{,}352n^2 - 0{,}357\delta^2 - 0.0104c^2 \qquad (5.15)$$

The dependences of the cleaning effect on individual factors according to equation (3.15) are shown in Fig. 5.14, 5.15, 5.16.

Figure 5.14 shows the graphs of the dependence of the cleaning effect on the number of mesh surface faces: the first curve on the graph corresponds to the lower values of *δ* and *with,* the second graph - intermediate, the third - upper values. The graphs show that with an increase in the number of mesh surface faces from 3 to 9, the cleaning effect increases, then decreases [153, 154].

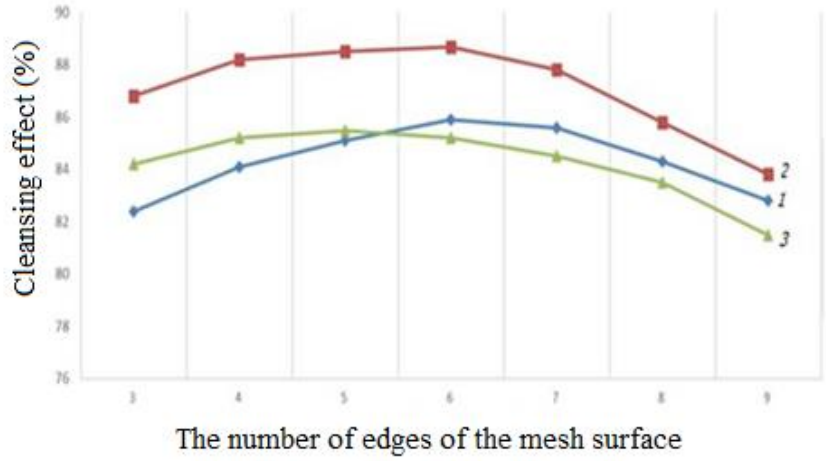

Fig. 5.14. Graph of the change in the cleaning effect depending on the number of mesh surface faces

The first graph in the diagram in Fig. 5.14 is determined at *δ = 14 mm, c = 1,5·10 3 N/m.* In this case, when the number of faces was three, the cleaning effect was the lowest and amounted to 82,4%, with an increase in the number of faces to 6, the cleaning effect increased to 85,8%, a further increase in the number of faces to 9 reduces the cleaning effect to 82,8%. The second graph is determined at *δ* =

16 mm, c = 3·10 ^{3} N/m. In this case, when the number of faces was 3, the cleaning effect increased and reached the highest value of 87,0%, with an increase in faces to 6, the cleaning effect increased by 88,2%, with an increase to 9, the cleaning effect decreased and amounted to 83,6%. The third graph was obtained in experiments with high values of *δ = 18 mm, c = 4,5 10 ^{3} N/m* changes in the number of faces. In this case, when the number of faces of the mesh surface was 3, the cleaning efficiency was 84.5%, with an increase in faces to 6, the cleaning effect increased by 85,2%. Analysis of the graphs shows that with smaller values of the number of faces, the cleaning effect was small, with a further increase in the number of faces to the average value, the cleaning effect increased. In experimental studies with high values of the number of faces, i.e. at 9, as a result of reducing the forces in the zone of cleaning raw cotton from small debris, a decrease in the cleaning effect was observed. When the number of faces was 6, the greatest cleaning effect was achieved, which was 88,2%.

Fig. 5.15 shows graphs of the dependence of the cleaning effect on the gap between the drum pins and the mesh surface.

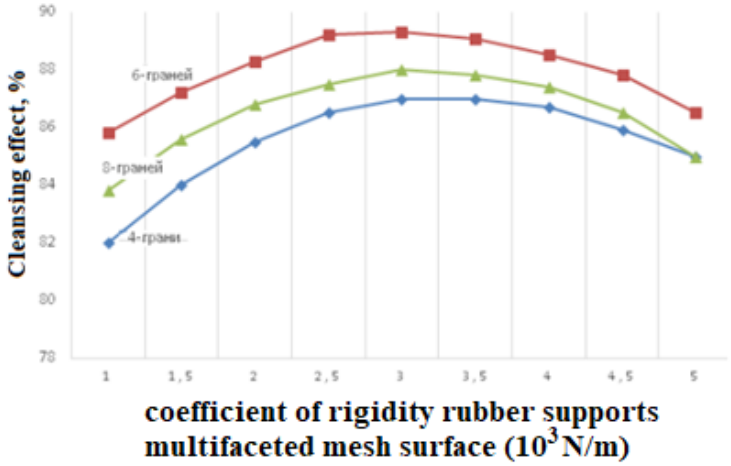

Fig.5.15. Graphs of changes in the cleaning effect depending on the gap between the pegs and the mesh surface

With an increase in the gap between the drum pins and the mesh surface from *δ = 12 mm, δ = 20 mm,* a graph of the change in the cleaning effect was obtained. Curve 1 at low values *of n* and c, i.e. *n =4, c=1,5·10 ^{3} N/m,* the result of the experiment with changing the gap between the drum pins and the mesh surface was carried out. In this case, when the gap between the pins and the mesh surface is *δ = 12 mm,* the cleaning effect is 83,4%, when *δ =16 mm,* the cleaning effect was the highest, up to 86%. However, with a further increase in the gap *δ = 20 mm,* the cleaning effect decreased to 81,2%. Curve 2 shows the nature of the change in the cleaning effect at average values of *n = 6, c = 3·10 ^{3} N / m.* When the gap between the pegs and the mesh surface *δ = 12 mm,* the cleaning effect was

86,0%, and at $\delta = 16$ mm it increased to 88.9%, when $\delta = 20$ mm the cleaning effect decreased and was 83,4%. The third graph shows the result of the change in the cleaning effect at high values of δ and c, i.e. at n = 8, $c = 4.5\ 10^3$ N / m. When the gap between the pegs and the mesh surface $\delta = 12$ mm, the cleaning effect was 83%, and at $\delta = 16$ mm the cleaning effect increased to 87%, with an increase in $\delta = 20$ mm, a decrease in the cleaning effect to 82,0% was observed.

The obtained results and constructed graphs showed that with a gap between the pegs and the mesh surface of 15-16 mm, the greatest cleaning effect is achieved.

Fig. 5.16 shows graphs of the influence of the rigidity coefficient of the rubber bushing on the supports of the multifaceted mesh surface on the cleaning effect. In the graph, curve 1 is obtained for low values *of n* And δ , curve 2 for average and curve 3 for high values. The influence of the stiffness coefficient of the rubber bushing was studied, with an increase from $c = 1{,}5{\cdot}10^3$ N/m to $c=4{,}5{\cdot}10^3$ N/m.

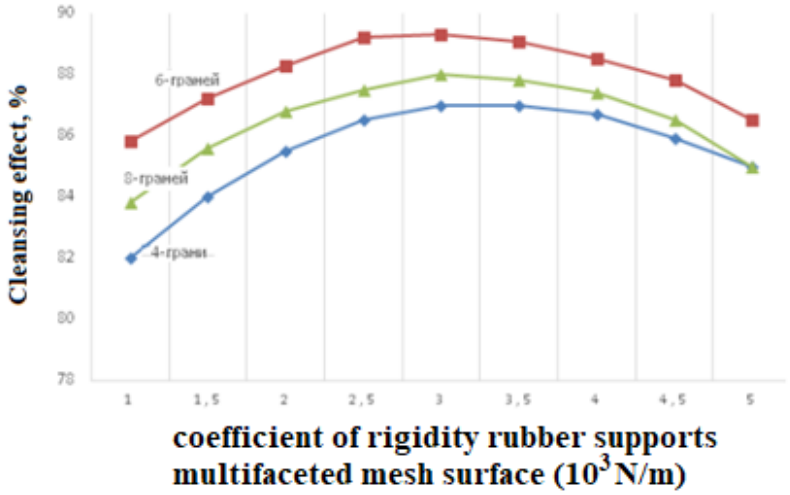

Fig.5.16. Graph of the change in the cleaning effect depending on the rigidity coefficient of the rubber support of the multifaceted mesh surface

An experiment was conducted at low values of $n = 4$, $\delta = 14$ mm with a change in the stiffness coefficient of the rubber bushing. When the rubber stiffness was $c = 1{,}5{\cdot}10^3$ N/m, the cleaning effect was 84,9%, with an increase in stiffness to $c = 3{\cdot}10^3$ N/m, the cleaning effect increased to 87,2%. A further increase in the stiffness coefficient to $c = 4{,}5{\cdot}10^3$ N/m the cleaning effect decreased to 85,2%. Graph 2 of the diagram shows the results of studying the cleaning effect at average values of $n = 6$, $\delta = 16$ mm. At low values, $c = 1{,}5{\cdot}10^3$ N/m, the rigidity coefficient of the rubber support of the multifaceted mesh surface, the cleaning effect was 85.8%, and at a rigidity *of* $c = 3{\cdot}10^3$ N/m increased to 89,2%, further increase in rigidity to $c=4{,}5{\cdot}10^3$ N/m led to a decrease in the cleaning effect to

87,8%. Graph 3 of the diagram shows the results of experiments at high values, $n = 8$, $\delta = 18$ *mm*. When the stiffness coefficient of the rubber support of the mesh surface was $c = 1{,}5 \cdot 10^3$ *N/m*, the cleaning effect was 83,8%. With an increase in $c = 3 \cdot 10^3$ *N/m*, the cleaning effect increased to 88,0%, a further increase in the stiffness of the rubber bushing to $c = 4{,}5 \cdot 10^3$ *N/m* the cleansing effect decreased to 85,2%

Analysis of the graphs shows the influence of the rubber bushing stiffness coefficient on the cleaning effect. The greatest cleaning effect is achieved with a rubber bushing stiffness coefficient within the range of $(3\text{-}3{,}5) \cdot 10^3$ *N/m* .

Thus, based on multifactorial experiments, the optimal values of the mesh surface parameters were determined. Recommended parameter values: $n=6$, $\delta = 15$ *mm*, the stiffness coefficient of the rubber support of the mesh surface $c=3 \cdot 10^3$ *N/m*. With these optimal values, the cleaning effect of the UHK machine is 89,2%.

5.3. Experimental study of the large debris cleaning section of the separation and cleaning unit

5.3.1. Measuring the loading and vibrations of composite grates on elastic supports

Based on the analysis of existing grate designs, a new design of a grate for cotton cleaners to remove large impurities is developed in Chapter 2. A theoretical analysis of the proposed technical solutions is carried out in Chapter 4.

The new cotton cleaner grate contains tubular composite grates mounted in arched sidewalls by means of elastic bushings, in the sidewalls and in intermediate brackets.

Cyclic effects on the grate contribute to the emergence of complex oscillations of the grate and cotton, which results in an intensification of the release of large impurities from the cotton.

It is important to determine the amplitude and frequency of oscillations of composite grates on elastic supports, which directly affect the effect of cleaning cotton from large debris.

In order to study dynamic and force loading in operating modes using modern methods and devices for measuring machine parameters and grate operation, a grate with composite grates was manufactured.

5.3.2. Experimental methodology and measuring devices used

The main objective of the experimental studies is to study the nature of the

oscillatory motion of composite grates installed on rubber bushings in the sidewalls of the cotton cleaner. It is important to study the grate loading, the amplitude and frequency of forced grate oscillations, based on the analysis of which it is possible to justify the necessary parameters of the grate, elastic support and cotton cleaning modes.

To conduct comparative studies, a grate with composite grates installed on elastic supports was manufactured, the general appearance of which is shown in Fig. 5.17.

To increase the rigidity of the grate, rods with a diameter of 16 mm are additionally fixed to the sidewalls and brackets are welded to them at certain distances, on which there are guide bushings on which rubber guides are put on. In total, the grate has three brackets along the entire length, four spans of the grate with a distance of each section of 497 mm, on which rubber bushings are put on, through the opening of which composite rods (pipes) with a diameter of 20 mm are passed. The main physical and mechanical properties of rubber grades SKF36, SKF26 and SKF260 and others are given in Table 5.10.

a-when using composite grates on elastic supports

b-when using metal grates

Fig.5.17. Working area of the cotton cleaner for large debris

Table 5.10

Physical and mechanical properties of rubbers

No.		Shore hardness	Conditional strength at calculations	Rel. elong. at resolution	density	Compressive stiffness	
						$d-l$ C_1, 10^4 N/ m	$d+l$ C_1, 10^4 N/ m
1	1847	40-55	14,2	550	1500	4,5	2,6
2	NO-68	56-55	13,4	445	725	3,0	1,6
3	1338	70-55	12,2	360	430	2,2	1,3
4	SKF 32	70-75	26-30	500	450	2,2	2,0
5	SKF26	70-80	16-18	450	400	1,8	1,5
6	SKF 260	100	20	500	400	2,2	1,8

To obtain the simplest possible design, the bushings were cast in the form of tubes of certain sizes from different grades of rubber with properties according to Table 5.6. The main design dimensions of the bushings are given in Table 5.11. The general design of the rubber bushings is shown in Fig. 5.18.

Table 5.11

Brand of rubber	SKF36	SKF26	SKF260	1847

Outer diameter of the	26	26	26	26
Inner diameter of the	20	20	20	20
Sleeve length mm.	40	40	40	40

Fig.5.18. Rubber bushings for installing grates in the sides and intermediate brackets

Currently, grates are made of steel rods with a diameter of 20 mm. They have great rigidity, which makes it impossible to provide the required amplitude of oscillations. Another disadvantage is the possibility of sparks appearing when small stones, which are part of the litter in small quantities, hit the grate. This leads to combustion of cotton.

To eliminate the above mentioned disadvantages, we have proposed to use grates made of composite. The technology for producing rods from composite is similar to the technology used in the production of composite pipes, which are widely used in water supply, sewerage, and in various technological machines. Over the years, experience has been gained in the production of composite pipes and rods from polyvinyl chloride (PVC), polyethylene (PE), polypropylene (PP), and fiberglass.

Polypropylene, polyethylene, and polyamides were studied for the manufacture of grates. Based on the price-quality ratio, polyamide (PA) was adopted as the basis for the manufacture of grates.

Table 5.12 presents the main characteristics of PA rods.

Table 5.12.

Technical characteristics of PA rods

No.	Rod diameter, *mm*	16	18	20	22	24
1	Mechanical force on rod bending, N (at *l=1000 mm)*	17	20	24	28	35

2	Maximum operating temperature, °C	70	80	85	90	95
3	Surface roughness, class	7	7	7	7	7
4	Weight, kg *(l=1000 mm)*	0,5	0,58	0,72	0,8	0,95
5	Relative elongation at break, in %	12.0	16	18	20	22
6	Tensile yield strength, MPa	34.5	40	42	44	46
7	Impact resistance, scratch up to 1,5-2,0 mm, (TIR)	Not more 5%	Not more 5%	Not more 5%	Not more 5%	Not more 5%

Their main drawback is their weak resistance to scratches, which occur when they interact with cotton and litter. To increase scratch resistance, it is proposed to add 5% basalt fiber with an average length of 10 mm to the grate material.

As a result, a composite material was obtained that meets operational requirements [154, 155, 156].

To measure the vibration parameters of the proposed grates, a computerized measuring system was used.

information system, which included a four-channel strain gauge amplifier UT-4-1 and an electronic device LTR -154 for entering measurement information into a computer. The general appearance and diagram of the measuring device are shown in Fig. 5.19 and 5.20.

Fig. 5.19. General view of the experimental setup

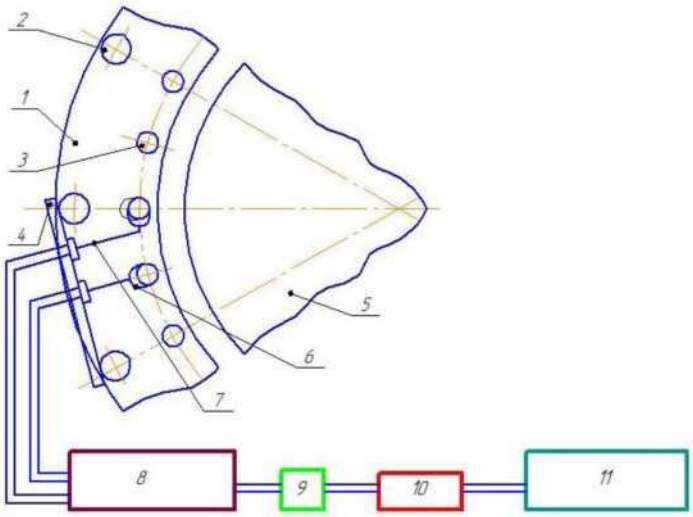

Fig.5.20. Scheme for measuring the movements (oscillations) of grate bars in two coordinates

1- grate fastening sidewalls, 2- steel rods, 3- grate bars, 4- dynamic sensor fastening bracket, 5- saw drum, 6- dynamic sensor of displacement along the YY axis. 7- dynamic sensor of displacement along the XX axis, 8- high-frequency amplifier, 9- modulator, 10- ADC, 11- computer.

Fig. 5.21 shows the installation location of the vibration sensors on the grate. Structurally, the measuring device [155, 156] for measuring the vibrations of the grate is made autonomously and has the ability to move along the grate, which allows measuring the vibrations of the grate elements along the entire width along the machine.

Fig.5.21. Location of the measuring device in the working area of the machine

Fig. 5.22 shows the design diagram of the displacement sensors along the XX and YU axes.

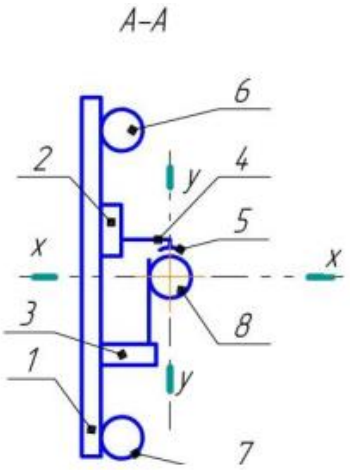

Fig.5.22. Scheme of displacement measurement and coordinates of the location of measuring dynamic sensors.

1- bracket; 2-movement mechanism for installing sensors relative to the grate bars along the YY axis ; 3-dynamic displacement sensors along the XX axis; 4-displacement sensors along the XX axis; 5-adapter; 6,7- metal fastening rods. 8-composite grate bars.

The calibration of sensors for measuring the vibrations of composite grates along the X and Y axes is given in Appendix P.1.2. of the dissertation. Fig. 5.23 shows a general view of the calibration stand [155].

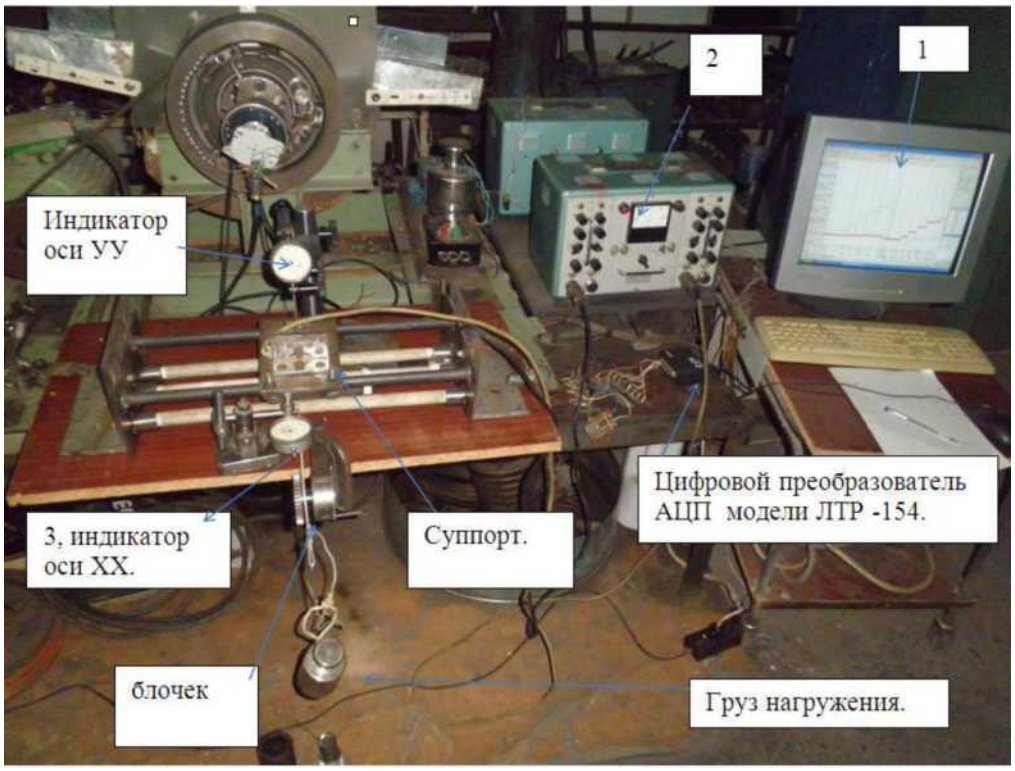

Fig.5.23. General view of the installation during calibration of sensors

5.3.3. Analysis of the results of measuring the load and vibrations of composite

grates

The experiments were conducted under production conditions at the Karasuv cotton mill in the Tashkent region of the Republic of Uzbekistan. The grate vibrations were measured for both composite grates on elastic supports and serial grates.

It is known that the technological load from the cotton on the metal grates, rigidly installed in the sides, slightly deforms the grates, since it does not exceed 18,0-22,0 N. Therefore, in the existing design of the grate, the grates are stationary, the cleaning effect is low. The vibration of the grates occurs together with the cleaning unit due to unbalanced masses in the machine drive. Fig. 5.24 shows oscillograms of the grate movements of a serial design along the X and Y axes. Analysis of the oscillograms shows that the amplitude of the grate oscillations along the X and Y axes reaches $0{,}05 \cdot 10^{-3}$ m at a saw drum rotation frequency of 270 rpm and a productivity of 5,0 t/h, and with an increase in the saw drum rotation frequency to 320 rpm and productivity to 7,0 t/h, the oscillation frequency of the serial grate increases and corresponds to 30-70 Hz, and the amplitude of the oscillations along the X axis reaches 0,2 mm (see Fig. 5.24 a, b, c).

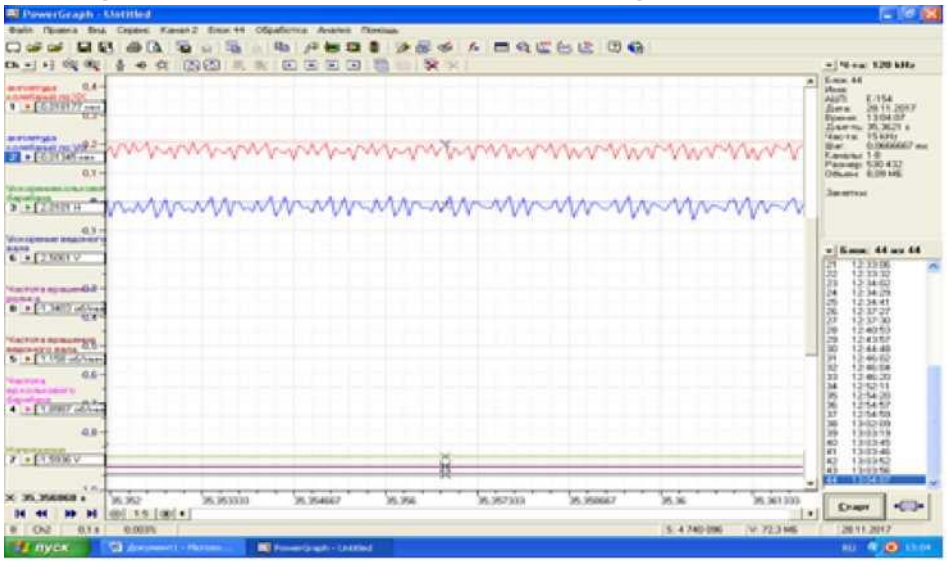

a - n=270 rpm; P=5,5 t/h

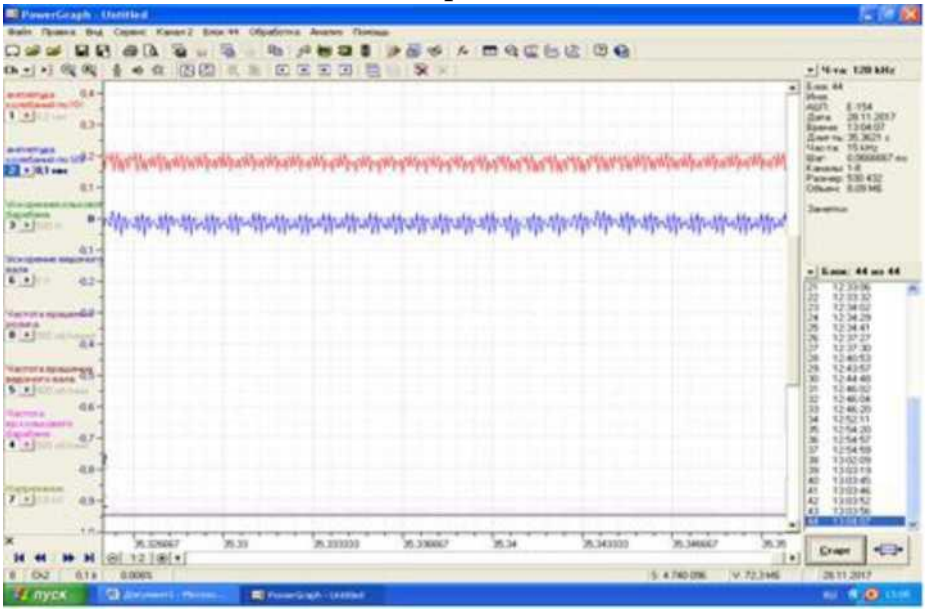

b - n=300 rpm; P=6,5 t/h

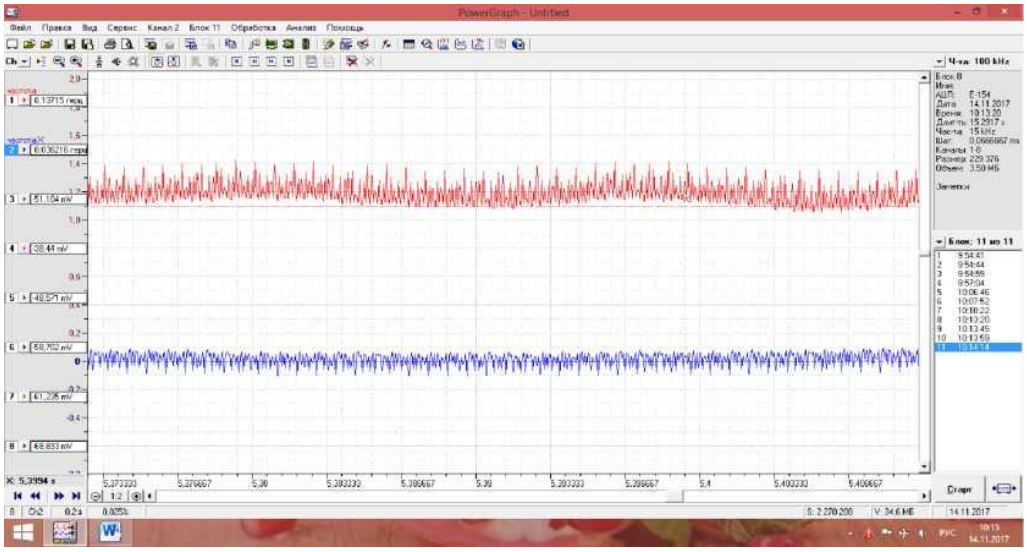

in - n = 310 min/min; P = 8,0 t/h

Fig.5.24. Oscillograms characterizing the oscillations of the serial grate

Figure 5.25 shows oscillograms characterizing the oscillations of the composite grate along the X and Y axes . Thus, with a rotation frequency of the saw drum of 300 rpm, a machine productivity of 5,0 t/h and a grate rubber support stiffness of $1{,}8 \cdot 10^{4}$ N/m, the oscillation range of the composite grate along the Y axis reaches $0{,}55 \cdot 10^{-3}$ m, while along the X axis the grate does not actually oscillate (see Figure 5.25 a). With an increase in the cotton cleaner productivity to 7,0 t/h and the rotation frequency of the saw drum to 310 rpm with the rigidity of the rubber supports, the amplitude of the oscillations of the composite grate at $c=1{,}4 \cdot 10^{4}$ N/m increases to $0{,}6 \cdot 10^{-3}$ m along the X axis, and along the Y axis the amplitude of the oscillations of the composite grate on the elastic support reaches $3{,}0 \cdot 10^{-3}$ m.

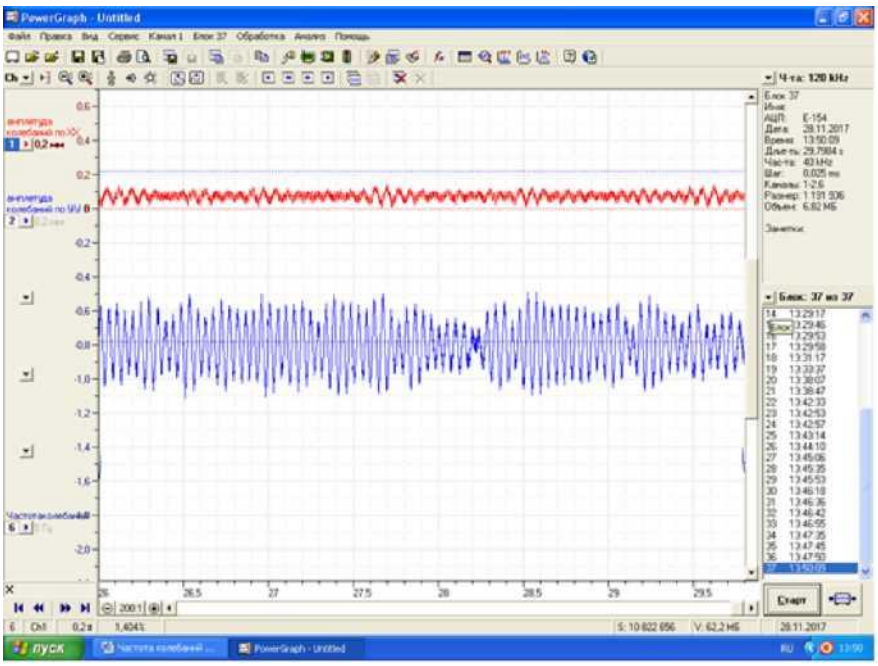

a - at n = 300 rpm; P = 5,5 t/h, s = 1,6·10 ^{4} N/m

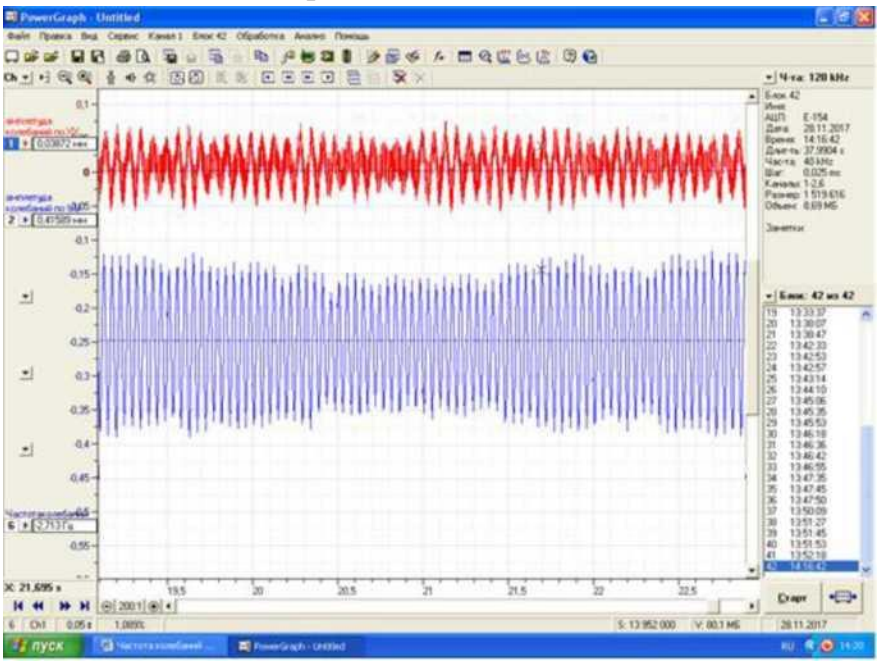

b - at n = 310 rpm; P = 7,5 t/h, s = 1,5-10 ^{4} N/m

Fig.5.25. Oscillograms characterizing the oscillations of a composite grate on elastic supports

Based on the processing of oscillograms, graphical dependencies of the change in grate oscillations of both variants along the X and Y axes on the change in the load from the cleaned raw cotton were constructed, which are shown in Fig. 5.26. AX and AY are nonlinear. The AY value is important for the composite grate, which directly affects the effect of cleaning raw cotton from large debris. Thus, with an increase in the load from H to 23,0 N, the amplitude of oscillations in the existing version of the grate AX and AY do not exceed 0,5·10 $^{-3}$ m. At the same time, the amplitude of oscillations of the composite grate on elastic supports

along the X axis reaches 1,0·10 $^{-3}$ m, and along the Y axis it reaches 3,15·10 $^{-3}$ m. In this case, the composite grates oscillate vertically with an amplitude of 1,575·10 $^{-3}$ *m* and with a frequency 6,5-15,5 times exceeding the rotation frequency of the saw drum. This means that during the operation of the cleaner, with one revolution of the saw drum, on average 6,5-15,5 times the raw cotton flies pulled by the saw cylinder hit the grate, i.e. the frequency of forced oscillations of the composite grate reaches 30-70 Hz.

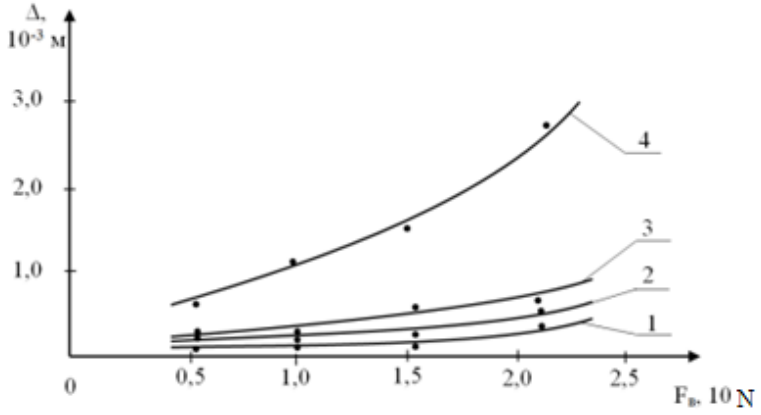

Fig. 5.26. Change in the amplitude of grate oscillations from the load from the side of the cleaned raw cotton 1,2 - for the metal (serial) version of the grate; 3,4 - for the composite grate on elastic supports.

It is known from machine mechanics that increasing the rigidity of elastic elements leads to a decrease in the amplitude of oscillations. Fig. 5.27 shows examples of oscillograms characterizing the oscillations of a composite grate at different values of the rigidity coefficient of the rubber bushings through which the grates are installed in the sidewalls of the cleaner.

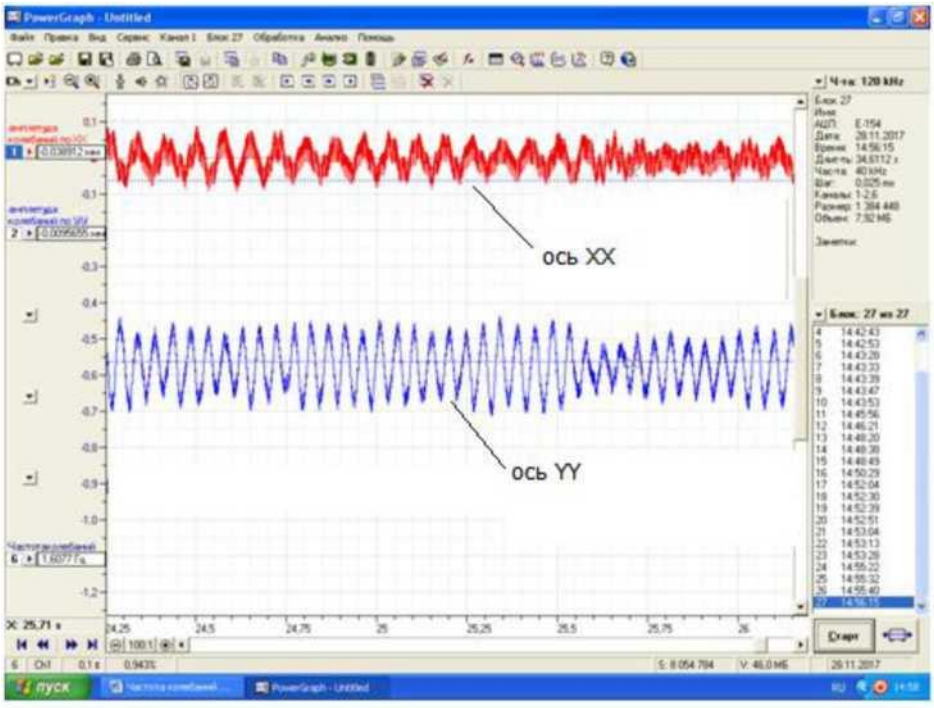

a - at c=2,15·10 ^{4} N/m n =310 rpm; P=7,0 t/h,

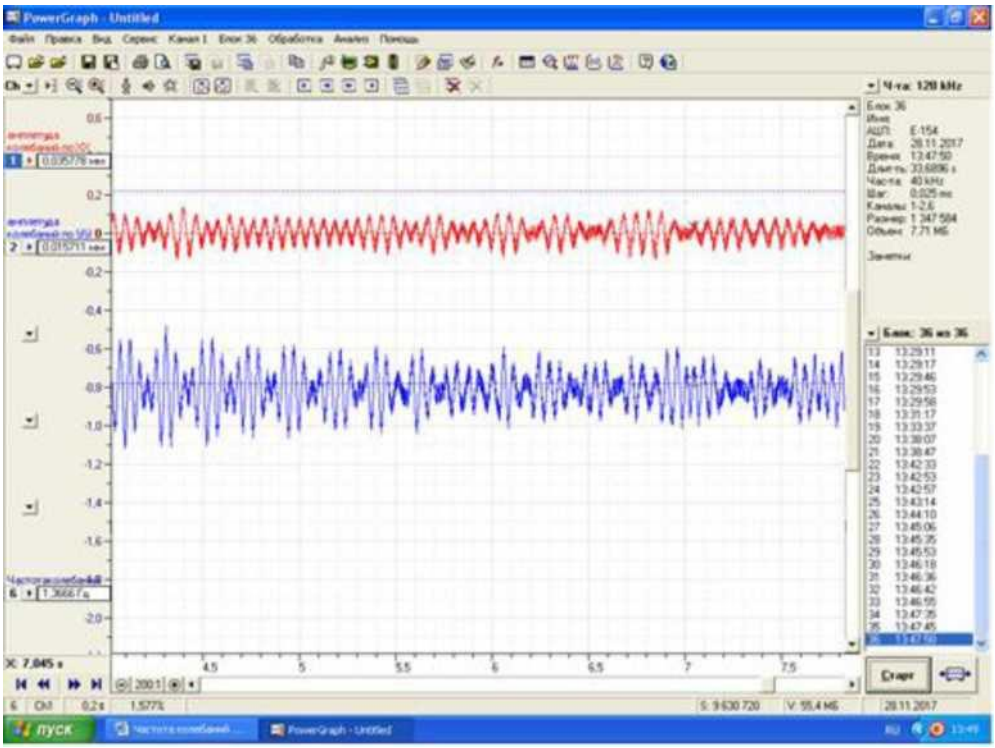

b - at c=2,5·10 ^{4} N/m n =310 rpm; P=7,0 t/h,

Fig. 5.27. Samples of grate oscillation oscillograms

Analysis of the oscillograms in Fig. 5.27 shows that an increase in the stiffness coefficient of the rubber bushings of the composite grate supports leads to a significant decrease in the amplitude of the grate oscillations both along the X axis and along the Y axis . A decrease in the stiffness of the elastic supports (see Fig. 5.27) leads to an increase in the amplitude of the composite grate oscillations.

In this case, the amplitude of the oscillations increases to 0,6·10 $^{-3}$ m along the X axis and to 2,15·10 $^{-3}$ m along the Y axis with a machine productivity of 5,0 t/h.

Based on the processing of the obtained oscillograms, graphical dependencies of the change in the oscillations of the composite grate on the increase in the stiffness coefficient of the rubber elastic grate supports were constructed, which are shown in Fig. 5.28. It is evident from the graphs that with an increase in the stiffness coefficient of the rubber bushing from 1,2·10 ^{4} N/m to 2,15·10 ^{4} N/m, the amplitude of the oscillations of the composite grate along the X axis decreases from 0,67·10 $^{-3}$ m to 0,18·10 $^{-3}$ m, and the amplitude of the oscillations of the grate along the Y axis decreases from 2,25·10 $^{-3}$ m to 0,58·10 $^{-3}$ m according to a nonlinear pattern. Experimental studies have shown that the maximum effect of cleaning raw cotton for large debris is achieved with the amplitude of oscillations of the composite grate within the limits of (1,7-2,0) ·10 $^{-3}$ m. Therefore, for the case under consideration, the recommended values of the

stiffness coefficient of the rubber bushing of the grate support are (1,6-2,0) ·10 ^{4} N/m (rubber brand SKF 32).

Research into determining the oscillation frequency [157, 158] of composite grates is important. Figure 5.28 shows the graphical dependences of the change in oscillation frequency along the Y axis of a composite grate on the increase in the stiffness coefficient of the elastic support.

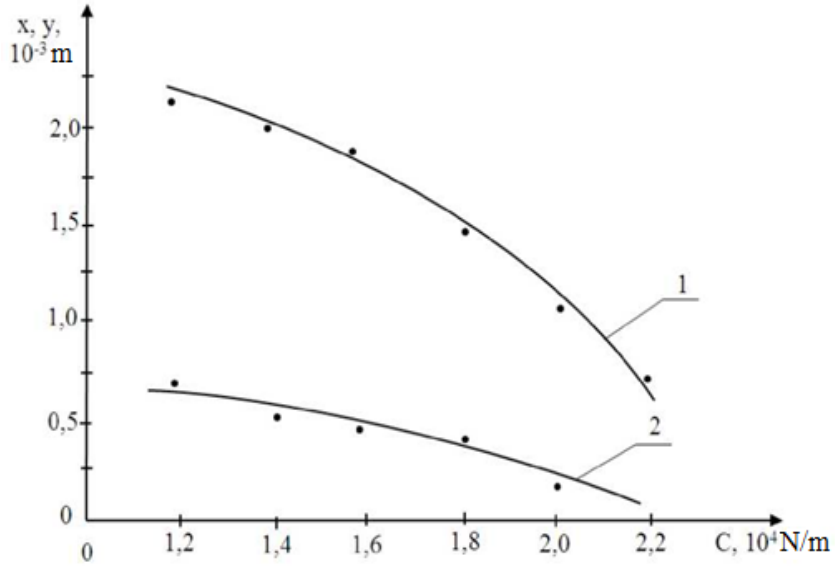

Fig.5.28. Dependences of the change in the amplitude of oscillations of the composite grate on the change in the stiffness coefficient of the elastic support 1 - y = f(c); 2 - x = f (c); at n = 290 rpm; P = 7,0 t/h.

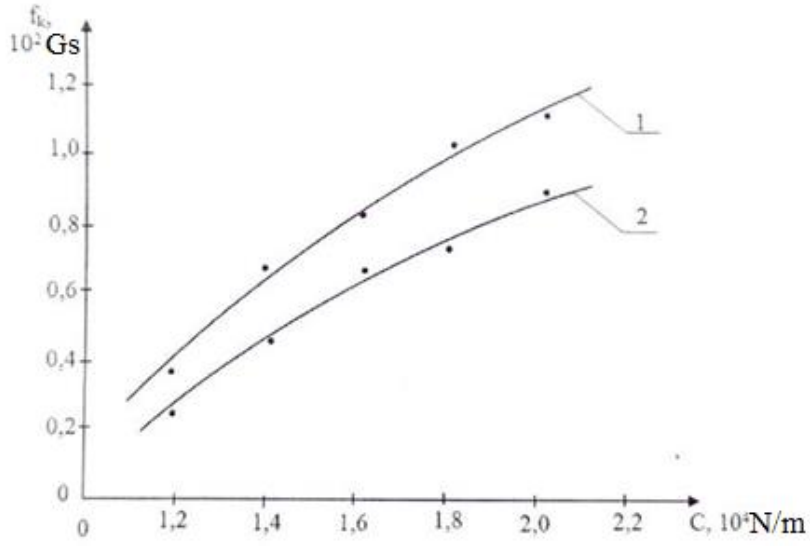

Fig.5.29. Graphic dependences of the change in the oscillation frequency of the composite grate on the change in the stiffness coefficient of the elastic support 1-at n =280 rpm, P =5,0 t/h; 2-at n =310 rpm; P =7,0 t/h

It should be noted that an increase in the stiffness coefficient of the elastic support from 1,2·10 ^{4} N/m to 2,15·10 ^{4} N/m leads to an increase in the oscillation

frequency of the composite grate at n = 280 rpm and P = 5,0 t/h according to a nonlinear pattern from $0{,}2\cdot10^{2}$ Hz to $0{,}92\cdot10^{2}$ Hz, and at n = 310 rpm and P = 7,0 t/h the oscillation frequency along the Y axis reaches $1{,}22\cdot10^{2}$ Hz. The highest effect of cleaning raw cotton from large debris is obtained at (45 - 75) Hz. Taking this into account, the most suitable value of the stiffness coefficient is (1,6—2,0) $\cdot10^{4}$ N/m, while the grate oscillation frequency along the Y axis will be (0,8—1,1) $\cdot10^{2}$ Hz.

The analysis of the obtained results revealed that the frequency of oscillations of composite grates on elastic supports is also affected by the rotation frequency of the saw drum. In this case, the raw cotton bats pulled by the saw cylinder, colliding with the composite grates, form forced oscillations of the grates. Fig. 5.30 shows the patterns of change in the frequency of forced oscillations of composite grates from an increase in the rotation frequency of the saw drum. With an increase in the rotation frequency of the saw drum from $0{,}5\cdot10^{2}$ rpm to $3{,}1\cdot10^{2}$ rpm, the grate oscillation frequency increases at $c = 1{,}4\cdot10^{4}$ N/m from $0{,}125\cdot10^{2}$ Hz to $0{,}52\cdot10^{2}$ Hz, and at $c = 2{,}2\cdot10^{4}$ N/m and P = 7,0 t/h, the forced oscillation frequency of the composite grates reaches $1{,}28\cdot10^{2}$ Hz. Therefore, the most effective way to increase the grate oscillation frequency is to increase the rotation frequency of the saw drum. But this may increase the percentage of damage to fibers and cotton seeds due to the increased impact forces on the grates. Therefore, the rotation frequency of the saw drum must be set within the range of (3,0—3,15) $\cdot10^{2}$ rpm.

The studies of the change in the gap between the saw cylinder and the composite grate bars of the cotton cleaner for large debris are important.

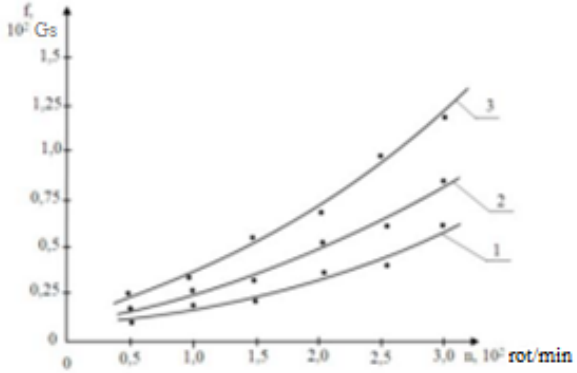

Fig.5.30. Graphic dependences of the change in the frequency of forced oscillations of the composite grate on the variation in the rotation frequency of the saw drum
1-at $c=1{,}4\cdot10^{4}$ N /m; 2-at $c=1{,}8\cdot10^{4}$ N /m; 3-at $c=2{,}2\ 10^{4}$ N /m; at P=7,0 t/h

Based on the processing of oscillograms, graphical dependencies of the grate oscillation amplitude on the change in the gap were constructed, which is shown in Fig. 5.31.

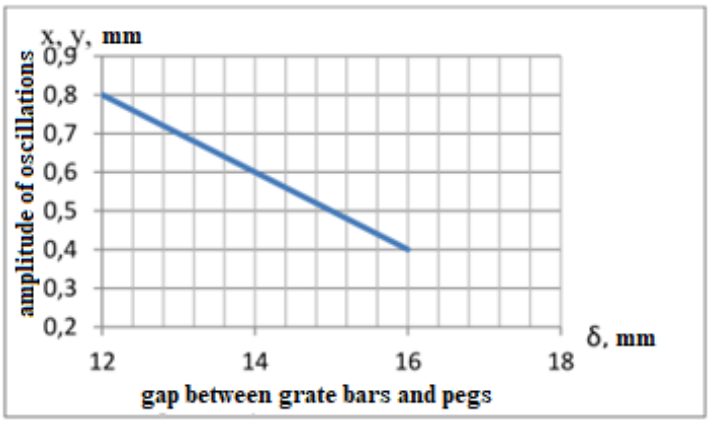

Fig.5.31. Dependence of the grate oscillation amplitude on the gap between the saw cylinder and the grate

A full factorial experiment was conducted to determine the recommended value for the gap between the pin cylinder and the grate bars.

5.3.4. Influence of technological parameters of the coarse debris cleaner on the quality of raw cotton cleaning

To study the performance of the proposed design
grate bars installed on the UHK machine, a full factorial experiment was conducted. There are a number of foreign literary sources, Internet materials, which evaluate the quality indicators of seeds and cotton during the processing of raw cotton.

The input parameters of the experiment are:

1. Rigidity coefficient of rubber bushings installed on composite grate supports - s, N/m
2. Machine productivity - P, t/hour
3. The gap between the grate and the saw drum is 5 mm.

When conducting experiments, the cleansing effect of U was chosen as the output parameter.

5.3.5. Procedure for conducting research

When conducting experimental measurements, in order to increase the accuracy of measurements and eliminate errors, a comparative assessment was made with the parameters of a standard machine.

When conducting the research, a full factorial experiment [144] (hereinafter PFE) 2^3 was chosen.

All the identified main factors vary at two levels (+1 and -1), and the number of experiments is $2^3 = 8$. After selecting the main factors and their variation levels, it was determined by which main output parameters it is possible to judge and

evaluate the work, as well as optimize the technological and design parameters of the cleaner with the recommended composite grate with elastic rubber bushings. Based on this analysis, a planning matrix was compiled, which is presented in Tables 5.14 and 5.15. Table 5.13 shows the variation levels of the factors.

The actual values of the factors were coded using the formula;

$$X_1=(c-1,5)/0,5;\ X_2=(П-6)/1;\ X_3=(\delta-14)/2;$$

The accuracy and reliability of the experimental results largely depend on the accuracy of control of all input and output parameters and their constancy. Therefore, each experiment was preceded by preparation with multiple control of the input and output parameters of the cotton cleaner from large debris. The results obtained are presented in Tables 5.14 and 5.15.

Table 5.13

Name of the factor	Coded designations	Values of factors.			Variation interval
		-1	0	+1	
Rubber bushing hardness, *s* 10^4 N/m	X_1	1,0	1,5	2,0	0,5
Machine productivity P, t/hour.	X_2	5	6	7	1
The gap between the grate and the saw cylinder is δ,10^{-3} m	X_3	12	14	16	2

Experimental results for a composite grate using grade II raw cotton.

Table 5.14

No.	X_1	X_2	X_3	Y_1	Y_2	Y_3	Y_{av}	$S^2[Y]$
1	-	-	-	82,5	81,7	81,8	82	0,19
2	+	-	-	89,8	89,7	89,5	89,67	0,023
3	-	+	-	85,8	85,1	84,3	85,07	0,563
4	+	+	-	82,4	82,6	82,8	82,6	0,04
5	-	-	+	81,8	82,5	82,5	82,27	0,163
6	+	-	+	86,8	87,8	87,9	87,5	0,37
7	-	+	+	83,4	83,1	82,9	83,13	0,063
8	+	+	+	80,8	80,2	80,1	80,37	0,143

We determine the dispersion from the following expression [157; pp. 5-12].

$$S^2[\,У\,]=\frac{\sum_{1}^{8} y_u}{m-1}; \qquad (5.16)$$

where m is the number of experiments conducted under identical conditions.

The dispersion values are given in Tables 5.9 and 5.10.

We calculate the Cochran criterion using the formula [144, 182-c].

$$G_p= S^2[\,У\,]/\sum_{i-1}^{x} S_i^2(Y) = 42{,}28/166{,}16=0{,}2544 \qquad (5.17)$$

For probability q = 0.05 from table [144, 157] we select Cochran's coefficient for N = 8, m = 5 G_{tab} = 0.7043.

Since $G_p < G_{tab}$ we can assume that the dispersion is homogeneous.

$$b_0 = \frac{1}{8}(82 + 89{,}67 + 85{,}07 + 82{,}6 + 82{,}27 + 87{,}5 + 83{,}13 + 80{,}37) = 80{,}1$$

$$b_1 = \frac{1}{8}(-82 + 89{,}67 - 85{,}07 + 82{,}6 - 82{,}27 + 87{,}5 - 83{,}13 + 80{,}37) = 0{,}95$$

$$b_2 = \frac{1}{8}(-82 - 89{,}67 + 85{,}07 + 82{,}6 - 82{,}27 - 87{,}5 + 83{,}13 + 80{,}37) = -1{,}28$$

$$b_3 = \frac{1}{8}(-82 - 89{,}67 - 85{,}07 - 82{,}6 + 82{,}27 + 87{,}5 + 83{,}13 + 80{,}37) = -0{,}76$$

$$b_{12} = \frac{1}{8}(82 - 89{,}67 - 85{,}07 + 82{,}6 + 82{,}27 - 87{,}5 - 83{,}13 + 80{,}37) = -2{,}26$$

$$b_{13} = \frac{1}{8}(82 - 89{,}67 + 85{,}07 - 82{,}6 - 82{,}27 + 87{,}5 - 83{,}13 + 80{,}37) = -0{,}34$$

$$b_{23} = \frac{1}{8}(82 + 89{,}67 - 85{,}07 - 82{,}6 - 82{,}27 - 87{,}5 + 83{,}13 + 80{,}37) = -0{,}28$$

$$b_{123} = \frac{1}{8}(-82 + 89{,}67 + 85{,}07 - 82{,}6 + 82{,}27 - 87{,}5 - 83{,}13 + 80{,}37) = 0{,}26$$

$$b_3 = \frac{1}{8}(-82 - 89{,}67 - 85{,}07 - 82{,}6 + 82{,}27 + 87{,}5 + 83{,}13 + 80{,}37)$$
$$= -0{,}76$$

$$b_{12} = \frac{1}{8}(82 - 89{,}67 - 85{,}07 + 82{,}6 + 82{,}27 - 87{,}5 - 83{,}13 + 80{,}37) = -2{,}26$$

$$b_{13} = \frac{1}{8}(82 - 89{,}67 + 85{,}07 - 82{,}6 - 82{,}27 + 87{,}5 - 83{,}13 + 80{,}37) = -0{,}34$$

$$b_{23} = \frac{1}{8}(82 + 89{,}67 - 85{,}07 - 82{,}6 - 82{,}27 - 87{,}5 + 83{,}13 + 80{,}37)$$
$$= -0{,}28$$

$$b_{123} = \frac{1}{8}(-82 + 89{,}67 + 85{,}07 - 82{,}6 + 82{,}27 - 87{,}5 - 83{,}13 + 80{,}37)$$
$$= 0{,}26$$

Let's calculate the variance of the regression coefficient

$$S^2\{b_i\} = \frac{1}{N} S^2\{\bar{Y}\} = 0{,}0081, \quad S\ \{b_i\} = 0{,}08999$$

Where $S^2\{\bar{Y}\} = \frac{1}{mN} S^2\{Y\}$

Calculated values of the Student's criterion

$$t_R\{b_i\} = \frac{|b_i|}{S\{b_i\}}$$

$$t_R\{b_1\} = \frac{0{,}95}{0{,}08999} = 10{,}65$$

$$t_R\{b_2\} = \frac{-1{,}28}{0{,}08999} = -14{,}26$$

$$t_R\{b_3\} = \frac{-0{,}76}{0{,}08999} = -8{,}43$$

$$t_R\{b_{12}\} = \frac{-2{,}26}{0{,}08999} = -25{,}18$$

$$t_R\{b_{13}\} = \frac{-0{,}34}{0{,}08999} = -3{,}79$$

$$t_R\{b_{23}\} = \frac{-0{,}28}{0{,}08999} = -3{,}15$$

$$t_R\{b_{123}\} = \frac{0{,}26}{0{,}08999} = 2{,}98$$

As a result of processing the obtained results, regression equations were obtained for grade II cotton:

$$У = b_0 + b_1X_1 + b_2X_2 + b_3X_3 + b_{12}X_1X_2 + b_{13}X_1X_3 + b_{23}X_2X_3 + b_{123}X_1X_2X_3 \quad (5.18)$$

$$У = 80,1 + 0,95X_1 - 1,28X_2 - 0,76X_3 - 2,26X_1X_2 \quad (5.19)$$

Experimental results for a composite grate using grade IV raw cotton.

Table 5.15

No.	X_1	X_2	X_3	Y_1	Y_2	Y_3	Y_{tab}	$S^2[Y]$
1	-	-	-	82,8	81,7	81,8	82,1	0,37
2	+	-	-	85,8	86,1	85,5	85,8	0,09
3	-	+	-	78,8	78,1	77,3	78,07	0,563
4	+	+	-	82,4	81,6	81,8	81,93	0,173
5	-	-	+	80,2	81,1	80,9	80,73	0,223
6	+	-	+	77,8	77,2	75,2	76,73	1,853
7	-	+	+	78,7	78,5	77,3	78,17	0,573
8	+	+	+	77,8	77,5	76,5	77,27	0,463

We determine the dispersion from the following expression.

$$S^2[У] = \frac{\sum_1^8 Y_u}{m-1}; \quad (5.20)$$

where m is the number of experiments conducted under identical conditions.

The dispersion values are given in Tables 5.14 and 5.15.

We calculate the Cochran criterion using the formula [144].

$$G_p = S^2[У] / \sum_{i-1}^{x} S_i^2(Y) = 42,28/166,16 = 0,2544 \quad (5.21)$$

For probability q = 0,05 from table [144, 157] we select Cochran's coefficient for N = 8, m = 5 G_{tab} = 0.7043.

Since $G_p < O_{tab,}$ we can assume that the dispersion is homogeneous.

$$b_0 = \frac{1}{8}(82,10 + 85,80 + 78,07 + 81,93 + 80,73 + 76,73 + 78,17 + 77,27) = 80,1$$

$$b_1 = \frac{1}{8}(-82,10 + 85,80 - 78,07 + 81,93 - 80,73 + 76,73 - 78,17 + 77,27) = 0,33$$

$$b_2 = \frac{1}{8}(-82,10 - 85,80 + 78,07 + 81,93 - 80,73 - 76,73 + 78,17 + 77,27) = -1,24$$

$$b_3 = \frac{1}{8}(-82{,}10 - 85{,}80 - 78{,}07 - 81{,}93 + 80{,}73 + 76{,}73 + 78{,}17 + 77{,}27)$$
$$= -1{,}87$$

$$b_{12} = \frac{1}{8}(82{,}10 - 85{,}80 - 78{,}07 + 81{,}93 + 80{,}73 - 76{,}73 - 78{,}17 + 77{,}27)$$
$$= 0{,}40$$

$$b_{13} = \frac{1}{8}(82{,}10 - 85{,}80 + 78{,}07 - 81{,}93 - 80{,}73 + 76{,}73 - 78{,}17 + 77{,}27)$$
$$= -1{,}55$$

$$b_{23} = \frac{1}{8}(82{,}10 + 85{,}80 - 78{,}07 - 81{,}93 - 80{,}73 - 76{,}73 + 78{,}17 + 77{,}27)$$
$$= 0{,}73$$

$$b_{123} = \frac{1}{8}(-82{,}10 + 85{,}80 + 78{,}07 - 81{,}93 + 80{,}73 - 76{,}73 - 78{,}17 + 77{,}27)$$
$$= 0{,}36$$

Let's calculate the variance of the regression coefficient

$$S^2\{b_i\} = \frac{1}{N}S^2\{\bar{Y}\} = 0{,}022438, \quad S\ \{b_i\} = 0{,}149792$$

$$S^2\{\bar{Y}\} = \frac{1}{mN}S^2\{Y\}$$

Where

Calculated values of the Student's criterion

$$t_R\{b_1\} = \frac{0{,}33}{0{,}149792} = 2{,}20$$

$$t_R\{b_2\} = \frac{1{,}24}{0{,}149792} = 8{,}27$$

$$t_R\{b_3\} = \frac{1{,}87}{0{,}149792} = 12{,}51$$

$$t_R\{b_{12}\} = \frac{0{,}4}{0{,}149792} = 2{,}72$$

$$t_R\{b_{13}\} = \frac{1{,}55}{0{,}149792} = 10{,}39$$

$$t_R\{b_{23}\} = \frac{0{,}73}{0{,}149792} = 4{,}9$$

$$t_R\{b_{123}\} = \frac{0{,}36}{0{,}149792} = 2{,}45$$

As a result of processing the obtained results, a regression equation was obtained for the IV grade of cotton:

$$У = 80,1 + 0,93X_1 - 1,24X_2 - 1,87X_3 + 0,4X_1X_2 + 0,73X_2X_3 \quad (5.22)$$

Verification of the obtained equations (5.19) and (5.22) using the Fisher criterion showed their adequacy.

Let us consider the influence of factors on the output parameter, i.e. on the cleaning effect. Analysis of the regression equation shows that the main influence on the cleaning efficiency *Y* is exerted by the rigidity of the rubber bushings (x_1 productivity (x_2 the gap between the grate and the saw drum (x_3)) and the interaction of factors *($x_1 x_3$, $x_2 x_3$, $x_1 x_2 x_3$).*

To study these dependencies, a numerical calculation of the curves was carried out using the regression equation for different values of the main factors [159-169].

5.3.6. Results of the experiments and analysis of regression equations

The results of the calculations after processing are presented in the form of graphs (Fig. 5.32). Fig. 5.32, *a* shows the dependences of the efficiency of cotton cleaning on the hardness of the rubber, where four curves *y = y (x)* are given.

The first curve corresponds to the minimum, the second and third to the intermediate, and the fourth to the maximum values of the factors x_2 and x_3. On the first curve, at x_2 = 5,0 t/h, x_3 = 12 mm, it increases from 83,04% to 89,01%, on the second curve, at x_2 = 5,66 t/h, x_3 = 13,32 mm, it increases from 82,8% to 83,7%, on the third curve at x_2 = 6,32 t/h, x_3 = 14,64 mm, respectively, from 83,04% to 83,7%, on the fourth curve at x_2 = 7,0 t/h, x_3 = 16,0 mm, respectively, from 82,47% to 80,9%.

Fig. 5.32, b shows the graphical dependences of the efficiency of cleaning raw cotton on the machine productivity. The presented curves show that with an increase in productivity from 5,0 t/h to 7,0 t/h, depending on the specified x_2 and x_3, the cleaning efficiency is characterized by descending curves. On the first curve at x_1=1,0·10 ^{4} N/m; x_3 = 12 mm from 82,5% to 85,2%, on the second curve at x_2=1,33·10^{4}N/m, x_3 = 13,3 mm from 84,4% to 83,3%, on the third curve at x_7 = 1,66·10^4 N/m, x_3 = 14,64 mm from 86,17% to 82,12%, on the fourth curve at x_1= 2,0·10 ^{4} N/m, x_3=16 mm from 87,63% to 80,9%.

Fig. 5.32, c shows the effect of changing the gap between the grate and the saw drum on the effect of cleaning raw cotton. The presented curves show that with an increase in the gap from 12 mm to 16 mm, depending on the specified x_1 and x_2 , the cleaning efficiency is characterized by descending curves, on the first curve at x_1 = 1,0·10 ^{4} N/m; x_2 = 5,0 t/h from 82,59% to 82,25%, on the second curve at x_1 = 1,33·10 ^{4} N/m; x $_2$ = 5,56 t/h from 84,6% to 83,35%, the third curve at x_7 = 1,66·10 ^{4} N/m; x $_2$ = 6,32 t/h from 83,6% to 82,9%, the fourth curve at x $_1$ =

2,0·10 ^{4} N/m; x $_{2}$ = 7 t/h from 82,5% to 80,9%.

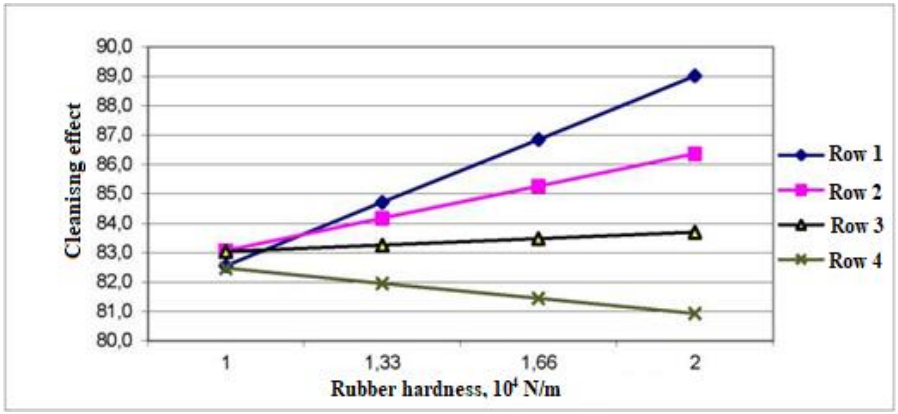

a - graphs of changes in the cleaning effect depending on hardness rubber bushing of composite grates, where, 1 - at x $_{2}$ = 5,0 t/h, x $_{3}$ = 12 mm, 2 - at x $_{2}$ = 5,33 t/h, x $_{3}$ = 13,32 mm, 3 - at x $_{2}$ = 5,66 t/h, x $_{3}$ = 14,64 mm, 4 - at x $_{2}$ = 7,0 t/h, x $_{3}$ = 16,0 mm

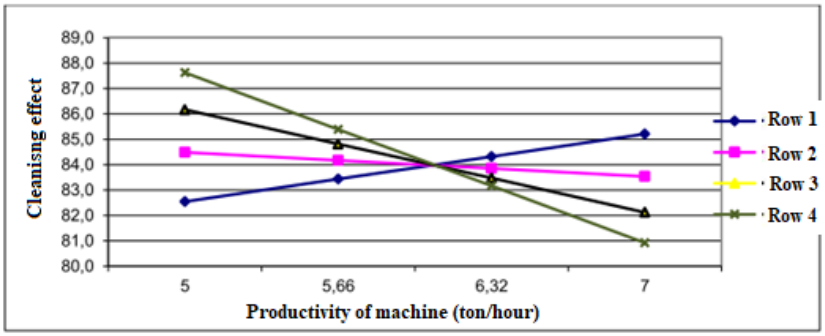

b - graphs of the change in cleaning effect from the machine productivity, where, 1 - at x $_{1}$ = 1,0·10 ^{4} N/m; x $_{3}$ = 12 mm, 2 - at x $_{1}$ = 1,33·10 ^{4} N/m; x $_{3}$ = 13,32 mm,3-at x$_{1}$ =1,66·10^{4} N/m;x $_{3}$ =14,64 mm, 4 - at x $_{1}$ = 2,0·10 ^{4} N/m; x $_{3}$ = 16,0 mm

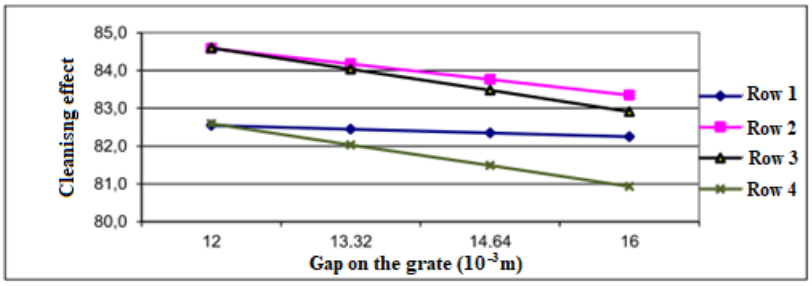

c - graphs of the change in the cleaning effect from the gap between the grate and the saw cylinder. 1 - at l $_{1}$ = 1.0 x 10 ^{4} N/m; x $_{2}$ = 5.0 t/h, 2 - at x7 = 1.33 x 10 ^{4} N/m; x $_{2}$ = 5.56 t/h, 3 - at x7 = 1.66 x 10 ^{4} N/m; x $_{2}$ = 6.32 t/h, 4 - at x7 = 2.0 x 10 ^{4}

N/m; x $_2$ = 7.0 t/h.

Fig. 5.32. Graphical dependencies of the cleaning effect on technological parameters

The calculation results after processing are presented in the form of graphs (Fig. 5.33). Fig. 5.33, *a* shows the dependences of cotton cleaning efficiency on rubber hardness, where four curves *y = y (x)* are given. On the first curve, at the values of factors x $_2$ = 5,0 t/h, *x $_3$ = 12* mm, it increases from 82,08% to 85,8%, on the second curve at x $_2$ = 5,66 t/h, x $_3$ = 13,32 mm it increases from 80,45% to 81,9%, on the third curve at x $_2$ = 6,32 t/h, x $_3$ = 14,64 mm it decreases from 79,17% to 79,14%, and at maximum values, i.e. *x $_2$ = 7* t/h, *x $_3$ = 16* mm, it decreases from 82,47% to 80,93%.

Fig. 5.33, b shows the graphical dependences of the efficiency of cleaning raw cotton on the machine productivity. The presented curves show that with an increase in productivity from 5.0 t/h to 7.0 t/h depending on the specified *x $_2$* and *x $_3$* The cleaning efficiency is characterized by descending.

On the first curve at x $_7$ = 1,0·10 ^{4} N/m; x $_3$ = 12 mm from 82,01% to 78,52%, on the second curve at x $_7$ = 1,33·10 ^{4} N/m, x $_3$ = 13,3 mm from 85,52% to 78,6%, on the third curve at x $_7$ = 1,66·10 ^{4} N/m, x $_3$ = 14,64 mm from 80,25% to 78,08%, on the fourth curve at x $_7$ = 2,0·10 ^{4} N/m, x $_3$ = 16 mm from 76,4% to 77,26%.

Fig. 5.33, c - shows the effect of changing the gap between the grate and the saw drum on the effect of cleaning raw cotton. The presented curves show that with an increase in the gap from 12 mm to 16 mm, depending on the specified *x$_7$* and *x$_2$* , the cleaning efficiency is characterized by descending curves, on the first curve at x $_7$ = 1,0·10 ^{4} N/m; x $_2$ = 5,0 t/h from 82,08% to 80,74%, on the second curve at x $_7$ = 1,33·10 ^{4} N/m; x $_2$ = 5,56 t/h from 82,0 % to 78,89 %, the third curve at x $_7$ = 1,66 x 10 ^{4} N/m; x $_2$ = 6,32 t/h from 82,04% to 77,74%, the fourth curve at x $_7$ = 2,0·10 ^{4} N/m; x $_2$ = 7 t/h from 81,9% to 77,2%.

The gap between the grate and the saw drum affects the cleaning process linearly. By changing the gap, the cleaning effect can be adjusted.

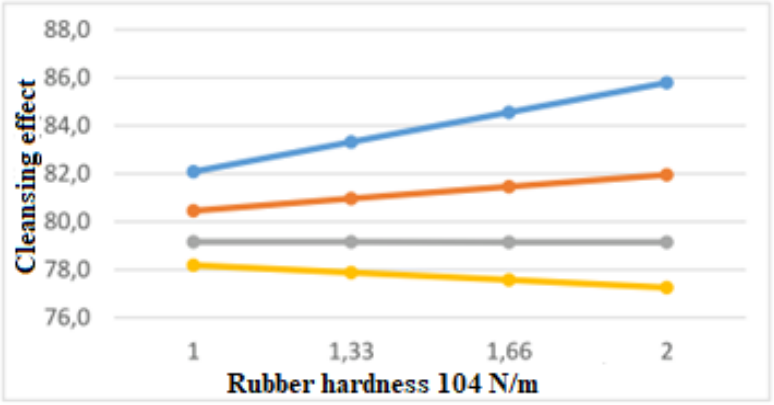

a - graphs of the change in the cleaning effect from the rigidity of the

rubber bushing of the composite grates, where, 1 - at x_2 = 5,0 t/h, x_3 = 12 mm, 2 - at x_2 = 5,33 t/h, x_3 = 13,32 mm, 3 - at x_2 = 5,66 t/h, x_3 = 14,64 mm, 4 - at x_2 = 7,0 t/h, x_3 = 16,0 mm.

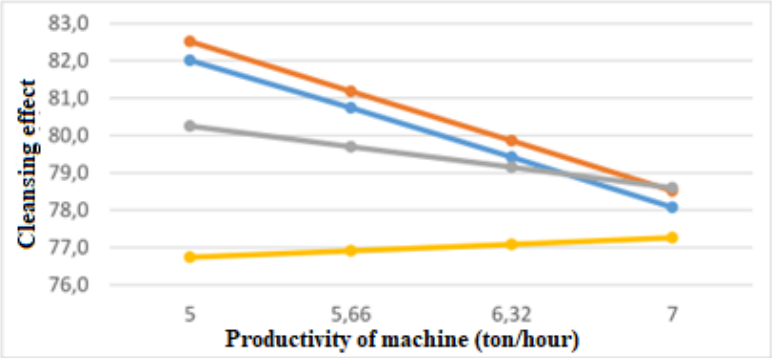

b - graphs of the change in the cleaning effect from the machine performance. 1 - at x_1 = 1,0·10 ^{4} N/m; x_3 = 12 mm, 2 - at x_1 = 1,33·10 ^{4} N/m; x_3 = 13,32 mm, 3 - at x_1 = 1,66·10 ^{4} N/m; x_3 = 14,64 mm, 4 - at x_1 = 2,0·10 ^{4} N/m; x_3 = 16,0 mm.

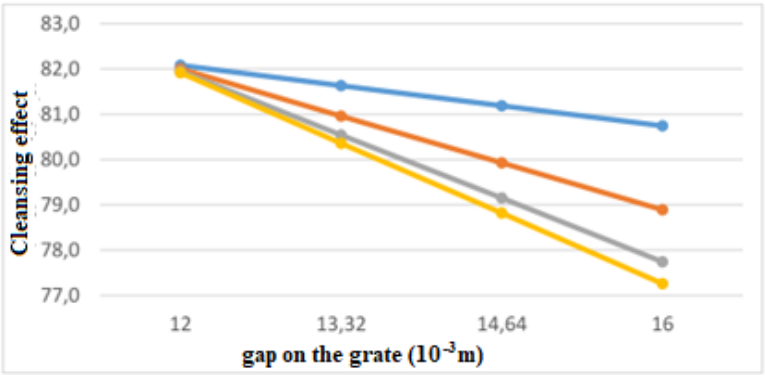

c - graphs of the change in the cleaning effect from the gap between the grate and the saw cylinder. 1 - at x_1 = 1,0·10 ^{4} N/m; x_2 = 5,0 t/h, 2 - at x_1 = 1,33·10 ^{4} N/m; x_2 = 5,56 t/h, 3 - at x_1 = 1,66·10 ^{4} N/m; x_2 = 6,32 t/h, 3 - at x_1 =2,0·10 ^{4} N/m; x_2 =7,0 t/h.

Fig. 5.33. Graphs of changes in the cleansing effect

The main result of the conducted full-factorial experiment is to determine the influence of input factors on the output factor. All the above parameters and their ratio affect the process of cleaning raw cotton. It is necessary to select such parameters of input factors that would work to improve the cleaning process. Analysis of the obtained experimental results allows us to recommend the following values for the selected main factors:

- productivity, t/h – 5,0;
- the hardness of rubber bushings is 2,0·10 ^{4} N/m;
- the gap between the grate and the saw drum is 16 mm.

With these values of factors, the raw cotton cleaner operates efficiently, i.e. the cleaning effect is above 90%.

The technical solutions and recommendations obtained as a result of completing the dissertation have been implemented in:

- Karasuv and Piskent cotton factories in Tashkent region.
- Kagansky and Peshkunsky cotton factories of the Bukhara region.
- Chelak cotton factory in Samarkand region.
- Sherabad cotton factory, Surkhandarya region.

This is confirmed by the relevant implementation acts (Appendix 7-12).

The quality of the fiber after the separation and cleaning section was tested using the HVI system in the laboratory of the Tashkent Textile Institute. The experiments were conducted on the selection variety "Namangan-77" and "Bukhara-6" I, II and III industrial grades. The test results for the existing and proposed cleaning systems are given in Appendix 13. From the data provided it follows that the contamination of the fiber is reduced by 14-17% for the "Bukhara-6" variety and by 14-29% for the "Namangan-77" variety. The short fiber index is reduced by an average of 3% regardless of the selection variety.

5.3.7. Conclusions for Chapter 5

1. Experiments have shown that installing a curved guide at the entrance to the separator's separation chamber reduces seed damage by 1.5 times.
2. The use of an insulating separator chamber allows to reduce the pressure of cotton on the mesh at the point of removal, which leads to a decrease in the amount of free fibers by 33-39%, depending on the type of fiber.
3. Based on a full factorial experiment, a mathematical model was obtained for the dependence of the level of seed crushing on the controlled factors of air velocity at the entrance to the separator, the angle of inclination of the guide and productivity, which makes it possible to determine rational values of the process parameters.
4. It has been established that with an increase in the number of edges or the width of the multifaceted mesh, the cleaning effect decreases. An increase in the width of the mesh surface edges leads to significant cotton braking, increased interaction with the mesh and pins. This leads to some increase in damage to the fibers and seeds of the cleaned cotton. Therefore, a mesh with six edges and a width of *70,8 mm* is recommended for use in cleaners.
5. When increasing the distance between the ends of the pegs and the mesh to mm with the recommended version of the multi-faceted mesh, the cleaning effect will be 4-5,8% greater than when using a serial mesh. The recommended gap value is 14,0-16,0 mm. At the same time, compared to the serial version, small debris in cotton after its cleaning in the recommended version decreases on

average to 17%, and the cleaning effect increases to 21%.

6. Based on multifactorial experiments of the second order, rational values of technological parameters of cotton cleaning from small debris were determined. It is recommended to select the number of mesh edges - *6* (width 70.8 mm), technological gap between the pegs and the mesh - 15 mm, the coefficient of rubber rigidity on the supports of the mesh surface is $3 \cdot 10^{3}$ N/m. With these values, the cleaning effect of the UHK machine is 89,2%.

7. Based on multifactorial experiments, the best parameters of the cotton cleaner for small debris were determined: the number of peg faces is 6, the technological gap between the pegs and the mesh is 15 mm, the number of drum revolutions is *310 rpm,* which ensures the maximum cleaning effect of UHK cotton up to 89,8%.

8. The laws of oscillatory motion of composite grates on elastic supports were determined experimentally depending on the load from the side of the cleaned raw cotton, the rigidity coefficient of the rubber bushings (supports) and the rotation frequency of the saw drum:

- regularities of the change in the amplitude of oscillations of composite and metal (serial) grates from the change in the load from the side of the cleaned raw cotton were obtained. In this case, the amplitude of oscillations of the composite grate is 5-6 times greater than the amplitude of oscillations of the serial grate under the same conditions, which contributes to an increase in the cleaning effect;
- Graphic dependences of the change in the oscillations of the composite grate on the increase in the stiffness coefficient of the rubber elastic supports of the grate were constructed. To ensure the required amplitude of oscillations of the composite grate $(1,7\text{-}2,0) \cdot 10^{-3}$ m, it is recommended to install bushings with a stiffness coefficient of $(1,6\text{-}2,0) \cdot 10^{4}$ N/m;
- The regularities of the change in the frequency of forced oscillations of composite grates from the increase in the rotation frequency of the saw drum were obtained. The recommended values of the rotation frequency of the saw drum are $(3,0\text{-}3,15) \cdot 10^{2}$ rpm;

9. Experimental studies of a new grate with composite grates on elastic supports were conducted. A mathematical model was obtained that adequately describes the process of cleaning raw cotton from large debris in the form of regression equations. Optimization of the parameters of the section for cleaning cotton from large debris was carried out, based on which the following parameters are recommended: productivity 5,0 t/h; rubber hardness $2,0\text{-}10^{4}$ N/m, gap between the saw drum and grates 16 mm, while the cleaning effect achieved is above 90%.

10. The results of fiber testing for the existing and proposed cleaning

systems according to the HVI system showed that fiber contamination is reduced by 14-17% for the Bukhara-6 variety and by 14-29% for the Namangan-77 variety. The short fiber index is reduced by an average of 3% regardless of the selection variety.

CHAPTER 6. ECONOMIC EFFICIENCY FROM THE IMPLEMENTATION OF A MODERNIZED SEPARATION AND PURIFICATION UNIT

6.1. Calculation of economic efficiency from the implementation of a modernized separation and purification unit

Tests on the introduction of new equipment were conducted at the Karasuv cotton mill in Tashkent region. The existing SS-15A designs and the UHK unit were installed, and a prototype of the modernized separation and cleaning unit was installed in parallel. Fig. 6.1 shows the equipment diagram and Fig. 6.2 shows the general appearance of the unit.

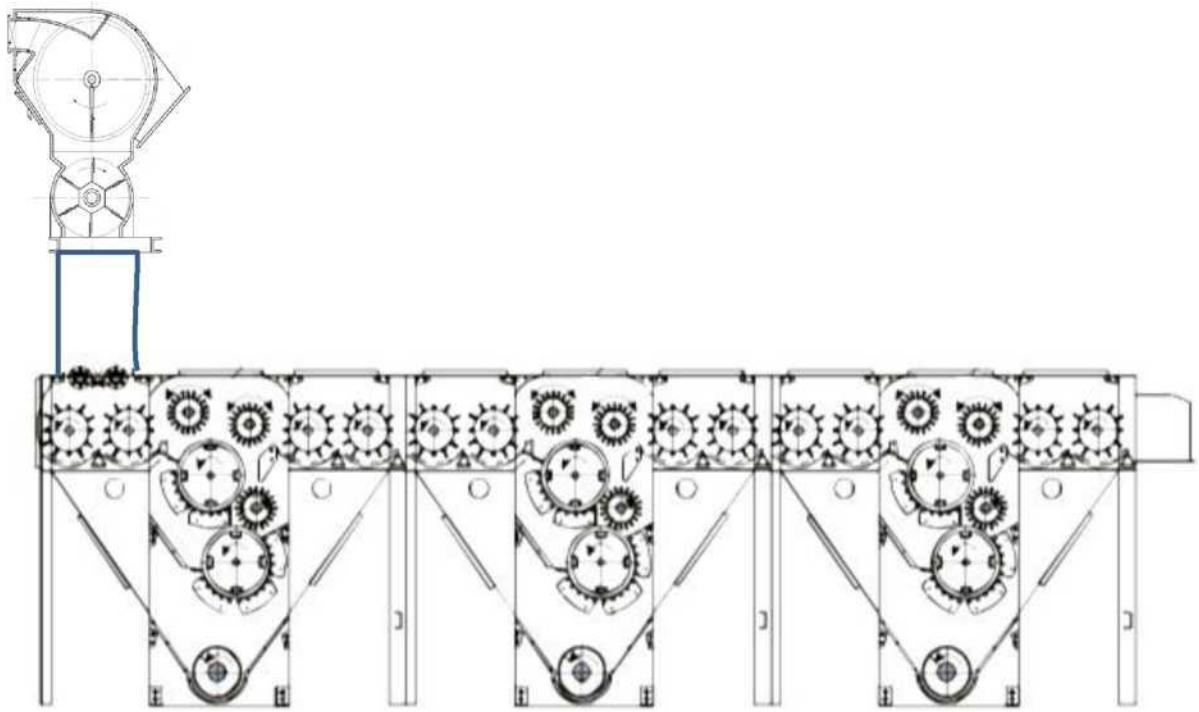

Fig.6.1. Scheme of the separation and cleaning unit SS-15A-UKhK

Based on the test results, the annual economic effect from using the upgraded equipment in the form of the SS-15A-UKhK separation and cleaning unit was calculated.

Economic efficiency was calculated on the basis of the current methodology "Methodology (basic provisions) for determining the economic efficiency of using new technology, inventions and rationalization proposals in the national economy" [170].

The calculation of the annual economic effect is based on a comparison of the reduced costs for the basic and new technology.

Fig.6.2. General view of the recommended separation and cleaning unit

The main indicators characterizing the economic efficiency of introducing a new technology are: cost price of production, specific capital investments, labor costs, labor productivity, profitability, profit, payback period of additional investments or the standard capital investment coefficient.

The payback period (T) or efficiency coefficient (E) is determined by the following formula.

$$T = \frac{K_1 - K_2}{C_1 - C_2} \tag{6.1}$$

$$E = \frac{C_2 - C_1}{K_1 - K_2} \tag{6.2}$$

where K_1, K_2 are specific capital investments in basic and new technology;

C_1, C_2 - the cost of production of a unit of output using basic and new technology.

The costs incurred are an indicator of the comparative effectiveness of capital investments and are used to select the best options for technical and economic solutions. Costs are determined by next formula:

$$C_i + E_n \ K_i \rightarrow \min \text{ или } K_i + T_n \ C_i \rightarrow \min \tag{6.3}$$

where K_i is the capital investment spent on each solution option.

C_i - this is the price of a product produced using a certain technology.

T_n is the standard payback period for capital investments.

E_n is the standard coefficient of comparative efficiency of capital investments.

The annual economic effect is determined by the following formula:

$$Э_г=(З_1-З_2)\ A_2 \qquad (6.4)$$

where $З_1$,$З_2$ are the sum of the costs of producing a unit of output using old and new technology, sum ;

A_2 is the annual volume of production of the product using the new technology in the estimated year, in physical units.

The economic efficiency of production and use of new equipment is determined by the following formula:

$$Э_г=\left(З_1\cdot\frac{в_2}{в_1}\cdot\frac{P_1+E_н}{P_2+E_н}+\frac{\left(U_1^{'}-U_2^{'}\right)-E_н\left(K_2-K_1\right)}{P_2+E_н}-З_2\right)\cdot A_2 \qquad (6.5)$$

where $З_1$, $З_2$ are the reduced costs of the old and new equipment, respectively, in sum;

$\frac{в_2}{в_1}$ – the coefficient of growth of productivity of new equipment compared to old one;

b_1, and b_2 — annual volumes of products (work) produced using a unit of basic and new equipment, respectively, in physical terms;

$\frac{P_1+E_н}{P_2+E_н}$ — coefficient of taking into account the service life of new equipment in comparison with the basic version;

P_1, P_2 - percentage of deductions from the book value for the complete restoration of basic and new equipment, taking into account obsolescence.

If the complete recovery rate is 16,4%, then P = 0,164;

E_n - standard efficiency coefficient E_n = 0,15;

$\frac{(U_1-U_1)-E_н(K_2-K_1)}{P_2+E_н}$ consumer savings on current operating costs and deductions from capital investments over the entire service life of new equipment compared to the new base version;

K_1, K_2 – accompanying capital investments of the consumer in basic and new equipment;

U_1, U_2 - annual operating costs of the consumer when using new equipment based on the volume of products produced using the new equipment;

A_2 - the annual volume of products manufactured on new equipment in the reporting year, in physical terms.

At the same time, as a result of the introduction of more advanced equipment into production, the quality of finished products will be improved. At the same time, as a result of the improvement of equipment and its working parts of the main production process at cotton ginning plants, the output of high-grade cotton fiber increases, and the quality of the seeds obtained increases due to the reduction

of their damage.

Therefore, when calculating the annual economic efficiency of introducing improved equipment into production, it is necessary to take into account the additional economic effect of increasing the overall quality of manufactured products.

The economic efficiency of improving quality indicators is determined by the following formula:

$$Эк = (Ц_2^1 - Ц_1^1) * A_2 \qquad (6.6)$$

where, $Ц_1^1$is the price of the product in the basic version;

$Ц_2^1$- the price of the product in the new version;

A_2 - annual production of a new version, size.

The information required to calculate the annual economic effect from the introduction of a new type of separation and purification unit, brand SS-15A-UKhK, is presented in Table 6.1.

Table 6.1

Necessary data for calculation of a new type of separation and cleaning unit of the SS-15A-UKhK brand

INDICATORS	Units measurement	Options	
		Basic	New
Annual volume of processed raw cotton	tons	24000	24000
Quantity established equipment	pcs .	2	1
Performance equipment	t/h	10	11
Installed power equipment	kW	131,5	131,5
Coefficient demand	-	0.7	0.7
Electricity fee for 1 kW of maximum load per year for 1 kW/hour of consumed energy	sum .	325	325
Amount of payment for installed capacity	sum .	36800	36800
The amount of depreciation charges for major repairs	%	15	15
Deductions on current repair	%	5	5
Minimum wage established for settlements	sum .	821000	821000
Deductions By social insurance	%	25	25

I. Calculation capital expenses.

The book value of the equipment, taking into account the coefficient for transportation and installation of 10%, is:

In the basic version:

Separator brand SS-15A and cleaning unit brand UHK: 195580 thousand soums ;

Total: 195580 thousand sums.

In the implemented version:

Separation and cleaning unit brand SS-15A-UHK: 195580 thousand sums;

Total, taking into account expenses for R&D: 220180 thousand sums.

II. Calculation operational costs.

These costs include expenses for major repairs, current repairs, electricity, and material consumption.

1. Cost on capital repair:

In the basic variant

195580*0,15 = 29337 thousand sums

In being implemented variant

220180*0,15 = 33027 thousand sums

2. Cost on current repair:

In the basic variant

195580*0,05 = 9779 thousand sums

In being implemented variant

220180* 0,05 = 11009 thousand sums

3. Cost on electricity:

In the basic variant

(131.5x0.7x0.7x3556x325)/1000 = 74467,5 thousand sums;

In the implemented version

(131.5x0.8x0.7x3556x325)/1000 = 85105,7 thousand sums.

4. R&D costs: 24600 thousand sums.

5. Material costs:

In the basic version: 14400 thousand sums;

In the implemented version: 2328 thousand sums.

The obtained data are entered into table 6.2.

Table 6.2

Determination of reduced and operating costs in the basic and implemented options, in thousands of sums.

INDICATORS	Options	
	Basic	New
Initial price equipment	177800	177800
Costs of transportation and installation	17780	17780
Straight capital cost	154508	154508
R&D costs	-	24600
Capital expenditures in R&D	154508	179108
Presented costs for the acquisition of equipment	218756	222446
Operational expenses , total	159898	152746
Including: - depreciation charges	29337	33027
- deductions on current repair	9779	11009
- expenses on electricity	106382	106382
- material cost	14400	2328

6.2 Definition accompanying capital investments

Associated capital investments related to the production of a new means of labor are determined in the amount of 10% of the cost of the basic and implemented equipment:

$$K_1 = \frac{195580 \times 10}{100} = 19558{,}0$$

thousand sums

$$K_2 = \frac{220180 \times 10}{100} = 22018{,}0$$

thousand sums

Substituting the obtained data into the formula, we calculate the annual economic effect from the introduction of improved equipment [171, 172]:

$$Э_г = 218756 \times 1{,}1 \times 1{,}0 + \frac{(159898 - 152746) - 0{,}15 \times (22018 - 19558)}{0{,}164 + 0{,}15} - 222446 = 39787{,}53$$

thousand sums

Let's define general economic effect:

$$Эобщ. = Эг. + Эс.вол. + Э_{кач.воз.} = 39787{,}53 + \frac{24000 \times 32{,}5 \times 0{,}5}{100 \times 100} \times 12860{,}72 + (14789{,}83\text{-}14318{,}24) \times 228{,}2$$

$$= 39787{,}53 + 50156{,}08 + 10761{,}84 = 64897{,}45 \cdot \textit{thousand sums}$$

6.3. Conclusions on Chapter 6

1. According to the results of research in production, as a result of mechanical damage to seeds and loss of fibrous products in the proposed improved isolation chamber and directional separator, an economic benefit of 490,592 thousand sums was achieved.

2. It is recommended to use a mesh surface with a face width of 70,8 mm, when using which the cleaning effect in the UHK unit will be 7,3% greater than in the serial version.

3. Based on the results of tests of JSC “Korasuv pakhta tozalash” of the Tashkent region cotton cleaning plant, it was revealed that the modernized unit of the UHK using hexagonal meshes with a width of 70,8 mm allows to obtain a cleaning effect of 7,0-7.5% greater than in a serial cotton cleaner.

4. The implementation of the recommended design of a multifaceted mesh surface in the EN.178 section of the cotton ginning unit of the UHK allows one cotton mill to obtain an annual economic effect of 52,466 thousand sums.

5. The results of comparative production tests of the developed design of the separation and cleaning unit in the conditions of cotton mills showed that the cleaning effect of raw cotton in the proposed separation and cleaning unit is on average 12-14% higher than in serial machines. In addition, mechanical damage to cotton seeds due to the use of a composite guide in the separator and shock-absorbing bushings in the supports of the cleaner grates made it possible to reduce 0,75-0,82% relative to the serial design. At the same time, free fiber in cotton is reduced almost twice, the service life of the machine has increased significantly, and it has become possible to increase the productivity of the machine.

6. The implementation of the recommended separation and cleaning unit with the developed working bodies allows to obtain an annual economic effect for one cotton mill of 648972,45 thousand sums.

GENERAL CONCLUSIONS AND RECOMMENDATIONS FOR THE DISSERTATION

1. Analysis of works on improvement of cotton separators and cleaners showed that currently there is no information on research on combination and continuity of processes of separation of cotton and air with its subsequent cleaning. Due to imperfection of working bodies of cotton separators and cleaners, high damage of fibers and seeds of cotton occurs. Combination and provision of continuity of technologies of separation of raw cotton from air and cleaning is proposed. On this basis, a technological scheme of separation and cleaning section of flow line of cleaning of raw cotton is proposed.

2. Efficient and resource-saving design schemes of working parts and elements of cotton separators have been developed:

- a separator with a curved cotton guide in the inlet part of the chamber;
- diagram of a raw cotton separator with a composite guide and elastic shock absorber;
- raw cotton separator with improved design of perforated disc and isolation chamber;
- diagram of a separator with a spherical shape of the design of the mesh surface of the chamber.

3. The technological parameters of the working parts of the cotton separator are theoretically substantiated: the pressure at the entrance to the separator, the position of the guide, the law of movement of the scraper shaft with a separating chamber, ensuring a reduction in mechanical damage to seeds by 1,5 times, and the formation of free fibers by 33-39%.

4. The regularities of movement, trajectory and speed of cotton fly are determined taking into account the guide at the entrance to the separator. The forces of interaction of seeds with the wall of the separating chamber are determined by finite element modeling methods.

5. Regularities have been established that allow calculating the shear forces of the cotton layer on the surface of the separator mesh taking into account the geometry of the holes with it; the parameters of the mesh and conical holes that ensure the minimum value of their shear forces have been substantiated.

6. A formula for determining the movement and speed of a cotton particle along a curvilinear vibrating surface of a composite separator guide has been obtained, and technological parameters have been recommended that ensure efficient separation of dust and small debris.

7. Based on the results of research in production conditions, it was established that as a result of reducing mechanical damage to seeds and fiber loss in the proposed separation technology with an isolation chamber and a separator

guide, an economic benefit of 490 350,26 thousand sums was achieved.

8. It has been established that the use of multifaceted meshes in small debris cleaners reduces the monotony of cotton movement across their surface and thereby increases the cleaning effect.

9. A mathematical model of the movement of a fly on the surface of a polyhedral mesh has been obtained, which makes it possible to determine the values of the technological angle of interaction of cotton fly with the polyhedral surface of the mesh, the speed of the impact interaction of the cotton fly with the polyhedral mesh surface and the rebound value of the cotton fly after interaction with the mesh.

10. Graphic dependences of the change in the speed of movement of cotton bats on a multifaceted mesh surface on the change in the angle of inclination of the flight of bats in the cleaning zone are constructed. It is revealed that in order to increase the rapid movement of cotton bats in the cleaning zone, it is advisable to sufficiently loosen the cotton so that the mass of the dragged lump of raw cotton does not exceed 0,5-0,7 g.

11. Small oscillations of a polyhedral mesh under the effect of a technological load from the cotton being cleaned are studied. Dependences of the change in the amplitude of oscillations of a polyhedral mesh on the torsional rigidity of the elastic support and on the moment of inertia of the mesh are obtained, allowing to increase the efficiency of separation of small debris.

12. A method for determining the rigidity of the elastic support of a polyhedral mesh is proposed, providing the required level of its amplitude from a variable technological load. Operating modes of the cleaner are established, providing the necessary gap between the ends of the pegs and the mesh surface of 0.014-0.016 m.

13. The dependence of the cleaning effect on the number of mesh edges and the gap between the mesh pins was established, which made it possible to reasonably approach the selection of rational parameters from the point of view of reducing damage to seeds and fiber.

14. Based on multifactorial experiments, the best parameters of the cotton cleaner for small debris were determined, at which the UHK cleaner provides the maximum cotton cleaning effect of up to 89,8%.

15. Based on the test results, it was found that the modernized UHK unit using hexagonal meshes allows for a cleaning effect of 7,0-7,5% greater than in a serial cotton cleaner. The introduction of the recommended design of a multifaceted mesh surface allows for an annual economic effect of 52,466 thousand sums for one cotton plant.

16. Based on the analysis of the grate designs of cotton cleaners for large

debris, lightweight composite grate designs on elastic supports have been developed. A classification of grate bars has been developed taking into account the mobility and materials of manufacture, as well as the functional and technical properties of the grate bars.

17. A differential equation of oscillatory motion of a lightweight composite grate on an elastic support with nonlinear rigidity is obtained, formulas are obtained for determining the period and frequency of natural oscillations of the grate on an elastic support with a nonlinear restoring force. It is revealed that with an increase in the reduced mass of the grate, the frequency of natural oscillations of the grate decreases according to a nonlinear dependence.

18. The dependences for determining the distance and deviation angle of the cotton fly with variable rotation of the saw drum and the use of composite grates, as well as the dependences of the change in oscillations of the displacement, speed and acceleration of the composite grate depending on the stiffness coefficient of the elastic support of the grate are obtained. It is revealed that with an increase in the load on the composite grates, the values of displacement, speed and acceleration increase according to nonlinear patterns, and the influence of the random component of the load is within 8,0-10%. To ensure the required oscillation amplitudes of the composite grate $(1,0\text{-}1,4)10^{-3}$ m, the average value of the disturbing force should not exceed 15-20 N.

19. Tests of the separation and cleaning unit with the proposed changes in the conditions of cotton mills showed that the cleaning effect of raw cotton is on average 12-14% higher than in serial machines. In addition, mechanical damage to cotton seeds due to the use of a composite guide in the separator and shock-absorbing bushings in the supports of the cleaner grates is reduced by 0,75-0,82% relative to the serial design.

20. The results of fiber testing for the existing and proposed cleaning systems according to the HVI system showed that fiber contamination is reduced by 14-17% for the Bukhara-6 variety, and by 14-29% for the Namangan-77 variety. The short fiber index is reduced by an average of 3% regardless of the selection variety.

21. The introduction of a separation and cleaning unit with developed working bodies and recommended technological modes allows obtaining an annual economic effect for one cotton mill of 648972,45 thousand sums.

LIST OF USED LITERATURE

1. Распоряжение Правительства РФ от 6 июня 2020 г. № 1512-р «Об утверждении Сводной стратегии развития обрабатывающей промышленности РФ до 2024 г. и на период до 2035 г.». [Электронный ресурс]-Режим доступа: https://www.garant.ru/products/ipo/ prime/doc/74142592/.
2. Указ Президента Республики Узбекистан, «О стратегии действий по дальнейшему развитию Республики Узбекистан» от 07.02.2017 г. № УП-4947. [Электронный ресурс]-Режим доступа: https://lex.uz/uz/docs/3107042
3. Жабборов Г.Ж. и др. / Технология первичной обработки хлопка. //Т.: Укитувчи, 1987. 465 с.
4. Амиров Р., Тихомиров Г.А., Суслин А.К. К вопросу о поврежденности семян при транспортировках хлопка-сырца //Хлопковая промышленность. - Ташкент, 1975. №1.- С.4-5.
5. Максудов И.Т. / Справочник по первичной обработке хлопка // © По заказу Научно-производственного объединения «Хлопкопром», 1995 г. Ташкент-«Мехнат»-1995. 389 с.
6. Рахматуллин Х.А. «К теории пневматической хлопкоуборочной машин». //Известия, сер.техн.наук. 1957. №1.
7. Кадырходжаев С.К. Разработка сепаратора для хлопка-сырца с целью сохранения его качественных показателей и сокращения потерь волокна. Дисс.канд.тех.наук, Ташкент, 1986.
8. Муродов О. Ж. Изучение изменения технологических показателей хлопка сырца при складировании / Муродов О. Ж., Рузметов М.Э. // Костромской государственный университет ISSN 2587-6147. Технологии и качество. 2021. № 4(54). С. 30-36. https: doi 10.34216/2587-6147-2021- 4-54-30-36.
9. Муродов О.Ж. О новом способе переработки семенного хлопка-сырца / О.Ж. Муродов, А. Джураев, К. Собиров // Министерство образования республики Беларусь Учреждение образования «Витебский Г осударственный технологический университет» Новое в технике и технологии текстильной и легкой промышленности. Витебск-2005. С. 53-54.
10. Муродов О.Ж. Улучшение конструкции сушилки хлопка-сырца и

повышение эффективности очистки / О.Ж. Муродов, Р.Х. Нурбоев, Д.Х. Бафоев // Бух ТИП и ЛП. Материалы V-научной конференции магистров. Бухара-2005.

11. Бурнашев Р.З. и др. Экспериментальное исследование ударного взаимодействия летучек хлопка-сырца с колосниками очистителя крупного сора. // «Хлопковая промышленность», 1980, №1. с.7-8.
12. Атаметов А.Т. Исследование рабочих поверхностей хлопкоочистительной машин с целью повышения качества волокна тонковолокнистого хлопка. // Автореф. дисс. канд. техн. наук, Тошкент, 1980.
13. Авдеев Н. Е. «Центробежные сепараторы для зерна». М.: Колос.1975.
14. Урбан Я. «Пневматический транспорт». М.: Машиностроение. 1967 (перевод с чешского).
15. Хасанов М.Р. Повышение эффективности технологической надежности элементов пневмотранспортных систем хлопка. // Дисс. кан. тех. наук. Ташкент, 1989.
16. Байдюк П.В. «Влияние природных особенностей хлопка-сырца на процесс транспортирования». Автореф.канд.дисс. Ташкент. ТТИ. 1952.
17. Шамсутдинов Т. «Некоторые вопросам аэродинамики хлебоуборочных машин». Автореф.канд.дисс. М., 1960.
18. Артиков Н.А. «Исследования и разработки пневмотранспортной установки с пневмосепараторы для хлопка-сырца». Автореф.канд.дисс. Ташкент, 1972.
19. Амиров Р. Исследования влияния средств механизации пневмотранспортных установок на качество волокна. // Дисс.кан.техн. наук. Ташкент, 1976.
20. Янгибоев Ю.Д., Мардонов Б., Мурадов Р. Изучение процесса съема хлопка-сырца с поверхности сепаратора СС-15А с наклонным скребком». // Журнал. Хлопковая промышленность, 1984, №5, С. 12-14.
21. Мурадов Р., Махкамов А. Создание возможности очистки хлопка от мелких сор за счет изменения конструкции вакуумного клапана. // АндМИИ тезис. Андижон - 2008 г. С. 45-48.
22. Мурадов Р.М., Каримов А., Маматкулов О.Т. Изучить движение хлопка в рабочей камере сепаратора // НамДУ. Научный вестник №1. 2010 г. С. 101 104.

23. Кадырходжаев С.К. Разработка сепаратора для хлопка-сырца с целью сохренения его качественных показателей и сокращения потерь волокна. Дисс.канд.тех.наук, Ташкент, 1986.

24. Ходжиев М.Т., Шодиев 3.0. Предварительные испытания при разработке сепаратора СХМ // Стратегия и развитие науки и техники в XXI веке. Материалы Республиканской научно-практической конференции. Бухара: Бух ТИП и ЛП, 2009. С.95-96.

25. АпШопу W.S. 8nd Wil^m D. МауйеШ. Сойоп gin^s handbook. /М^пси1Шга1 handbook. ШтЬег 503. Unted States Department of Agriculture. December 1994. 337 p.

26. Сепаратора «BAJAJ» Баджадж сталь индастриз лимитед [Электронный ресурс]-Режим доступа: https://baj ajngp.com/products-services/baj aj - ginning- pressing-machinery/ginning-pressing-machinery/air-separator/

27. Компания Shandong Swan Cotton Industrial Machinery Stock Co., Ltd. [Электронный ресурс]-Режим доступа: http://www.sdmj.com.cn/en/index.aspx.

28. Технологические машины и оборудование хлопкоочистительных заводов США. [Электронный ресурс]-Режим доступа: https://www.lummus.com/.

29. Мирошниченко Г. И. Основы проектирования машин первичной обработки хлопка. М.: Машиностроение, 1972, 486 с.

30. Гуляев Р.А., Лугачев А.Е., Усманов Х.С., Современное состояние производства, переработки, потребления и качества хлопковой продукции ведущих хлопкосеющих странах мир. Ташкент-2017 г. с. 15-18.

31. Зикриёев З. Первичная обработка хлопка. Издательство «Мехнат», Ташкент,1999,398с.

32. Лугачев А. Е., Зияев У. К. Влияние предварительной подготовки хлопка сырца в пильчатой секции очистителя на показатели процесса очистки // Хлопковая промышленность. 1986. № 1. С. 10 -11.

33. Котов Б. С. и др. Интенсификация процесса за счет уменьшения геометрических размеров зуба пилы волокноочистителей // Хлопковая промышленность. 1985. № 3. С. 10 -11.

34. Мирошниченко Г.И., Тютин П.Н., Лугачев А. Е. К вопросу Расчета и конструирования очистительных машин // Хлопковая

промышленность. 1974. № 1. С. 16.

35. Бурнашев Р.З. и др. Экспериментальное исследование ударного взаимодействий летучек хлопка - сырца с колосником очистителя крупного сора // Хлопковая промышленность. 1980. № 1. С. 7 - 8.

36. Мирошниченко Г.И Справочник по первичной обработке хлопка. Книга I // Ташкент-«Мехнат-1994». - 574 С.

37. Махкамов Р.Г. Повышение технологической надежности хлопкоочистительных машин, работающих в ударном режиме. Ташкент, Фан, 152 С.

38. Болдинский Г.И и др. Оптимальное направление полета хлопковой летучки на зуб очистителя хлопка - сырца поточной линии // Хлопковая промышленность. 1978. № 1. С. 6 - 7.

39. Лугачев А.Е. О работе питающих валиков в хлопковых машинах // Хлопковая промышленность. 1978. № 3. С. 10 - 11.

40. Лугачев А.Е. Новые подходы к разработке эффективных процессов питания и очистки волокнистого материала к питателям в линейно-поточной технологии хлопкозавода. Научно - техн. Журнал «Пахтачилик» N4, Ташкент, 1996, с. 25-27.

41. Мирошниченко Г. И. и др. Исследование возможностей вибрационного способа очистки хлопка - сырца // Хлопковая промышленность. 1983. № 1. С. 6 - 7.

42. Нестеров Г.П. и др. Исследование влияния параметров колосниковых решеток пильчатых секции хлопкоочистительного агрегата на технологические показатели хлопка - сырца и волокна // Хлопковая промышленность. 1981. № 3. С. 9 - 10.

43. Будин Е.Ф., Агзамов М. Влияние параметров вращающихся колосников на показатель очистки хлопка - сырца // Хлопковая промышленность. 1980. № С. 4 - 5.

44. Будин Е. Ф. Бородин П. И. Результаты исследований по созданию секции комбинированного хлопкоочистительного агрегата // Хлопковая промышленность. 1983. № 1. С. 18 - 19.

45. Бурнашев Р.З. и др. Определение коэффициента динамической жесткости летучки хлопка - сырца при ударе о колосник // Хлопковая промышленность. 1981. № 4. С. 10 - 12.

46. Нестеров Г. П. и др. Поточная линия сушки и очистки хлопко - сырца

ЛХ - 2 // Хлопковая промышленность. 1981. № 2. С. 13 - 15.

47. Лугачев А.Е., Куриезов Ж.Ш., Рустамов Б.Б. Исследование процесса и разработка устройства для закрепления хлопка-сырца в модуле очистителя крупного сора. Проблемы текстиля. Ташкент, 2003. №1. с. 51-53.

48. Лугачев А.Е. Разработка теоретических основ питания и очистки хлопка применительно к поточной технологии его переработки. Дисс. док. тех. наук - Ташкент, ТИТЛП, 1998. -422 с.

49. Будин Е. Ф. Разработка поточных линий сушки и очистки средневолокнистого хлопка - сырца ЛХ - 2 // Хлопковая промышленность. 1980. № 5. С. 7 - 8.

50. Бородин П. Н. и др. Новая поточная линия сушки и очистки хлопка - сырца // Хлопковая промышленность. 1968. № 1. С. 11

51. Тхипхавонгсай П., Тютин П.Н., Лугачев А.Е. Исследование изменения структуры хлопка-сырца от кратности пропуска через барабаны питателя джина. Реф.сб. Хлопковая промышленность №2, Ташкент 1992, с 10-11.

52. Балтабоев С.Д. Предварительная очистка хлопка-сырца машинного сбора от сорных примесей. Дисс. канд. тех. наук.- Ташкент, ТИТЛП, 1971. - 222 с.

53. Бурнашев Р.З и др. Экспериментальное исследование ударного взаимодействия летучек хлопка-сырца с колосником очистителя крупного сора. Сб. Хлопковая промышленность. Ташкент, 1980. №1, с. 7-8.

54. Гробер А.Д. Некоторые особенности ударного взаимодействия хлопковых материалов с рабочими органами хлопкообработывающих машин. Сб. Хлопковая промышленность. -Ташкент, 1980. №6, с. 9-10.

55. Хлопкоочистительная Машина «Murray» - Укомплектована И Г отова К Отправке По Всему Миру. [Электронный ресурс]-Режим доступа: http: //murraycottongin.com/

56. Расулов Р. Х. Обоснование параметров пильчатой - колосниковой системы очистителя хлопка - сырце от крупного сора. Канд. дисс. Ташкент, 2008г, 130с.

57. Расулов Р.Х., Корабельников Р.В., Лугачев А.Е. Исследование некоторых физико-механических характеристик хлопка-сырца

применительно к модулю очистителя крупного сора// Журнал «Технология текстильной промышленности». - Иваново, 2004. - №1. - С. 16-19.

58. Будин Е.Ф., Бородин П.Н. Новые отбойные рабочие органы для пильчатых очистителей хлопка - сырца// Сб. Хлопковая промышленность - Ташкент, 1978, -№5. -с.17.

59. Фазылов С. Колосниковые узлы очистителей хлопка-сырца от крупных сорных примесей с регулируемыми параметрами: Дисс...канд. тех. наук. - Ташкент, 1985. -142 с.

60. Олимов К.Т. Разработка и обоснование параметров колосников на упругих опорах очистителей хлопка-сырца от крупных сорных примесей: Дисс... канд. тех. наук. -Ташкент: ТИТЛП, 1998. - 135 с.

61. Джураев А. Д. и др. Динамика вибрирующих рабочих органов очистителей хлопка - сырца, «ФАН», Ташкент, 2003, 192с.

62. Рахматкариев Ш. У. Динамический анализ и параметрический синтез машин с упругими элементами и нелинейностями различного происхождения. Ташкент, Издательство «ФАН» Академии наук Республики Узбекистан, 1997, 232 стр.

63. Лугачев А.Е. Резервы в повышении техники и технологии очитки хлопка - сырца в поточной линии хлопкозавода. Межд. Научно - практ конференция «Состояние техники и технология текстильной и легкой промышленности и перспективы их развития», Наманган, НМКИ, 1996, 144с.

64. Махкамов Р.Г. Бурнашев Р.З. Исследование контактных давлений при взаимодействии хлопкового волокна с переходными поверхностями рабочих органов машин. АН УзССР, Информационное сообщение № 154, Т., 1976.

65. Джабборов Г.Дж. и другие. Технология переработки хлопка-сырца. Т.: «Укитувчи», 1987. — 328 с.

66. Бобоматов А.Х. Создание эффективной конструкции и совершенствование на ученых основе методов расчета очистителя хлопка - сырца от мелкого сора. Дисс. (PhD) по техническим наукам: - Ташкент, 2017. -126 с.

67. Anthony W.S. and William D. Mayfield, Cotton ginners handbook // Agricultural handbook. Number 503. United States Department of Agriculture. December 1994. - 337 p.

68. Arude V.G., Manojkumar T.S., Shukla S.K. Axial flow pre-cleaner for on farm cleaning of cotton. Agricultural Mechanization in Asia, Africa and Latin Amerika. 2014, ISSN: 00845841.

69. Hardin R.G., Byler R.K. Removal of sheet plastic matetials from seed cotton using a cylinder cleaner. Journal of Cotton Science. - USA, 2016. - pp. 375-385.

70. Модернизированный хлопкоочистительный агрегат УХК Паспорт УХКМ. ООО ПС, АО «Paxtagin CB» - Ташкент, 2010. - 54 с.

71. Балтабаев С.Д. К теории и практике переработки хлопка-сырца советских тонковолокнистых разновидностей. - Ташкент: Издательство «Фан» - 1978. - С. 44-67.

72. Зикриёев Э.З. Первичная обработка хлопка-сырца: Учебник - Т.: «Труд», 2002. - 408с.

73. Лугачев А.Е. Первичная обработка натурального волокон: учебно - методический комплекс. - Ташкент: ТИТЛП, 2013. - 245 с.

74. Лугачев А.Е., Салимов А.М. Первичная обработка хлопка-сырца: учебное пособие - Ташкент, 2007. - 132 с.

75. А.С. № 651061. Сетка очистителя волокнистого материала / Тютин П.Н., Лугачев А.Е. // Бюлл. №9, 05.03.79.

76. Джабаров Г.Ж., Отаметов Т.У., Хамидов А.Х. Первичная обработка хлопка. - Т.: “Укитувчи”, 1987. - 102 с.

77. Максудов Р.Х., Мурадов Р.М., Джураев А.Ж. Разработка новых высокоэффективных рабочих органов и механизмов очистителей хлопка от мелкого и крупного сора: отчет № ИТД-15-061.-Ташкент, 2009. 138 с.

78. Джураев А., Элмонов С., Мирахмедов Дж. Рациональная компоновка рабочих органов в модернизированном хлопкоочистительном агрегате. Современные инструментальные системы информационные технологии и инновации: XII-я международная научно-техническая конференция. - Курск, 2015. - С. 188-191.

79. Якубов Б.Н. Совершенствование процесса очистки хлопка-сырца от сорных примесей в пильчатых очистителях с целью уменьшения потери волокнистой массы хлопка: Дисс... канд. тех. наук. -Ташкент: ТИТЛП, 1985. - 156 с.

80. Турсунов Х.К. Механика рабочих органов волокноочистительных

машин, Ташкент, Фан, 1997г, 126 с.

81. Патент Рес. Узб. FAP 00696. Сетчатая поверхность очистителя волокнистого материала / Бобоматов А.Х., Джураев А.Дж., Мирахмедов Дж.Ю., Мухамедов Ж.М, Бобомуродов Т.F. // Бюлл. №2. 29.02.2012.

82. А.С.912785. Колосниковая решетка очистителя волокнистого материала. Джураев А. БИ N10, 1982.

83. Будин Е.Ф., Агзамов М. Новые отбойные органы для очистителей хлопка - сырца. Ташкент. УзНИИНТ И 1979, с.5.

84. Абдуллаев А.В., Джураев А., Мирахмидов Дж. Анализ колебаний колосника на упругом основании с нелинейной жесткостью, Ж. Известия ВУЗ, Технология текстильной промышленности, №5, 2008 г.

85. Джураев А. и др. Колосниковая решетка очистителя волокнистого материала. Патент ДР 03338, Бюлл. №1, 2007.

86. Муродов О., Джураев А., Элмонов С. Очиститель волокнистого материала с колосниками на упругих резиновых втулках // «Молодежь и XXI век - 2017» Материалы VII Международной молодежной научной конференции 21-22 февраля 2017 Курск 2017. стр. 325-326

87. Джураев А. Колосниковая решетка очистителя волокнистого материала. А.С. №874776, бюлл № 39, 1981.

88. Справочник по первичной обработке хлопка. Книга I. Максудов И.Т., Нуруллаев А.Н. ISBN 5-8244-1048-8 // © По заказу Научно-производственного объединения «хлопкопром», 1994 г. С. 233-234.

89. А. Джураев Динамика рабочих механизмов хлопка перерабатывающих машин. Ташкент. изд. Фан УзССР, 1987 с. 142-146.

90. Murodov O.J. Perfection of Designs and Rationale of Parameters of Plastic Koloski Cleaning Cleaners / O.J. Murodov // International Journal of Innovative Technology and Exploring Engineering (IJITEE) ISSN: 2278-3075, Volume-8 Issue-12, October 2019. page 2640-2646.

91. Патент на изобретение UZB № IAP 06632 АПИС. D 01 B 1 02; 2006.01. Сепаратор хлопка-сырца / О.Ж. Муродов, А. Джураев. Хожиев М.Т., Рахимов А.Х. 13.05.2019; Опубл. 24.11.2021. Бюл. № 11.

92. Маматкулов О.Т. Создание рациональной конструкции хлопкоотделителя. Кандидатская диссертация по техническим наукам. Наманган, 2019, 125 стр.

93. Патент на изобретение РФ № 2701220 ФИПС, С 1. Сепаратор хлопка-сырца / О.Ж. Муродов, М.Т. Хожиев А. Рахимов и др. 19.04.2019; Опубл. 25. 2019, Бюл. № 27.

94. Патент на полезная модель UZB № FAP 01522 АПИС. D 01 B 1 02; Сепаратор хлопка-сырца / О.Ж. Муродов, М.Т. Хожиев А. Жураев. 01.04.2019; Опубл. 29.08.2020. Бюл. № 8.

95. SU 1285079. Барабан очистителя хлопка - сырца / Будин Е.Ф., Бородин П.Н. // Бюлл. №3. 23.01.87

96. Далиев Ш.Л., Джураев А.Д., Ражабов О.И. Сетчатая поверхность очистителя волокнистого материала от мелкого сора // Молодежь и XXI век - 2017: Материалы VII Международной молодежной научной конференции. - Курск, 2017. - С. 267-270

97. Муродов О.Ж. Влияние формы сетки очистителя мелкого сора для хлопка-сырца на очистительный эффект / О.Ж. Муродов, // Костромской государственный университет ISSN 2587-6147// технологии и качество №2(52) 2021 С.52-56. https: doi 10.34216/2587-6147-2021-2-52-52-55.

98. Муродов О.Ж. Результаты экспериментального исследования нагруженности и характера колебаний многогранной сетки на упругих опорах очистителя хлопка / О. Ж. Муродов., О.И.Ражабов // Издание Ивановского государственного политехнического университета. DOI 10.47367/0021- 3497_2021_5_191. Иванова 2021 г., С.191-197.

99. Патент на изобретение UZB № IAP 05853 АПИС, D 01 G 9 |14;2006.01. Колосниковая решетка очистителя волокнистого материала / О.Ж. Муродов, А. Джураев. Ж.Ю. Мирахмедов. С. Элмонов. 04.05.2016; Опубл. 31.05.2019. Бюл. № 6.

100. Патент на изобретение UZB № IAP 05652 АПИС. D 01 G 9 00; 2006.01. Колосниковая решетка очистителя волокнистого материала / О.Ж. Муродов, А. Джураев. Дж. Мирахмедов. С. Элмонов. 29.04.2016; Опубл. 28.08.2018. Бюл. № 10

101. Муродов О.Ж., А.Джураев. Groundation of the parameters of grate bar on elastic support with non-linear hardness. The european science review. №2 7-8 2017. July-August. Vienna Prague. 2017. page-109-111.

102. Муродов О.Ж., А.Джураев. Совершенствование конструкций и методы работе параметров пластмассовых колосников на резиновых опорах очистителей хлопка от крупного сора //Ташкентский институт

текстильной и легкой промышленности. Ташкент «Fan va texnologiya»-2018.136 с.

103. Муродов О.Ж. Янги пластмассали колосник урнатилган тозалаш машинасида тозаланган чигитли пахта сифат курсаткичларини тадкик килиш / О.Ж. Муродов, Х.К. Рахмонов О.И. Ражабов // «Развитие науки и технологий» Научно-технический журнал Бухарский инженерно-технологический институт 2017. № 4. С. 33-38.

104. Murodov O.J. Investigation of vibrations of a lightweight grate on elastic supports of a coarse litter cleaner with random disturbance from raw cotton / O.J. Murodov, Sh. Madrahimov Z. Shodiyev //ISSN (Online): 2455-3662. EPRA International Journal of Multidisciplinary Research (IJMR) - Peer Reviewed Journal. Volume: 7 | Issue: 1 January 2021. Article DOI: https://doi.org/10.36713/epra6042. Page-49-53.

105. Муродов О.Ж. Снижение повреждаемости семян в сепараторе хлопка-сырца / О.Ж. Муродов // Костромской государственный университет ISSN 2587-6147. Технологии и качество. 2021. № 3(53). С. 48-51. https: doi 10.34216/2587-6147-2021-3-53-48-51.

106. Murodov O.J. Researches Gained in Process with Developed CC-15A Separator / O.J. Murodov, M. T. Khojiev // ISSN: 2350-0328 International Journal of Advanced Research in Science, Engineering and Technology Vol. 6, Issue 4, April 2019. page-8735-8738.

107. Кодиралиев А. Исследование падения компонентов хлопкасырца. Машины, агрегаты и процессы. Проектирование, создание и модернизация 2020, №3, С. 73-76. https://doi.org/10.26160/2587-7577-2020-3-73-76

108. Холтураев Х.П., Джураев А., Мавлянов А.П., Дж.Мирахмедов Эффективная новая конструкция колкового барабана очистителя Модернизация производства, инновации в техническом и технологическом перевооружении, экономичные методы и нетрадиционные решения: Тезисы докладов Республиканской научно-технической конференции. - Фергана, - с. 224-227.

109. Ахмедходжаев Х. Т., Алиев М.А. О повреждаемости семян при пневмотранспортировании хлопка - сырца. “Хлопковой промышленность”. - Ташкент, 1977. - №2. - С.7-8

110. Бурнашев Р.З. и др. Экспериментальное исследование ударного взаимодействий летучек хлопка - сырца с колосником очистителя

крупного сора. «Хлопковая промышленность» - Ташкент, 1980. - № 1. - С. 7 - 8.

111. Попов О.Н. Принцип Лагранжа - Даламбера. Теория и задание: Исследование движения механической системы с двумя степенями свободы с помощью принципа Лагранжа - Даламбера и уравнений Лагранжа второго рода относительно положения равновесия: Учебное пособие. - Томск: ТГАСУ, - 65 с.

112. Rajabov O., Mavlyanov A., Yakubova A. Study of the influence of the parameters of the plastic grate on elastic supports with nonlinear stiffness on the oscillation frequency // International scientific and practical conference "Innovative ideas of modern youth in science and education", - USA, 2019. - pp. 152-154.

113. Тураев Н.Т. Теоретическая механика.-Ташкент: “Ношир”, 2012. -304 с.

114. Ражабов О.И., Джураев А., Рустамов Б. Определение реакции при взаимодействии летучек хлопка с сетчатой поверхностью очистителя хлопка от мелкого сора. «Развитие науки и техники». -Бухара, 2018.- №3. - С. 20-26

115. Мвлянов Т.М. и другие. Теоретическая механика: учеб. - Ташкент: ТТИЛП. - 2001.

116. Ражабов О.И., Джураев А. Обоснование жесткости упругой опоры сетчатой поверхности очистителя хлопка от мелкого сора // Проблемы и перспективы развития инновационного сотрудничества в системе научных исследований и карточного обучения: Материалы международной научнопрактической конференции. - Бухара, 2017. - С. 31-33.

117. Ражабов О.И., Джураев А., Анализ колебаний упругой пластины сетчатой поверхности очистителя при случайном возмущении от хлопка- сырца. «Развитие науки и техники». - Бухара, 2017. - №4 - С. 114-118.

118. Ражабов О.И., Далиев Ш.Л., Джураев А., Мавлянов А.П. Сетчатая поверхность очистителя волокнистого материала от мелкого сора // Молодежь и XXI век - 2017: Материалы VII Международной молодежной научной конференции. - Курск, 2017. - С. 256-260.

119. Мэнли Р. Анализ и обработка записей колебаний. Машиностроение, М.,1974, 368с.

120. Будин Е.Ф. Исследование колосниково - пильчатых рабочих органов

очистителей хлопка-сырца машинного сбора средневолокнистых сортов: Дисс...канд. тех. наук. Ташкент: ТИТЛП, 1968. - 156 с.

121. Тимошенко С.П., Янг Д.Х., Унвер У., Колебания в инженерном деле. Машиностроение, М., 1985, 472 С.

122. Потураев ВТ., Дырда В.И. Резиновые детали машин. М. Машиностроение 1977 г.

123. Муродов О.Ж. Колосниковая решетка очистителя хлопка с многогранными колками / О.Ж. Муродов, Х. Нуруллаева Ж.Ю. Мирахмедов., Ш. Мамадалиев // Сб. стат. Межд. НКТ «Молодёжь-производству» 21-22 ноября, Витебск-2006 г., С. 221-223.

124. Муродов О.Ж. Эффективная схема конструкции колосниковой решетки с пяти и шестигранными колосниками очистителя хлопка-сырца от мелкого сора / О.Ж. Муродов, Дж.Ю. Мирахмедов // «Современные материалы, оборудование и технологии в машиностроении», Международная научнотехническая конференция, секция 4. Ташкент-2016 г., С. 35-37.

125. Турсунов Х.К. Механика рабочих органов волокноочистительных машин, Ташкент, Фан, 1997г, 126 с.

126. Муродов О.Ж. Анализ влияния переменности угловой скорости пильчатого барабана на угол отклонения захваченной летучки в очистителе хлопка / О. Ж. Муродов // Российский государственный университет имени А.Н. Косыгина. Дизайн и технологии» 2021,81(123). С .73-77.

127. Муродов О.Ж. Совершенствование конструкции питающих валиков питателей хлопка / О.Ж. Муродов, Ж. Мирахмедов Ш. Мамадалиев // Тезисы Республиканской научно-практической конференции. Ташкент 2006 г., С. 284-285.

128. Муродов О.Ж. Эффективный сепаратор хлопка-сырца / О.Ж. Муродов, Б.Ч. Пардаев // Материалы Республиканской научно-практической конференции «Инновационные технологии на основе местного сырья и вторичных ресурсов». Ургенч, Том I. Ургенчский государственный университет, 2021. С. 529-530.

129. Методы динамических испытаний для резины (общие требования). ГОСТ 23926-78, - М. -1978, -18с.

130. Муродов О.Ж. Новые облегченные конструкции пильных цилиндров очистителей хлопка на упругих подшипниковых опорах / О.Ж.

Муродов, С. Юнусов, Дж.Ю. Мирахмедов // «Современные материалы, оборудование и технологии в машиностроении», Международная научно-техническая конференция, секция 2 Андижан-2016., С. 94-97.

131. Murodov O.J. Development of an effective design and justification of the parameters of the separation and cleaning section of raw cotton / O.J. Murodov // ICMSIT-II 2021 Journal of Physics: Conference Series 1889 (2021) 042012 IOP Publishing doi:10.1088/1742-6596/1889/4/042012. page-1889-1896

132. Murodov O.J Analysis of the vibrations of a console column made on a base with non-line protection in gin / O.J. Murodov, A. Djuraev, E.A. Narmatov, T. Yormamatov, // ICMSIT-II 2021 J ournal of Physics: Conference Series 1889 (2021) 042017 IOP Publishing doi:10.1088/1742-6596/1889/4/042017.page-1-5.

133. Муродов О.Ж. Исследование колебаний облегченного колосника на упругих опорах очистителя хлопка-сырца от крупного сора при случайном возмущении / О.Ж. Муродов, А. Джураев // Вестник Таш ГУ № 2, 2017 г., С. 95-100.

134. Патент на полезная модель РФ регистрационный №2021132612 ФИПС от 08.11.2021. входящий №068777. Пильный диск волокноочистителя / Муродов О.Ж., Мавлянов А.П., Абдусаматов А.А.

135. Murodov O.J. Analysis of harmful mixtures in air flow during cotton cleaning / O.J. Murodov, A.SH. Adilova // Tashkent state technical university named after Islam Karimov. Technical science and innovation. The Journal was established in 1993, Renamed in 2019. Published 4 times a year Tashkent-2021, №3(09). Page- 79-87.

136. Муродов О.Ж. Эффективная колосниковая решетка очистителя хлопка от крупного сора / О.Ж. Муродов, Х. Нуруллаева, О. Мавлянов // Материалы 58-й межвузовской научно-технической конференции молодых ученых и студентов «Студенты и молодые ученые КТТУ производству», 19-21 апреля 2006 г. Кострома, КТТУ 2006 г., С. 138-139.

137. Муродов О.Ж. Совершенствование системы питания и волокна отделения в пильных джинах / О.Ж. Муродов, Ш. Мамадалиев, Дж. Мирахмедов, С. Юнусов // Материалы 58-й межвузовской научно-технической конференции молодых ученых и студентов «Студенты и молодые ученые КТТУ производству», 19-21 апреля 2006 г. Кострома, КТТУ 2006 г., С. 140-141.

138. Патент на полезная модель UZB № FAP 01459 АПИС. D 01 G 9 14; Колосниковая решетка очистителя волокнистого материала / О.Ж. Муродов, А. Джураев. О.И. Ражабов. 02.03.2017; Опубл. 27.12.2019. Бюл. № 1.

139. Муродов О.Ж. Аналитический метод изучения колебаний колосника на упругих опорах очистителя шерсти от растительных примесей /

140. О.Ж. Муродов, Дж. Мирахмедов, С. Элмонов, Д. Ташпулатов // Роль интеграции науки в организации производства на предприятиях текстильной промышленности и решении актуальных проблем. Международная научнотехническая конференция. Часть 2, 27-28 июля, Маргилан-2017 г.,С. 111-114.

141. Муродов О.Ж. Разработка конструкции и обоснование параметров вибрационного пластмассового колосника очистителя хлопка от крупного сора. Дисс. (PhD) по техническим наукам: - Ташкент, 2018. - 156 с.

142. ГОСТ 23326-78 Резина. Методы динамических испытаний. Общие требования. База ГОСТов. Резиновая, резинотехническая, асбесто-техничекая и пластмассовая промышленность [Электронный ресурс]- Режим доступа: https://allgosts.ru/83/060/gost_23326-78

143. Патенты на программы для ЭВМ UZB №12975. ДГУ 20213002. Компьютерная программа для решения уравнения Навье-Стокса динамики движения пыли в канале / О.Ж. Муродов, А.Ш., 12.10.2021; Опубл.09.11.2021.

144. Муродов О.Ж. Собственные колебания колка на упругом основании рабочего барабана очистителя хлопка / О.Ж. Муродов, Ж.Ю. Мирахмедов, О.П. Мавлянов // Тезисы Республиканской научно-практической конференции. Ташкент 2006 г., С. 286-287.

145. Севостьянов А.Г. Методы и средство исследования механико-технологических процессов текстильной промышленности. -М.: МГТУ им А.Н. Косыгина, 2007. - 648 с. ISBN 5-8196-0091-6.

146. Murodov O.J. Creation of Scientific-Based Construction of the Separator with Insulation Camera / O.J. Murodov M.T. Khodjiev, D. Eshmurodov // International Journal of Innovative Technology and Exploring Engineering (IJITEE) ISSN: 22783075, Volume-9 Issue-4, February 2020. page 3231-3236

147. ГОСТ Стандарт УзГСт 598:2008. «Технические семена, методы отбора

образцов». Узбекское агентство стандартизации, метрологии и сертификации. Ташкент, 2014. с 3.

148. Murodov, O.J. Tests in the insulating cameras of the improved separator O.J. Murodov, M.T Khodjiev, D.D Eshmurodov, DA. Eshnazarov // MIP: Engineering-2020 IOP Conf. Series: Materials Science and Engineering 862 (2020) 032025 IOP Publishing doi:10.1088/1757-899X/862/3/032025. page-1-5.

149. Murodov O.J., M. T. Khojiev., A. Juraev., A. Rakhimov. Development of Design and Substantiation of the Parameters of the Separator for Fibrous Materials. International Journal of Recent Technology and Engineering (IJRTE) ISSN: 22773878, Volume-8 Issue-2, July 2019. page-5806-5811.

150. Муродов О.Ж. Ресурсосберегающий барабан для съема хлопка-сырца с пильных цилиндров и его транспортирования в очистителях / О.Ж. Муродов, С.М. Элмонов, Б.К. Хусанов // Поколение будущего: Взгляд молодых ученых Сборник научных статей 5-й Международной молодежной научной конференции 10-11 ноября, Курск 2016 г. С. 314-316.

151. Гост стандарт O'z DSt 643:2006 «Хлопок. Методы определения влажности», Узбекское агентство стандартизации, метрологии и сертификации. - Ташкент, 2006.

152. Стандарты России и СНГ «Хлопок-сырец. Методы определения влажности. Взамен O’z DSt 644-95. [Электронный ресурс]-Режим доступа: https://gostperevod.ru/o-z-dst-644-2006.html

153. Муродов О.Ж., Джураев А.Ж. Особенности конструкции пяти и шестигранных колосников очистителя хлопка. Минобрнауки России. Качество в производстеннных и социально-экономических системах. Сборник научных трудов 4-й Международной научно-технической конференции. 21-22 апреля 2016 года. Курск - 2016. С.265-266.

154. Муродов О.Ж. Новая конструкция пильного цилиндра хлопка на упругих подшипниковых опорах / О.Ж. Муродов, // Будущее науки-2021. Сборник научных статей 9-й Международной молодежной научной конференции. 21-22 апреля 2021 года, С. 212-214. https: //nauka46.ru/konferentsii

155. Веденяпин Г.В. Общая методика экспериментального исследования и обработка опытных данных. // Колос. - М. -1973. -199 с.

156. Немец И. Практическое применение тензорезисторов. // Пер. с

чешского. Энергия. М. -1970. -144 с.

157. Муродов О.Ж. Исследование показателей качества после очистки на хлопкоочистительной машине, оснащенной пластиковыми колосниками с эластичной опорой на семенах хлопка / О.Ж. Муродов, А.А. Умаров, Б.Ч. Пардаев // Актуальные проблемы инновационных технологий хлопкоочистки, текстильной, легкой промышленности, полиграфического производства и их решения в контексте интеграции науки, образования, производства. Республиканская научно-практическая конференция. Часть II. 21-22 апреля. Ташкент-2021. С.101-103.

158. Муродов О.Ж. Пахтани йирик ва майда хас-чуплардан тозалаш машинасидаги кайишкок элементли янги пластмассали колосникли панжаранинг параметрларини оптималлаштириш (Оптимизация параметров новой пластиковой колосниковой решетки с элластичним элементом в машине для очистки хлопка от крупных и мелких соров) / О.Ж. Муродов, О.И. Ражабов С.Х. Бобожонов // «Развитие науки и технологий» Научно-технический журнал №1. Бухарский инженерно-технологический институт 2018 г. С. 5-12.

159. Муродов О.Ж. «Ремонт сетевых машин». Учебник / О.Ж. Муродов., А.Х.Каюмов., Р.Х.Росулов // МВ и ССО Рес Узб. Наманганский инженернотехнологический институт. Учебное пособие «Ремонт сетевых машин» 5320300-Технологические машины и оборудование (текстильная, легкая и хлопчатобумажная промышленность) Ташкент-2019. -515 с.

160. Муродов О.Ж. Аналитический метод изучения колебаний колосника на упругих опорах очистителя шерсти от растительных примесей / О.Ж. Муродов, Дж. Мирахмедов, С. Элмонов, Д. Ташпулатов // Роль интеграции науки в организации производства на предприятиях текстильной промышленности и решении актуальных проблем. Международная научнотехническая конференция. Часть 2, 27-28 июля, Маргилан-2017 г.,С. 111-114.

161. Муродов О.Ж. Влияние производительности очистителя хлопка от крупного сора на колебания пластмассового колосника / О.Ж. Муродов, А. Джураев, С. Саидкулов, У.Бердимуродов // Республиканская научнопрактическая конференция «Анализ и решение проблем текстильной промышленности Узбекистана» Андижан 23-24 ноября 2021 года. С. 21-24.

162. Муродов О.Ж. Влияние жесткости упругой опоры колосника на показатели его колебаний очистителя хлопка / О.Ж. Муродов, А.Джураев, С.Саидкулов, У.Бердимуродов // Республиканская научно-практическая конференция «Анализ и решение проблем текстильной промышленности Узбекистана» Андижан 23-24 ноября 2021 года. 24-26.

163. Murodov O.J. Design development and parameters calculation methods of plastic diamond pattern bars on resilient supports in ginning machines / O.J. Murodov, D.S Tashpulatov, A. Juraev J.K. Gafurov, S. Vassiliadis // Aegean International Textile and Advanced Engineering Conference (AITAE 2018) IOP Conf. Series: Materials Science and Engineering 459 (2019) 012068. Scopus. page- 1-10.

164. Муродов О.Ж. Режимы движения барабана питателя при случайном сопротивлении от хлопка / О.Ж. Муродов, А. Джураев, Д.Ю. Мирахмедов, О.П. Мавлонов // «Проблемы текстиля». Научно-технический журнал. Ташкент. 2005. № 4. С. 8-11.

165. Справочник. Э.Л. Калинчаев., М.Б. Саковцева. Выбор пластмасс для изготовления и эксплуатации изделий. Справочное пособие. Ленинград. Издательство «Химия», Ленинградское отделение. 2007 г

166. Муродов О. Способы устранения износа деталей современной инновационной универсальной хлопкоочистительной машины / О.Ж. Муродов, Ф. Бобокулов // Материалы научно-практической конференции профессоров, преподавателей, старших научных сотрудников, магистрантов и студентов на тему «Проблемы и решения для развития инновационного сотрудничества в науке, образовании и производстве» Бухарский ИТИ (26-30 апреля 2016 г.) Бухара -2016 г., С. 276 -278.

167. Раевский Н.П. Датчики механических параметров машин. М. изд., 1999, 226с.

168. Муродов О.Ж. Динамика барабана питателя хлопка / О.Ж. Муродов, Ж.Ю. Мирахмедов., О.П. Мавлянов // Тезисы РНПК молодых ученых, «Инновации в модернизации производства, технико-технологическом перевооружении, экономическая эффективность и нетрадиционные решения», Фергана-2008 г., С. 6-8.

169. Муродов О.Ж. Эффективная конструкция барабана для съема хлопка-сырца с пильных цилиндров и его транспортирования в очистителях / О.Ж. Муродов, А. Джураев.С. Элмонов // Материалы научно-

практической конференции по совершенствованию оборудования и технологий в современных производственных условиях и повышению их экономической эффективности 24-25 ноября. Наманган - 2016 г., С. 195-197.

170. Murodov O.J. Improving the quality of lint by strengthening the cleaning of cotton seeds from waste / O.J. Murodov, Kh. J Abdugaffarov, A.A Safoev // MIP: Engineering-2020 IOP Conf. Series: Materials Science and Engineering 862 (2020) 032026 IOP Publishing doi:10.1088/1757-899X/862/3/032026. page-1-6.

171. Муродов О.Ж. Эффективная конструктивная схема сепарационно-очистительного агрегата / О.Ж. Муродов, А.Джураев, С. Саидкулов, У. Бердимуродов // Республиканская научно-практическая конференция «Анализ и решение проблем текстильной промышленности Узбекистана» Андижан 2324 ноября 2021 года. С. 20-21.

172. Баранчикова С.Г. и др. под общ. ред. проф. Ершовой И.В. Экономическая эффективность технических решений: учебное пособие - Екатеринбург, 2016. - 140 с.

173. Габитова Е.В., Данилкин В.В., Старкова Т.Ю. Методические указания определению экономической эффективности научно-исследовательских работ новой техники. - Челябинск: издательский центр ЮУрГУ, 2011. -40 с.

174. Муродов О.Ж. Совершенствование конструкции и обоснование параметров сепаратора хлопка-сырца/ О.Ж. Муродов // Известия Высших учебных заведений. Технология текстильной промышленности. 2022, №1, С. 248-253. DOI 10.47367/0021-3497_2022_1_248.

175. Муродов О.Ж. Обоснование параметров и конечно-элементное моделирование движения хлопковоздушной смеси в сепараторе хлопка/ О.Ж. Муродов, П.Н. Рудовский, А.Р. Корабельников// Известия Высших учебных заведений. Технология текстильной промышленности. 2022, №1, С.266-271. DOI 10.47367/0021-3497_2022_1_266.

176. Муродов О. Ж., Рудовский П. Н., Корабельников А. Р. Определение собственных частот и форм свободных колебаний колосниковой решетки очистителя хлопка-сырца // Технологии и качество. 2022. № 1(55). С. 24-28. https: doi 10.34216/2587-6147-2022-1-55-24-28.

177. Джураев, А. Д., Давидбаев, Б. Н., & Давидбаева, Н. Б. (2019). Обоснование параметров амартизирующий пластины резиновой подушке сепаратора хлопка-сырца. Наманганский инженерно-технологически институт. Научно-технический журнал, 4.

178. Давидбаев Б. Н., Джураев А., & Давидбаева Н.Б. (2024).\\ Разработка эффективной конструкции хлопкового сепаратор для хлопка-сырца.\\ Механика и технология, (3 (10) Спец.выпуск), 172-176.

179. Давидбаев Б. Н., Джураев А., Зулпиев С. М., Давидбаева Сепаратор для волокнистых материалов. Патент Кыргизской Респ. № 36о 30.08.2023.

180. Зулпиев С.М, Давидбаев Б., ДжураевА.Д., Давидбаева Н.Б, Сепаратор для хлопка-сырца. Патент Кырг. Рес. По заявке 135. № 20230011,2 от 30.08.23 г. №360

181. Djuraevich D. A., Nizomitdinovich D. B., Bakhtiyerdjanovna D. N.Substantiation Parameters Of Reflector With Rubber Shock Absorber Of Cotton Separator //Solid State Technology. – 2020. – Т. 63. – №. 6.– С.1718-1726.

182. Давидбаев Б. Н., Джураев А., Алимов, О, Давидбаева Н.Б. Сепаратор для волокнистых материалов // Ўзб. Рес. патенти IAP 06300 Расмий ахборотнома №10, 2020

183. A.Djuraev, B.N.,Davidbaev, A.S.Jumaev Improvement of the design of the belt conveyor and scientific basis for calculation of parameters (monograph \\ Global Onlihe Book Publisihg (Publisiher) 1211 polk St, Orlahdo,32805 USA.24 05.2022,144 стр.

184. Джураев, А., Давидбаев, Б., & Давидбаева, Н. (2020). Влияние взаимодействие летучки с амортизирующей пластин. Сепаратора на качественные показателей хлопка-сырца. Сепаратора на качественные показателей хлопка-сырца. Збірник науко вихпраць ΛΌГОΣ, 72-76.

185. Давидбаев Б.Н., Джураев А.Д., Давидбаева Н.Б. Разработка эффективной конструкции хлопкового сепаратора для хлопка. \\Наманган мухандислик курилиш институти. Механика ва технология илмий журнали. Махсус сон №3, 2024

186. Джураев А., Давидбаев Б. Н., Давидбаева Н. Б. Разработка эффективной конструкции и результаты испытаний сепаратора хлопка–сырца Сборник материалов Республиканской научно-практической конференции “посвященной к 100 летую Академика ХХ Усмонхужаева //года, ТОМ. – 2019. – №. 1. – С. 86.

187. Джураев А. Д., Давидбаев Б. Н., Давидбаева Н. Б. Обоснование параметров амартизирующий пластины резиновой подушке сепаратора хлопка-сырца //Наманганский инженерно-технологически институт. Научно-технический журнал. – 2019. – Т. 4.

188. Джураев А., Давидбаев Б., Давидбаева Н. Анализ процесса выпадения частиц хлопка в зоне взаимодействия с амортизирующем отражателям сепаратора //Научно-технический-журнал Ферганского политехнического института. – 2020. – С. 144-147

189. Давидбоев Б.Н., ДжураевА.Д., Давидбоева Н.Б. Сепаратор для хлопка-сырца. // Talabnoma raqami IAP 20220095 буйича O‘zbekiston Respublikasining “Ixtiro патент № IAP 7689.2024й

190. Давидбаев Б.Н., ДжураевА.Д., Давидбаева Н.Б. Разработка эффективной конструкции хлопкового сепаратора для хлопка.\\ Наманган муҳандисликқурилиш институти.Механика ва технология илмий журнали. махсус сон №3,2024,172-176 бет.

191. Давидбаев Б.Н., Давидбаева Н.Б. Разработка и теоретическая исследования рычажно-шарнирных \\ НТЖ ФерПИ, 2024, Т.27.спец. выпуск №28) 2021 №2.Наманган. 9-15 бет.

192. Djuraev A., Davidboev B. N., Davidboeva N. B. Determination of Oscillatiom Amplitude of Cotton Particle at Interaction with Plate and Shock Absocber of the Separator //International Journal of Abvanced Research in Science, Engineering and Technology. – 2020. – Т. 7. – №. 9.– С. 14977-14981.

193. Зулпиев С. М., Давидбаев Б. Н., Давидбаева Н. Б. О движение летучки хлопка-сырца по поверхности перфорированной сетки сепаратора сс-15а //известия национальной академии наук кыргызской республики. – 2022. – №. 5. – С. 173-178.

194. Давидбаев Б., Джураев А., Давидбаева Н. Исследование взаимодействия частицы хлопка–сырца с амортизирующей пластин сепаратора //Збірник наукових праць ΛΌГОΣ. – 2020. – С. 82-86

195. Давидбоев Б.Н., ДжураевА.Д., Давидбоева Н.Б. Сепаратор для хлопка-сырца. // Talabnoma raqami IAP 20220095 буйича O‘zbekiston Respublikasining “Ixtiro патент № IAP 7689.2024й